

ULTRA-FAST LINE-CAMERA KALYPSO FOR fs-LASER-BASED ELECTRON BEAM DIAGNOSTICS

M. M. Patil*, M. Caselle, E. Bründermann, G. Niehues, A. Ebersoldt, M. J. Nasse, M. Reißig,
A. Kopmann, J. L. Steinmann, S. Funkner, C. Widmann, T. Dritschler, S. Chilingarayan,
M. Weber and A.-S. Müller
Karlsruhe Institute of Technology, Karlsruhe, Germany

Abstract

A very common bottleneck to study short electron bunch dynamics in accelerators is a detection scheme that can deal with high repetition rates in the MHz range. The KIT electron storage ring KARA (Karlsruhe Research Accelerator) is the first storage ring with a near-field single-shot electro-optical (EO) bunch profile monitor installed for the measurement of electron bunch dynamics in the longitudinal phase-space. Using electro-optical spectral decoding (EOSD) it is possible to imprint the bunch profile on chirped laser pulses subsequently read out by a spectrometer and a camera. However, commercially available cameras have a drawback in their acquisition rate, which is limited to a few hundred kHz. Hence, we have developed KALYPSO, an ultra-fast line camera capable of operating in the MHz regime. Its modular approach allows the installation of several sensors e.g. Si, InGaAs, PbS, PbSe to cover a wide range of spectral sensitivities. In this contribution, an overview of the EOSD experimental setup and the detector system installed for longitudinal bunch studies will be presented.

INTRODUCTION

In an electron storage ring, investigation of ultra-fast dynamics in short electron bunches of a few ps length requires diagnostic methods that allow non-destructive measurements (e.g. longitudinal bunch profile of the electron bunches) at MHz repetition rate. Most commonly used methods involving the measurement of synchrotron radiation with a streak camera. This method is not capable of single-shot acquisitions, as this diagnostic tool averages the bunch profile over a few turns. On the other hand commercial line array cameras have a disadvantage of being slow with readout rate in the kHz range. In this paper, a diagnostic method based on EOSD combined with a novel line array camera KALYPSO (KARlsruhe Linear arraY detector for MHz rePetition-rate SpectrOscopy) developed at KIT will be presented. Electro-optic techniques are based on the so-called Pockels effect [1]. This effect leads to a phase or polarization modulation of the laser pulse passing through an electro-optic active crystal, e.g. gallium phosphide (GaP), in the presence of an external electric field. The phase modulation can be effectively converted to intensity modulation via a detection scheme based on one of different polarization-based methods [2].

EOSD is a well-known technique in THz spectroscopy. It dates back as early as 1998, when this method was used

for the measurement of freely propagating sub-ps electromagnetic pulses using a linearly chirped optical beam [3]. Near-field EO measurements of sub-ps relativistic electron bunches were demonstrated for the first time at the linear accelerator FELIX, a free electron laser facility in the Netherlands [4]. Since then, several facilities have implemented this technique for characterizing electron bunches [5–12]. At the KIT storage ring KARA, far-field EO sampling measurements for the detection of CSR (Coherent Synchrotron Radiation) emitted by short electron bunches were pioneered in 2009 [13]. However, it was in 2013 when the first single-shot measurements based on near-field EO were performed in a storage ring [14].

Such measurements of the near-field in a storage ring are challenging due to the high repetition rate with a requirement for a single-shot non-destructive method without averaging. Another challenge is the deposited heat load on the EO crystal, especially on its coatings. The EOSD technique allows for the direct measurement of the Coulomb field, which gives additional insights into micro-bunching instabilities in storage rings [15].

While this method allows for single shot measurements of electron bunch profiles, the technological limitations posed by commercially available data acquisition systems (DAQs), e.g. low repetition rate of a few kHz, do not allow for the continuous study of the evolution of electron bunch dynamics. Hence, to overcome these challenges, a novel FPGA-based DAQ system combined with an ultra-fast line array camera was developed, KALYPSO [16, 17]. This line array camera offers a modular approach, allowing for the use of different micro-strip sensors based on Si, InGaAs, PbS, and PbSe depending on the required wavelength range. It has a maximum frame rate of 2.7 MHz, but a version operating at 12 MHz is currently being commissioned. In the further sections of this paper, the EOSD setup installed at KARA, the working principle of KALYPSO, data analysis and results from the experiment will be explained.

NEAR-FIELD EOSD SETUP

The measurements were carried out during single bunch operation at the storage ring KARA accelerator at a beam energy of 1.3 GeV. In order to study the micro-bunching instability, a low-alpha optics setup was used to compress the longitudinal bunch length to a few ps. The experimental setup is illustrated in Fig. 1.

First, chirped laser pulses generated by a self-built ytterbium-doped fiber laser (emitting around 1060 nm) are

* meghana.patil@kit.edu

RECOMMISSIONING OF THE CERN INJECTOR COMPLEX BEAM INSTRUMENTATION

R. Veness*, European Organisation for Nuclear Research (CERN), Geneva, Switzerland

Abstract

During the last two years, the CERN injector complex has been completely renovated with the aim of providing high intensity and smaller emittance beams to the LHC.

A new Linac providing H⁻ has been constructed and major upgrades in the Proton Synchrotrons (PS Booster ring, PS ring and Super PS ring) have been performed. A full suite of new beam diagnostics has been implemented and commissioned. This includes fast wire scanners, beam gas ionization monitors, quadrupolar pick-ups and diamond beam loss detectors. New radiation-hard beam position monitoring system was also successfully deployed in the SPS. This talk will present an overview of the performance of the newly built instruments.

INTRODUCTION

The LHC injectors are the heart of the CERN accelerator complex, producing and accelerating proton and ion beams upto LHC injection energies, as well as producing beams for fixed-target and other facilities on the site.

2019–2020 saw the second major shutdown of the whole CERN accelerator complex since the start of LHC operations, called LS2. This was required principally to complete the LHC Injectors Upgrade (LIU) project [1], with changes across the whole injection chain to produce brighter, more intense beams in preparation for the High-Luminosity LHC (HL-LHC) upgrade [2]. Table 1 shows the target beam parameters for this upgrade at the time of the instrumentation conceptual design in 2014.

Table 1: Achievable LIU Proton Beam Characteristics at Injection

Machine	PSB	PS	SPS	LHC
Kinematic energy [GeV]	0.16	2	25	449
Number of bunches	1/ring	29.6	1.5	650
Bunch separation [ns]	-	284	25	25
Bunch intensity [10^{10} p/b]	29.6	28.1	2.2	2
Transverse emittance [μ s]	1.5	1.6	1.7	1.9
Bunch length [ns]	650	205	4.2	1.65

The major change has been the construction of a new LINAC (LINAC4) which produces hydrogen ions (H⁻) at 160 MeV, rather than the 50 MeV protons from the previous LINAC2. These are stripped to p⁺ with carbon foils and accelerated in the existing Proton Synchrotron Booster (PSB) to 2 GeV. The existing Proton Synchrotron (PS) ring takes this new higher energy injection and accelerates into the

* raymond.veness@cern.ch

Super Proton Synchrotron (SPS) at 26 GeV which gives the final boost to 450 GeV for LHC injection.

In parallel with the LIU project, LS2 has also seen a significant consolidation project (called CONS) of the injector systems, taking advantage of the unprecedented access to machines, with the aim of ensuring reliable operations for the HL-LHC era. The injectors have been operating for, in some cases, more than 60 years and were historically separated by machine in instrument design and operations. One of the strategic goals of the Beam Instrumentation group was to use this major upgrade to standardize whole instrument groups across the injector complex, replacing mechanics, electronics and software where possible with the aims of decreasing commissioning time, improving maintainability and coping with reductions in expert manpower.

These LIU and CONS projects have led to a number of new in-vacuum beam instrumentation requirements, coming from the completely new LINAC4 and its injection into the PSB, instruments with a new specification due to the increased energies and intensities in the rings and for the consolidation of obsolete instruments, many of which were 30+ years old. The numbers are summarized in Table 2.

Table 2: In-vacuum Instruments Newly Commissioned Post-LS2

Machine / Complex	'New for old' Replacements	Additional Instruments
LINAC4	–	36
PSB	20	12
PS	9	2
SPS	4	3
LHC	3	1
ISOLDE / HIE	20	11
ELENA	–	31
TOTALS	56	96

A total of 152 in-vacuum instruments were built and newly commissioned post-LS2, plus some 348 new BLM channels. Not all of this work will be covered in this paper, in particular, there are two significant new installations, ELENA, the extra-low energy ion ring and an extension to the High Energy and Intensity isotope separator, HIE-ISOLDE, which have between them 42 new instruments. However, these are not part of the LHC injector chain so will be presented elsewhere. The paper will also cover the new acquisition system for SPS beam positioning system that has been designed, deployed and successfully commissioned with beam.

OVERVIEW OF RAON BEAM INSTRUMENTATION SYSTEM AND CONSTRUCTION STATUS OF THE LOW-ENERGY LINAC*

Y. S. Chung[†], H. J. Woo, G. D. Kim, J. W. Kwon, E. H. Lim¹,
Institute for Basic Science, Daejeon 3400, Korea,
¹also at Korea University, Sejong City, Korea

Abstract

RAON is a heavy ion accelerator for researches using Rare Isotopes (RI) as a major research facility in Korea. RAON uses both In-flight Fragmentation and Isotope Separation On-Line methods to provide various RI beams. The ultimate goal of the driver Linac of RAON is to accelerate uranium and proton beams up to 200 MeV/u and 600 MeV, with a maximum beam currents of 8.3 μA and 660 μA , respectively. After 9 years of RAON construction, commissioning of the low-energy Linac front-end system that consists of 14.5 GHz ion source, low energy beam transport, a 500 keV/u radio frequency quadrupole, and medium energy beam transport has been carried out since late 2020. And beam injection to the low-energy superconducting Linac is planned to start in December 2021. Here, we introduce RAON beam instrumentation and diagnostics systems as well as the construction status of the low-energy Linac.

INTRODUCTION

RAON is a heavy ion accelerator facility to accelerate both stable and rare isotope (RI) beams up to the power of 400 kW with an energy higher than 200 MeV/u [1]. This facility is planned to have both Isotope Separation On-Line (ISOL) and In-Flight (IF) fragmentation method [2,3] to produce RI beams. Using both ISOL and IF method, this facility can provide the high intensity and quality RI beams to the experiment.

RAON accelerator is composed of an injector system and the superconducting linear accelerator. An injector system accelerates a heavy ion beam to 500 keV/u and creates the desired bunch structure for injection into the superconducting Linac. The injector system comprises two electron cyclotron resonance ion sources (ECR-IS), a low energy beam transport (LEBT), a radio frequency quadrupole (RFQ), and a medium energy beam transport (MEBT). The superconducting linear accelerator is divided into two sections, the low-energy superconducting Linac (SCL3) and the high-energy superconducting Linac (SCL2). Two superconducting Linac sections are connected by a Post-accelerator to Driver Linac (P2DT) which consists of a charge stripper and 180 degree bending system.

This article is to document the construction status of RAON. Beam instrumentation system and the early results of beam commissioning of the injector system will also be briefly discussed.

* Work supported by the IBS/RISP funded by the Ministry of Science and ICT and the National Research Foundation of the Republic of Korea under Contract 2013M7A1A1075764

[†] yschung@ibs.re.kr

CONSTRUCTION STATUS OF RAON

Recently RAON construction project was evaluated thoroughly and it was decided that the whole construction project would be staged to two phases. The low-energy Linac section which consists of injector, SCL3 and low experimental system will be completed in the phase 1. ISOL system and high-energy experimental system are also constructed in the phase 1 as well. The high-energy superconducting Linac, SCL2 will be constructed in the 2nd phase launched in 2022.

The installation of injector system (14.5 GHz ECR-IS, LEBT, RFQ, and MEBT) was completed in October 2020, and immediately followed by the beam commissioning.

The superconducting cryomodule is being installed in the SCL3 tunnel since April 2020. As of August 2021, 22 QWR cryomodules, 13 HWR type-A (2 cavities) cryomodules, and 10 HWR type-B (4 cavities) cryomodules were installed in the SCL3 tunnel as shown in Fig. 1. The first beam injection to the SCL3 is planned to be in December 2021.

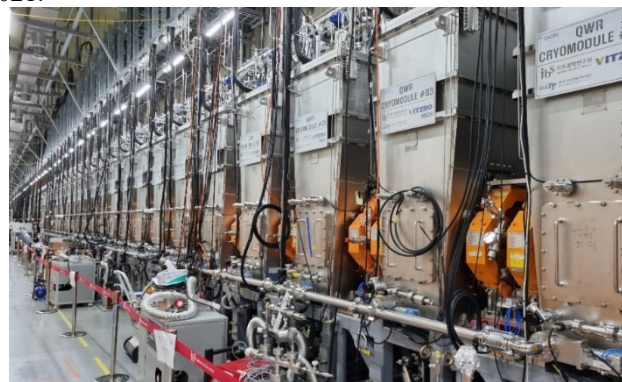


Figure 1: A photograph of SCL3 tunnel.

BEAM INSTRUMENTATION SYSTEM

For initial beam commissioning and component tuning, we will use $^{40}\text{Ar}^{9+}$ beam with $\sim 30 \mu\text{A}$, 100 μs pulse width, and a repetition rate of 1 Hz. Faraday Cup (FC), Wire Scanner (WS), Beam Viewer (BV), AC-Current Transformer (ACCT), and Beam Position Monitor (BPM) are properly used for beam tuning. During normal operation, on-line device such as BPM, ACCT, and Beam Loss Monitor (BLM) are used to monitor beam transport and acceleration function without destructing beam. The ACCT is to measure a beam current and transmission, and Differential Beam Current Measurement (DBCM) using ACCT networks is to primary detect beam loss in a certain section. Every BLM and the DBCM outputs will be linked to the RAON Fast Machine Protection System (MPS). Those on-

SUMMARY OF THE ARIES WORKSHOP ON MATERIALS AND ENGINEERING TECHNOLOGIES FOR PARTICLE ACCELERATOR BEAM DIAGNOSTIC INSTRUMENTS*

R. Veness, R. Jones, CERN, Geneva, Switzerland

U. Iriso, ALBA-CELLS Synchrotron, Cerdanyola del Vallès, Spain

G. Kube, K. Wittenburg, Deutsches Elektronen-Synchrotron DESY, Hamburg, Germany

P. Forck, GSI, Darmstadt, Germany

V. Schlott, PSI, Villigen, Switzerland

D. Eakins, University of Oxford, Oxford, UK

Abstract

ARIES is an EU-sponsored programme for accelerator research and innovation. An international workshop was held online as part of this programme in June 2021 on the topic of 'Materials and Engineering Technologies for Particle Accelerator Beam Diagnostic Instruments'. The aim of the workshop was to bring together instrument designers, experts and industry and research groups to review the state of the art in the field, present designs and discuss future challenges, whilst also developing and strengthening collaborations between groups. There were sessions covering 'Instrument design and operation', 'Novel materials and applications' and 'New technology and components' over the three half-days of the online meeting. This paper reviews the key topics presented at the workshop.

INTRODUCTION

Over the years 2017 to 2021 the EU-funded ARIES programme [1] is funding a number of topical meetings on specific areas of interest to the accelerator beam instrumentation community through the work-package ARIES-ADA [2,3]. The workshop [4] under consideration within this publication was targeted at design and technology of physical instruments – an area which receives relatively little coverage in the literature. It was originally planned as a face-to-face meeting at Wadham College, Oxford but was postponed and finally re-structured as a remote meeting in June 2021 with a programme of 20 talks, reduced from the original 32. This included four talks from European industry, demonstrating close links to science in the field.

There were 205 participants registered from around the globe resulting in lively online discussions performed in dedicated break-out rooms for each talk.

BEAM INSTRUMENT DESIGN, PRODUCTION & OPERATION

Thibaut Lefevre (CERN) opened the scientific part of the workshop introducing the current beam instrumentation highlights from CERN. He showed how the trends in particle physics accelerators, both on the energy/brightness frontier and in areas such as antimatter and rare isotope physics are creating new challenges for beam instrumentation. CERN has just completed a major upgrade to the LHC

injector complex. This required new instrument designs for highly radioactive environments, such as the BTV in the SPS synchrotron [5] as well as new simulation-driven designs for the mitigation of impedance heating. Designs for beam-intercepting devices such as screens and wire scanners have been upgraded with modern thermally resistant materials and faster movements. However, most innovation for current and future machines is related to non-invasive beam profile devices. New devices based on laser stripping of the LINAC4 H⁻ beams [6] and beam-gas ionisation in the Proton Synchrotron [7] are now operational at CERN whilst upgraded devices using synchrotron light and diffraction radiation are developed for the future High Luminosity LHC.

Gian Luca Orlandi (PSI) presented a collaboration between the Paul Scherrer Institut and Sincrotrone Trieste on electron beam lithography fabricated, freestanding wire scanners [8]. The project aims for minimally invasive electron beam profile measurements with sub-micron resolution. Applications are for FEL user operation and ultra-high precision, transverse beam diagnostics at novel laser and plasma driven accelerators. PSI produced 800 nm and 500 nm wide Au wires of 2 μm thickness and 2 mm beam clearance. FERMI manufactured a set of wires consisting of 3 μm thick sandwiches made of Au (1 μm) and Si₃N₄ (2 μm) and a Ti (20 nm) middle layer with a width of 0.7 μm , 0.8 μm , 1 μm and 2 μm , respectively [9, 10]. Beam tests were successfully conducted at SwissFEL, where a 300 MeV, low charge (1 pC), and low emittance ($\epsilon_y \sim 55$ nm) beam can be focused to transverse beam sizes of < 500 nm, see Fig. 1 and [11].

William Andrezza (CERN) presented a new generation of fast wire scanners built for the LHC Injector Upgrade project at CERN and the European Spallation Source in Lund, Sweden [12]. The high power beams require a wide

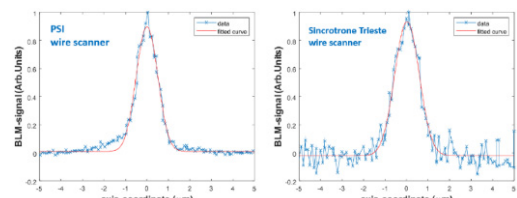


Figure 1: Vertical beam profiles at SwissFEL taken with single shot data acquisitions. The measured beam sizes are 434 ± 7 nm (PSI wire scanner) and 443 ± 33 nm (Sincrotrone Trieste wire scanner).

* This project has received funding from the European Union's Horizon 2020 Research and Innovation programme under Grant Agreement No 730871.

AN EXPERIMENTAL COMPARISON OF SINGLE CRYSTAL CVD DIAMOND AND 4H-SiC SYNCHROTRON X-RAY BEAM DIAGNOSTICS

C. Houghton*, C. Bloomer, L. Bobb, Diamond Light Source, OX11 0DE, Didcot, United Kingdom

Abstract

As synchrotron beamlines increasingly use micro-focus techniques with detectors sampling at kHz rates, the need for real-time monitoring of the beam position at similar bandwidths is vital. Commercially available single-crystal CVD diamond X-ray diagnostics are well established as excellent non-destructive monitors for synchrotron X-ray beamlines. Silicon carbide (4H-SiC) X-ray beam position monitors (XBPMs) are a recent development with the potential to provide the same benefits as their diamond counterparts with larger usable apertures and lower cost. At Diamond Light Source a comparison between single-crystal CVD diamond and 4H-SiC XBPMs has been carried out. The sc-diamond and 4H-SiC beam position monitors are mounted in-line along the beam path, so that synchronous kHz measurements of the synchrotron X-ray beam motion can be measured. Several tests of the two position monitors performance are presented: comparing kHz beam position measurements from the detectors, temporal response, and signal uniformity across the face of the detectors. Each test is performed with varying bias voltages applied to the detectors. A discussion of the benefits and limitations of 4H-SiC and diamond detectors is included.

INTRODUCTION

With the recent upgrades to synchrotron beamline optics that allow for sub-micron X-ray beam sizes at the sample point, and beamline detectors with operating frequencies in the kHz range, the need for accurate beam position monitoring at similar bandwidths is essential. Destructive X-ray beam position diagnostics such as fluorescent screens can not be used during experimental data collection as the transmission of X-rays through the materials used for these screens is low. For example 50 μm of LuAG scintillator has a transmission of just 7% at 9 keV [1]. Modern beamlines require real-time non-destructive beam position monitoring to ensure the micro-focus beam is stable throughout any data collection. This demand led to the research and development of diamond X-ray Beam Position Monitors (XBPMs) due to their excellent transparency, radiation hardness, and thermal conductivity.

Early experiments with polycrystalline diamond [2,3] have led to modern, commercially available single-crystal chemical vapour deposition (scCVD) diamond XBPMs with beam position resolutions of a few 10 nm [4]. These XBPMs perform as excellent non-destructive monitors for synchrotron X-ray beamlines.

Silicon carbide (4H-SiC)¹ XBPMs are a more recent development that have the potential to provide the same benefits as their diamond counterparts with the added benefit of larger usable apertures and potentially lower cost [5]. In this paper a direct comparison of these two devices is conducted on a synchrotron X-ray beamline.

EXPERIMENTAL SET-UP

The experiment was conducted on the I18 [6] beamline at Diamond Light Source. The two XBPMs used in this experiment were a 10.5 μm thick 4H-SiC detector and a 50 μm thick single-crystal CVD diamond, referred to as sc-diamond. The thicknesses of these devices were chosen such that the two detector plates have similar X-ray transmission at typical synchrotron beamline photon energies. For example, the following experiments were conducted at 9 keV, where transmission is 95% and 90% for the sc-diamond and 4H-SiC XBPM respectively [1].

As shown in Fig. 1, the 4H-SiC detector was mounted in front of the sc-diamond as the sc-diamond XBPM has a smaller transparent aperture. These were placed in a nitro-

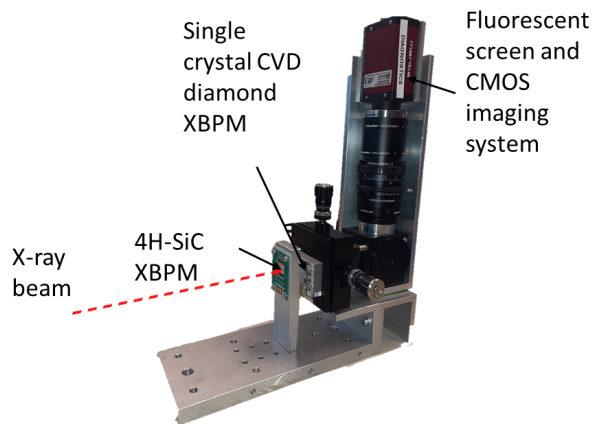


Figure 1: Image of the mounting stage used for the direct comparison of a 4H-SiC XBPM with a sc-diamond XBPM, complete with a CMOS camera imaging system.

gen environment. Behind both the XBPMs was a fluorescent screen CMOS imaging system, used to capture beam images at 700 Hz for independent verification of beam motion. The three devices were secured to a X-Y motion stage just upstream of the sample point, allowing for the X-ray beam to be moved across the surface of the XBPMs. The applied bias voltages and the flux, by use of filters, could be changed throughout the experiment. Generally a 25 μm Al filter was

* claire.houghton@diamond.ac.uk

¹ 4H-SiC refers to the polytype of silicon carbide

SOLEIL UPGRADE PROJECT AND FORESEEN BEAM INSTRUMENTATION

N. Hubert, A. Bence, R. Broucquart, M. El-Ajjouri, M. Labat, D. Pédeau, J-P. Ricaud
Synchrotron SOLEIL, Gif-Sur-Yvette, France

Abstract

SOLEIL Synchrotron has an upgrade plan to replace its storage ring by a new one based on multi-bend (7/4BA) achromat lattice. The Conceptual Design Report (CDR) has been published recently and the Technical Design Report (TDR) phase should be finished for the end of 2023.

For the beam instrumentation, most of the equipment will have to be replaced, to overcome cases of electronics obsolescence and to fulfil the new tight requirements. Among them, the most challenging ones are the micron resolution transverse beam size measurement, the beam position monitoring and the stability feedbacks. The present machine will be used to validate some prototypes and it is planned to upgrade part of the diagnostics ahead of the dark period to speed-up the commissioning of the new storage ring.

This paper presents the diagnostics systems that are foreseen for the SOLEIL upgrade project.

SOLEIL UPGRADE

SOLEIL Synchrotron is a third-generation light source in operation since 2006. The 2.75 GeV storage ring based on a Double-Bend achromat (DBA) lattice provides a broad spectrum of photon ranging from the far infra-red to hard X-rays to 29 beamlines.

SOLEIL is working on an upgrade project plan based on Multi-Bend Achromat (MBA) lattice. The Conceptual Design Report (CDR) has been published [1] and the Technical Design Report (TDR) phase has started recently. The CDR reference lattice is based on 20 non-standard alternating 7BA and 4BA Higher-Order Achromat (HOA) cells reaching a horizontal natural emittance of about 80 pm.rad at the energy of 2.75 GeV and equal horizontal and vertical β -functions of between 1.5 to 1.0 m at the center of all Insertion Device (ID) straight sections [2]. Figure 1 compares the arrangement of the magnets in the 7BA cell of this new lattice and the one in the Double Bend Achromat (DBA) cell of the existing machine.

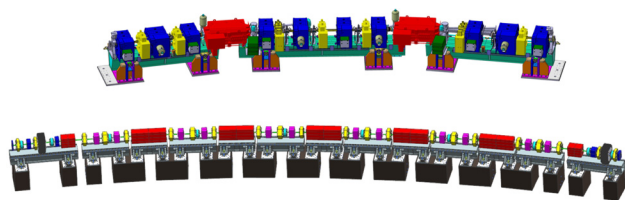


Figure 1: Engineering layout of the 7BA cell type of the new MBA-ARC (bottom) and the SOLEIL DBA-ARC cell (top).

The new machine implementation should minimize the impact on the ID source point position and reuse the existing tunnels and their radiation shielding walls [3].

The achieved natural horizontal emittance is about 50 times smaller than that of the existing SR (Fig. 2) and the effective emittance calculated in the straight section source points would be about 100 times smaller than the average value in those of the current SR.

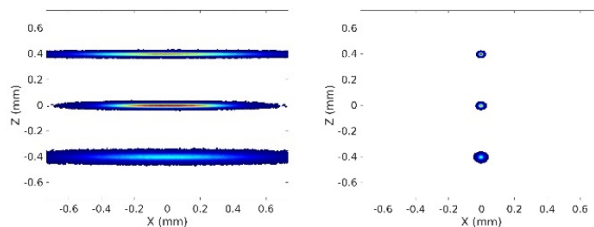


Figure 2: Comparison of the transverse beam profiles of the present SOLEIL (left) for the three straight sections with 1% coupling and SOLEIL Upgrade CDR reference lattice (right) with 50 pm.rad emittance in each plane.

With appropriate low gap IDs, this emittance reduction will improve the brilliance and coherent flux by more than two order of magnitudes [2].

FORESEEN BEAM INSTRUMENTATION

Most of the SOLEIL present diagnostics systems will have to be renewed to fit the new technical specifications of the upgrade (Table 1), but also to overcome obsolescence of the electronics.

Table 1: Current and Future Beam and Machine Parameters

	SOLEIL	SOLEIL-Upgrade
H. Emit. [pm.rad]	4000	80
V. Emit. [pm.rad]	20.3	80
H. Beam Size (min value at source point) [$\mu\text{m rms}$]	180	7.4
V. Beam Size (min value at source point) [$\mu\text{m rms}$]	8	2.8
BPM Aperture [mm]	84x25	16
Pos. and Angle Stability (wrt size and divergence)	10%	2-3%
Orbit Feedback Efficiency	200 Hz	1 kHz

CONCEPTUAL DESIGN OVERVIEW OF THE ELECTRON ION COLLIDER INSTRUMENTATION*

D. M. Gassner[†], J. Bellon, M. Blaskiewicz, A. Blednykh, K. A. Drees, T. Hayes, C. Hetzel, D. Holmes, R. Hulsart, P. Inacker, C. Liu, R. Michnoff, M. Minty, C. Montag, D. Padrazo Jr, M. Paniccia, V. Ptitsyn, V. Ranjbar, M. Sangroula, T. Shaftan, P. Thieberger, E. Wang, F. Willeke
 Brookhaven National Laboratory, Upton, NY, USA
 L. Dalesio, Osprey DCS LLC, Ocean City, USA

Abstract

A new high-luminosity Electron Ion Collider (EIC) is being developed at Brookhaven National Laboratory (BNL). The conceptual design [1] has recently been completed. The EIC will be realized in the existing RHIC facility. In addition to improving the existing hadron storage ring instrumentation, new electron accelerators that include a 350 keV gun, 400 MeV Linac, a rapid-cycling synchrotron, an electron storage ring, and a strong hadron cooling facility will all have new instrumentation systems. An overview of the conceptual design of the beam instrumentation will be presented.

INTRODUCTION

The EIC [1, 2] will be realized in the existing Relativistic Heavy Ion Collider (RHIC) facility, the primary additions will be a chain of electron accelerators and systems that will reside inside the RHIC tunnel and service buildings. The well-established beam parameters of the present RHIC facility are close to what is required for the highest performance of the EIC, except for the total hadron beam current which will be increased by a factor of approximately three by increasing the number of bunches. A strong hadron cooling facility will utilize 100 mA of 150 MeV electrons to reduce the hadron beam emittance and control emittance growth due to intrabeam scattering. Polarized electrons will be generated in a new 350 keV DC gun from a strained superlattice GaAs photocathode and will be accelerated to 400 MeV in an S-band normal conducting Linac. The 3.8 km rapid cycling synchrotron (RCS) then increases the electron energy to 5, 10 or 18 GeV in 100 - 200 ms, then fills the electron storage ring (ESR). The 3.8 km ESR will provide ~70% polarized electron beams at 5, 10 or 18 GeV for collisions with the polarized protons or heavy ions in the hadron storage ring (HSR) at 41, 100 and 275 GeV. To maintain high spin polarization, each of the ESR electron bunches will be replaced every one to three minutes.

ELECTRON PRE-INJECTOR LINAC

Beam instrumentation (shown in Table 1) for the 350 keV DC gun and the 400 MeV electron LINAC [3] will be designed to measure beam properties at a repetition frequency of 1 Hz with single-bunch charge ranging from

100 pC to the design charge of 10 nC per bunch. Beam position monitors will measure the trajectory of the beam that has a bunch length range of 2 ns to 4.5 ps with better than 100 μ m resolution. A pair of selected BPMs will provide time-of-flight measurements to determine the beam energy.

Table 1: Electron Pre-Injector Instrumentation

Type	Quantity
Beam Position Monitors	9
Beam Loss Monitors	5
Fast Current transformers	1
Integrating Current transformers	7
Faraday Cups	4
YAG/OTR Screen profile monitors	9
Longitudinal Profile Monitors	2
Mott Polarimeters	2
Slit scanner	1
Wire scanners	7

Transverse profile monitors using plunging YAG/OTR screens will be located throughout the beamlines. Slit scanners and wire scanners will be used to measure beam emittance. Longitudinal bunch profiles will be measured with a plunging radiator at low energy, and using synchrotron light emitted downstream of a bending magnet at 400 MeV, with a shared streak camera. Relative bunch lengths will be non-destructively measured using a ceramic gap with waveguide-coupled fast diodes downstream of the 4.5 ps bunching section. Mott polarimeters will be installed at the cathode preparation system (100 eV) and in the first diagnostic beamline upstream of the Linac (350 keV). Scintillators coupled to photo-multiplier tubes (PMTs) and/or Geiger counters, used to detect X-ray and gamma ray, will be placed after the gun, after the first dipole, in the bunching sections and between the acceleration sections to localize beam loss. Additionally, a long optical-fiber beam loss monitor will be used between the gun and the entrance of the Linac. All EIC current and charge monitors (DCCT, ICT, FCT) will be commercially provided [4].

RAPID CYCLING SYNCHROTRON

The EIC RCS [5] will accelerate two batches of four 7 nC bunches in adjacent buckets that are 1.69 ns apart that will subsequently be merged into two 28 nC electron bunches that are 2.43 μ s apart by means of two steps of pairwise merging on a 1 GeV porch using the 591 MHz,

* Work supported by Brookhaven Science Associates, LLC under Contract No. DE-SC0012704 with the U.S. Department of Energy.

[†] gassner@bnl.gov

THE FRASCATI BEAM TEST FACILITY NEW LINE: FROM DESIGN TO BEAM COMMISSIONING

B. Buonomo, F. Cardelli, C. Di Giulio*, D. Di Giovenale, L. G. Foggetta,
on behalf of the BTF Upgrade team[†], INFN-LNF, Frascati, Italy

Abstract

The request of beam time for long-time experiments and contemporary the need to provide beam time to the detector developers community, drive the INFN to invest in the commissioning of a new beam line test facility. In this work we describe the necessary steps followed from the design to the commissioning of the new beam line in the Frascati Beam Test Facility.

INTRODUCTION

In the development of the detectors for the high energy physics (HEP) and astro-particles physics, the test beam and irradiation facilities are the key enabling infrastructures.

From 2005 the Beam-Test Facility (BTF) of the DAΦNE accelerator complex in the Frascati laboratory of the Italian National Institute of Nuclear Physics (INFN) has gained an important role in the European infrastructures devoted to the development and testing of particle detectors [1–3].

The presented proposal in 2016 aimed at improving the performance of the facility extending the range of application for the LINAC beam extracted to the BTF lines, in the directions of hosting fundamental physics long term experiments [4] and providing electron irradiation also for industrial users.

To achieve this, it was requested to double the BTF beam-lines, in order to cope with the significant increase of users due to the much wider range of applications.

The original BTF line is in operation since 2002 [5, 6], and from 2004 operates in opportunistic mode [7] during the running of the DAΦNE electron-positron collider. The full LINAC beam can also be extracted towards the BTF line without being intercepted by the target (within the 3×10^{10} particles/s limit established radio-protection rules for the current shielding configuration).

In the next paragraphs the steps from the Conceptual Design Report presented in 2016 [8] to the commissioning of the new line are described. The issues necessary to be discussed for the reconstruction of the first line of the BTF (BTF1) for a long term experiment and the processing dif-

iculties of the commissioning of the second line of BTF (BTF2) are described.

THE DESIGN OF THE NEW BTF LINE

The main requirements from the users concerning the detector testing beam-test activities can be easily summarized:

- Good quality beam, in particular from the point of view of beam size, divergence and background, down to the low end of the BTF energy range, i.e., few tens of MeV. This requirement is particularly difficult to match if the setup is in air, downstream of the exit window.
- Extending the energy range towards higher energies: tracking and efficiency studies suffer from the Coulomb scattering of electrons, which scales as $1/p$. Higher energies are also very useful for extending the range for the calibration of calorimeters.

The Beam-Test Facility (BTF) is an extraction and transport line, to produce electrons or positrons in a wide range of intensity, energy, beam spot dimensions and divergence, starting from the primary beam of the DAΦNE LINAC. The LINAC accelerate 50 pulses/s, one transported in the spectrometer, the other can be either transported to a small ring for emittance damping (and from there injected into the collider rings), or to the BTF line, by means of pulsed dipoles. A variable depth target (from 1.7 to 2.3 X_0) spreads the momentum distribution of the incoming beam, then secondary electrons (or positrons) are momentum selected by means of a 45 degree bending dipole and collimators (in the horizontal plane). The beam intensity is thus greatly reduced, depending on the chosen secondary beam energy central value (from about 30 MeV up to almost the primary beam energy) and spread (typically better than 1 percent at higher energy, depending on the collimators settings). The beam is then transported to the experimental hall and focused by means of two quadrupole FODO doublets. The layout of the beam selection and transport line is shown in Fig. 1, together with the shielded experimental area.

The original idea for the new layout consists in a beam-splitting dipole, wrapped around a double-exit pipe, that can drive beam pulses from the upstream BTF beam-line alternatively to the two new lines [9]. In case, the dipole can be connected to a pulsed power supply for a fast switch between the two lines. The first line drives the beam in the existing experimental hall (“BTF 1”), also profiting of the existing concrete block-house, while the second will transport the beam, with three additional dipoles, in the area previously used as BTF control room (“BTF 2”), with few civil engineering work. A complete optimization of the new lines optics has been performed, in order to define the

* claudio.digiulio@lnf.infn.it

[†] D. Alesini, M. Belli, B. Bolli, B. Buonomo, S. Cantarella, F. Cardelli, P. Carinci, G. Catuscielli, R. Ceccarelli, A. Cecchinelli, O. Cerafogli, P. Ciuffetti, M. Chiti, R. Clementi, O. Coiro, D. Di Giovenale, C. Di Giulio, E. Di Pasquale, R. Donghia, A. Esposito, O. Frasciello, L. G. Foggetta, F. Galletti, A. Ghigo, S. Incremona, F. Iungo, S. Lauciani, A. Liedl, V. Lollo, R. Mascio, M. Martini, A. Michelotti, M. Paris, L. Pellegrino, G. Piermarini, F. Putino, L. Sabbatini, F. Sardone, G. Sensolini, A. Stecchi, R. Ricci, L. A. Rossi, U. Rotundo, A. Stella, S. Strabioli, A. Vannozzi, R. Zarlenga (INFN Laboratori Nazionali di Frascati); P. Valente (INFN Roma)

BEAM POSITION MONITOR FOR MYRRHA 17-100 MeV SECTION*

M. Ben Abdillah[†], F. Fournier, University Paris-Saclay, CNRS/IN2P3, IJClab, France

Abstract

MYRRHA (Multi-Purpose Hybrid Research Reactor for High-Tech Applications) aims to demonstrate the feasibility of high-level nuclear waste transmutation at industrial scale. MYRRHA Facility aims to accelerate 4 mA proton beam up to 600 MeV. The accurate tuning of LINAC is essential for the operation of MYRRHA and requires measurement of the beam transverse position and shape, the phase of the beam with respect to the radiofrequency voltage with the help of Beam Position Monitor (BPM) system. MINERVA is the first phase of MYRRHA. It includes several sections allowing beam acceleration up to 100 MeV. A BPM prototype was realized for the single spoke section (17 MeV-100 MeV). This paper addresses the design, realization, and calibration of this BPMs and its associated electronics. The characterization of the beam shape is performed by means of a test bench allowing a position mapping with a resolution of 0.02 mm.

GENERAL DESCRIPTION OF MYRRHA

MYRRHA is a high power proton accelerator with strongly enhanced reliability performances. The conceptual design is on-going for more than 15 years. The adopted LINAC scheme to fulfil the reliability goal is based on 2 distinct sections, as illustrated in Fig. 1

The first phase (MINERVA) currently ongoing until 2026 aims at demonstrating the fault compensation strategy for the 600 MeV linac on a 100 MeV linac. The MYRRHA phase 1 accelerator will deliver a 100 MeV, 4 mA CW proton beam. The accelerated beam will be sent to a PTF (Proton Target Facility) for various applications including fusion research and isotope production.

MINERVA addresses the topics that have been identified as priority ones to successfully pursue the research, design and development of the MYRRHA accelerator and prepare for its actual construction. Among the topics, beam characterization would deliver data of fundamental importance in all beam dynamics simulation tools.

Beam Position Monitor (BPM) is a non-destructive beam diagnostic system, it measures beam position, phase shift regarding the accelerating signal and also gives an indication on the beam transverse shape. IJClab is in charge of the realization of a BPM prototype in order to contribute to the characterization of the beam along 17-100 MeV section that accelerates the beam from 17 MeV to 100 MeV. This document details the steps of design, fabrication and qualification of this prototype.

GENERAL DESCRIPTION OF BPM

BPMs allow measuring the vertical and horizontal coordinates of the center of gravity of the beam position and

assessing the transverse size of the beam. Capacitive BPM is used. Each BPM is equipped with 4 probes formed by a sealed 50 Ohm feedthroughs attached to an electrode. The probes (feedthrough + electrode) should be as identical as possible and they should be symmetrical regarding the center of the BPM.

BPM must meet a set of constraints (vacuum, magnetism, positioning, steaming, resistance to ionizing radiation) in order to ensure its integration into the machine.

The beam induces electrical signal on each electrode, beam position, transverse shape and energy are induced from these electrical signals. The electronic module provides the following information by processing the electrical signals delivered by the electrodes:

- The horizontal and vertical position of the center of gravity of the beam.
- The phase of the beam with respect to the main Radio Frequency reference signal. Beam velocity and energy are processed from this measurement.
- Beam Ellipticity figuring in the second order moment of the beam transverse distribution.

BPM SPECIFICATIONS

Table 1 summarizes beam properties and BPM specifications for 17-100 MeV section of the MINERVA project.

- The precision on the position should be less than 100 μm on both axes. The phase shift relative to the accelerating signal should be measured with a precision less than 1 degree. The beam ellipticity should be less than 1.6 mm^2 for circular beam while it should be measured within 20% precision for elliptical beams.

Table 1: Beam Parameters and BPM Specifications

Parameter	Range	Precision
Energy E	17 MeV- 100 MeV	
Current I	0.1 mA-4 mA	
Duty cycle	2.10^{-4} to 0.125	
Bunch length @17 MeV	15° ; 230 ps	
Bunch length @100 MeV	5° ; 80 ps	
F_{acc}	176.1 MHz	
Beam pipe	28 mm	
Measured Position	± 5 mm	100 μm
Measured Phase	360degrees	1degree
Measured Ellipticity	± 5 mm	Max (1.6 mm^2 ;20%)

* Work supported by SCK-CEN

[†] sidi-mohammed.ben-abdillah@ijclab.in2p3.fr

DESIGN OF A CAVITY BEAM POSITION MONITOR FOR THE FLASH 2020+ UNDULATOR INTERSECTION PROJECT AT DESY

D. Lipka*, Deutsches Elektronen-Synchrotron DESY, Hamburg, Germany

Abstract

The FLASH 1 beamline at DESY will be upgraded from fixed to variable gap undulators in the next years. For this the vacuum beamline has to be adapted. This reduces the inner diameter compared to the existing chamber. The vacuum components should fit to the new dimension to minimize transitions and therefore reduce wakefields which could interact with the electron beam and disturb the SASE effect. The electron beam position in the intersection of the undulators should be detected with a high resolution and a large charge dynamic range. Cavity BPMs are known to fulfill these requirements. The existing design with 10 mm inner diameter for the European XFEL is reduced to 6 mm. Additional improvements are: widening of the dipole resonator waveguide to adapt to the dipole mode and antenna transmission. The resonator frequency of 3.3 GHz and loaded quality factor of 70 are maintained to use electronic synergies to other projects. The design considerations and simulation results of the cavity BPM are presented.

MOTIVATION

The superconducting free-electron laser user facility FLASH [1] at DESY in Hamburg routinely delivers several thousand high brilliance XUV and soft X-ray photon pulses per second. The user facility FLASH is in operation since 2005 and since 2014 the bunch train from the superconducting linac can be split between the original FLASH 1 undulator beamline and a new second beamline FLASH 2. In 2016 a significant Mid Term Refurbishment Program was started for FLASH. Its program will persist for the next years. As part of the DESY strategy process DESY 2030 [2] that was initiated 2016, a second substantial upgrade, FLASH 2020+ was proposed [3]. In April 2019 the internal conceptual design report (CDR) for FLASH 2020+ [4] was finalized. The mid and long term upgrades are described in [5].

There are several key aspects of the upgrade in 2024: the important one is in order to enhance the independence of the two beamlines and their over all operability, FLASH 1 needs to be equipped with variable gap undulators. To be able to close the undulators further a smaller inner vacuum chamber is proposed. This implies a reduction of the available Cavity Beam Position Monitor (CBPM) design from the European XFEL with an inner vacuum diameter of 10 mm [6] to 6 mm. The reduction of the diameter minimizes transition of the vacuum boundaries and therefore the impact of reduce wakefields which would interact with the electron beam and disturb the SASE production. Many institutes are developing such CBPM [7–19] to provide the beam position with the best resolution which consists of a dipole and a reference

resonator. In this contribution the design considerations of both resonators are described.

DESIGN

For the general design the resonance frequency and quality factor have to be chosen for the dipole and reference resonator of the CBPM. Both parameters should be similar for the dipole and reference resonator to simplify the signal processing. Since the inner tube diameter is 6 mm with a cut-off frequency of 29 GHz this high cut-off this is not a limitation. To provide synergies for the already developed electronics the resonance frequency of $f = 3.3$ GHz is defined. The repetitive bunch frequency of 1 MHz allow only for a fast decaying signal, therefore a low loaded quality factor of $Q_L = 70$ is chosen which results in a bandwidth of 47 MHz. This allows a monitor production in stainless steel. The basic design is depicted from the SACLA facility [7] which was modified for the European XFEL [6]; in addition a design for the SINBAD accelerator with 34 mm diameter was developed in 2018 [19]. The quality factor and resonance frequency of the new design for FLASH 1 are similar to the European XFEL and SINBAD CBPMs for synergy but with other tube diameters and resonator thicknesses.

Dipole Resonator

The TM_{11} mode of the dipole resonator provides a signal proportional to beam offset and charge. The amplitude sensitivity is $S = \pi f \sqrt{\frac{Z}{Q_{ext}}} \left(\frac{R}{Q}\right)$ [19, 20], with the line impedance $Z = 50 \Omega$ and the normalized shunt impedance $\left(\frac{R}{Q}\right)$ and the external quality factor Q_{ext} . The antenna position defines the value of the external quality factor; a small value dominates the loaded quality factor because $\frac{1}{Q_L} = \frac{1}{Q_{ext}} + \frac{1}{Q_0}$ with Q_0 the internal quality factor (which is still relative large compared to Q_{ext} for stainless steel) and therefore increases the sensitivity too. To obtain a larger sensitivity the normalized shunt impedance can be increased by using a large resonator thickness l because $\left(\frac{R}{Q}\right) \propto l$ [21], in this design $l = 5$ mm is applied. The Eigenmode solver of the simulation tool CST [22] is used to design and investigate the resonator properties. The resulting geometry is shown in Figures 1 and 2.

The resonator has a kink to decrease the resonator diameter which bends the dipole field. This is an advantage for a smaller overall monitor transverse size. The dipole field is propagating into the four slots where the dominating monopole field TM_{01} can not propagate due to the geometry and is therefore in comparison with the dipole signal negligible at the antenna positions [23]. The thickness of the slots are increased compared to [6, 19] to provide the low external quality factor shown in Table 1.

* dirk.lipka@desy.de

RESEARCH ON THE OPTIMAL AMPLITUDE EXTRACTION ALGORITHM FOR CAVITY BPM*

J. Chen[†], S. S. Cao, Y. B. Leng[#], T. Wu, Y. M. Zhou, B. Gao
Shanghai Advanced Research Institute, CAS, Shanghai, China

Abstract

The wake field of different modes of cavity BPM carries different bunch information, the amplitude and phase of the signals of different modes can be extracted through the signal processing method to obtain the characteristic parameters of the source bunch. In the application of bunch charge and position measurement, the accurate amplitude extraction method for cavity BPM signal is the primary issue to be considered when designing the data acquisition and processing system. In this paper, through theoretical analysis and numerical simulation, it is proved that the optimal algorithm of amplitude extraction for CBPM exists, and the dependence between the data processing window size and the decay time of the cavity BPM under the optimal design is given. In addition, the relationship between the optimized amplitude extraction uncertainty and the noise-to-signal ratio, sampling rate of data acquisition and processing system, and the decay time of the cavity BPM is also proposed, which can also provide clear guidance for the design and optimization of the CBPM system.

INTRODUCTION

Cavity BPM (CBPM) adopting a resonant cavity structure and using the characteristic modes excited by the electron beam to measure the beam parameters, has the advantage of high resolution and is widely used in FEL facilities and Linear Colliders. A typical CBPM system is composed of a cavity pickup, a radio frequency signal conditioning front end, and a data acquisition and processing electronic. The factors that affect system performance mainly include the signal-to-noise ratio (SNR) of the cavity pickup, crosstalk between different modes, beam trajectory with a finite angle, noise figure of RF front-end, performance of Analog to Digital Converter (ADC) and digital signal processing algorithms.

For cavity BPM pickups, it can be divided into low-Q (Quality factor) and high-Q from the Q value of the pickup. In theory, as long as the ADC sampling rate and number of bits are high enough, the multi-point sampling of the signal can always obtain a processing gain greater than 1. Therefore, the best signal acquisition and processing method must be the amplitude and phase extraction after full waveform sampling.

However, in the actual measurement system, due to the limitation of sampling rate and effective number of bits of

ADC, when the Q value is exceedingly small, the duration time of signal is short, the data acquisition and processing schemes mostly choose analog IQ demodulation combined with peak sampling of phase locked. However, since this paper discusses general rules, technical limitations of ADC are not specifically considered.

As for the high-Q cavity BPM system, in terms of data acquisition and processing methods, the conventional method is to sample and quantize the full waveform of the IF signal conditioned by the RF front-end. And then the amplitude and phase information were extracted in the digital domain by the algorithm such as digital down-conversion (DDC), time-domain fitting, harmonic analysis, etc. In general, all waveform data are used in digital signal processing, and there is no systematic research on the optimal signal processing method. In addition, for the design and optimization of the system, there is also have no clear guiding formula for the parameters selection among the various components of the CBPM system.

In this paper, based on theoretical analysis and numerical simulation, the optimal algorithm of amplitude extraction for CBPM is discussed, and the guidance formula about the optimized amplitude extraction uncertainty and the parameters of CBPM system is also studied.

THEORETICAL ANALYSIS

The output signal of the cavity BPM can be expressed by the Eq. (1):

$$V_{port}(t) = A \cdot e^{-\frac{t}{\tau}} \cdot \sin(\omega t + \varphi). \quad (1)$$

So, the envelope of the signal can be expressed by:

$$y_{sig} = A \cdot e^{-t/\tau}. \quad (2)$$

Assume the white gaussian noise level of the signal can be expressed by:

$$y_n = A \cdot \sigma. \quad (3)$$

Where σ represents the relative noise-to-signal ratio.

The number of data points of the signal waveform after being quantized by ADC is represented by N , and the sampling rate of ADC is represented by F_s , when taking N points for digital signal processing, the total signal can be written as:

$$y_{signal} = \sum_{n=1}^N A \cdot e^{-\frac{n}{F_s \cdot \tau}}. \quad (4)$$

*Work supported by National Natural Science Foundation of China (2016YFA0401903) and Ten Thousand Talent Program and Chinese Academy of Sciences Key Technology Talent Program

[†] chenjian@zjlab.org.cn

[#] lengyongbin@sinap.ac.cn

OBSERVATION OF WAKEFIELD EFFECTS WITH WIDEBAND FEEDTHROUGH-BPM AT THE POSITRON CAPTURE SECTION OF THE SuperKEKB INJECTOR LINAC

M. A. Rehman*, T. Suwada

High Energy Accelerator Research Organization (KEK), Tsukuba, Japan

Abstract

At the SuperKEKB injector linac, positrons are generated by striking electron beam at tungsten target. The secondary electrons are also produced during positron creation and accelerated in the positron capture section. A new wideband feedthrough-beam position monitor (BPM) system was developed for synchronous detection of secondary produced e^- and e^+ beams with temporal separation of about 180 ps. When e^+/e^- bunches pass through the accelerating structure or vacuum duct of different radius, they generate wakefields. These wakefields can be directly observed with the feedthrough-BPM. A simulation study has also been carried to validate the observed wakefield effects with the feedthrough-BPM. The effects of wakefields on beam parameters will be reported in this paper.

INTRODUCTION

The SuperKEKB (SKEKB) [1, 2] is an electron and positron collider with asymmetric energies to study CP violation in B mesons and also to search for new physics beyond the Standard Model, with the target luminosity of $8 \times 10^{35} \text{ cm}^{-2}\text{s}^{-1}$, which is 40 time higher than its predecessor KEKB [3]. The SKEKB collider consists of e^- and e^+ rings of energy 7 GeV (HER) and 4 GeV (LER) with the stored beam current of 2.6 A and 3.6 A, respectively.

The SKEKB injector linac generates e^-/e^+ bunches of 5 nC and 4 nC to directly inject into HER and LER, respectively, at their designed energy. The low emittance e^- beam is produced by a RF-photocathode gun. The e^+ beam is produced by striking the e^- beam of energy 3.5 GeV and bunch charge of 10 nC at a tungsten target. The positrons are generated as secondary particles and have a large transverse emittance. To capture a large amount of positrons, a pulsed solenoid called flux concentrator and a large aperture S-band (LAS) accelerating structures [4] are placed in the downstream of the e^+ target. The secondary electrons are also produced in a similar amount of charges during the e^+ creation process and accelerated in the capture section. Because of phase slipping process in the capture section, the time interval between secondary produced e^- and e^+ bunches is about only 135 ps under nominal operation.

Due to low frequency response and high-frequency cable losses, conventional beam monitors, i.e., stripline beam position monitors, are difficult to detect such closely spaced and opposite polarities bunches in the capture section. For this reason in the past capture section there were no beam moni-

toring devices. As a result of a lack of information about the beam properties such as transverse positions, bunch lengths and, bunch charges, the e^+ beam suffers some amounts of beam loss after the capture section.

Therefore, a new wideband feedthrough type BPM was developed to overcome the above-mentioned challenges. This new monitor can synchronously detect e^- and e^+ bunch properties, i.e., transverse positions, bunch lengths, time interval, and bunch charges. It provides an opportunity to enhance positron beam transport through the capture section. The detailed analysis of bunch properties is reported in [5,6]. The modal analysis of electromagnetic coupling between SMA-feedthrough and beam is described in [7]. The effect of wakefields induced by the passage of e^-/e^+ bunches through the end of the accelerating structure on the BPM signal will be discussed in detail in this report.

WIDEBAND FEEDTHROUGH BEAM POSITION MONITOR

The feedthrough-BPM consists of a vacuum pipe of length 431 mm which has an inner diameter of 38 mm, four SMA-type feedthroughs having inner conductor made of Kovar with $\pi/2$ rotational symmetry are installed at the upstream direction of the vacuum pipe. The diameter of the central connector pin of feedthroughs is 1.8 mm, and they extend 1 mm to the center of the beam pipe from the inner surface of the vacuum pipe. The vacuum pipe of BPM also has bellows mounted at the downstream and upstream direction for flexible installation. The upstream bellow is shielded in order to any suppress unwanted wakefields. In the upstream direction, BPM is attached with the LAS accelerating structure. The 3-D model of the new wideband feedthrough-BPM with LAS structure is shown in Fig. 1 (a). Figure 1 (b) shows the front view of the new monitor with dimensions. Two new feedthrough-BPMs were installed in the positron capture section. The horizontal and vertical steering coils are also installed at the same locations in the capture section to optimize the e^+ transmission through the capture section. The entire capture section is enclosed in the DC solenoid coils for efficient transmission of large emittance e^+ beam. For the sake of simplicity, they have been omitted from Fig. 1. The details can be found elsewhere [2, 5].

The SMA connectors of the feedthroughs are first connected to 2 m-long semirigid coaxial cable due to its protection against a high radiation environment. Later the semirigid cable was connected to 15 m-long 10D and 2 m-long RG223 coaxial cable [8]. The RG223 coaxial cables are then connected to a real-time keystone oscilloscope of bandwidth

* rehman@post.kek.jp

DEVELOPMENT OF AN X-BAND CBPM PROTOTYPE FOR SHINE*

S. S. Cao[†], Y. B. Leng^{*}, R. X. Yuan, R. T. Jiang

Shanghai Advanced Research Institute, Chinese Academy of Sciences, Shanghai, China

Abstract

SHINE (Shanghai High repetition rate XFEL aNd Extreme light facility) is a newly proposed high-repetition-rate X-ray FEL facility and will be used to generate brilliant X-rays between 0.4 and 0.25 keV. To guarantee the high performance of FEL light pulses, it is required to precisely monitoring the trajectory of the electron bunch. The position resolution of each bunch at the undulator section is required to be better than 200 nm at a bunch charge of 100 pC and 10 μ m at a bunch charge of 10 pC. Since the cavity beam position monitor (CBPM) is widely used in FEL facilities for its unique high resolution and high sensitivity and the output signals of an ideal pillbox cavity are proportional to the resonant frequency, thus the X-band CBPM is preferred because it is expected to obtain better results at low bunch charge compared with the C-band CBPM. Therefore, an X-band CBPM prototype is also developed for SHINE. This paper will focus on the design and production process of the X-CBPM.

INTRODUCTION

SHINE is designed to become one of the most efficient and advanced free electron laser user facilities in the world and provide an ultra-powerful tool for cutting-edge research. The facility is composed of a superconducting linear accelerator, 3 underlines, 3 optical beam lines, and the first 10 experimental stations[1, 2]. The facility is designed to operate at a maximum repetition rate of 1 MHz and the beam energy is 8 GeV. The bunch charge is ranging from 10 pC to 300 pC. The pulse length is only 20 to 50 fs.

To build such an ultra-high performance FEL facility, stringent requirements are placed on the beam position monitor system so as to establish and maintain precise beam trajectory and prevent emittance growth. At the undulator section, the bunch position resolution is required to be better than 200 nm at a bunch charge of 100 pC and 10 μ m at 10 pC bunch charge. Since the cavity beam position monitors (CBPM) can couple high signal-to-noise ratio (SNR) RF signals for high-resolution bunch position detection and the reported position resolution can even reach nm-scale, thus the CBPM is utilized in this section. Generally, the CBPM can work at S-band, C-band and X-band. In this research, the X-band CBPM is selected for three reasons. Firstly, the X-band CBPM has a more compact structure. Secondly, the X-band CBPM is expected to extract the RF signals with better SNR. Thirdly, it could test the machining techniques of the manufacturers.

This paper will mainly introduce the design and cold test of the X-CBPM as well as the high-bandwidth feedthrough.

* Work supported by National Key Research and Development Program of China under Grant 2016YFA0401903.

[†] lengyongbin@zjlab.org.cn

REQUIREMENTS

As described in [3], the X-CBPM will operate at 11.483 GHz which has a 59.5 MHz deviation from the quadruple frequency of 2856 MHz. The bandwidth is ranging from 1.59 MHz to 3.18 MHz. Thus the decay time constant is ranging from 100 ns to 200 ns. In order to reduce the influence of beam jitter in the X/Y direction on the beam position measurement in the Y/X direction, the XY crosstalk is required to be smaller than -34 dB under a dynamic range of $\pm 100 \mu$ m. The fundamental requirements of the X-CBPM have been summarized in Table 1.

Table 1: Requirements of X-CBPM

Parameters	Value	Unit
Frequency	11483	MHz
Decay time constant	100~200	ns
Qload	3611~7222	~
Bandwidth	1.59~3.18	MHz
XY crosstalk	<-34	dB
Crosstalk between Ref. and Pos. cavity	<-60	dB

DESIGN OF X-CBPM

The X-CBPM is composed of a position cavity and a reference cavity. The position cavity of X-CBPM is equipped with four rectangular waveguides and thus demands four high-bandwidth feedthroughs. The waveguides are mainly used to reject the TM010 mode and extract the TM110 mode. The structure of this cavity is shown in Fig. 1(a).

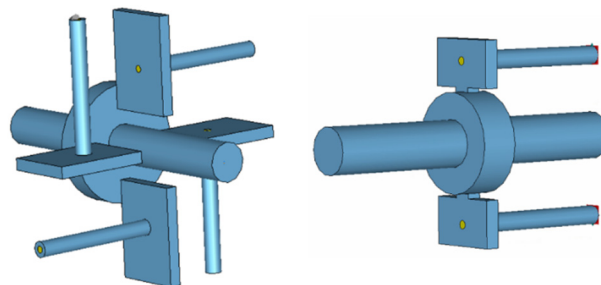


Figure 1: A 3-D view of X-CBPM vacuum parts: (a) position cavity; (b) reference cavity.

Unlike the previous CBPM reference cavity, the reference cavity of X-CBPM additionally contains two rectangular waveguides. This is mainly because of the limited space for installation of feedthrough. The diameters of the beam pipe and the reference cavity resonating at 11.483 GHz are 10 mm and 20 mm, respectively. Excluding the thickness of the cavity wall, the space left for installing feedthrough in the radial direction is less than

DESIGN OF SUPPORT FOR BPM DISPLACEMENT MEASUREMENT SYSTEM FOR HALF AND EPICS CONNECTION*

C. H. Wang, T. Y. Zhou, L. L. Tang, P. Lu, B. G. Sun[†]

NSRL, University of Science and Technology of China, Hefei, Anhui, China

Abstract

The beam orbit stability is an important parameter to measure the stability of the synchrotron radiation source. As for the fourth-generation storage ring, the emittance and beam size continue to decrease and higher requirements are being put forward for beam orbit stability. There are two main factors that affect the stability of the beam orbit. One is the vibration of the ground and other systems, which requires highly mechanically stable support. The other is due to synchrotron radiation and changes in ambient temperature, which lead to the expansion and deformation of the vacuum chamber, causing BPM movement and misjudging the position of the beam orbit. The misjudging will introduce errors in the orbit feedback system and decrease the stability of the beam orbit. Therefore, a set of offline BPM (beam position monitor) displacement measurement system with high stability was built. However, considering the adverse effect of the INVAR36 on magnetic field and the drift of the displacement data [1], we added carbon fiber to the new support for BPM displacement measurement probes. Besides we realized the function of real-time reading BPM displacement data through EPICS. This article mainly introduces the support design and EPICS connection of the BPM displacement measurement system.

INTRODUCTION

The Hefei Advanced Light Facility (HALF), a fourth-generation diffraction-limited storage ring, has completed pre-research. For the fourth-generation storage ring, ultra-high beam orbit stability is essential. The beam orbit stability is generally required to be less than 10% of the beam size, and near the insert device, it's usually required to be less than 5% of the beam size [2]. For HALF, the minimum beam size in the horizontal and vertical directions is 5 μm and 2 μm , which means the stability of the beam orbit should be less than 500 nm in the horizontal direction and 200 nm in the vertical direction. In order to meet the stability of beam orbit, a high-precision, a high-precision displacement measurement system and a high stable support for the high-precision probe are needed. The vibration amplitude of the support is also expected to be less than 50 nm and 20 nm in the horizontal and vertical directions.

We choose CapaNCDT6200 series from Micro Epsilon to measure the displacement of BPMs. The CapaNCDT-6200 has a measuring range of 1 mm, a static resolution of 0.75 nm and a dynamic resolution of 20 nm.

* Work supported by National Natural Science Foundation of China (Grant No. 12005223, 12075236) and the Fundamental Research Funds for the Central Universities (WK2310000080)

[†] bgsun@ustc.edu.cn

DESIGN

A single-sided INVAR36 support has already been processed before. The data drift in the one-sided measurement of BPM displacement, as it is shown in Fig. 1. It is difficult to know whether the data drift is due to the movement of the BPM, the movement of the support or the thermal expansion of the BPM, so a new support was designed. We plan to measure the movement of BPM from both sides at the same time and change the material. The upper part is carbon fiber composite and the lower part still uses INVAR36 alloy. Based on these, the support is designed.

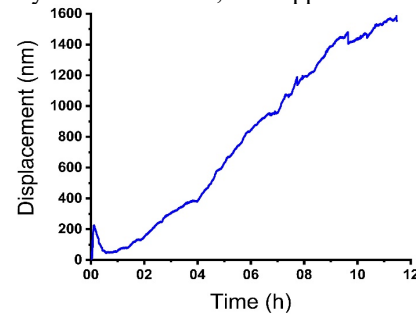


Figure 1: Data drift measured in the one-sided measurement of BPM displacement.

Analysis of Vibration Model

The support system can be simplified to the model [3] shown in Fig. 2, where k represents for stiffness and c represents for damping coefficient.

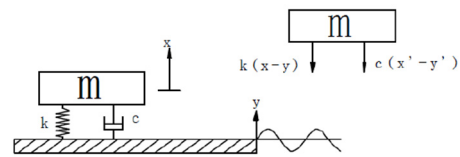


Figure 2: Vibration model.

The relationship between eigen-frequency ω_n and the support vibration amplitude X at the base vibration with amplitude Y and frequency ω can be expressed in Eq. (1) and shown in Fig. 3:

$$\beta = \frac{X}{Y} = \sqrt{\frac{1 + (2\zeta\frac{\omega}{\omega_n})^2}{[1 - (\frac{\omega}{\omega_n})^2]^2 + [2\zeta\frac{\omega}{\omega_n}]^2}} \quad (1)$$

where $\zeta = c/2\sqrt{km}$ represents for damping ratio and $\omega_n = \sqrt{k/m}$ represents for eigen-frequency, $\beta = X/Y$ represents for the vibration amplitude amplification factor of the support.

PRECISE SINGLE BUNCH MEASUREMENTS USING FAST RF SWITCHES*

W. Cheng[#], A. Brill, Argonne National Laboratory, Lemont, IL 60439, USA

Abstract

To measure the swap-out injection/extraction bunches of the Advanced Photon Source Upgrade (APS-U) storage ring, single-pass Beam Position Monitor (BPM) electronics will be installed in the first sectors after the injection with fast RF switches. The fast RF switch will select a bunch signal to be processed by the single pass BPM electronics, and have the remaining bunches processed by the regular BPM electronics. In addition to measuring the swap-out bunch during injection, the setup will be able to carry out various other measurements of any selected single bunch (or bunches). This paper presents the performance of the fast RF switches and related electronics.

INTRODUCTION

APS-U is an ultimate low emittance storage ring [1] that is being constructed at Argonne National Laboratory. The machine has small dynamic aperture, hence swap-out injection will be used. It is of great interest to measure one selected bunch (like the swap-out bunch) during machine studies and operation. Precise 1-bunch measurement of the X/Y positions (and sum signals) in turn-by-turn (TBT) rate will supply important information to machine physicists. For example, it will make sure the swap-out bunch get pre-kicked; it allows single-turn trajectory measurement during the injection/extraction period; and it will be able to confirm that a fresh bunch is captured with a desired intensity.

Modern BPM electronics typically use 125 MHz, 16-bit ADC digitizers. There are band-pass filters (BPF) implemented in the analog front end to select button BPM signal around the RF frequency (or at its harmonics). For example, APS-U storage ring will be equipped with such BPM electronics [1], with +/-10 MHz BPF and ADC sampling at 108 MHz (revolution frequency \times 398). Due to the BPF, the single bunch signal will be stretched to ~300 ns, making single-bunch position measurement impossible if the bunch-to-bunch spacing is less than that. For the APS-U machine, the bunch spacing will be either 11.4 ns (324-bunch mode) or 76.7 ns (48-bunch mode), both are small enough so that regular BPM electronics will not be able to measure individual bunches.

Wider band digitizers allow bunch-by-bunch (BxB) measurements. These new digitizers have been tested at various machines [2-4]. However, due to its wider bandwidth, there are limitations of the BxB position measurements:

- The BxB resolution is worse due to the wider bandwidth, and the ADC digitizer will have less

resolution (8 to 12-bit for a broadband ADC vs. 16-bit for a regular BPM electronics).

- The number of turns that can be saved is limited.
- It is more difficult to process and stream out the data.
- The measurement may be sensitive to clock jitter, bunch lengths and synchronous phases, and depends on the algorithm to process the BxB positions.

As in many cases, it is good enough to measure one selected bunch at the TBT rate. Fast RF switches have been proposed to select the 1-bunch signals before sending them to regular BPM processing electronics. It has been demonstrated that the regular BPM electronics have very good single bunch TBT position resolution. The single-bunch BPM electronics setup is illustrated in Fig. 1. At each selected BPM pickup location, the four button signals (namely A/B/C/D) pass through a fast RF switch box. The fast RF switch will choose a single-bunch signal for the single pass BPM electronics, and the remaining bunch signals continue feed to the regular BPM electronics (Libera Brilliance+ or LB+). The fast RF switch unit (gray box on the left which includes four switch boxes; and a dedicated Spark BPM electronics (gray box on the bottom right) select and measure the one-bunch TBT positions/sum. The blue line box shows the regular LB+ electronics which measures the position of all bunches except one.

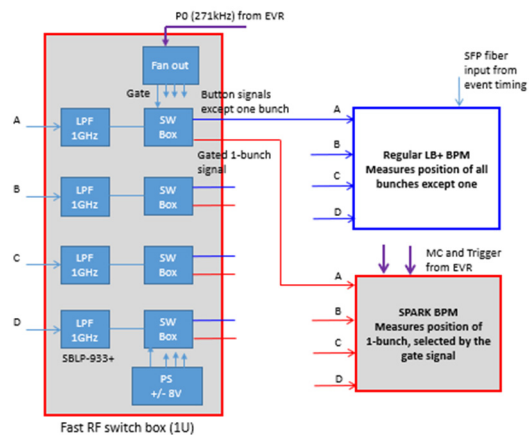


Figure 1: Schematic setup of the single pass BPM.

There will be about 20 BPMs (selected in the first three sectors right after injection) in the APS-U storage ring to be equipped with the single bunch TBT BPM electronics. Using these BPMs, the injected bunch phase space can be measured [5, 6]. Additionally, TBT position and sum signals from these BPMs will be useful to track the swap-out bucket for the pre-kick, extraction, and injection process. The idea of fast RF switches to select 1-bunch signal has been implemented in KEK's ATF and SuperKEKB [7, 8]. We report the procurement status and

*Work supported by DOE contract No: DE-AC02-06CH11357

[#]wcheng@anl.gov

WIRE TEST OF LARGE TYPE BPM FOR P2DT IN RAON

J. W. Kwon[†], Y. S. Chung, G. D. Kim, H. J. Woo, E. H. Lim¹

Institute for Basic Science, Daejeon 34000, Korea

¹also at Department of Accelerator Science, Korea University, Sejong, 30019, Korea

Abstract

RAON (Rare isotope accelerator complex for On-line experiments) is accelerator to accelerate heavy ion such as uranium, oxygen, and proton. At P2DT(Post to Driver linac Transport line) section where is located between SCL3 and SCL2, particle beam would be higher charge state by stripper. In bending area in P2DT, BPM(Beam Position Monitor) should accept the beam that has large size (~10 cm) horizontally. Required BPM transverse position resolution is 150 μm . We simulated Large type BPM with CST particle studio. Fabricated LBPM was tested on the developed wire test bench that could move BPM for width of ± 80 mm, height of ± 40 mm with manual steering knob.

INTRODUCTION

Rare isotope Accelerator complex for ON-line experiments (RAON) include of superconducting linear accelerators, which comprise superconducting linac2 (SCL2) and superconducting linac 3 (SCL3) sections [1]. The extracted beam from ECR ion source of injector will be accelerated and transferred from SCL3 to SCL2 through P2DT section. The layout of the post linac to driver linac transport (P2DT) section of RAON is depicted in Fig.1. In the P2DT section, the charge state of the beam is changed to a higher charge state by charge stripper using carbon foil, and only the beam of a specific charge is transmitted by the Charge Selector. The beam selected by the charge selector is transmitted and accelerated to the experimental area through SCL2.

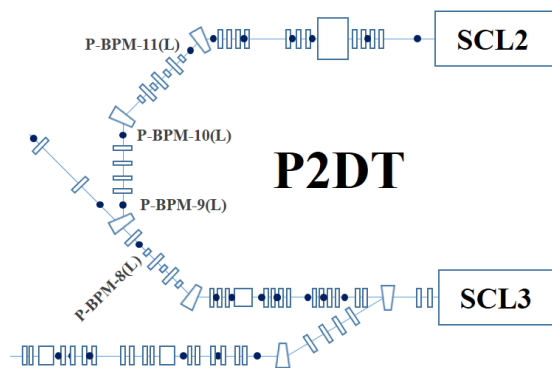


Figure 1: Layout of P2DT section of RAON, there are 4 large type BPMs for only P2DT section.

The P2DT section has four dipole magnets and 2 charge selector, which are used to select the design charge state for

[†] jangwonk@ibs.re.kr

acceleration in the SCL2. As the beam passes through the charge stripper, particle beam has higher charge state and charge selector has a role of collimator to pass the beam that has charge state between 77+ and 81+.

In the P2DT region, the energy, and bunch length of a uranium beam are 18.5 MeV/u and 0.3 ns rms, respectively. The designed input beam pulse current of P2DT is 340 μA , and the output beam current is 660 μA

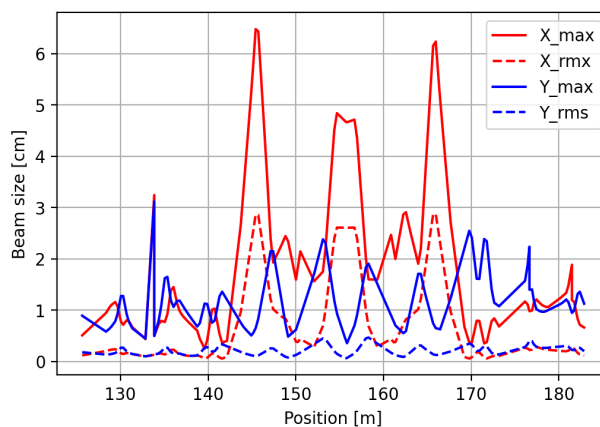


Figure 2: Beam size in P2DT section.

As the particle beam passes through a dipole magnet, the beam size increases horizontally. The increased beam size caused by multi charge state is greater than for single charge state beams. It is caused by different A/Q for same dipole magnetic field.

In the case of a uranium beam, the maximum beam size along the horizontal direction is greater than 6 cm after passing the first dipole magnet as depicted in Fig. 2. Four BPMs will be installed at the bending areas, which are placed between the four dipole magnets. The BPMs are required to accept large-size beams for measuring the positions and phases of the beams. For the bending areas where the BPMs are installed, the BPMs can be damaged because dipole magnet failure. Although MPS(machine protection system) is configured, we fundamentally want to avoid direct damage to the BPM electrode. In case of dipole magnet failure, an accelerating particle beam will hit the BPM electrode. The electrode of BPM has low heat capacity and the only place to dissipate heat is brazed feedthrough.

The required transverse position resolution is 150 μm at 81.25 MHz, that is the fundamental RF frequency and bunch repetition rate of the RAON. The formula of Δ/Σ will be used to calculate the position on the basis of the signal strength of BPM. We prepared an electronic system to calculate the signal strength and phase of all electrodes using the IQ method of 81.25 MHz [2]. BPM pickup signals were simulated using CST Particle Studio [3].

CURRENT STATUS OF ELETTRA 2.0 eBPM SYSTEM

G. Brajnik*, R. De Monte, Elettra-Sincrotrone Trieste, Trieste, Italy

M. Cargnelutti, P. Leban, P. Paglovec, B. Repič, Instrumentation Technologies, Solkan, Slovenia

Abstract

In the last years, there has been a growing interest in using the pilot-tone technique for long-term stabilization of electron beam position monitors in synchrotrons. At Elettra, after an internal development, the effectiveness of this approach was proven with tests in the laboratory and on the storage ring. The pilot-tone scheme will be adopted for the eBPMs that will equip Elettra 2.0, the low-emittance upgrade of the present machine. In order to support the development, industrialisation and production of the overall system, a partnership with Instrumentation Technologies has been signed. With the extensive experience with the Libera instruments, the company will be engaged in improving the BPM system developed by Elettra and getting it ready for serial production. This paper presents the current status of the BPM system, with an emphasis on the efforts done to improve the key performances of the system and to address its weaknesses (e.g. enhancing single bunch response and low currents sensitivity) within the industrialisation process, with the goal to get to a reliable system, easy to maintain and that meets the multiple project requirements for the new storage ring, the booster, the pre-injector and the transfer lines.

INTRODUCTION

Elettra 2.0 will be the new diffraction limited storage ring that will start serving the users at the end of 2026, replacing the current machine (Elettra). Even if the lattice length will remain more or less the same, the number of beam position monitors (BPMs) will increase to 147 [1]. In order to reduce costs and optimize resources, the same electronics will be used in preinjector, transfer lines, booster and storage ring. Thus, different operation modes are required for a correct behaviour: single pass (first turn) mode, gated mode, close orbit mode.

As a consequence of the excellent results obtained during the development of the overall prototype [2], the machine will be equipped with BPM controlled by electronics based on pilot tone. A modular approach was chosen, with analog front ends detached from the digital part (Figure 1). The front ends will be placed in machine tunnel, powered and controlled via Ethernet links, while the analog-to-digital conversion and processing unit will remain in accelerator service area (radiation safe), with sufficient computing power to manage two BPMs each. The required connections to machine infrastructure will be optical (e.g., 10 Gb Ethernet link for global orbit feedback data) or copper-based (interlock, synchronisation).

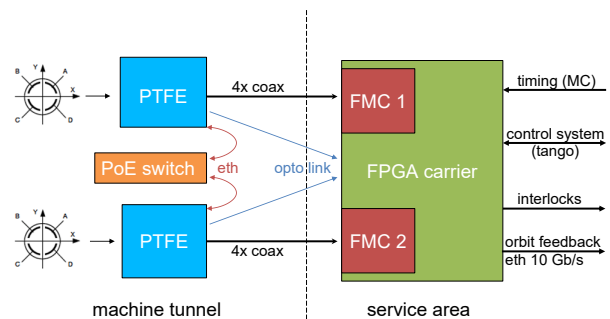


Figure 1: Block diagram of the system.

The process of building such a system for a high number of units (about 200 for the analog front ends, 100 for the digital platform) is not straightforward. Many aspects have to be considered, especially those related to manufacturing, maintenance and reliability. For this reason, a partnership was signed with Instrumentation Technologies after a tender procedure, in order to industrialize and produce all the components of the system. In this way, Instrumentation Technologies' long-term experience in manufacturing diagnostic tools for particle accelerators will be combined with Elettra's knowledge of the overall aspects of a light source. This collaboration is already making improvements over the original prototype, and these results will be discussed in the following sections.

PILOT TONE FRONT END

The analog front end has been presented already at IBIC 2016 [3]: it consists of an RF analog processing chain with pilot tone injection. Compared to the first working prototype, we have made improvements on various aspects, both in terms of performance improvement and in terms of reliability and the production process.

Radiation Sensor

In order to compensate the overall signal path, the front end has to be installed in the machine tunnel, as near as possible to the pick-ups. This area presents unavoidable and unpredictable ionizing radiations due to multiple sources, that can damage the electronics and cause malfunctions. So, special care must be taken in correct positioning of the electronics, preferring low radiation zones. For this reason, a commercial radiation sensor (Teviso BG51 [4]) has been integrated in the front end (Figure 2). It is capable to detect beta radiation, gamma radiation and X-rays, in a measurement range of dose rate from 0.1 $\mu\text{Sv/h}$ to 100 mSv/h . The pulse count rate is about 5 cpm for 1 $\mu\text{Sv/h}$, and the energy response ranges from 50 keV to above 2 MeV. Its output

* gabriele.brajnik@elettra.eu

BEAM POSITION DETECTION OF A SHORT ELECTRON BUNCH IN PRESENCE OF A LONGER AND MORE INTENSE PROTON BUNCH FOR THE AWAKE EXPERIMENT

Eugenio Senes^{*1}, P. N. Burrows^{1,2}, R. Corsini¹, W. Farabolini¹, T. Lefevre¹,
A. Gilardi³, M. Krupa¹, S. Mazzoni¹, C. Pakuza^{1,2}, M. Wendt¹

¹ CERN, Geneva, Switzerland

² JAI and University of Oxford, Oxford, United Kingdom

³ Lawrence Berkeley National Laboratory, Berkeley, California, USA

Abstract

The AWAKE experiment studies the acceleration of electrons to multi-GeV levels driven by the plasma wakefield generated by an ultra-relativistic and high intensity proton bunch. The proton beam, being considerably more intense than the co-propagating electron bunch, perturbs the measurement of the electron beam position achieved via standard techniques. This contribution shows that the electrons position monitoring is possible by frequency discrimination, exploiting the large bunch length difference between the electron and proton beams. Simulations show that the measurement has to be carried out at a frequency of a few tens of GHz, which is far higher than the spectrum produced by the 1 ns long (4 sigma) proton bunch. As operating a conventional Beam Position Monitor (BPM) in this frequency range is problematic, an innovative approach based on the emission of coherent Cherenkov Diffraction Radiation (ChDR) in dielectrics is being studied. After describing the monitor concept and design, we will report about the results achieved with a prototype system at the CERN electron facility CLEAR.

INTRODUCTION

The AWAKE experiment successfully demonstrated the acceleration of an electron bunch in 10 meters of Rubidium plasma driven by a high energy proton bunch [1]. Due to the high accelerating gradients produced in the plasma, the research in this technology is promising for a new generation of compact high energy accelerators [2]. A new experimental run has started recently, the AWAKE Run 2, with the first protons delivered to the experiment during summer 2021. The AWAKE Run 2 is a new experimental program that aims to further study the proton-driven Plasma Wakefield Acceleration (PWFA) in the next decade, while finding technical solutions to apply the PWFA to operational accelerators. Among the copious experimental program, one finds the development of even stronger accelerating gradients, the conservation of the accelerated beam quality and the scalability of the acceleration scheme [3]. The present layout of the AWAKE experiment is shown in Fig. 1. A 400 GeV, 1 ns-long proton driver bunch is extracted from the SPS and reaches the AWAKE experiment through a dedicated transfer

line. Few meters upstream to the plasma cell, it merges with a common beamline with the electron bunch and the plasma ionising laser pulse [4]. The electron bunch is considerably shorter and less intense than the proton bunch. The beam parameters are reported in Table 1. The two beams may travel with different trajectories, in order to select the merging point distance inside the plasma cell. The plasma is created out of rubidium vapour [5], ionised by a high power laser pulse [6]. Downstream the plasma cell, diagnostic devices can be inserted to analyse the beams [7]. The electrons are then sent to a spectrometer [8] to measure their energy, while the spent laser and proton beams are finally dumped.

Two different BPM systems measure the electron [9] and the proton [10] bunch transverse position, upstream the plasma cell. Due to the very different bunch structure of the electron and proton beam (see Table 1), the whole instrumentation installed in the common beamline is perturbed when both beams are present. This originates from the very different electromagnetic field of the proton bunch, that is considerably more intense than that of the electrons. As a result, the former overshadows the latter, limiting the possibility to measure the electron beam only in the absence of the proton beam. However, with shorter bunch length, the electron spectrum extends to higher frequencies compared to the proton spectrum and it would provide an opportunity to perform measurements on the electron beam in presence of the proton bunch. Currently, the experiment can operate either by setting up the two beams separately or by relying on the different repetition rate of the electron and proton beams. In fact, while the electrons are produced with a 10 Hz repetition rate, the protons are extracted every 30 s or more [11]. Therefore, during operation, the electron bunch position was extrapolated by the electron position in a number of shots before and after the proton pulse. This approach, although successful for a test experiment, may prove insufficient for an operational accelerator or to study beam-beam effects [12].

Table 1: AWAKE Beam Parameters

Beam	proton	electron
Charge [nC]	48	0.1 – 0.6
Length (1σ) [ps]	250	1 – 5
Energy [MeV]	4×10^5	16 – 20

* eugenio.senes@cern.ch

DEVELOPMENT OF A PASS-THROUGH DIAGNOSTIC FOR NEXT-GENERATION XFELs USING DIAMOND SENSORS*

I. Silva Torrecilla[†], B. Jacobson, J. MacArthur, D. Zhu

SLAC National Accelerator Laboratory, Menlo Park, California, USA

J. Bohon, D. Kim, J. Smedley, Los Alamos National Laboratory, Los Alamos, New Mexico, USA

E. Gonzalez, S. Kachiguine, F. Martinez-Mckinney, S. Mazza, M. Nizam, N. Norvell, R. Padilla,

E. Potter, E. Ryan, B. Schumm, M. Tarka, M. Wilder, Santa Cruz Institute for Particle Physics and the University of California at Santa Cruz, Santa Cruz, California, USA

C. T. Harris, Sandia National Laboratory, Albuquerque, New Mexico, USA

Abstract

X-ray FELs deliver rapid pulses on the femtoseconds scale, and high peak intensities that fluctuate strongly on a pulse-to-pulse basis. The fast drift velocity, and high radiation tolerance properties of CVD (chemical vapor deposition) diamonds, make these crystals a good candidate material for developing a multi-hundred MHz pass-through diagnostic for the next generation of XFELs. Commercially available diamond sensors work as position-sensitive pass-through diagnostics for nJ-level pulses from synchrotrons. Supported by the University of California and the SLAC National Laboratory, a collaboration of UC campuses and National Laboratories have developed a new approach to the readout of diamond diagnostic sensors designed to facilitate operation for FEL-relevant uJ and mJ pulses. Single-crystal diamond detectors have been tested on the XPP end station of the Linac Coherent Light Source beam at SLAC. We present results on the linearity and charge collection characteristics as a function of the density of deposited charge.

INTRODUCTION

Monocrystalline diamonds are recognized to exhibit a number of properties that make them attractive options for a broad range of sensor applications. Superior radiation tolerance, a fast saturated drift velocity (approximately 200 $\mu\text{m}/\text{nsec}$) and superior thermal conductivity (2200 W/m-K) distinguish diamond among other semiconductor sensor materials such as silicon and gallium-arsenide.

Here, we explore the use of diamond sensors as a pass-through diagnostic for X-ray Free Electron Laser (XFEL) beams. For this application, involving intense X-ray beams being trained directly on the diagnostic sensor, diamond properties that might be disadvantageous for other applications provide additional advantages relative to other sensor materials. The low atomic number of carbon leads to a relatively small scattering cross section for X-ray above the carbon K-shell edge of 0.28 keV, limiting the absorption of

the XFEL beam as it passes through the diagnostic. In addition, the large diamond band gap of 5.5 eV, and resulting pair excitation energy of 13.3 eV [1], limits the production of signal charge relative to other sensor materials.

In this study, we explored the characteristics of diamond-sensor charge collection in limits relevant to their application as pass-through diagnostics for high-intensity, high repetition-rate X-ray beams. These studies were performed at the XPP beamline of the Linac Coherent Light Source (LCLS) at the SLAC National Accelerator Laboratory on April 5-6, 2021. The studies made use of a monochromatic beam of 11.89 keV X-rays with individual pulse varying in energy from 1 μJ to nearly 100 μJ . Both the duration and efficiency of charge collection were studied as a function of the density of deposited charge within the diamond sensor.

SENSOR AND READOUT

The studies made use of a 4x4 mm² monocrystalline diamond substrate, provided by the Element Six corporation and thinned by Applied Diamond, Inc. The diamond was plated with planar platinum electrodes of area approximately 3.5x3.5 mm² and 25 nm thickness at the Center for Integrated Nanotechnologies (CINT) facility in Albuquerque, New Mexico, USA. The thickness of the diamond substrate was measured to be $37 \pm 10 \mu\text{m}$ in the laboratory of the Santa Cruz Institute for Particle Physics (SCIPP) on the campus of the University of California at Santa Cruz.

The sensor was mounted on a printed-circuit board (PCB), produced by the SCIPP laboratory, featuring a low-impedance signal path designed to circulate large amounts of signal charge at high bandwidth. Figure 1 shows the details of the PCB signal path, including the loaded diamond sensor described above. To reduce inductive load associated with bond wires, the sensor is connected to the readout path through a metallic band composed of indium. This band carries signal charge to a series array of two resistors – a 1 Ω resistor followed by a 10 m Ω resistor, with contacts on the long side to minimize inductance – that shunt the signal current directly to ground. 50 Ω pick-off traces make contact with the sensor side of both the 1 Ω and 10 m Ω resistors, each of which terminates at an SMA connector close to the pickoff point, providing signals that can be digitized and recorded with a high-bandwidth digital storage oscilloscope. Figure 2 provides a larger-scale view of

* Work supported by the UC-National Laboratory Fees Research Program grant ID #LFR-20-653232, the U.S. Department of Energy, grant number DE-SC0010107 (SCIPP), contract 89233218CNA000001 (LANL), Contract DE-NA-0003525 (Sandia), Contract No. DE-AC02-76SF00515(SLAC).

[†] email address isleydys@slac.stanford.edu

BEAM POSITION MONITOR CALIBRATION BY RAPID CHANNEL SWITCHING*

R. Hulsart†, R. Michnoff, S. Seletskiy, P. Thieberger
Brookhaven National Laboratory, Upton, NY, USA

Abstract

One of the requirements for low-energy RHIC electron cooling (LEReC) is a small relative angle between the ion and electron beams as they co-propagate. In order to minimize relative electron-ion trajectories angle, BPM measurements of both beams must be very accurate. Achieving this requires good electronic calibration of the associated cables and RF components, due to their inherent imperfections. Unfortunately, these are typically frequency dependent, especially in the RF filter and amplifier stages. The spectral content of the ion vs. electron bunch signals varies significantly, presenting a calibration challenge, even when using the same sampling channels and electronics to measure both beams.

A scheme of rapidly swapping the BPM signals from the pickup electrodes between the two signal cables (and sampling channels), using switches installed near the BPM was implemented to combat these calibration issues. Bias in each signal path appears as an offset which has an equal and opposite component when the cables are reversed. Taking the average of the two measurements with the channels in normal and reverse positions reduces this offset error. Successful transverse cooling of the RHIC ion beam has been verified after using this switching technique to provide continuous calibration of the BPM electronics [1]. Details of the processing hardware and switch control methodology to achieve this result will be discussed.

INTRODUCTION

Beam position measurements in accelerators are commonly performed by sampling the induced signals on a pair of pickup electrodes mounted in the vacuum chamber. In order for them to be precise and accurate, small differences in signal amplitude need to be measured between these two sampling channels. In most BPM systems, separate analog signal paths consisting of cables, amplifiers, attenuators, and filters are used to process each signal before being sampled by an analog to digital convertor (ADC). Each of these circuit elements has inherent properties that can attenuate or reflect signals with a dependence on frequency.

Typically, a calibration procedure is followed by using a known test signal to match the gain and offset of each of these channels, in order to balance their response. In theory once these channels are matched the true position of the beam will be the only contributor to any difference. In reality, the circuit response due to the test signal can differ significantly from that produced by a real beam. There are also accelerators where the spectral content of the beam signal can change during operation due to variations in RF

frequencies such as with rebucketing. The presence of two beams of different bunch length and/or structure also has the same effect of changing the response of the individual circuit elements of each sampling channel. This leads to a situation where a static calibration using a test signal is inadequate to remove the electronic offsets for all beam conditions. Another source of offsets that can't be removed with static calibrations is the presence of radiofrequency interference (RFI) at the bunch frequency or its harmonics picked up by the long cables and enhanced by ground-loops. Such RFI can vary with time and can produce offsets that are bunch-intensity dependent.

One method of removing these offsets is to periodically swap the channels that each of the pickup electrodes (PUE) is connected to. By placing a set of switches close the BPM, each PUE can be connected to either of the sampling channels, including cables, analog processing electronics, and ADC. When using a BPM with two PUE's, this will produce two separate position measurements, where the differences due to the sampling channels are equal and opposite in sign. By rapidly switching and averaging these two together, a true measurement is obtained that is free from the offsets produced by elements downstream of the point of switching.

SWITCHING TECHNIQUE

Theory of Operation

To simplify this description, we will consider a single plane BPM measurement derived from two PUE's. An enclosure containing an arrangement of solid-state transistor switches is placed close to the BPM and connected via short cables. We will call these PUE signals A and B and these are the inputs to the switch. The outputs will be labelled 1 and 2 and are connected via longer cables to the BPM processing electronics.

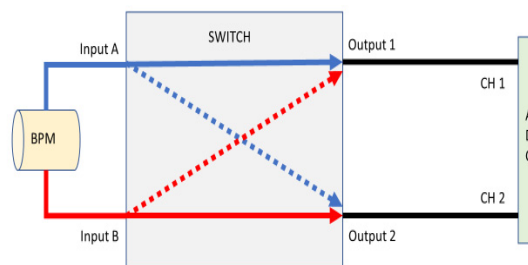


Figure 1: Switching Block Diagram.

The switch circuit is designed such that in the 'Normal' position, input A is connected to output 1 and B is connected to 2. When a control signal is applied to the switch,

* Work supported by BSA under DOE contract DE-AC02-98CH10886

† rhulsart@bnl.gov

RESEARCH ON RESOLUTION OF ORBIT BASED ON CLUSTERING ANALYSIS AND BP NEURAL NETWORK IN SSRF*

R. T. Jiang[†], N. Zhang, Y. M. Deng, Y. B. Leng[‡]

Shanghai Advanced Research Institute, Chinese Academy of Sciences, Shanghai, China

Abstract

Keeping the beam current's normal motion is an important mission for Shanghai Synchrotron Radiation Facility (SSRF). So the Orbit (rms)x/y is an main parameter for SSRF's running. However, the orbital resolution has been constrained by the accuracy of acquired data. To eliminate BPM's failure causing the inaccurate orbital resolution, the work based on clustering analysis and BP neural network to removed the abnormal BPM and recalculate the resolution of orbit. Experiment data came from the machine research. The analysis results showed that the rms value of orbit was 100.75 μm (x direction) and 14.9 μm (y direction) using all BPM's data but the recalculate value was 98.03 μm (x direction) and 2.6 μm (y direction) when eliminated the data of faulty BPM. The analysis result indicated that the method can optimize the resolution of orbit and next work is further to evaluate the orbital resolution with more operation data.

INTRODUCTION

The storage ring in SSRF is equipped with different machine parts located at 20 cells of the storage ring to monitor the beam dynamics [1]. Due to the accidental error of machine parts and the collimation error of each magnet, particles usually deviate from ideal orbit to form orbit and it can result in machine performance degradation or even failure. Good orbit is the foundation of accelerator operation, and orbit correction is the most basic of current accelerator beam adjustment. And it is also one of the most widely studied fields at present. As a beam monitoring system, the BPMs at the beam lines after the insertion devices (ID) or the bending magnets are also of great importance, because they also serve as the orbit feedback system to ensure stability of the electron Beams [2]. Meanwhile, the BPM confidence levels included in the feedback system can be used to estimate stability of the beam dynamics. The BPMs can monitor the stability of beam Orbit. Therefore, an abnormal BPM should be found and treated to avoid the deviation calculation for beam orbit.

A typical BPM system consists of the probe (button-type or stripline-type), electronics (Libra Electronics/ Brilliance in SSRF) and transferring component (cables and such). Ever since the SSRF commissioning in 2009, the BPM have occurred all kinds of malfunction. They were permanently damage of individual probe or corre-sponding cable, misaligned (position/angle) probes, high-frequency vibrations, electronics noise, and others. These faults mean

totally useless of the signals from the BPM, which should be ignored until its replacement or repair. Hence, it is essential to find an effective method to detect the faulty BPM and revise the beam orbit.

With development in machine learning methods, a series of powerful analysis approaches make it possible for detecting beam position monitor's stability. Cluster analysis is one of machine learning methods. It is aimed at classifying elements into categories on the basis of their similarity [3]. Its applications range from astronomy to bioinformatics, bibliometric, and pattern recognition. Clustering by fast search and find of density peaks is an approach based on the idea that cluster centres are characterized by a higher density than their neighbours and by a relatively large distance from points with higher densities [4]. This idea forms the basis of a clustering procedure in which the number of clusters arises intuitively, outliers are automatically spotted and excluded from the analysis, and clusters are recognized regardless of their shape and of the dimensionality of the space in which they are embedded. In addition to, it is able to detect non-spherical clusters and to automatically find the correct number of clusters.

Based on the advantage of clustering by fast search and find of density peaks, this study located and removed the faulty BPM at SSRF. Through we removed the faulty BPMs, considering the beam integrity, the research work used the BP neural network to fit the beam position in all BPM's data (the removed BPMs's collected data were replaced the fitted data).

EXPERIMENTAL DATA AND ANALYSIS METHOD

Experimental Data and Acquisition System

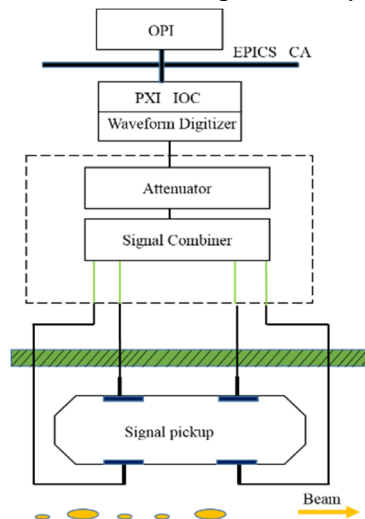


Figure 1: Acquisition system layout.

* Work supported by National Nature Science Foundation of China (No.11375255)

[†] jiangruitao@sinap.ac.cn

[‡] lengyongbin@sinap.ac.cn

SIGNAL ANALYSIS AND DETECTION FOR THE BPMs OF THE LHC HOLLOW ELECTRON LENS

G. Bantemits, M. Gasior, A. Rossi, M. Wendt, CERN, Geneva, Switzerland

Abstract

The Large Hadron Collider (LHC) at CERN will be equipped with two hollow electron lenses (HEL) for the high luminosity upgrade, which allow for scraping of the LHC proton or ion beams transverse tails by overlapping a coaxial hollow electron beam over a 3 m length. A precise alignment of the two beams is essential for the HEL functionality, the bunched LHC hadron beam of up to 7 TeV beam energy, and the non-relativistic, DC-like electron hollow beam of 10 keV energy. The absolute and relative transverse positions of both beams will be monitored by two stripline beam position monitors (BPM), located in the HEL, and the pickup signal processed by a narrowband signal detection system. This paper summarizes the analysis of the expected proton and electron beam signals, including laboratory measurements, with aim of a narrowband diode-detection read-out electronics as BPM signal processor.

INTRODUCTION

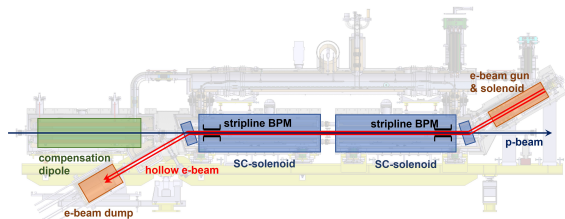


Figure 1: Sketch of the HL-LHC hollow electron lens (HEL).

A high-luminosity LHC upgrade project (HL-LHC) is in progress at CERN [1], with the goal to boost the yearly integrated luminosity from presently $50-65 fb^{-1}$ to $> 250 fb^{-1}$ at the two collision experiments ATLAS and CMS. Among the many changes and improvements required, a new particle collimation strategy was developed to enhance the transverse beam halo depletion, which includes the use of a hollow electron lens (HEL) for each of the two circulating hadron beams [2]. It utilizes a “non-material” hollow electron beam scraper, placed coaxially around the proton beam, to increase the diffusion rate of protons or ions with large emittance. Figure 1 shows the schematic of the approximately 6-meter-long HEL system in a sectional view, which consists of a thermionic electron beam gun, accelerating a hollow electron beam of up to 5 A current to approximately 12 keV beam energy, before being bent onto the LHC proton beam orbit. The beam is controlled by two main superconducting solenoid magnets and a set of auxiliary solenoids and steering magnets, before being bent downwards to a beam dump. Inside the 120 mm warm bore of each superconducting solenoid, a beam position monitor (BPM) pickup

with four symmetrically arranged electrodes is located. The horizontal and the vertical pairs of stripline electrodes of 400 mm length are used to monitor the beam position of both beams, i.e. the hollow electron beam and the counter-propagating proton beam, each detected separately at the upstream ends of the electrodes by a high-resolution BPM signal processor, enabling a precise relative alignment of both beams.

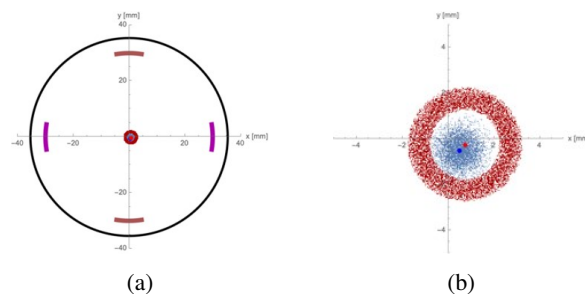


Figure 2: Hollow electron beam position measurement with a BPM pickup (left), proton and hollow electron beam close-up (right).

Figure 2 (left) gives an idea of the BPM pickup of 60 mm diameter aperture in a cross-section view, indicating the beam pipe and the stripline electrodes, as well as both beams near the center. Figure 2 (right) illustrates a close-up cross-section view of the proton and the hollow electron beam in a non-optimized beam position, both beams should be perfectly centered to each other. Also indicated are their center-of-charges, by a blue dot (for the proton beam) and a red dot (for the hollow electron beam), as they would be monitored by the proposed BPM system. The proton and hollow electron beams to be detected have very different beam formats, see Table 1.

Table 1: Proton and Hollow Electron Beam Specifications

	Time structure	Beam charge /current	Relativistic factor β	Transverse size
Proton beam	2760 bunches ~ 1 ns (4σ)	$1 - 2.3e^{11}$ p/b	1	$\sigma_x \approx \sigma_y$ $\approx 0.3 - 1.2$ mm
Hollow electron beam	“DC-like” 1.2 – 86 μ s pulse duration	0.1 – 5 A	0.2 – 0.24	Inner diameter $\approx 2 - 8$ mm Outer diameter $\approx 4 - 16$ mm

Figure 3 illustrates the situation of the two beams at the location of the HEL stripline BPM in a longitudinal section view. Let’s name the two symmetric stripline electrodes “A” and “B”, either the horizontal, or the vertical pair of electrodes. With the help of a signal pre-processing scheme,

COMMISSIONING OF ALPS, THE NEW BEAM POSITION MONITOR SYSTEM OF CERN'S SUPER PROTON SYNCHROTRON

A. Boccardi*, J. Albertone, M. Barros Marin, T. Bogey, V. Kain, K.S.B. Li, P. A. Malinowska¹, A. Topaloudis, M. Wendt, CERN, Geneva, Switzerland
¹also at AGH University of Science and Technology, Kraków, Poland

Abstract

The Super Proton Synchrotron (SPS) is both the final machine in the pre-accelerator chain of the Large Hadron Collider (LHC) at CERN and a machine providing several fixed target experiments with proton and ion beams. In the framework of CERN's LHC Injectors Upgrade (LIU) project, aimed at improving the performances of the pre-accelerators in view of the high-luminosity upgrade of the LHC, the Beam Position Monitor (BPM) system of the SPS was redesigned during Run 2 of the LHC and deployed during the subsequent Long Shutdown 2 (LS2). This new system is called ALPS (A Logarithmic Position System) and acquires the signals from some 240 BPMs. It is designed to improve the system's reliability and reduce the required maintenance with respect to its predecessor. During the restart of the SPS in 2021, the BPM system was a key element of the fast recommissioning of the machine, proving the validity of the chosen design approach and pre-beam commissioning strategy. This paper aims to illustrate the design choices made for ALPS, the strategy for commissioning it with beam in parallel with the machine restart, the commissioning procedure and the results obtained.

INTRODUCTION TO ALPS

The Super Proton Synchrotron (SPS) is the second largest accelerator in the CERN complex. It can accelerate both proton and ion beams to fill the Large Hadron Collider (LHC) but also provides beams to several fixed target experiments. The beams accelerated by the SPS may vary in bunch intensity from 5E8 up to 5E11 protons per bunch, but also in bunch spacing, from single bunch to trains spaced from 5 ns to 75 ns. Table 1 summarises the beam types accelerated in the SPS.

The majority of the pick-ups in the SPS are of the shoebox type, with very low sensitivity: 0.1 dB/mm and 0.2 dB/mm respectively for the horizontal and the vertical planes. Because of the limited BPM sensitivity, the system needs to cover the 70 dB dynamic range, mostly deriving from intensity (see Table 1), with an expected resolution in the order of 0.01 dB, corresponding to about 100 μ m. ALPS (A Logarithmic Position System) uses logarithmic amplifiers to compress the dynamic range, as described in details in [1]. The chosen amplifiers have a dynamic range of about 40 dB, in which processing errors are acceptable for the system requirements. In order to cover the full 70 dB required, the electrode signal is split in 3 channels with different sensi-

tivity ranges, each separated by about 15 dB [1]. The 3 channels are acquired in parallel and the online processing algorithm automatically selects the ranges which can be used for position calculation.

The logarithmic amplifiers only approximate the logarithm function, and the error function is specific for each amplifier. The mismatch between the error functions in the different channels, as well as the integral error, need to be compensated for in the processing chain to achieve a precision compatible with the target resolution, otherwise they would lead to position- and intensity-dependent systematic errors. This is achieved with a correction polynomial applied in the online processing chain, and computed from calibration measurements performed in the lab on each amplifier. Figure 1 illustrates the residual integral error of the measured power at the input of the front-end after the calibration. ALPS' front-end electronics, both analogue and digital, is indeed installed in the SPS tunnel and exposed to radiation but no digital processing is performed there after digitisation: the digitised signals are directly transmitted to the surface via optical fibres after packaging and serialisation. The front-end as a whole, as well as each of its active components individually, was qualified for radiation with the help of CERN's Radiation to Electronics (R2E) working group and, whenever possible, radiation-tolerant by design ASICs designed by the CERN PH-ESE group were used. As a result, the front-end electronics, installed in small crates located under the beamline itself, is expected to properly operate, i.e. without significant drifts, up to an integrated dose of 750 Gy [2].

The use of radiation-tolerant front-end electronics, with digitisation in the tunnel and optical transmission, eliminated the need for the long cables used in the previous system. Those cables were the main reason for maintenance interventions: due to the low sensitivity of the pick-ups, even small drifts in the cable characteristics had to be measured and compensated for between each run.

Table 1: SPS Beam Types

Spacing	Charges per bunch	Charges per bunch
	MAX	MIN
5 ns	5e10	5e8
25 ns	3e11	1e9
50 ns	3e11	1e9
75 ns	3e11	1e9
single bunch	5e11	1e9

* andrea.boccardi@cern.ch

SIGNAL PROCESSING ARCHITECTURE FOR THE HL-LHC INTERACTION REGION BPMs

D. R. Bett*, University of Oxford, Oxford, UK

A. Boccardi, I. Degl'Innocenti, M. Krupa, CERN, Geneva, Switzerland

Abstract

In the HL-LHC era, the Interaction Regions around the ATLAS and CMS experiments will be equipped with 24 new Beam Position Monitors (BPM) measuring both counter-propagating beams in a common vacuum chamber. Numerical simulations proved that, despite using new high-directivity stripline BPMs, the required measurement accuracy cannot be guaranteed without bunch-by-bunch disentanglement of the signals induced by both beams. This contribution presents the proposed signal processing architecture, based on direct digitisation of RF waveforms, which optimises the necessary computing resources without a significant reduction of the measurement accuracy. To minimise the number of operations performed on a bunch-by-bunch basis in the FPGA, some of the processing takes place in the CPU using averaged data.

INTRODUCTION

The Large Hadron Collider (LHC) will undergo major upgrades in the context of the High Luminosity LHC (HL-LHC) project with the goal to deliver 3000 fb^{-1} of integrated luminosity over twelve years of operation from 2027 [1]. New Inner Triplets (IT) consisting of several high-gradient focusing magnets around ATLAS and CMS experiments will squeeze the proton beams to a $7.1 \mu\text{m}$ RMS beam size at the collision point [2]. In order to reliably collide such exceptionally small beams, each HL-LHC IT will feature six Beam Position Monitors (BPM) of two different types [3]. Since these BPMs will be installed in regions where both proton beams circulate in a common vacuum chamber, they must be able to clearly distinguish between the positions of the two counter-propagating particle beams.

The longitudinal positions of the BPMs were optimised to guarantee that the temporal separation between the two beams at each BPM location will always be greater than 3.9 ns, which is approximately 3 times longer than the bunch length. Nevertheless, using directional-coupler BPMs (also known as stripline BPMs) is unavoidable to reduce the inter-beam cross-talk. In such BPMs the passing beam couples to four long stripline electrodes parallel to the beam axis. Each electrode is connectorised on both ends but the beam couples predominantly to the upstream port with only a relatively small signal generated at the downstream port. This feature, referred to as directivity, allows both beams to be measured by a single array of electrodes. Figure 1 shows a 3D model of one of the HL-LHC stripline BPMs. Most of the HL-LHC IT BPMs incorporate four tungsten absorbers protecting the superconducting magnets from the high-energy collision

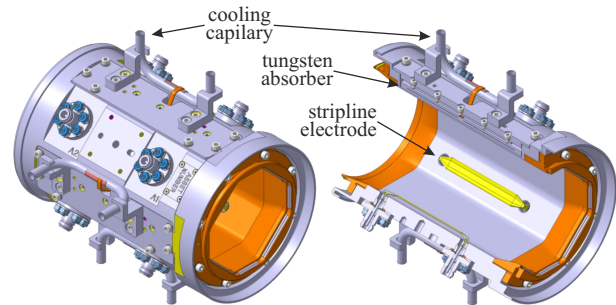


Figure 1: Tungsten-shielded cryogenic directional coupler BPM design for HL-LHC.

debris [4]. As the absorbers must be placed in the horizontal and vertical plane, the BPM electrodes are installed at $\pm 45^\circ$ and $\pm 135^\circ$ significantly increasing the measurement non-linearity for large beam offsets.

To cope with the very demanding requirements of precise beam position measurements near the experiments, a new state-of-the-art acquisition system for the HL-LHC IT BPMs is under development. It will be based on nearly-direct digitization by an RF System-on-Chip (RFSoc) [5]. This unique family of integrated circuits combines a set of Analogue-to-Digital Converters (ADC), Digital-to-Analogue Converters (DAC), Programmable Logic (PL) and several embedded CPUs, referred to as the Processing System (PS), on a single die. Each of the 8 ports of each BPM will be connected to a dedicated RFSoc 14 bit ADC channel sampling at 5 GSa s^{-1} . The acquisition electronics and signal processing software will use this raw data to compute the beam position applying a correction algorithm to minimize the parasitic contribution of the other beam as well as taking into account the BPM rotation, non-linearity and scaling factors.

ACQUISITION ELECTRONICS DESIGN CRITERIA

The final specification for the HL-LHC IT BPMs is not yet available but some preliminary design criteria have been set to guide the design of the future acquisition electronics.

The HL-LHC beam will consist of up to 2808 bunches spaced by multiples of 25 ns with intensities spanning close to two orders of magnitude from 5×10^9 up to 2.2×10^{11} charges. However, for most common operational scenarios it is assumed that the intensity of bunches within the same beam might vary by a factor of four, while the ratio of bunch intensity between the two beams can reach a factor of ten. HL-LHC bunches are not expected to be longer than 1.2 ns (4σ) but for some special operational modes the BPM system should be able to measure bunches as short as 0.5 ns.

* douglas.bett@physics.ox.ac.uk

HARMONIC BASED BEAM POSITION MEASUREMENTS ON DEBUNCHED BEAMS

M. Bozzolan[†], CERN, Geneva, Switzerland

Abstract

In some accelerator environments, e.g. in linear accelerator (LINAC), the beam position is measured with a BPM operating at one particular strong harmonic component present in the beam signal. This approach has limitations once the beam gets debunched and the harmonic components drops. Nevertheless, from a signal processing point of view the signal-to-noise ratio can be still acceptable with highly debunched beams, leading, in principle, to a reasonable, even if degraded, position measurement. A simplified beam transport model developed for the CERN BI transfer line between LINAC4 and the PS Booster demonstrates, that in some case, the harmonic component cannot be used anymore for position measurement despite the fact it is still significative in amplitude.

INTRODUCTION

Beam Position Monitors (BPMs) are one of the most used instruments in a particle accelerator. Their main functionality is the monitoring of the beam trajectory in linear accelerators (LINACs) and transfer lines and the closed orbit in circular machines. In addition, BPMs can provide other beam parameters such as beam intensity, kinetic energy and longitudinal distribution.

The basic idea of most BPM is to measure the image current flowing on the conducting beam pipe [1]. Typically, for the estimation of the transverse beam position, a set of two opposite electromagnetic pickups or electrodes is used, for the horizontal and the vertical plane.

Different types of BPM pickups exist and, depending on the machine and the required measurements, a specific BPM type is chosen accordingly.

The signals at the BPM electrodes can be degraded by electromagnetic interference of nearby devices. Also, depending on the BPM type, its signal can be corrupted by beam loss and secondary emitted particles. If the beam has a fixed pattern, this feature can be exploited in order to mitigate these effects. For example, in LINACs, where the acceleration process bunches the beam at a rate defined by the frequency of the accelerating cavities, the signals present strong components at the harmonics of the RF frequency. In this case, the receiver could be tuned at a single harmonic and use the envelope of the received signal for the position estimation.

CURRENT HARMONICS OF A GAUSSIAN BEAM

Assuming a train of bunches with a Gaussian longitudinal distribution [2], with individual bunch charge q , spaced by $T=1/f_{RF}$, the beam current intensity is

$$I(t) = \frac{q}{\sqrt{2\pi}\sigma} \sum_{n=-\infty}^{+\infty} e^{-\frac{(t-nT)^2}{2\sigma^2}} \quad (1)$$

and the harmonics can be made explicit by expanding the summation using the cosine series[§]

$$I(t) = I_0 \left[1 + \sum_{n=1}^{+\infty} K_n \cos\left(\frac{2\pi n t}{T}\right) \right] \quad (2)$$

where I_0 is the DC beam average current and

$$K_n = e^{-\left(\frac{\omega_{RF} n \sigma}{\sqrt{2}}\right)^2} \quad (3)$$

CURRENT HARMONICS OF A NON-GAUSSIAN BEAM

In the case of non-Gaussian longitudinal distribution, the same expansion in cosine series as with the Gaussian beam can be made, but with the difference that one or more harmonics can vanish and hence cannot be used.

For example, a train of rectangular square bunches of duration W and period $T=1/f_{RF}$ is described by Eq. (2) with

$$K_n = \text{sinc}\left(\frac{n\pi W}{T}\right) = \frac{\sin\left(\frac{n\pi W}{T}\right)}{\frac{n\pi W}{T}} \quad (4)$$

vanishing for pulse duration W multiple of T/n [2]. This means that for specific bunch lengths the signal from the electrodes of a BPM pickup will not have the f_{RF} harmonic component

In practice this condition can be reached along the transfer line of LINACs where the beam energy spread associated with the non-relativistic beam energy, and space charge effect, results in increasing long bunches. This debunching process also modifies the shape of the longitudinal bunch distribution so that the harmonic vanishing can happen even if a Gaussian beam is injected into the line.

Furthermore, a so called “de-buncher cavity” can be present at the end of a LINAC in order to provide the energy spread demanded by the downstream machine, which causes the vanishing of the harmonic content at a range of locations depending on the settings of this cavity.

[†] michele.bozzolan@cern.ch

[§] Cosine series can only be used for even functions but it's not reducing generality

PERFORMANCE OF BPM READOUT ELECTRONIC BASED ON PILOT-TONE GENERATOR AND A MODIFIED LIBERA SPARK AT ALBA

L. Torino*, U. Iriso, ALBA-CELLS, Cerdanyola del Vallès, Barcelona, Spain

Abstract

As many synchrotron radiation sources, ALBA is also going through an upgrade project. At the same time, the world of BPM electronic is evolving fast to keep up with the stringent requirement of new facilities. In order to follow the situation closely and develop know-how for the future, we decided to install and test in our storage ring a BPM readout system composed by a Pilot-Tone generator (developed by Elettra) and a modified Libera Spark (by Instrumentation Technologies). We compare position measurement results and stability with the ones obtained by our standard Libera Brilliance and a Libera Brilliance+ electronics.

INTRODUCTION

As other third generation Synchrotron Light Sources, ALBA [1] is also starting its upgrade project which will lead to the new ALBA-II machine [2]. In this frame, an upgrade of the BPMs readout system, composed nowadays by Liberas Brilliance [3], will be needed and, for this reason, alternative electronics are being studied. In particular, the system proposed by ELETTRA in collaboration with I-Tech has been tested at ALBA storage ring. The system is based on the idea of using a Pilot-Tone signal (PT) to calibrate online fluctuations related to external factor acting on cables and readout electronics [4].

This method is intended to avoid the use of quasi-crossbar switches which are now running in Libera Brilliance and Libera Brilliance+ electronics to minimize effects of the electronics on the beam measurement [3]. Main disadvantages of this compensation technique are that:

1. signal pollution due to cables is not kept into account for the compensation;
2. the switching mechanism generates glitches in the Fast Signal and might compromise the final position measurement.

Both these disadvantages may be solved using the PT method.

PILOT-TONE + LIBERA SPARK

The system is composed by a PT generator and a modified Libera Spark. The PT generator produces a sinusoidal RF signal at a frequency close to the RF frequency. The PT signal is injected after each BPM buttons in order to pass along all the electronics path.

The idea is that, since the beam and the PT frequencies are similar, any fluctuation induced by variation in the electronics path will be similar for both signals. Moreover, since

frequencies are slightly different, it is possible to separate the responses of the two signals thanks to Fourier analysis, and to compensate the Raw Signal coming from the beam with using the one of the PT [5].

The PT generator, designed by ELETTRA, is optimized to produce frequencies close to the 499.65 MHz of ALBA RF frequency. It is powered over Ethernet and can easily be located inside the tunnel and controlled via a Tango device. The signal is splitted and added to the beam signal inside the generator. It is possible to regulate the amplitude of the PT signal in order to have it similar to the one produced by the beam. Also, individual output attenuator can be set for each channel.

The Libera Spark has been modified in order to be able to actually see the PT signal: to do so, saw filters at the entrance of the electronics were removed. As a downside, the removal of these saw filters makes impossible to perform measurements during single bunch operation. Saw filters, apart from filtering, also have the function of spreading the single bunch signal over several ADC samples. This allows the signal processing for this operation mode, which is not measurable using this technique nowadays.

Libera Spark software has been modified to separate beam and PT signal through Fourier analysis and to finally calculate the compensated data. The device server provided by I-Tech, shows:

- Raw Signal: Sum of PT and Beam signal as passing through the whole electronics.
- PT Signal: PT signal resulting after Fourier analysis of the Raw Signal inside the Libera.
- Compensated Signal: obtained by compensating the Raw Signal using the PT one.

At ALBA the RF frequency is 499.654 MHz. The PT frequency is set to be 501.41 MHz. The ADC of the modified Spark, adjusted for ALBA, under-samples these signals with a frequency of 118.2217 MHz. The resulting intermediate frequencies for the beam and the PT are $if_{RF} = 26.76$ MHz and $if_{PT} = 28.52$ MHz. The plot of the Fourier transform of the Raw Signal for each of the four BPMs buttons is presented in Fig. 1, two main peaks are present at if_{RF} and if_{PT} .

CONFIGURATION

The PT generator has been located in the tunnel and connected to a spare BPM. In order to have consistent results, data has been compared to the one obtained from a second and a third BPM connected respectively to a Libera Brilliance and a Libera Brilliance+.

* Itorino@cells.es

EPU-PBPM WITH CVD-DIAMOND BLADE AT PLS-II

J. Ko*, D-T. Kim, G. Hahn, S. Shin and T. Ha

Pohang Accelerator Laboratory, POSTECH, Pohang, Republic of Korea

Abstract

All 18 photon beam position monitors (PBPM) installed on the PLS-II are tungsten blade types. The elliptical polarized undulator (EPU) has the characteristic that the spatial profile of the beam varies depending on the polarization mode. This is related to the thermal load of the blade and therefore changes in blade material are inevitable on fixed blades. In this paper, we analyze power density and flux density according to EPU mode and describe the process of installing new PBPM with CVD-diamond blades on the PLS-II EPU beamline for the first time.

INTRODUCTION

The Pohang Light Source II (PLS-II), a third-generation synchrotron-radiation source, has been operational since 2013, with electron-beam energy of 3 GeV and natural emittance of 5.8 nm-rad [1]. The maximum average beam current stored in the storage ring is 400 mA and operates in top-up mode to achieve stable electron-beam orbit as well as synchrotron-radiation flux. Currently, a total of 35 beamlines including 19 insertion-device beamlines are in operation for user service.

One of the major operational issues in electron-storage ring as a light source is the stability in the transverse position for the photon beam as well as the electron beam. To monitor the transverse position of the photon-beam the PLS-II installs 18 photon-beam position monitors (PBPM) at the front-end of the beamline. 13 of these operate on the planar undulator beamline and 5 on the bending magnet beamline. A pick-up usually has two or four blades. For beamlines using BM as a light source, it has two blades. For the blades, 0.5 mm-thick tungsten plates are used, which are installed on the top and bottom of the detector head [2].

For beamlines using an elliptically polarized undulator (EPU) as a light source a new type of PBPM is required. Because the spatial profile of the beam varies with the polarization of light, the blade can cut a large part of the photon beam from EPU. Thus, structural changes of the blades due to thermal loads could cause a problem because the existing blades are optimized for photon beams from bending magnets and planar undulators. Thus we built the new type of PBPM for EPU beamline (EPU-PBPM) invented by the Taiwan Light Source (TPS) [3]. In this paper, an analysis is described to verify that this EPU-PBPM satisfies the characteristics of the PLS-II EPU source.

DESIGN OF EPU-PBPM

Table 1 shows the parameters according to the polarization of EPU72 which is the light source of 10A1-Soft X-ray

* kopearl@postech.ac.kr

Nanoscopy beamline (BL10A) at PLS-II. EPU72 with a length of 2.6 m was divided into 72 mm intervals. Figure 1 shows a schematic diagram of the pick-up of EPU-PBPM, which is installed at the front-end 10 m away from EPU72. The blade spacing is 5 mm horizontally and 3 mm vertically. And the blades of EPU-PBPM were decoupled horizontally, this structure may be useful to suppress the cross-talk effect of scattered beams affecting the opposite blade.

Table 1: PLS-II BL10A EPU72 Parameters

	Hor. mode	Cir. mode	Ver. mode
$B_x(T)$	0	0.48	0.6
$B_y(T)$	0.79	0.48	0
K_x	0	3.24	4.09
K_y	5.33	3.24	0
Total power (kW)	3.30	2.44	1.94

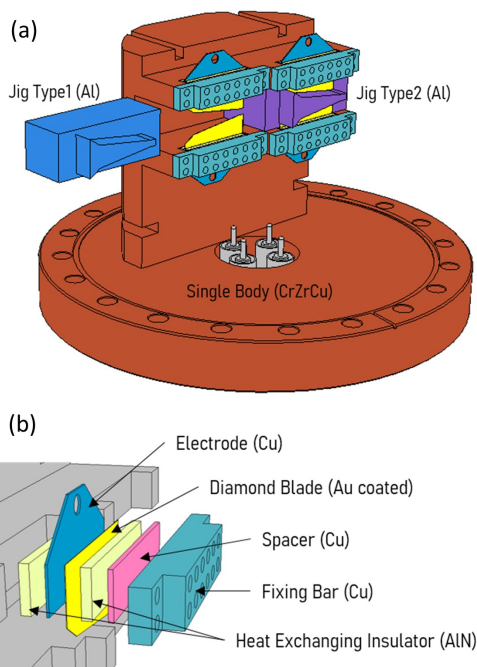


Figure 1: (a) A schematic diagram of the structure of the pick-up of EPU-PBPM. (b) Layered construction of blades.

ANALYSIS OF EPU-PBPM

Power Density

The power density according to the mode is shown in Figure 2. These properties were calculated using SPECTRA code [4]. Angular power density can evaluate the thermal

DEVELOPMENT OF 8 STRIPLINE BPM FOR MEASUREMENT OF MOMENTUM SPREAD OF ELECTRON BEAM AT INJECTOR TEST FACILITY OF POHANG ACCELERATOR LABORATORY

C. Sung, S. Kim, B. Shin, M. Chung*

Ulsan National Institute of Science and Technology, Ulsan, Republic of Korea
I. Nam, C. Kim, Pohang Accelerator Laboratory, Pohang, Republic of Korea

Abstract

A stripline beam position monitor has been developed with 8 feedthroughs in order to nondestructively measure the momentum spread of beam. The beam momentum spread causes the variation of transverse beam width at a dispersive section and can be detected by the multipole moment based analysis of the beam-induced electromagnetic field. The feasibility of such a device will be tested with electron beam generated in the beamline of Injector Test Facility (ITF) at Pohang Accelerator Laboratory (PAL). The experimental preparation with electron beam test will be presented and the future plan for an application to bunch compressors at X-ray Free Electron Laser (XFEL) of PAL will be followed.

INTRODUCTION

A beam position monitor was proved that it enables to non-destructively measure an energy spread of an electron beam with multi-striplines by T. Suwada *et al.* [1]. At a dispersive section such as a bending point with dipole magnet, the transverse beam width is varied in the bending plane depending on a momentum spread of beam so that the quadrupole moment becomes non-negligible in the transverse plane. R. H. Miller demonstrated the beam position monitor can be used to measure the quadrupole moment [2].

The 8-stripline BPM has been developed to non-destructively control the momentum spread of electron beam for X-ray Free Electron Laser at Pohang Accelerator Laboratory (PAL-XFEL). The striplines were designed to match the characteristic impedance as 50Ω following [3, 4]. It is tested with a conducting wire and thin Cu sheet for the resolution to quadrupole moment before the electron beam test.

Beam dynamics simulations were also performed to predict the relation between the quadrupole moment and momentum spread of PAL-XFEL electron beam with the ELEGANT [5].

The device is implemented for the electron beam test at the Injector Test Facility (ITF) of PAL [6]. The PAL-ITF consists of a photocathode RF gun, a booster cavity (accelerates up to 70 MeV), dipole and quadrupole magnets within about 10 meter space [7].

MOMENTUM SPREAD AND MULTIPOLE MOMENT ANALYSIS

When the particle beam travels at a dispersive section such as a dipole magnet, the path length of particles differ with its longitudinal momentum so that the transverse distribution will be changed at the exit. For example, if a particle is bent in the horizontal plane (x), the particle position will be changed as

$$x_f = x_i + D_x (\Delta P_x / P_0). \quad (1)$$

with x_i, x_f for the initial and final horizontal positions. D_x is the dispersion function at dispersive section and $(\Delta P / P_0)$ is the fraction of momentum deviation to the total momentum, P_0 .

The difference of squared RMS beam size defines a quadrupole moment and it can be written as

$$\sigma_x^2 - \sigma_y^2 = \beta_x \epsilon_x - \beta_y \epsilon_y + D_x^2 \langle (\Delta P / P_0)^2 \rangle. \quad (2)$$

where $(\sigma_x^2 - \sigma_y^2)$ in the L.H.S is the quadrupole moment. In the R.H.S, the β_x, β_y are the beta functions in x and y direction. ϵ_x, ϵ_y are the RMS emittances in x and y directions, respectively, and $\langle (\Delta P / P_0)^2 \rangle$ is the RMS momentum spread.

The RMS momentum spread can be figured out by the measurement of quadrupole moment defined as above non-destructively with the stripline monitor.

Multipole Moment Analysis

A charged particle beam induces an image current on a surface of surrounding conducting chamber and the image current density is described by the series representation as below

$$J = \frac{I_{\text{beam}}}{2\pi r} \left[1 + \frac{2\rho}{r} \cos(\theta - \phi) + \frac{2\rho^2}{r^2} \cos(2\theta - 2\phi) + 2 \frac{\sigma_x^2 - \sigma_y^2}{r^2} \cos(2\theta + 2\alpha) \right]. \quad (3)$$

In the Eq.(3), the (r, θ) and (ρ, ϕ) represent the position of electrode and beam centroid, respectively, and the I_0 is the beam current and α is the skew angle of transverse beam distribution.

Thus, the quadrupole moment will be reconstructed from the measurement with multiple striplines (in this proceeding,

* mchung@unist.ac.kr

DESIGN AND OPTIMISATION OF BUTTON BEAM POSITION MONITOR FOR SPS-II STORAGE RING*

S. Naeosuphap[†], P. Sudmuang, Synchrotron Light Research Institute, Nakhon Ratchasima, Thailand

Abstract

The Beam Position Monitors (BPMs) for the new Thailand synchrotron light source, Siam Photon Source II (SPS-II), has been designed utilizing as the essential tool for diagnosing the position of the beam in the storage ring. Its design with four-button type BPM has been optimized to obtain the high precision of position data in normal closed orbit and feedback mode as well as turn by turn information. We calculate feedthroughs capacitance, sensitivities, induced power on a 50 Ω load, and intrinsic resolution by using Matlab GUI developed by ALBA, to find the appropriate position, thickness, and gap of the BPM button. Extensive simulation with the electromagnetic simulation packages in CST Studio Suite was also performed to investigate the dependence of the induced BPM signal, wakefield, Time Domain Reflectometry (TDR), and power loss on different BPM geometry.

INTRODUCTION

Four-button pick up electrodes have designed for a stable and precise beam position monitor in the SPS-II storage ring. They are an essential part to provide information about the position of the beam in the vacuum chamber during machine commissioning, beam tuning and routine operation. The preliminary design of the button electrode is performed by using ALBA/DIAMOND Matlab tool [1]. The button diameter, thickness and the gap between button and chamber wall are necessary to optimize for archiving low power losses, high signal transmission, Time Domain Reflectometry (TDR), Thermal transferring and proper impedance matching. These simulations are performed by using simulation packages in CST Studio Suite. [2]. The model was used in the simulation shown in Fig. 1.

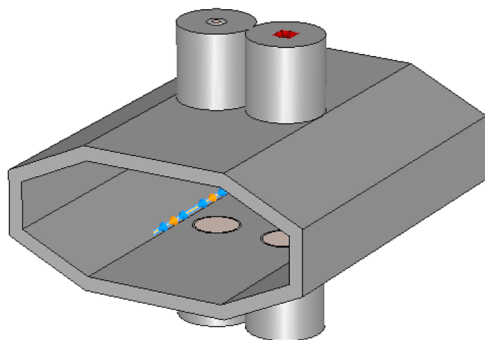


Figure 1: A simulation model of SPS-II storage ring BPM.

SPS-II BPM REQUIREMENT

The SPS-II storage ring consists of 14 Double Triple Bend Achromat (DTBA) cells and each cell is equipped with 10 BPMs. In total, there are 140 BPMS utilized for the machine operation. Since the beam size at the center

of an IDs is approximately 2.6 μm, the beam position stability of 0.2 μm level needs to be obtained. The BPM button geometry, especially for button diameter has been considered to provide about 100 nm position resolution at 100 mA and 2 kHz bandwidth.

GENERAL CONSIDERATION OF BPM BUTTON

The BPM chamber has been modeled based on a standard storage ring vacuum chamber which is designed as an octagonal shape with a vertical inner aperture of 16 mm, a horizontal inner aperture of 40 mm and sides of 6.6 mm. To achieve the required resolution, the calculation of sensitivity, signal power and intrinsic resolution are performed by using Matlab tool. This software can study the basic geometries and related parameters of BPM at a preliminary design phase. The goal of this calculation is to optimize the button diameter, button gap and thickness, as well as the button separation on the storage ring vacuum chamber.

Mechanical Design

In order to achieve sufficient induced power, sensitivity, and mechanical limitation of the storage ring vacuum chamber the BPM button diameter is considered to be 6 mm. The gap size between button electrode and housing should be smallest as possible as a mechanical limitation, to increase the button capacitance and shifts the high order modes (HOM) resonances to higher frequencies [3]. The trapped HOMs can be caused by beam instabilities and will leak inside the button when the button thickness is too thin. To avoid this issue, we considered increasing the button thickness to be 4 mm. Design parameters of the SPS-II button pick up electrodes are shown in Table 1.

The simulation results of sensitivity, signal power and intrinsic resolution are shown in Fig. 2. To obtain the horizontal and vertical sensitivities (S_x and S_y), a Delta over Sum method is used [4], the slope at no beam displacement gives us the S_x and S_y is 0.1359 and 0.1343, respectively. Considering a bandwidth of 2 kHz, which is the expectation value for a fast orbit measurement system, the calculated intrinsic resolution of the BPM button at 100 mA beam current is 14.63 nm, which meets the specific requirements for the measurement resolution.

Table 1: Preliminary Design Parameters for the SPS-II BPM Button

Button calculation parameters (mm)	
Button diameter	6
Button thickness	4
Button gap	0.3
Button separation	10.5

TESTS OF A NEW BPM LONG TERM DRIFT STABILIZATION SCHEME BASED ON EXTERNAL CROSSBAR SWITCHING AT PETRA III

G. Kube, F. Schmidt-Föhre, K. Wittenburg, Deutsches Elektronen-Synchrotron DESY, Germany
 A. Bardorfer, L. Bogataj, M. Cargnelutti, P. Leban, P. Paglovec, B. Repič, I-Tech, Solkan, Slovenia

Abstract

For the new PETRA IV project at DESY, about 800 high resolution BPMs will be installed with the readout electronics system based on MTCA.4 as technical platform. In order to fulfill the requested long-term drift requirement to be less than 1 micron over a period of six days (one week of user operation), due to the machine-specific geometry the BPM cable paths have to be stabilized in addition. To achieve this demand, the well proven concept of crossbar switching was extended such that the analogue switching part is separated from the read-out electronics and brought as close as possible to the BPM pickup. This contribution summarizes first proof-of-principle measurements which were performed at PETRA III using a modified Libera Brilliance+ with external switching matrix. These measurements indicate that the concept of external switching works well and that the performance of this modified test setup fulfills the specifications.

INTRODUCTION

The PETRA IV project at DESY aims to upgrade the present synchrotron radiation source PETRA III into an ultralow-emittance source which will be diffraction limited up to X-rays of about 10 keV [1]. Using a hybrid six bend achromatic (H6BA) lattice with a unit cell providing an emittance of 45 pm rad, the target emittance of about 20 pm rad will be recovered by a large number of damping wigglers distributed in the short straights of the octants not equipped with user beamlines [2]. This small PETRA beam emittance translates directly into much smaller beam sizes of 7 μm in both planes at the insertion device source points, thus imposing stringent requirements on the machine stability. In order to measure beam positions and control orbit stability to the requisite level of accuracy, a high resolution BPM system will be installed which consists of about 800 individual monitors with the readout electronics based on MTCA.4 as technical platform.

In Table 1 the BPM readout specifications are summarized. As demonstrated already in Refs. [3, 4], the listed requirements are achievable with the commercial Libera Brilliance+ (LB+) system [5]. However, in order to fulfill the requested long-term drift requirement for the case of PETRA IV, the specific machine geometry has to be taken into account. Originally, PETRA was built in 1976 as an e^-/e^+ collider for high-energy physics, later on acting as pre-accelerator for the hadron-electron ring accelerator HERA, then converted into the 3rd generation synchrotron light source PETRA III which started operation in 2009 [6]. Due to the history as high-energy physics collider, the PETRA machine circumference of 2304 m is much larger compared

Table 1: Readout electronics specifications. The single bunch / turn resolution holds for 0.5 mA bunch current, the closed orbit one for 1 kHz bandwidth, the beam current dependency for a 60 dB range with centered beam, and the long term stability should be measured over 6 days and a temperature span of ± 1 deg within a stabilized rack.

Requirement	Value
single bunch / single turn	< 10 μm
closed orbit resolution	< 100 nm (rms)
beam current dependence	$\pm 2 \mu\text{m}$
long term stability	< 1 μm

to light sources built in the last two decades, and the machine infrastructure is distributed in the former experimental halls with the result of long cable lengths between monitor and readout electronics. Driven by considerable cost saving, the plan for PETRA IV is to reuse again the existing ring tunnel in the areas between the experimental halls as shown in Fig. 1. However, the tunnel cross section is too small for housing all required cables, i.e. it will not be possible to interconnect BPM pickups in the accelerator with their corresponding readout electronics in an experimental hall using cable paths inside the accelerator tunnel. As consequence, additional cable access shafts will be required to minimize the arising load inside the tunnel, and it is not guaranteed that cable routing will be in a perfectly stabilized temperature and humidity environment, thus affecting the BPM position readings [7, 8]. Therefore, in order to fulfill the requested long-term drift stability the BPM cable paths have to be stabilized in addition.

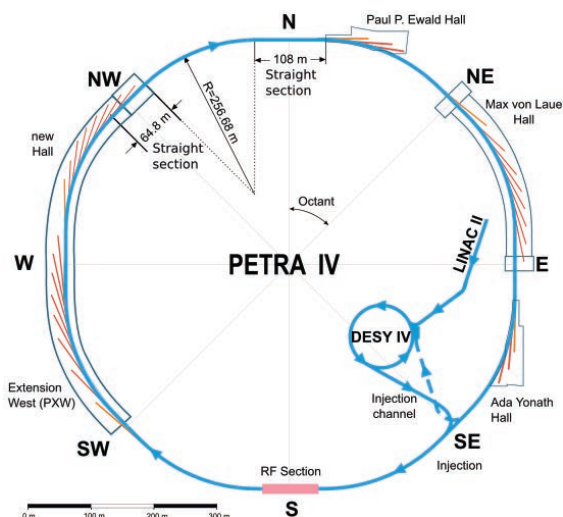


Figure 1: Layout of the PETRA IV facility.

PRELIMINARY STUDIES FOR THE SOLEIL UPGRADE BPM

M. El Ajjouri, N. Hubert, A. Gamelin, P. Alves, Synchrotron SOLEIL, 91192 Saint-Aubin, France

Abstract

Synchrotron SOLEIL is currently preparing a machine upgrade based on multibend achromat lattice with a drastically reduced horizontal electron beam emittance ($<100 \text{ pm}\cdot\text{rad}$). Foreseen quadrupole and sextupole strengths will impose a small vacuum chamber diameter and the future Beam Position Monitors (BPM) will have a 16 mm inner diameter (circular shape). To minimise the BPM contribution to the longitudinal impedance, and induced heating on their mechanics, the feedthrough and button shapes must be optimised. This paper summarises the systematic electromagnetic simulations that have been carried on in order to distinguish the effect of single dimension changes (such as button thickness and shape, ceramic thickness and diameter) on the amplitudes and frequency position of the resonances. It also introduces the preliminary BPM design for the SOLEIL upgrade project.

INTRODUCTION

Synchrotron SOLEIL has recently published the Conceptual Design Report (CDR) of the SOLEIL Upgrade [1]. The specifications are challenging for the new beam parameters especially the beam size and emittance below 100 pm rad (Fig. 1). The energy will remain the same as today (2.75 GeV). The project includes considerable modification of the accelerator and especially the replacement of the storage ring for a new multi bend achromat lattice. Natural bunch length will be 9 ps RMS, lengthened to 30 ps RMS by a harmonic cavity to preserve the transverse emittance and beam lifetime.

The main parameters of the SOLEIL upgrade SR and the existing SOLEIL SR are compared in Table 1.

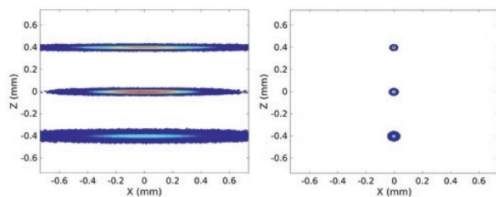


Figure 1: Comparison of the transverse beam profiles (x: horizontal, z: vertical plane) of the present SOLEIL (left) for 3 types of straight sections (short, medium and long / plots shifted for convenience) with 1% coupling and SOLEIL upgrade CDR reference lattice (right) with 50 pm.rad emittance.

Table 1: Main Parameters of the Present and CDR Reference Lattice

	<i>SOLEIL</i>	<i>SOLEIL Upgrade</i>
Circumference (m)	354.097	353.74
Beam energy (GeV)	2.75	2.75
maximum beam current (mA)	500	500
Natural emittance (pm.rad)	3900	80
Bunch length rms (ps)	15	9
BPM vacuum chamber (mm)	70/25	16
Number of BPM	122	~200

The SOLEIL upgrade project pushes the vacuum system conception to a new limit: the high gradient quadrupoles and the large strength of the sextupoles require the minimum size of the vacuum chamber inner diameter to be as low as 12 mm.

BPM SPECIFICATION AND CHALLENGING

The Beam Position Monitor (BPM) system is the largest (and one of the most critical) diagnostic systems for a synchrotron light source: about 200 position measurement units are considered in the CDR reference lattice. The system should deliver beam position measurement with a resolution of less than 50 nm RMS in closed orbit measurement (used for feedback loops). The measurement stability is also very important with a drift that must be below 1 μm over 24 hours. The BPM sensors for the SOLEIL upgrade will be the usual RF button pickups installed at 45° on the vacuum chamber. In order to protect the BPM from possible heating due to synchrotron radiation, its internal diameter is enlarged to 16 mm. The challenge will be the manufacturing of a small dimension pickup and its positioning on the BPM body with respect to tight tolerances in order to maintain an absolute position.

FIRST 2D SIMULATIONS

Preliminary studies have been carried out to design the future BPM pickups. With the usual delta over sum equation used to compute the position, the response is linear on a $\pm 1 \text{ mm}$ range around the BPM center with an on-axis error below 3 % (Fig. 2). We can consider a polynomial response to enlarge the linear range if needed for machine physics studies at large amplitude.

BPM SYSTEM FOR THE PIP-II INJECTOR TEST FACILITY*

N. Eddy[#], J. Diamond, B. Fellenz, R. Santucci, A. Semenov, D. Slimmer, D. Voy,
Fermilab, Batavia, IL 60510, USA

Abstract

A new BPM system was used for commissioning and operation of the PIP2 Injector Test Facility. The system of 13 warm and 12 cold BPMs was based upon custom 250 MS/s digitizers controlled and readout over gigabit ethernet by a single multi-core rackmount server running linux. The system provided positions, intensity, and phase for each bpm as a pulse average or pulse waveform from 10 μ s to 4.4 ms at a 20 Hz pulse repetition rate.

INTRODUCTION

The PIP-II Injector Test facility was developed to perform an integrated test for the front-end of the PIP-II linac upgrade project at Fermilab [1]. The beamline shown in Fig. 1 includes the warm front-end consisting of the ion source, low energy beam transport (LEBT), radio-frequency quadrupole (RFQ), and the medium energy beam transport (MEBT) sections. It also includes the first two superconducting cryomodules consisting of the half-wave resonator (HWR) module and the 1st single spoke resonator (SSR1) module which are followed a high energy beam transport (HEBT) section with diagnostics and beam dump. The PIP-II Injector provides bunched beam out of the RFQ at 162.5 MHz with pulse lengths from 10 μ s to 4 ms at up to a 20 Hz pulse repetition rate with up to 10 mA instantaneous beam current.

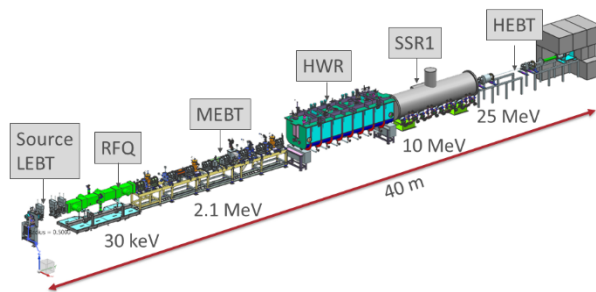


Figure 1: Beamline layout of the PIP-II Injector Test Facility.

After the RFQ, there are 9 warm button BPM pickups in the MEBT section, then 8 cold button BPM pickups in the HWR, 4 cold button BPM pickups in the SSR1, and 4 warm button BPMs in the HEBT. A completely new data acquisition system was developed for the final PIP-II Injector Test run in 2020.

BPM SYSTEM

The new readout electronics are shown in Fig. 2. The main components of the new system are analog signal conditioning modules, custom digitizer modules, a commodity rackmount PC, and Gigabit ethernet control and readback for the system via a standard Gigabit switch.

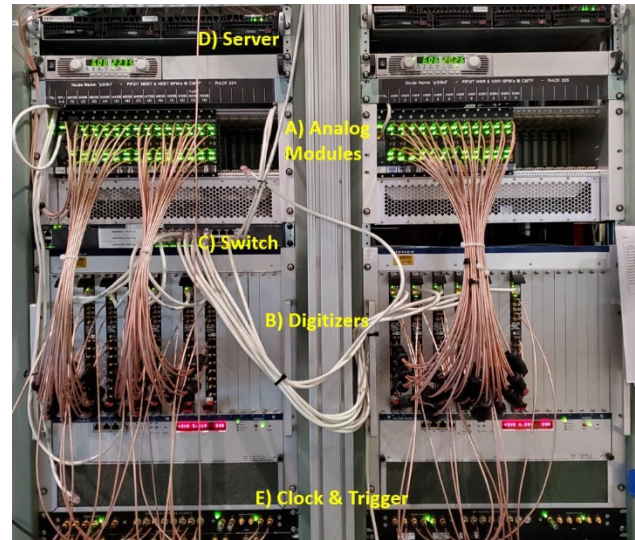


Figure 2: The PIP-II injector test BPM electronics.

Analog Signal Conditioning Module

The Analog Signal Conditioning Modules provide filtering and signal level control (see Fig. 3). There is a 500 MHz low pass filter and programmable 0-32db in 0.5db steps attenuator at the input. A removable daughter card handles the filtering. For PIP-II Injector Test, the daughter card splits the signal to provide band pass filters for both the 1st and 3rd beam harmonics at 162.5 MHz and 487.5 MHz. The daughter card also provides programmable high (26db) and low (6db) gain for each signal path. There is also a variable gain amplifier on the board output with 64 settings from 0-31db. The modules reside in two Eurocard crates which each have a controller board. All settings on each analog module are controlled via ethernet by a raspberry-pi module on the controller board.

* This work was supported by the DOE contract No.DEAC02-07CH11359 to the Fermi Research Alliance LLC.

[#] eddy@fnal.gov

PERFORMANCE OF THE SLAC-PAL-VITZROTECH X-BAND CAVITY BPMs IN THE LCLS-II UNDULATOR BEAM LINES*

Christopher Nantista†, Patrick Krejcik, Bobby McKee, Andrew Young, Sonya Hoobler, Dennis Martinez-Galarce and Michael Rowen, SLAC National Accelerator Laboratory, Menlo Park, U.S.A.
Changbum Kim, Pohang Accelerator Laboratory, Pohang, Korea

Abstract

The hard X-ray and soft X-ray undulator beamlines of the LCLS-II X-ray FEL incorporate 65 X-band cavity beam position monitors for accurate tracking of the electron beam trajectories and Beam-Based Alignment. For this crucial function, a design was jointly developed between PAL and SLAC, consisting of a monopole reference cavity and a dipole position cavity, with signals coupled out through coaxial vacuum feed-throughs. For the relatively large quantity needed, the production of completed units was contracted to the Korean company Vitzrotech, who developed the manufacturing process to successfully fabricate the needed quantity. Herein, an overview is given of the production experience, tuning, installation and performance of these devices.

INTRODUCTION

The LCLS-II free electron laser at SLAC requires monitoring of the beam position with sub-micron level resolution in both x and y . The device chosen by the project to achieve this is an X-band cavity beam position monitor, or RFBPM, of a unique configuration whose design was developed over the last couple of decades [1-3]. It consists of two independent resonant cavities, dipole and reference, with signals coupled out through coaxial vacuum feed-throughs. A distinguishing feature benefiting sensitivity is the magnetic coupling of the dipole cavity fields into side waveguide stubs in a way that shields the pickups from the monopole mode [4]. The design adopted had been recently deployed in the PAL-XFEL in Pohang, Korea. For production of the 65 units required in the soft X-ray and hard X-ray undulator beamlines of LCLS-II, the technology was transferred to the Korean industrial firm Vitzrotech in Gyeonggi-do. The full complement of RFBPMs was completed, installed and recently commissioned at SLAC.

DEVICE DESCRIPTION

Developed through a Cooperative Research and Development Agreement (CRADA), with final design by PAL, the 10 cm beamline device passes the beampipe through two resonant pillbox cavities (Fig. 1a). As sensitivity roughly scales with wavelength, an X-band cavity frequency of nominally 11.424 GHz was chosen, equal to four times that of the SLAC normal conducting and PAL S-band linacs. The main cavity operates in the TM_{110} mode. Each polarization component, excited by either an x or y offset of the beam, couples through its radial magnetic field into

a pair of slot-coupled longitudinal waveguide stub resonators. Capacitive probes couple signal out through coaxial feedthroughs brazed into the sides of these in a pin-wheel pattern. The smaller second cavity, excited on axis in the fundamental TM_{010} mode, provides a phase reference for the sign of the position cavity signals and an amplitude reference for their bunch charge dependence. Its signal is coupled out through a pair of coaxial feedthroughs magnetically coupled through the edge of its end wall.

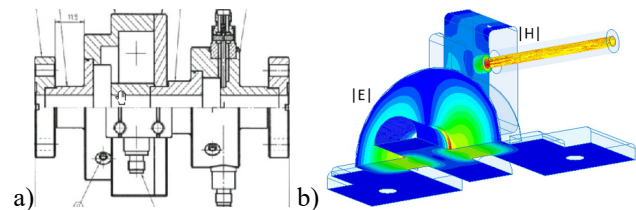


Figure 1: a) cutaway and external view of RFBPM geometry and b) field simulation of dipole cavity coupling.

Two feedthroughs couple to each of the three cavity modes. Each incorporates a ceramic coaxial vacuum window. Four threaded tuning pins are provided around the edge of each cavity at the 45° positions. Split-ring collars are used with special tuning tools to provide push-pull capability on these pins for fine-tuning of the cavity frequencies (Fig. 2b).

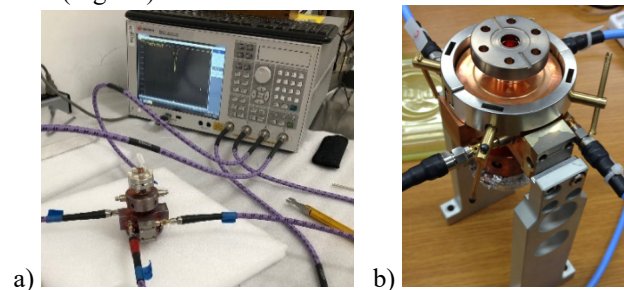


Figure 2: a) RF testing on 4-port network analyzer and b) fine tuning of cavity with tuning collar and tools.

PRODUCTION EXPERIENCE

After an initial 3 prototypes were received and one was beam tested, fabrication of production units began at Vitzrotech, in batches of about 15–25. Upon receipt of each batch, acceptance testing at SLAC would proceed via mechanical inspection, vacuum testing and RF characterization (Fig. 2a). Over the 2–3 year production span, with roughly a hundred units produced, problems were encountered and overcome by the vendor, with advisory input from SLAC and from PAL via regular video meetings and a couple of factory visits.

* Work supported by U.S. Department of Energy under Contract Numbers DE-AC02-06CH11357.

† nantista@slac.stanford.edu

COMMISSIONING AND RESULTS OF SPIRAL2 BPMs

C. Jamet, P. Legallois, GANIL, Caen, France

Abstract

Construction of a new accelerator is always an opportunity to face challenges and make new developments. The BPM diagnostics installed in the SPIRAL2 linac and the associated instrumentation are part of these developments. BPM instrumentations are, of course, used to measure positions and phases of ion beams but also transverse shapes, called ellipticity, as well as the beam velocity. Specifications involve knowing and calculating the sensitivities in position and in ellipticity as a function of the beam velocities. These impose small amplitude differences between channels, which require precise calibration of electronics. This paper describes the modelling and analysis of the BPM behaviour according to the beam velocity, the technical solutions, modifications and improvements. An analysis of the results and evolutions in progress are also presented.

INTRODUCTION

The SPIRAL2 accelerator is a new facility built on the GANIL site at Caen in France. The first ECR ion source produce ion beams, the second proton and deuteron beams. A CW RFQ accelerates beams with $A/Q \leq 3$ at energy of 0.74 MeV/A ($\beta \approx 0.04$). The injector commissioning took place from end 2015 to 2019 [1] with the qualification of the diagnostic monitors [2].

A high power CW superconducting linac produces up to 5 mA beams with a maximum energy of 33 MeV for protons and 20 MeV/A for deuterons. The linac is composed of 19 cryomodules, 12 with one $\beta = 0.07$ cavity and 7 with 2 $\beta = 0.12$ cavities. The HEBT lines distribute the linac beam to a beam Dump, to NFS (Neutron For Science) or to S3 (Super Separator Spectrometer) experimental rooms [3]. A proton beam at 33 MeV, 5 mA and a power of 16 kW was produced in 2020.

BPMs are installed inside quadrupoles in the warm sections of the linac between cryomodules. BPMs are composed of 4 squared electrodes with a radius of 24 mm, a length of 39 mm and an electrode angle of 60° .

LINAC CAVITY TUNING

The β values in the linac are from 0.04 up to 0.26 for the 33 MeV proton beam. The first cavity tuning step consists to tune the phase and amplitude of the cavities one by one at low beam power, the downstream cavities being detuned to avoid beam energy changes. Three BPM phase measurements, one before and two after the cavity to tune, allow to measure the beam velocity. After aligning the beam using the BPM positions, the cavity phase is scanned over 360° to find the buncher phase. Comparisons with theoretical values allow to compute the cavity voltage and phase to be applied. The second step is to match the beam to the linac with quadrupole tunings in the MEBT by an iterative process. The matching method

uses the ellipticity values given by the BPMs. The last step is to gradually increase the beam power while monitoring beam losses.

BPM SPECIFICATIONS

The BPM specifications to tune the SC linac cavities are given in (Table 1).

Table 1: BPM Specifications

Parameter	Resolution	Range
Position	+/- 150 μm	+/-20 mm
Phase	+/-0.5 deg.	+/-180 deg.
Ellipticity	+/-20 % or +/- 1.2 mm ²	

At low velocities, sensitivities in position and ellipticity are function of the beam beta and the frequency harmonic [4]. One of our objectives was to find a formula to calculate the ellipticity sensitivity correction.

BPM MODEL

Equations

Beam bunches generate a periodical beam current represented by a Fourier series [4].

$$I_b(t) = \langle I_b \rangle \left[1 + 2 \sum_{n=1}^{\infty} A_n \cos(n\omega_0 t + \phi_n) \right]$$

- I_b the beam intensity
- $\langle I_b \rangle$ the average beam intensity
- A_n the Fourier component amplitudes
- ω_0 the fundamental pulsation
- ϕ_n the Fourier component phases

The wall current density i_w , at frequency $n\omega_0/2\pi$, induced by a pencil beam on the conducting cylindrical tube is given by the equation [5]:

$$i_w(n\omega_0, r, \theta, \phi_w) = \frac{A_n \langle I_b \rangle}{\pi a} \left[\frac{I_0(gr)}{I_0(ga)} + 2 \sum_{m=1}^{\infty} \frac{I_m(gr)}{I_m(ga)} \cos(m(\phi_w - \theta)) \right]$$

- r the beam radius
- a the radius of the tube
- ϕ_w the position angle on the cylindrical tube
- θ the beam angle
- $I_m()$ the modified Bessel function of order m

With

$$g = \frac{n\omega_0}{\beta\gamma c} = \frac{n\omega_0 \sqrt{1-\beta^2}}{\beta c}$$

- λ the wave length
- γ the Lorentz factor
- $n\omega_0$ the pulsation

COMPARISON OF TWO LONG TERM DRIFT STABILIZATION SCHEMES FOR BPM SYSTEMS

Frank Schmidt-Foehre, Gero Kube, Kay Wittenburg
Deutsches Elektronen-Synchrotron, 22607 Hamburg, Germany

Abstract

For the planned upgrade of synchrotron radiation sources PETRA (called PETRA IV) at DESY a much higher beam brilliance is requested. In order to measure according beam positions and to control orbit stability to the corresponding level of accuracy, a future high-resolution BPM system has to deliver the necessary requirements on machine stability. This needs to enable long-term drift requirements of even less than 1 micron beam position deviation per week. Such a specification goal requires an additional long-term drift stabilization of the beam position monitor (BPM) readout scheme for PETRA IV, which will include a compensation of BPM cable parameter drifts. This paper discusses a comparison of two common compensation schemes using different signal conditioning features, typically needed at machine topologies with long BPM cable paths. Certain critical aspects of the different schemes are discussed in this report, while existing successful measurements are referred in some references.

INTRODUCTION

Some 3rd generation synchrotron radiation sources like PETRA III at DESY are planned to be upgraded into 4th generation low-emittance synchrotron light sources over the next years [1]. These new machines require much smaller beam sizes at the insertion device source points for generation of high brilliant photon beams. In addition, improved long-term drift performance of BPM position measurement will be needed to cope with the corresponding level of accuracy for the required control orbit stability [2, 3].

A large amount of well-known high-resolution button BPM systems will be used as workhorses around such a ring for appropriate beam position measurement and stability control (orbit-feedbacks). PETRA IV will utilize considerably long frontend cables up to 100 m for the BPM system due to:

- avoiding radiation sensitive electronics in the tunnel
- the large accelerator circumference (2.3 km)
- space limitations inside the tunnel.

The cables connect the BPMs in the tunnel with their readout electronics outside the tunnel. Certain parts of the cable will be conducted outside the tunnel under harsh, unstable environmental conditions. Compensation schemes will be used, to control the environmental impact on BPM cable parameters, resulting in long-term drifts of the measured beam position, to a sufficiently low level. These long cables, carrying sensitive analog button RF-signals, are exposed to long-term deviation of critical signal propagation properties like the relative dielectric permittivity (ϵ_r)

through drifts of environmental parameters like temperature, humidity and mechanical stability [4, 5].

The compensated signal path has to incorporate as much of the BPM cable as possible to cope for parameter deviations along this cable segment. In consequence, this needs an electronic device for handling of the compensation scheme, located at the beginning (close to the BPM) and another one at the end of the compensated signal path (e.g. included in the BPM frontend).

Two main compensation concepts and their technical implementations will be discussed below, together with their common similarities and differences, their individual pro's and con's in comparison to the needs and preferences for use in the future PETRA VI synchrotron light source [2, 3].

COMPENSATION SCHEMES

Four years ago, a new BPM frontend compensation scheme was introduced for the ELETTRA storage ring at the Sincrotrone Trieste in Italy [6-8], which has been tested and is now in use at different accelerators [9]. Meanwhile, this system is manufactured in collaboration with the Instrumentation Technologies d. d. company at Solkan, Slovenia. It is mainly used in combination with the Libera Spark readout electronics of the same company [7, 10]. This compensation scheme uses an artificial pilot tone (PT), which is added into each BPM button signal chain inside an electronic box located at the foremost coupling opportunity just behind the button output connector as shown in Fig. 1 (signal combiner/splitter combination is used for equalization of button signals here). A pre-series PT frontend has been tested in a test setup as shown in Fig. 1 in combination with the non-switching Libera Spark readout electronics at the PETRA III ring at DESY in 2019 for performance comparison against other existing BPM readout electronics (Libera Brilliance+ and Libera Brilliance) [11].

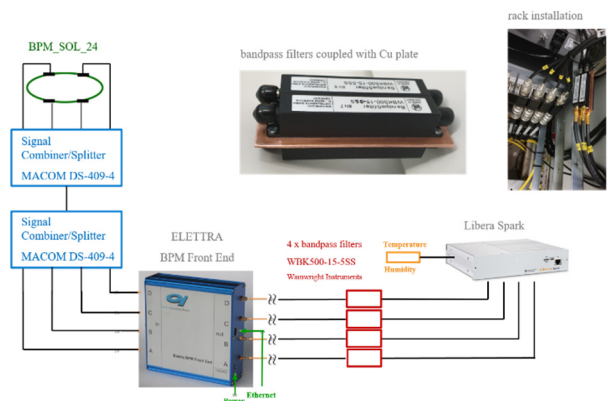


Figure 1: Button BPM setup with PT frontend and adapted Libera Spark readout electronics [11].

AN AUTOMATIC FOCALIZATION SYSTEM FOR ENHANCED RADIOISOTOPE PRODUCTION WITH SOLID TARGETS*

P. Casolaro[†], P. D. Häffner, G. Dellepiane, I. Mateu, P. Scampoli¹, N. Voeten, E. Zyaee, S. Braccini
Albert Einstein Center for Fundamental Physics, Laboratory for High Energy Physics,
University of Bern, Bern, Switzerland

¹also at Department of Physics “Ettore Pancini”, University of Napoli Federico II,
Complesso Universitario di Monte S. Angelo, Napoli, Italy

Abstract

A research program aimed at the production of novel radioisotopes for theranostics is ongoing at the 18 MeV cyclotron laboratory in operation at the Bern University Hospital (Inselspital). A method based on the bombardment of isotope enriched materials in form of compressed 6 mm diameter pellets was developed. To accomplish this challenging goal, accurate knowledge of beam energy, positioning and focusing as well as production cross sections are crucial. Investigations are carried on to assess all these items. In particular, an automatic compact focalization system was conceived and constructed to optimize the irradiation procedure. It is based on a 0.5 m long magnetic system, embedding two quadrupoles and two steering magnets, and a non-destructive beam monitoring detector located in front of the target. The profiles measured by a fiber detector are elaborated by a feedback optimization algorithm that acts on the magnets and keeps the beam focused on target to enhance the production yield. Following the first successful functional tests, the preliminary results on the production of medical radioisotopes are presented.

INTRODUCTION

Medical cyclotrons for radioisotope production are nowadays optimized for providing standard radioisotopes as the ^{18}F used in Positron Emission Tomography (PET) applications. Theranostics is a novel approach in cancer treatment based on the combined use of diagnostic (γ or β^+ emitters) and therapeutic (α or β^- emitters) radioisotopes. The production of radioisotopes for theranostics is currently a reserach topic. The University of Bern is equipped with an IBA 18/18 HC medical cyclotron for both routine production of radiopharmaceuticals and scientific research. Figure 1 shows a picture of the cyclotron and of its Beam Transfer Line (BTL), which ends in a separate bunker with independent access. Multidisciplinary research activities are carried out at the Bern cyclotron laboratory. These include the study of new radioisotopes for theranostics, radiation hardness, fundamental physics, radiation protection and particle detector physics [1].

In particular, the production of novel radioisotopes for theranostics is performed by irradiating solid targets in form



Figure 1: The Bern medical cyclotron.

of 6 mm diameter pellets made of compressed powder [2, 3]. Beams extracted from medical cyclotrons for standard radioisotope production have a typical dimension of the order of 10 mm. Thus, in order to achieve a safe, reliable and optimized production for theranostics, the beam should be focused on target over the whole irradiation. However, the focused beam is very sensitive to any beam instability due, for example, to drifts of the main coil of the cyclotron caused by the temperature increase. To address these scientific requirements, a new Automatic Focalization System (AFS) has been developed. Its operating principle as well as first functional tests carried out on a AFS-prototype installed in the BTL are presented in this work.

MATERIALS AND METHODS

The production of non-conventional radioisotopes at the Bern medical cyclotron is carried out by irradiating solid targets contained in a specifically designed target coin. It is made of two halves, typically made of aluminum, held together by permanent magnets. The overall thickness of the target coin is 2 mm. A picture of the target coin with the permanent magnets and 6 mm diameter pellet is shown in Fig. 2.

A new beam line has been implemented to enhance the performance of the production of new radioisotopes for theranostics (Fig. 3). It is made of a Mini-PET Beamline (MBL), a UniBEaM detector and a IBA Nirta solid target station.

* Work partially supported by the Swiss National Science Foundation (SNSF). Grants: 200021_175749 and CRSII5_180352.

[†] pierluigi.casolaro@lhep.unibe.ch

ANALYSIS OF MULTI-BUNCH INSTABILITIES AT ALBA USING A TRANSVERSE FEEDBACK SYSTEM

U. Iriso and T.F. Günzel
ALBA-CELLS Synchrotron, Cerdanyola del Vallès, Spain

Abstract

Since 2015 Alba is equipped with a transverse bunch by bunch feedback system, which not only damps the transverse coupled bunch instabilities in the machine, but also allows the impedance characterization of the storage ring. This characterization is produced by an internal sequence, which is programmed to excite and measure the growth and damping rates of each of the multi-bunch modes. This paper describes the measurement technique, presents the studies carried out to characterize the machine and different movable systems like the scrapers or in-vacuum undulators. Results are compared with the transverse impedance spectra obtained from computer simulations.

INTRODUCTION

Transverse betatron oscillations associated with beam instabilities limit the machine performance in current synchrotron light sources. These instabilities are driven by long range wakefields, usually trapped modes in cavity-like structures in the vacuum chamber, resistive wall (RW) impedances, and occasionally from multibunch ion instabilities when the machine vacuum is not the optimum.

Since 2015, ALBA uses the transverse bunch-by-bunch (BBB) feedback system described in [1] to damp these instabilities. It is based on the Libera BBB electronics (iTech) and controlled using the firmware and software developed at Diamond Light Source (DLS) [2,3]. This system not only allows to damp instabilities, but it also allows to program sequences that apply different control parameters at the same time as data acquisition. This is used to measure the growth rates of the individual multi-bunch modes, and so to 1) evaluate the ALBA impedance model, and 2) assess the most dangerous modes for the ALBA Storage Ring.

In this report, similarly to what is done in [4], we analyze the results of these scans for different machine configurations, like different chroms or different position of movable systems like scrapers or in-vacuum undulators (IVUs).

IMPEDANCE THEORY

For a beam with M bunches and N particles per bunch and non-zero chromaticity ξ , the complex frequency shift of mode (m, l) is [4,5]:

$$\Omega_{m,l} - \omega_\beta = -i \frac{MNr_0c}{2\gamma T_0^2 \omega_\beta} \sum Z_\perp(\omega_{m,l} \cdot h_l(\omega_{m,l} - \omega_\xi)) , \quad (1)$$

where r_0 the classical radius of the electron, c is the speed of light, γ is the Lorentz factor, and T_0 is the revolution period. While the $\text{Re}(\Omega_{m,l})$ corresponds to the coherent beam

frequency shift, the $\text{Im}(\Omega_{m,l})$ corresponds to the growth rate of mode (m, l) , which we will measure experimentally using the BBB in the following sections.

The oscillation frequency of the discrete modes (m, l) is:

$$\omega_{m,l} = (pM + m)\omega_0 + \omega_\beta + l\omega_s , \quad (2)$$

with $p = [-\infty, +\infty]$, and $\omega_0, \omega_\beta, \omega_s$ the (angular) revolution, betatron and synchrotron frequencies. We note that the spectrum of a real signal is folded anti-symmetrically around half of the harmonic number, $h/2$, so that the peak at m_0 has its mirror at $(h - m_0)$ [4,5].

But to infer the beam growth rate of mode (m, l) , it is crucial to have a good impedance model Z_\perp in Eq. 1. At ALBA, the contribution of Z_\perp is considered to be composed of two parts, namely the Resistive Wall (RW) Z_\perp^{RW} contribution and the narrow-band resonators $\sum Z_\perp^{\text{res}}$:

$$Z_\perp = Z_\perp^{RW} + \sum Z_\perp^{\text{res}} . \quad (3)$$

These two contributions can be expressed as:

$$Z_\perp^{RW} = G_1 L \frac{\text{sgn}(\omega) + i \sqrt{\frac{Z_0 \rho c}{2\omega}}}{\pi b^3} , \quad \text{and} \quad (4)$$

$$Z_\perp^{\text{res}} = \frac{R_s}{\frac{\omega}{\omega_r} + iQ \left(\left(\frac{\omega}{\omega_r} \right)^2 - 1 \right)} . \quad (5)$$

Here, b is the chamber half-aperture, G_1 is the chamber form Yukoya factor, Z_0 is the vacuum impedance and ρ is the chamber resistivity, R_s is the resonator shunt impedance, Q its quality factor, and ω_r is the resonator eigenfrequency.

Next, we compare the BBB measurements with the impedance model assuming the contributions described by Eq. 3. For simplicity, we assume $l = 1$ and so we will refer to the excitation modes simply as mode m .

EXPERIMENTAL SETUP

We program the BBB to produce a "super-sequence" with the following steps:

- excite mode "m" during 250 turns at the frequency given by Eq. 2;
- leave the BBB inactive to characterize the evolution of mode "m" during the following 500 turns;
- switch the feedback "on" to damp the (possible) instability created by mode "m" for the next 500 turns.

The sequence is then repeated for mode "m+1" and a full characterization spans up to mode 448 (ALBA harmonic

SINGLE-CRYSTAL DIAMOND PIXELATED RADIATION DETECTOR WITH BURIED GRAPHITIC ELECTRODES

C. Bloomer*¹, L. Bobb, Diamond Light Source Ltd, Didcot, UK
M. E. Newton, University of Warwick, Coventry, UK
¹also at University of Warwick, Coventry, UK

Abstract

A new type of transmissive pixel detector has been developed for synchrotron radiation diagnostics at Diamond Light Source. A thin single-crystal CVD diamond plate is used as the detector material, and a pulsed-laser technique has been used to write conductive graphitic electrodes inside the diamond plate. Instead of using traditional electrodes formed from a layer of surface metallisation, the graphitic electrodes are buried under the surface of the diamond and result in an all-carbon imaging detector. Within the instrument's transmissive aperture there are no surface structures that could be damaged by exposure to radiation beams, and no surface metallization that could introduce unwanted absorption edges. The instrument has successfully been used to image the X-ray beam profile and measure the beam position to sub-micron accuracy at 100 FPS at Diamond Light Source. A novel modulation lock-in technique is used to read out all pixels simultaneously. Presented in this work are measurements of the detector's beam position resolution and intensity resolution. Initial measurements of the instrument's spread-function are also presented. Numerical simulations are used to identify potential improvements to the electrode geometry to improve the spatial resolution of similar future detectors. The instrument has applications in both synchrotron radiation instrumentation, where real-time monitoring of the beam profile is useful for beam diagnostics and fault-finding, and particle tracking at colliders, where the electrode geometries that buried graphitic tracks can provide increased the charge collection efficiency of the detector.

INTRODUCTION

Synchrotron light sources are particle accelerators which are used to generate highly intense beams of UV and X-ray light. At modern synchrotrons monochromatic photon beams of up to 1×10^{14} photons/s and of energies from a few 10 eV up to 100 keV are used to examine a range of biological, chemical, and physical samples. The light produced can be focused down to sub-micron spot sizes [1]. Experimental timescales range from picoseconds, up to years [2, 3].

Common to all the experiments conducted at synchrotrons globally is the requirement to monitor and maintain the stability of the photon beam incident upon the sample: in spatial position, in beam profile, in intensity, in photon energy; and to do so over the range of timescales utilised by the synchrotron users. The typically required photon beam stability at a 3rd generation synchrotron is $< 10\%$ of the beam size,

$< 1\%$ of beam intensity, over kHz timescales [4, 5]. New 4th generation synchrotrons have even stricter stability requirements [6]. To provide this level of beam stability, the measurements of the incident photon beam must correspondingly be at least as accurate as these stringent requirements. It is also required that the instruments used to make beam stability measurements are minimally invasive, and mostly transparent to the incident light: a diagnostic instrument that makes a perfect measurement of the beam but does not transmit any of the incident photons through to the sample would not be acceptable! If measurements of the photon beam can be obtained then real-time optics adjustments can be made to keep the beam position stabilised at the sample, and to keep the X-ray intensity maximised.

Non-destructive X-ray beam profile monitoring is essential as synchrotron and XFEL beamlines increasingly aim to deliver sub-micron beam sizes at their samples points. Significant effort is put into ensuring that precision optics can meet these requirements, from ex-situ measurement and optimisation [7], to in-situ beam profile monitoring and adaptive improvement [8]. It is increasingly common to consider real-time feedback and adaptive optics to ensure that the mirror performance is maintained [9]. The ability to reliably and non-destructively monitor the beam profile is an essential step in ensuring the reliability of the beamline optics.

DIAMOND DETECTORS

To fulfil these requirements for non-destructive monitoring, single crystal chemical vapour deposition (scCVD) diamond makes for an excellent non-invasive detector material: a $50 \mu\text{m}$ plate is mostly transparent to $> 4 \text{ keV}$ photons, radiation tolerant, and exhibits good detector properties. The

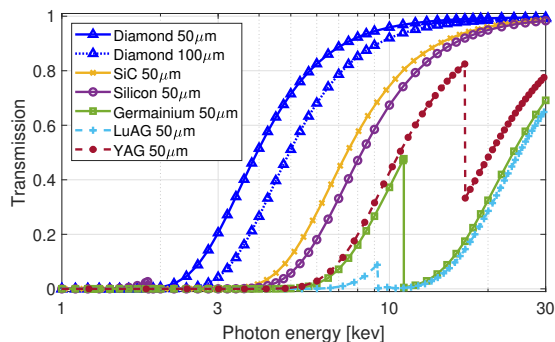


Figure 1: The X-ray transmissivity of scCVD diamond alongside other common solid-state detector materials for ionizing radiation, and common fluorescent materials.

* chris.bloomer@diamond.ac.uk

TRANSVERSE BEAM EMITTANCE MEASUREMENT BY UNDULATOR RADIATION POWER NOISE*

I. Lobach[†], The University of Chicago, Chicago, Illinois

K. J. Kim¹, ANL, Lemont, Illinois,

V. Lebedev, S. Nagaitsev¹, A. Romanov, G. Stancari, A. Valishev, Fermilab, Batavia, Illinois

A. Halavanau, Z. Huang, SLAC, Menlo Park, California

¹also at The University of Chicago

Abstract

Generally, turn-to-turn power fluctuations of incoherent spontaneous synchrotron radiation in a storage ring depend on the 6D phase-space distribution of the electron bunch. In some cases, if only one parameter of the distribution is unknown, this parameter can be determined from the measured magnitude of these power fluctuations. In this contribution, we report the results of our experiment at the Integrable Optics Test Accelerator (IOTA) storage ring, where we carried out an absolute measurement (no free parameters or calibration) of a small vertical emittance (5–15 nm rms) of a flat beam by this new method, under conditions, when the small vertical emittance is unresolvable by a conventional synchrotron light beam size monitor. This technique may be particularly beneficial for existing state-of-the-art and next generation low-emittance high-brightness ultraviolet and x-ray synchrotron light sources.

Please see our Letter [1] for the details about our measurements of the transverse electron beam emittances using the turn-to-turn fluctuations of the undulator radiation power at the Integrable Optics Test Accelerator (IOTA) storage ring at Fermilab. The theoretical foundations of this method are described in Refs. [2, 3]. The design and the experimental program of the IOTA ring are described in Ref. [4].

REFERENCES

- [1] I. Lobach *et al.*, “Transverse beam emittance measurement by undulator radiation power noise,” *Phys. Rev. Lett.*, vol. 126, p. 134802, 13 Apr. 2021. doi: 10.1103/PhysRevLett.126.134802. <https://link.aps.org/doi/10.1103/PhysRevLett.126.134802>
- [2] I. Lobach *et al.*, “Measurements of undulator radiation power noise and comparison with ab initio calculations,” *Phys. Rev. Accel. Beams*, vol. 24, p. 040701, 4 Apr. 2021. doi: 10.1103/PhysRevAccelBeams.24.040701. <https://link.aps.org/doi/10.1103/PhysRevAccelBeams.24.040701>
- [3] I. Lobach *et al.*, “Statistical properties of spontaneous synchrotron radiation with arbitrary degree of coherence,” *Phys. Rev. Accel. Beams*, vol. 23, p. 090703, 9 Sep. 2020. doi: 10.1103/PhysRevAccelBeams.23.090703. <https://link.aps.org/doi/10.1103/PhysRevAccelBeams.23.090703>
- [4] S. Antipov *et al.*, “IOTA (Integrable Optics Test Accelerator): facility and experimental beam physics program,” *J. Instrum.*, vol. 12, no. 03, T03002, 2017.

* This manuscript has been authored by Fermi Research Alliance, LLC under Contract No. DE-AC02-07CH11359 with the U.S. Department of Energy, Office of Science, Office of High Energy Physics.

[†] ilobach@uchicago.edu

MEASUREMENT AND RECONSTRUCTION OF A BEAM PROFILE USING A GAS SHEET MONITOR BY BEAM-INDUCED FLUORESCENCE DETECTION IN J-PARC

Ippei Yamada*¹, Motoi Wada

Graduate School of Science and Engineering, Doshisha University, Kyoto, Japan

Katsuhiko Moriya, Junichiro Kamiya, Michikazu Kinsho

Japan Atomic Energy Agency, J-PARC center, Ibaraki, Japan

¹also at Japan Atomic Energy Agency, J-PARC center

Abstract

A non-destructive transverse beam profile monitor using interaction between a beam and a gas sheet has been developed and demonstrated in J-PARC. The gas sheet formed based on rarefied gas dynamics enables two-dimensional beam profile measurement by detection of induced fluorescence as a 2D image with a CCD camera. The relative-sensitivity spatial distribution of the developed monitor was measured to quantitatively reconstruct a beam profile from the captured image. The sensitivity distribution consists of the sheet-gas density spatial distribution, non-uniformity of the incident solid angle, and the detection efficiency distribution of the CCD camera. The J-PARC 3 MeV H⁻ beam profile was successfully reconstructed with deviation of 7% ± 2% by the integral equation derived from the monitor's principle with the sensitivity distribution.

INTRODUCTION

A non-destructive or a minimal destructive diagnostic system, which is advantageous for constant monitoring, plays an important role for high-intensity, high-energy beam accelerator operation. The system enables to minimize beam losses and radioactivations of the accelerator components. We have developed a non-destructive transverse beam profile monitor, *the gas sheet monitor*, using interaction between a beam and an injected sheet-shaped gas [1]. The gas sheet is formed based on a technique of rarefied gas dynamics to increase a local gas density. The sheet gas interacts with a high intensity beam and induces photons whose spatial distribution depends on the gas density spatial distribution and the beam intensity spatial distribution in transverse. The two-dimensional beam profile can be obtained by taking a picture of the fluorescence and applying a proper analysis considering the effect of the gas density distribution. Figure 1 shows the development flow of the gas sheet monitor. Development of the gas sheet monitor is separated into four components: (1) formation of gas sheet, (2) evaluation of the gas density spatial distribution, (3) test of the profile measurement using a high intensity beam, and (4) reconstruction of the beam profile. In this paper, we report the details of the beam profile measurement with the gas sheet monitor from the four viewpoints.

* ip_yamada@icloud.com

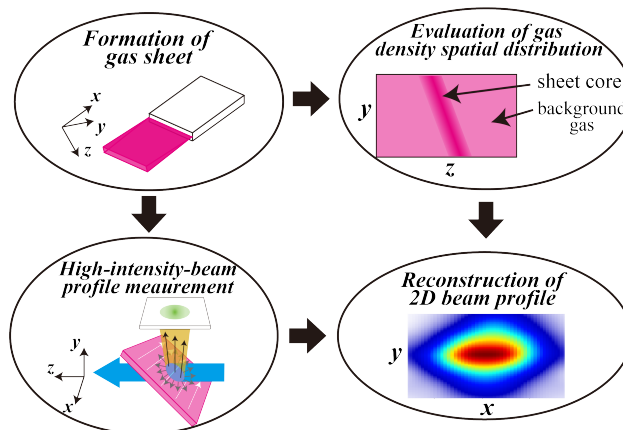


Figure 1: A development flow of the gas sheet beam profile monitor system.

PRINCIPLE

Gas Sheet Formation

The gas sheet is formed based on rarefied gas dynamics. When the mean free path of gas molecules is longer than the typical vacuum chamber dimension like in a beam pipe, the motion of gas molecules is determined not by intermolecular collisions but by the thermal motion and reflections with the chamber wall. The incident angle for reflections with a wall does not affect the reflection angle, and the probability distribution function of the reflection angle θ with respect to the normal direction of the wall is proportional to $\cos\theta$: cosine law. A long gas conduit of a thin cross section can form a gas sheet by increasing the number of reflections in the thickness direction for molecules to obtain a large angle. In this condition, the motion of gas molecules can be modeled by the individual motion of the constant velocity with reflections being subject to the cosine law, such as Molflow+ code [2].

Beam Profile Measurement

Figure 2 shows the gas sheet monitor consisting of a gas sheet flowing along x axis and a photon detector integrating fluorescence induced by beam-gas interaction along y axis. The high intensity beam passes through the gas sheet along z axis. The photons are induced by interaction between the beam and not only the gas sheet but also the background gas.

COMMISSIONING OF TIMEPIX3 BASED BEAM GAS IONISATION PROFILE MONITORS FOR THE CERN PROTON SYNCHROTON

H. Sandberg^{*1}, W. Bertsche², D. Bodart¹, S. Jensen¹, S. Gibson³, S. Levasseur¹, K. Satou⁴,
G. Schneider¹, J.W. Storey¹, and R. Veness¹

¹CERN, Switzerland

²University of Manchester, Cockcroft Institute, UK

³Royal Holloway University of London, John Adams Institute, UK

⁴Accelerator Laboratory, KEK, Japan

Abstract

A pair of operational Beam Gas Ionisation (BGI) profile monitors was installed in the CERN Proton Synchrotron (PS) at the beginning of 2021. These instruments use Timepix3 hybrid pixel detectors to continuously measure the beam profile throughout the cycle in the horizontal and vertical planes. In the weeks following their installation, both BGI's were commissioned in situ by equalizing and tuning the thresholds of the Timepix3 detectors.

First measurements were taken during the beam commissioning period, demonstrating the operational readiness of the instruments. Sextupolar components originating from the magnetic shield in the vertical BGI magnet were later discovered and required compensation to reduce their effect on the PS beams. With the compensation in place, operational measurements could be started and provided new insights into the dynamics of the PS beam cycles.

INTRODUCTION

A novel BGI profile monitor design aims at providing continuous, bunch-by-bunch and turn-by-turn measurement of the transverse beam profile in the CERN PS [1]. This instrument design uses electric and magnetic fields to transport electrons from rest-gas ionisation to a Timepix3 [2] based detection system installed directly inside the beam vacuum. The beam profile is inferred from the transverse distribution of the detected electrons. In 2017 a prototype was successfully installed in the CERN PS and was updated in 2018 with new detectors. It provided the first measurements of transverse horizontal beam profiles using this novel design and demonstrated the feasibility of the in-vacuum Timepix3 use [3, 4].

During the long shutdown 2 of the CERN accelerator complex, the prototype was replaced by an operational instrument and a second instrument was installed to measure the transverse beam profile in the vertical plane. The horizontal BGI reused the vacuum chamber, magnet and infrastructure from the prototype instrument, while the vertical BGI required the installation of a new vacuum chamber and a new 0.2 T triplet dipole magnet. Both instruments were ready for the first beam in the PS on March 2021.

* hampus.sandberg@cern.ch

DETECTOR SETUP AND EQUALISATION

A new generation of in-vacuum detector electronics was designed and manufactured for the operational vertical and horizontal instruments. This new design consist of an array of four modules each with one Timepix3 chip. This solves production yield issues discovered with the prototypes and improves the manufacturability and reliability of the detector. To ensure that the detectors were working as expected, each of them was tested twice, once in the lab prior to installation and once in the CERN PS after installation. The testing procedure consists of; measurements of the detector and sensor bias currents, temperature measurements, internal digital-to-analog converter (DAC) response scans, equalisation, threshold tuning and detection tests using radioactive sources. Equalisation and threshold tuning are the two most important step of the commissioning.

The equalisation process aims to create a uniform response of all pixels in the matrix by tuning 4-bit DACs that shifts the response of each pixel relative to a global threshold. All pixels have a slightly different response due to manufacturing process variations and for a fixed input signal some pixels are therefore below the threshold while others are above. The response is measured at the maximum and minimum range of the pixel DACs to find the ideal value for each pixel. Figure 1 presents the Timepix3 matrix response measurement before (two large distributions) and after equalisation (narrow central distribution). Equalisation

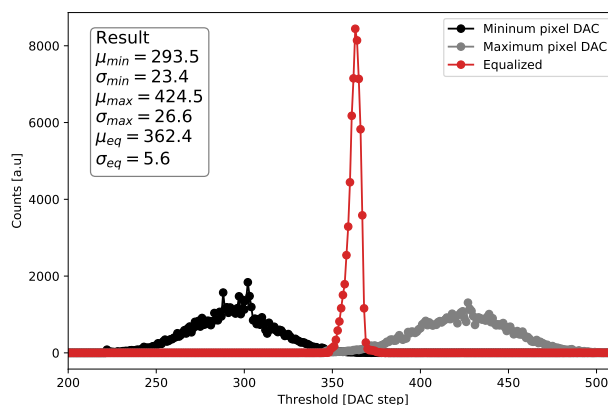


Figure 1: Equalisation result from a Timepix3 detector in the operational horizontal BGI instrument.

TWO-DIMENSIONAL BEAM SIZE MEASUREMENTS WITH X-RAY HETERODYNE NEAR FIELD SPECKLES

M. Siano*, B. Paroli, M. A. C. Potenza, L. Teruzzi, Università degli Studi di Milano, Milan, Italy
U. Iriso, A. A. Nosych, E. Solano, L. Torino, ALBA-CELLS, Cerdanyola del Vallés, Spain
D. Butti, A. Goetz, T. Lefevre, S. Mazzoni, G. Trad, CERN, Geneva, Switzerland

Abstract

We report on 2D beam size measurements with a novel interferometric technique named Heterodyne Near Field Speckles, capable of resolving few-micrometer beam sizes. It relies on the interference between the weak spherical waves scattered by a colloidal suspension and the intense transilluminating X-ray beam. Fourier analysis of the resulting speckles enables full 2D coherence mapping of the incoming radiation, from which the beam sizes along the two orthogonal directions are retrieved. We show experimental results obtained with 12.4 keV X-rays at the NCD-SWEET undulator beamline at ALBA, where the vertical beam size has been changed between 4 and 14 micrometers by varying the beam coupling. The results agree well with the estimated beam sizes from the pinhole calculations. Finally, we discuss recent investigations on alternative targets aimed at improving the signal-to-noise ratio of the technique.

INTRODUCTION

Two-dimensional (2D) beam size measurements are of utmost importance for present and future accelerators. Knowledge of the beam sizes enables to assess the beam emittance in storage rings [1]. Furthermore, beam size ultimately affects the transverse coherence properties of the emitted synchrotron radiation in current and forthcoming Synchrotron Light Sources (SLS), thus impacting many research areas that rely on coherence-based techniques [2].

Non-invasive beam size measurement methods can be divided into two main categories: direct imaging techniques and interferometric methods. Direct imaging techniques such as the X-ray pinhole camera directly provide a 2D image of the source, though they are typically limited in resolution to beam sizes larger than 10 μm [3]. Contrarily, interferometric methods such as the Young's double-pinhole interferometer provide higher resolutions, but are limited to one-directional measurements only [3].

Here we report on recent 2D beam size measurements with a novel, non-conventional interferometric technique named Heterodyne Near Field Speckles (HNFS). We show that the technique is intrinsically 2D and that it can resolve beam sizes as small as a few micrometers. As in all interferometric techniques, what we actually measure is the Complex Coherence Function (CCF) of the synchrotron radiation

$$\mu(\Delta\mathbf{r}) = \frac{\langle e(\mathbf{r})e^*(\mathbf{r} + \Delta\mathbf{r}) \rangle}{\sqrt{\langle i(\mathbf{r}) \rangle \langle i(\mathbf{r} + \Delta\mathbf{r}) \rangle}}, \quad (1)$$

* mirko.siano@unimi.it

from which the beam size is retrieved by means of Statistical Optics approaches. In Eq. (1), $e(\mathbf{r})$ is the electric field at a point \mathbf{r} on the wavefront of the synchrotron light, $i(\mathbf{r}) = |e(\mathbf{r})|^2$ is the corresponding intensity and $\langle \cdot \rangle$ denotes ensemble average over many electron bunches. The radiation CCF $\mu(\Delta\mathbf{r})$ quantifies the correlations of the emitted electric field between two points across the wavefront of the synchrotron light separated by $\Delta\mathbf{r}$ [4, 5].

THE HETERODYNE NEAR FIELD SPECKLES TECHNIQUE

The HNFS technique relies on the interference between the incoming partially-coherent synchrotron light and the weak spherical waves scattered by nanospheres suspended in water.

In the ideal case of a single scatterer, the self-referencing interference between the intense transilluminating field and the weak scattered spherical wave generates circular fringes whose visibility decays according to the 2D CCF of the incoming radiation, as shown in Fig. 1(a). Here, vertically elongated coherence areas have been assumed as typically encountered in undulator sources.

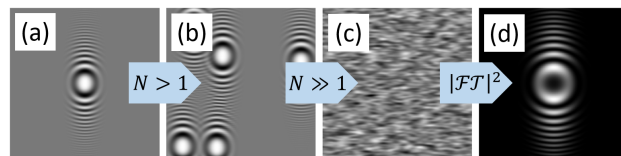


Figure 1: Fundamentals of the HNFS technique. (a) Single-particle interference image. Interference fringes are modulated by the 2D CCF of the synchrotron light. (b) and (c) Under heterodyne conditions, speckles are simply formed as the intensity sum of many equal single-particle interference patterns. (d) Power spectrum of heterodyne speckles, showing Talbot oscillations enveloped by the squared modulus of the 2D CCF.

Measurement of the visibility of the circular fringes as a function of the distance $\Delta\mathbf{r}$ from the center of the pattern allows to directly measure the 2D coherence properties of the incoming light. Furthermore, interference fringes are narrower at larger $\Delta\mathbf{r}$. This allows to introduce a one-to-one relation, known as the spatial scaling, between the spatial frequency of the interference fringes, \mathbf{q} , and transverse displacements, $\Delta\mathbf{r}$ [6–8]:

$$\Delta\mathbf{r} = z \frac{\mathbf{q}}{k}, \quad (2)$$

STUDIES OF BEAM LOSS MONITORS AT THE CHINA SPALLATION NEUTRON SOURCE*

Tao Yang^{†,1}, Jilei Sun, Jianmin Tian, Lei Zeng, Taoguang Xu, Weiling Huang, Fang Li,
Zhihong Xu, Ruiyang Qiu, Ming Meng, Anxin Wang, Mengyu Liu¹, Xiaojun Nie

Institute of High Energy Physics, Chinese Academy of Sciences, Beijing, China
Spallation Neutron Source Science Center, Dongguan, China

¹also at University of Chinese Academy of Sciences, Beijing, China

Abstract

Beam loss detection is essential for the machine protection and the fine-tuning of the accelerator to reduce the induced radioactivity. The beam loss monitors (BLM) at the China Spallation Neutron Source (CSNS) are mainly divided into the following types: the coaxial cylindrical ionization chamber (IC) filled with Ar/N₂ gas mixture, Xe, BF₃ gas, and the scintillator with photomultipliers, among which the Ar/N₂ IC is the main type. In the low-energy section of the linac (beam energy <20 MeV), the BF₃ BLMs enclosed by a high-density polyethylene (HDPE) moderator are utilized to detect the beam losses. The Monte Carlo program FLUKA is employed to perform the relevant simulations. This paper presents the summary of the beam-loss detection for the CSNS BLM system.

INTRODUCTION

The CSNS had generated the neutron beam by the spallation reaction of 1.6-GeV protons striking on the tungsten target in August 2017. At present, its beam power is 100 kW with a repetition rate of 25 Hz. In phase II of CSNS, the beam power will be raised to 500 kW and the remaining neutron instruments will be built. A schematic layout of the CSNS phase I complex is shown in Fig. 1. The CSNS accelerator is mainly comprised of a 50-keV H⁻ ion source, a 3-MeV radio frequency quadrupole (RFQ) accelerator, an 80-MeV drift tube linac (DTL), and a 1.6 GeV proton rapid cycle synchrotron (RCS) [1]. The main design parameters of CSNS are listed in Table 1.

Table 1: The Basic Design Parameters of the CSNS

Design parameter	Value
Beam power (kW)	100
Linac energy (MeV)	80
Beam current in the linac (mA)	15
Extraction energy (GeV)	1.6
Proton per pulse	1.56×10^{13}
Repetition rate (Hz)	25
Linac RF frequency (MHz)	324
Target material	Tungsten

Beam loss may bring out high energy deposition to damage the accelerator components or produce undesired radioactivation, so it is one of the most important issues during

the running and commissioning of an accelerator facility [2-4]. Monitors based on the IC and plastic-scintillator with photomultipliers are the two types of BLMs used in the CSNS. There are 190 IC-type BLMs (preliminary and the subsequent newly added amount) along the entire beam line at the CSNS, mostly filled with Ar/N₂ mixture gas, several filled with Xe or BF₃ gas, and there are also 15 scintillator-based BLMs. IC is the main BLM type for the CSNS as well as other hadron machines due to its robustness to radiation damage, large dynamic range, little maintenance, and ease for calibration [5-8].

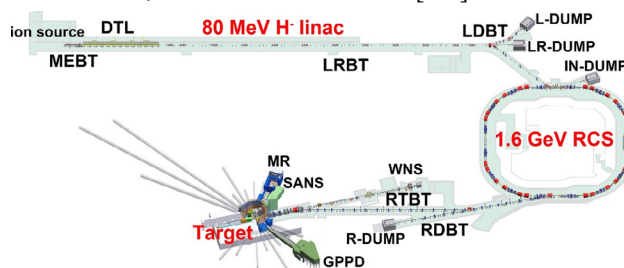


Figure 1: Schematics of the CSNS complex.

In this paper, the performance and some beam loss experiments of our IC BLMs are presented. The relevant Monte Carlo simulations with FLUKA are also executed to verify the experiments, simulates the induced current of different loss scenarios and then evaluates the suitability of electronics, and provide the basis of schemes for some special detections, e.g., the beam-loss detection in the low-energy section of linac for a proton accelerator based on the moderated secondary neutrons.

THE CSNS IC BLM

The schematic and the photograph of the CSNS IC BLM are shown in Fig. 2. The sensitive volume is the tube-like region enclosed by the outer and inner electrode with an effective length of 17.4 cm. The working gas is a mixture of argon and nitrogen with a volume ratio of 70:30 at a total pressure of 1 atm. The standard bias voltage is set to be -2100 V which falls well in the intermediate part of the plateau tested by the ⁶⁰Co source in our previous research [9]. The high voltage is applied on the outer electrode, while electrons are collected on the inner electrode. All electrodes and coverages of BLMs are made of stainless steel, and the insulators are made of alumina ceramics.

*This work is supported by the National Natural Science Foundation of China (Grants No. 11575219, No. 11705215, and No. 11805220).

[†] yangt@ihep.ac.cn

CMOS BASED BEAM LOSS MONITOR AT THE SLS

C. Ozkan Loch[†], A. M. Stampfli, R. Ischebeck, Paul Scherrer Institute, Villigen, Switzerland

Abstract

For several years, the SLS storage ring was not equipped with loss monitors to observe loss patterns around the storage ring; hence, any understanding of the operational losses, accidental losses, or manual beam dumps was missing. Initially, a long quartz fibre (350 m) was installed around the ring to locate losses, and read out with a photomultiplier tube. With the long fibre, we garnered some understanding yet, it was not easy to locate the position of the losses. Hence, we opted for scintillator based fibre loss monitors, installed in choice locations. All the fibres are read out together with a single CMOS based 2.3 MP camera. A device was built with 28 channels. Ten fibres were connected and are located in the injection kicker in the BTRL and three arcs of the storage ring. With these loss monitors, we were able to detect and locate the position of losses due to injection and sudden beam dumps/losses.

In this paper, we will introduce the concept and the components of this monitor, and present the data processing algorithm that identifies the individual fibres in the images, allowing us to locate and track the losses in the SLS storage ring.

INTRODUCTION

At SLS 2.0 [1], loss monitors will be used to monitor beam losses from the Booster-to-Ring transfer line down to the storage ring and around it, to detect low charge on-axis injection and provide loss patterns around the storage ring during filling and top-up operation. For commissioning and daily operation of the storage ring and insertion device protection, loss monitors that can detect “fast” losses (~100 ms) from faults or beam perturbations from injection are needed. The fast losses can be correlated to sudden changes in lifetime. We also need to identify “slow” losses that influence lifetime during standard operation.

At SwissFEL, a beam loss monitor system based on plastic fibre scintillators and photomultiplier tubes as detectors was developed [2]. This system was custom built for the stringent requirements of SwissFEL, where hardware interface to the machine protection system was required for dynamic regulation of beam rate to ensure operability of the facility within the allowed limits.

For the SLS 2.0, we took the SwissFEL BLM approach of distributed scintillating fibres and exchanged the single photomultiplier tube (PMT) per fibre readout with a CMOS camera because the camera would allow observing multiple fibres, simultaneously. A proof of principle experiment was carried out at the end of the injection straight by losing single injected bunches into the SLS storage ring. The CMOS camera was able to detect losses from the scintillating fibres. A prototype BLM system was built in-house

that can accommodate 28 fibres. Presented in this paper is the CMOS based BLM, the image processing and first results from the system installed in the SLS storage ring.

LOSS MONITOR SYSTEM

The beam losses cause scintillation light inside the scintillating fibres (Saint Gobain, BCF12 [3]), which is carried out of the tunnel with duplex plastic optical fibres (POF). One end of the POF is connected to an LED [4] for calibration purposes and the other end of the fibre is connected to the camera. The fibres from the tunnel connect to the front panel. The box that contains all the components of the system can be seen in Fig. 1a.

The beam loss system has the following functionalities:

- camera and LED control
- read the CMOS with a computer
- image the light from the fibres
- identify the individual fibres
- calibrate the fibres with LEDs
- display the measurements graphically
- archive the loss data

Hardware

The fibres that connect to the front panel are coupled to a bunch of short fibres inside the box. These fibres are arranged in a dense array by a holder that also serves to shield the fibres from each other and the external light (Fig. 1b). This holder also doubles as a polishing holder for the fibres. All fibre ends have been polished for improved light throughput.

The camera images the fibre holder with two objectives together in a tandem configuration. The focus of both objectives is set to infinity, such that the fibres, located at the flange focal distance of the first objective lens, are imaged onto the CMOS sensor located at the flange focal distance of the second lens. This system allows for a good light collection efficiency with two large-aperture, infinity-corrected objectives. The imaging ratio is the ratio of the focal lengths of the two lenses. We used objectives with $f=50$ mm and $f=16$ mm, respectively, resulting in a magnification of $M = -1/3.125$.

The image sensor is read out by a Jetson Nano [5] through a USB port. Software, written in Python, processes the images and makes the data available to the control system.

A fully functioning setup is installed in the rack at the SLS in a compact housing. All components inside the box and the front panels can be seen in Fig. 1.

[†] cigdem.ozkan@psi.ch

PARTICLE AND PHOTON BEAM MEASUREMENTS BASED ON VIBRATING WIRE

S.G. Arutunian, G.S. Harutyunyan, E.G. Lazareva, A.V. Margaryan
Yerevan Physics Institute, 0036, Yerevan, Armenia

M. Chung, D. Kwak, Ulsan National Institute of Science and Technology, 44919, Ulsan, Korea

Abstract

The instrumentation introduced herein is based on high-quality vibrating wire resonator, in which the excitation of wire oscillation is made through the interaction of the wire current with a permanent magnetic field. The high sensitivity of the oscillation frequency to the wire temperature allows the resonator to be used for measuring charged-particle/X-ray/laser/neutron beam profiles with wide dynamic range. The beam flux falling on the wire increases its temperature from fractions of mK to hundreds of degrees. Another application method is to use the vibrating wire as a moving target, in which signals created at beam interaction with the wire are measured synchronously with the wire oscillation frequency. This method allows to effectively separate the background signals. Also, the well-defined (in space) and stable (in time) form of the wire oscillation allows the vibrating wire to be used directly as a miniature scanner for measuring thin beams. The latter two methods enable a significant reduction in scanning time compared to the original thermal-based method.

INTRODUCTION

Vibrating wire (VW) resonators have a number of attractive characteristics: high quality factor, long-term stability, practical absence of irreversible drifts caused by component aging. On the basis of such resonators, we have developed several instruments for measuring the profiles of beams of different nature (charged particles, electromagnetic radiation in a wide wavelength range, from infrared to hard gamma rays, neutrons). Three principles of operation of such instruments have been proposed. The first uses the dependence of the resonator frequency on the wire tension, which is determined by the flux of particles falling on the wire. The second one uses the signals of secondary particles in the interaction of the beam with the wire, and measurements are made synchronously with the string oscillations. In the third, the wire oscillations are used as a miniature scanner to scan beams in the micrometer size range.

THERMAL METHOD

The Vibrating Wire Monitor (VWM) on the thermal principle can be described as a wire stretched between two clips mounted on the basis. Part of the wire is placed in a magnetic field created by permanent magnets. The oscillations of the wire at natural frequency are excited by the interaction of the current flowing through the wire with the magnetic field. The wire is connected to the input of operational amplifier with positive feedback, which leads

to autogeneration of natural oscillations of the wire (see [1] for details). The particles of the measured beam heat the wire, leading to a change in its tension and, accordingly, the frequency of oscillations, which serves as the output signal of the VWM. VWMs have good relative accuracy (several units per $1e-6$), long-term stability (many months) and a large dynamic range (up to 6 orders of magnitude).

Let us describe the operation of the VWM using the example of a profiling station for the Cyclon18 proton accelerator with the particle energy of 18 MeV [2] (the results of studies will be published in more detail in [3]). Figure 1 shows the main units of such a station.

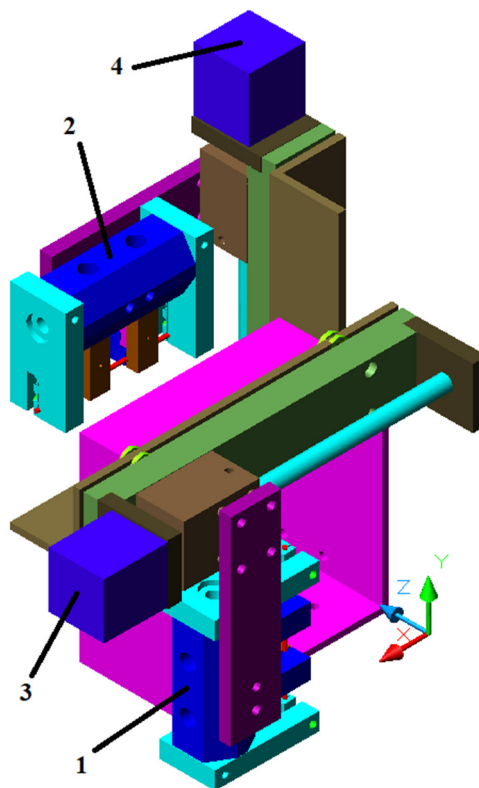


Figure 1: Profiling station for horizontal and vertical scanning, equipped with VWMs (1 and 2) and linear drive systems (3 and 4). Beam extends along the Z-axis.

Note that thermal monitors have response times ranging from fractions of a second to several seconds, depending on the wire material, the sensor geometry, and the atmosphere/vacuum in which the sensor is used. For the VWM used here (stainless steel string of length 56 mm, and 100 μm in diameter), this time is about 0.46 sec. The beam current was controlled by changing the current of the ion source located in the center of the cyclotron.

SPACE-CHARGE AND OTHER EFFECTS IN FERMILAB BOOSTER AND IOTA RINGS' IONIZATION PROFILE MONITORS *

V. Shiltsev[†], Fermi Accelerator Laboratory, Batavia, IL, USA

Abstract

Ionization profile monitors (IPMs) are widely used in accelerators for non-destructive and fast diagnostics of high energy particle beams. At low beam intensities, initial velocities of the secondaries to collect (ions or electrons) result in the IPM profile smearing. At high beam intensities, the space-charge forces make the measured IPM profiles significantly different from those of the beams. We analyze dynamics of the secondaries in IPMs, describe an effective algorithm to reconstruct the beam sizes from the measured IPM profiles and apply it to the Fermilab 8 GeV proton Booster and 70 MeV/c IOTA ring IPMs.

INTRODUCTION

Particle accelerators heavily rely on precise diagnostics and control of critical beam parameters such as intensity, pulse structure, position, transverse and longitudinal beam sizes, halo, etc [1]. Ionization profile monitors (IPMs) [2–7] are fast and non-destructive diagnostic tools used in proton and ion linacs, colliders, and rapid cycling synchrotrons (RCS) [8–10]. They operate by collecting ions or electrons created after the ionization of residual vacuum molecules by high energy charged particle beams [1, 11], which are then guided to a detector by a uniform external electric field E_{ext} . The detector is usually made of many thin parallel strips, whose individual signals are registered to make the beam profile signal ready for processing – see Fig.1.

Space-charge forces of the primary beams make the measured IPM profiles different from those of the beams and must be correctly accounted for. Brute force numerical modeling [12, 13] can successfully reproduce experimentally measured IPM profiles but offer limited predictive physics insights. Several phenomenological fits were proposed to relate the measured beam size σ_m and the initial beam size σ_0 - see, e.g., [3, 12, 14, 15] - but despite acceptable data approximation, they are not based on clear physical reasons for as many four free parameters and exponents. Below we briefly describe an effective algorithm developed in [16] to reconstruct the beam sizes from measured IPM profiles and known key parameters, such as high-energy beam intensity N and IPM extracting field E_{ext} is the guiding electric field. Based on that theory, we discuss the Booster IPMs measurements and possible upgrades, as well as specifications for the IOTA ring IPMs.

* This manuscript has been authored by Fermi Research Alliance, LLC under Contract No. DE-AC02-07CH11359 with the U.S. Department of Energy, Office of Science, Office of High Energy Physics.

[†] shiltsev@fnal.gov

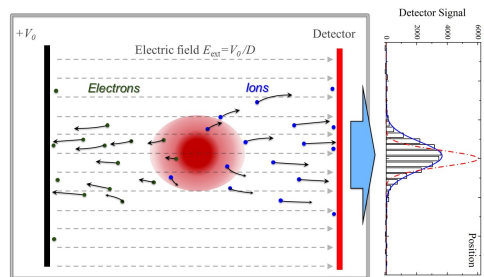


Figure 1: Transverse cross-section of a high energy beam (red) in vertical IPM and schematically shown motion of secondary ions (blue dots) and electrons (green dots) under the impact of horizontal extracting electric field E_{ext} and space-charge field of the primary beam. The diagram on the right shows the IPM detector signals at right before extraction of an intense beam of $N = 4.6 \cdot 10^{12}$ protons from the Fermilab Booster synchrotron. The actual rms proton vertical size of the proton beam is $\sigma_0 = 2.1$ mm - see dashed red curve, while the rms width of the IPM signal is $\sigma_m = 3.6$ mm, see blue line for the Gaussian fit.

SPACE-CHARGE DRIVEN IPM PROFILE EXPANSION

Ref. [16] presents a final-form solution of the general equations of transverse motion of non-relativistic ions with charge Ze and mass M born in the acts of ionization of the residual gas molecules by a high energy proton beam passing through IPM with extracting external electric field $E_{\text{ext}} = V_0/D$ due to the voltage gradient V_0 across the IPM gap D . No guiding external magnetic field is assumed. IPMs usually operate with electric fields $E_{\text{ext}} \sim O(100-1000 \text{ V/mm})$ which significantly exceed the space-charge field $E^{\text{SC}} \sim O(1-10 \text{ V/mm})$ and that assumption helps to solve the equations of motion.

Important beam parameters of the high energy beam are its current $J(t)$, velocity v_p and rms transverse size σ_0 . The space-charge potential of such beam is $U_{\text{SC}} = J/(4\pi\epsilon_0 v_p) \approx 30[\text{V/A}]J/\beta_p$, $\beta_p = v_p/c$, c is the speed of light, and ϵ_0 is the permittivity of vacuum [17]. Three characteristic times are of importance for the analysis: i) a characteristic time for the secondaries to get extracted out of the beam by the external electric field $\tau_0 = \sqrt{\frac{2M\sigma_0}{ZeE_{\text{ext}}}} = \tau_2 \sqrt{\frac{\sigma_0}{d}}$; ii) time for secondary particle to reaches the IPM detector plane $\tau_2 = \sqrt{\frac{2Md}{ZeE_{\text{ext}}}}$, where d is the average distance from the beam center to the detector; and iii) a characteristic expansion time due to the space-charge $\tau_1 = \left(\frac{eZU_{\text{SC}}}{M\sigma_0^2}\right)^{-1/2}$.

Proton beam space-charge fields result in *proportional magnification of the IPM profile* of the distribution of the secondary particles, i.e., $\sigma_m = \sigma_0 \cdot h$. Under a reasonable

SIMULATION OF A QUAD-SLITS INTERFEROMETER FOR MEASURING THE TRANSVERSE BEAM SIZE IN HLS-II*

Sanshuang Jin, Yunkun Zhao, Jigang Wang[†], Baogen Sun[‡], Fangfang Wu, Leilei Tang, Tianyu Zhou
National Synchrotron Radiation Laboratory (NSRL),
University of Science and Technology of China (USTC), Hefei, China

Abstract

A quad-slits interferometer using visible light is designed to measure the transverse beam size of Hefei Light Source-II (HLS-II). According to the basic beam parameters of the B7 source point, the preliminary simulation results are obtained by using the Synchrotron Radiation Workshop (SRW) code. Furthermore, the core parameters of the quad-slits components in the interferometer are optimized. Among, the optimum slits-separations of d_H and d_V are acquired to be 6.0 and 10.0 mm, respectively. It is shown that the simulated results are consistent with the theoretical values, which provides a reference value for performing the related experimental measurement in the future.

INTRODUCTION

It is known that the synchrotron radiation (SR) refers to the electromagnetic wave radiated when the acceleration state of the charged particles changes. So far the SR light source has been widely used in the fields of condensed-matter physics, medical research, biochemistry, materials and advanced manufacturing processes due to its significant characteristics of high-brightness, high polarization and good stability. With the advancement of accelerator science and technology, the transverse beam size becomes smaller and smaller and reaches few dozens of micrometers. There is no doubt that it requires a huge engineering challenge to accurately measure such a small beam size. The current mainstream technology for the measurement of the transverse beam size is to employ the SR optical system. It is especially pointed out that this SR system has the excellent advantage of real-time and online measurement without damage to the stored bunched beam [1]. Up to now, the traditional methods for measuring the transverse beam size include FZP imaging [2], double-slits and quad-slits interferometry [3,4], pinhole imaging [5] and so on [6,7]. Among them, the FZP imaging method is considered as uneconomical because of the smaller beamline layout in HLS-II and the expensive optical diffractive element FZP. As for the pinhole imaging method, it is difficult to measure the small transverse beam size owing to the inevitable optical diffraction effect. In addition to the double-slits interferometer proposed by T. Mitsuhashi [8], which possesses high resolution

that can be used in visible light and even X-ray bands. In combination with the remarkable merits of the optical interference measurement system, the B7 beamline of HLS-II has been achieved the online measurement of the transverse beam size. This previous double-slit interferometry occupies a large space and has a high maintenance cost. In order to further precisely obtain the beam size of B7 source point, we are devoted to designing a simple suitable quad-slits interferometer which can reduce the complexity of the optical system.

PRINCIPLE AND PHYSICAL DESIGN

HLS-II is a second-generation electron storage ring with low emittance of 36.4 nm-rad and with beam energy of 800 MeV. Note that a double-slits interferometer already has been applied to measure the transverse beam size of B7 source point. Then we are desired to design a new quad-slits interferometer for improving the measurement accuracy and system robustness. The parameters of B7 source point are clearly shown in Table 1.

Table 1: The Parameters of B7 Source Point

Parameters	Value
Electron beam energy E_e (GeV)	0.8
Beam current I (mA)	400
Circumference L (m)	66.1308
Radius of BM ρ (m)	2.1645
Vertical magnetic field of BM B (T)	1.2327
Transverse natural emittance ϵ (nm-rad)	36.4
Energy spread (RMS)	0.00047
β_x (m)	1.7668
β_y (m)	12.3485
α_x (m)	-3.002
α_y (m)	2.1319
η_x (m)	0.1059
η_x	-0.1990

According to the above parameters given in Table 1, the transverse beam size can be calculated by

$$\begin{cases} \sigma_x^2 = \epsilon_x \beta_x + (\eta_x \frac{\Delta p}{p})^2 \\ \sigma_y^2 = \epsilon_y \beta_y \end{cases} \quad (1)$$

where σ_x and σ_y are the horizontal and vertical beam size, respectively. ϵ_x and ϵ_y are the horizontal and vertical beam emittance, respectively. β_x and β_y are the horizontal and vertical beta function, respectively. $\Delta p/p$ is the energy spread and η_x is dispersion function. Through the calculation we

* Work supported by the National Natural Science Foundation of China under Grant 12075236, Grant 11575181, Grant 51627901, Grant 11805204, and Grant 11705203, the Anhui Provincial Natural Science Foundation under Grant 1808085QA24, and the Fundamental Research Funds for the Central Universities under Grant WK2310000080

[†] wangjg@ustc.edu.cn

[‡] bgsun@ustc.edu.cn

DEVELOPMENT OF A MULTI-CAMERA SYSTEM FOR TOMOGRAPHY IN BEAM DIAGNOSTICS

A. Ateş *, G. Blank, U. Ratzinger and C. Wagner
Institute of Applied Physics, Goethe University, Frankfurt, Germany

Abstract

Embedded visual systems in industry led to advancements of single board computers and single board cameras. Due to the lower power consumption and high flexibility of these miniature devices, a multi-camera system can be developed more effectively. A prototype of a beam-induced residual gas fluorescence monitor (BIF) has been developed and successfully tested at the Institute of Applied Physics (IAP) of the Goethe University Frankfurt. This BIF is based on a single-board camera inserted into the vacuum. The previous promising results led to the development of a multi-camera system with 10 cameras. One of the advantages of such a system is the miniature design, allowing this detector to be integrated within the vacuum and in regions that are difficult to access. The overall goal is to study the beam with tomography algorithms at a low energy beam transport section. We hope to reconstruct an arbitrary beam profile intensity distribution without assuming a Gaussian beam.

INTRODUCTION

Beam-induced fluorescence (BIF) monitors are standard detectors at accelerator facilities [1]. For ultrahigh vacuum beam diagnostics, scientific cameras are commonly used in combination with MCP photon amplifiers to determine the beam position and profile. New BIF monitors have been successfully tested at the low-energy beamline of the Frankfurt Neutron Source at the Stern Gerlach Center [2, 3]. These developments lead to new ways to study the beam. One idea is to view the beam from multiple angles. This allows the use of tomography algorithms to reconstruct the intensity distribution of the transverse beam profile. Beam tomography has previously been studied using a camera and a rotating vacuum chamber to rotate the camera and obtain any number of views. Another approach is to view the beam through viewing windows.

Our goal is to maximize the number of viewing angles and develop a fast tomographic detector with a minimal form factor to be as flexible as possible. Our approach is to use non-scientific single-board cameras with single-board computers and to put as many cameras as possible in the vacuum. Figure 1 shows a photo of the cameras mounted on the holder. It is designed to fit into a vacuum vessel with a diameter of 200 mm and a length of 300 mm.

The detector is built for low energy beam transport sections in high vacuum regions of about 10^{-7} mbar. To increase the emitted light, it is possible to introduce a buffer gas during image acquisition. We tested the cameras at a residual argon gas pressure down to 1×10^{-4} mbar. There

* ates@iap.uni-frankfurt.de

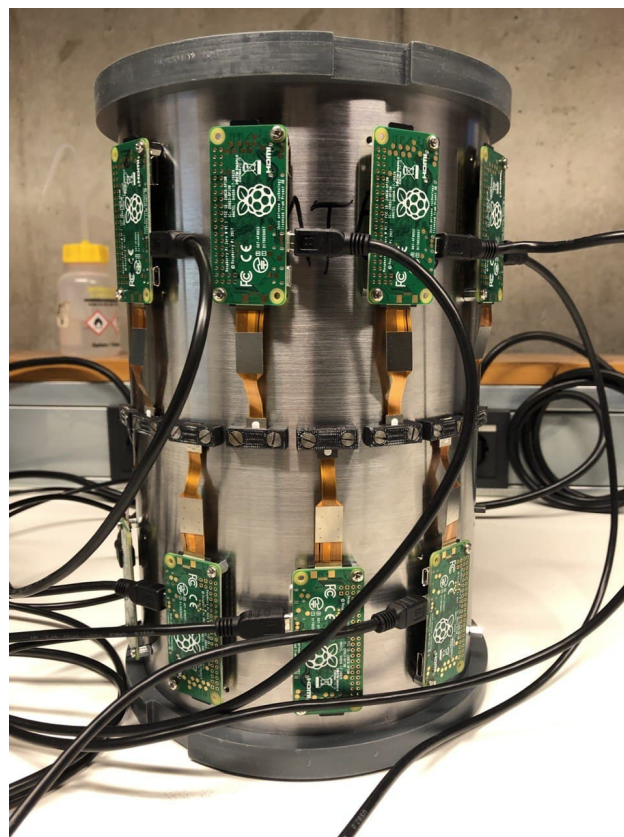


Figure 1: The picture shows a photo of the tomography detector with the Raspberry Pi Zero and its camera modules attached to a stainless steel pipe.

were several challenges to overcome in developing such a detector. One challenge was to get all cameras in parallel into full operation and retrieve all data. Another challenge was to align each of the cameras so that their center of field of view matched. The following sections present our approaches to solving these challenges.

HARDWARE SET UP

Raspberry Pi Zero and its Camera

The cameras you see in Fig. 1 are single-board cameras with so-called raspberry pi zero single-board computers. The Raspberry Pi Zero is the Raspberry Pi with the smallest dimensions among the Raspberry Pi computer models. The Raspberry Pi and especially its camera are gaining more and more attention not only in the Maker scene, but also in the scientific community [4]. Due to its compact dimensions and low power consumption of about 15 mW, they are predestined for projects like drones, robots or any mobile

DEVELOPMENT OF A BEAM HALO MONITOR USING VISIBLE SYNCHROTRON RADIATION AT DIAMOND LIGHT SOURCE

E. Howling*, L. Bobb, Diamond Light Source, Oxford, UK

Abstract

A Beam Halo Monitor (BHM) has been developed at Diamond Light Source (DLS). It is an optical system that uses visible synchrotron radiation (SR) to image the beam halo. In this paper, the design of the monitor is presented, including the introduction of a Lyot stop system to reduce diffraction effects. The BHM was used to take images of a source point of visible SR from a dipole at DLS. These images were analysed to investigate the beam halo and determine the limitations of the monitor. These results will help inform the design of the visible light extraction system and any future BHMs for Diamond-II.

INTRODUCTION

Diamond Light Source (DLS) is a third generation synchrotron light source. In the storage ring, most electrons in the beam reside in the beam core. Due to Touschek and gas scattering some are offset from the core and form a beam halo [1].

Synchrotron radiation from bending magnet sourcepoints at visible and X-ray wavelengths is commonly used for beam diagnostics. X-ray pinhole cameras are used to image the beam core for transverse profile measurements [2]. However, these do not have a great enough dynamic range to image the beam halo, as the halo is approximately 10^{-5} times as bright as the core. Furthermore, the beam core cannot be imaged using visible SR due to the diffraction limit. However, the beam halo is large enough to be imaged with visible SR [3].

A Beam Halo Monitor (BHM) has been developed to better understand the formation and properties of the beam halo. In circular colliders, damping rings and synchrotron light sources, beam halo is one of the critical issues limiting the performance as well as potentially causing component damage and activation [1]. In the case of synchrotron light sources, the beam core determines characteristic parameters such as brightness for beamlines. Therefore a significant beam halo is undesirable. This becomes all the more important upon considering planned synchrotron upgrades, such as Diamond-II [4], where increased brightness for beamline experiments is a key performance indicator.

Given the reduced emittance in Diamond-II, the beam core will be focused to a greater particle density and therefore will exhibit a greater rate of Touschek scattering [5]. These properties of the Diamond-II storage ring mean the beam halo is likely to be more significant than in the current machine. Thus it is beneficial to understand how we expect the beam halo to behave and how it could be observed.

Similar projects have previously been undertaken, including the successful development of a coronagraph BHM at

KEK [3]. A similar design was tested at CERN, where it was able to distinguish the halo from the core of a test lamp with a dynamic range of 10^7 [6]. A coronagraph BHM was also designed using a micro mirror array to mask the beam core and tested at the University of Maryland Electron Ring [7,8] and at DLS in collaboration with The Cockcroft Institute.

THE BEAM HALO MONITOR

Stage 1: Design and Installation

A BHM was designed to use visible SR emitted from a dipole magnet to image the beam halo, as shown in Fig. 1. The objective lens is a BORG77EDII apochromat, the characteristics of which are given in Table 1.

Table 1: Characteristics of the BORG77EDII Lens [10]

Parameter	Value
Aperture	77 mm
Focal length	510 mm
F ratio	6.6

Table 2: Properties of the Mako G-319B Camera with a Sony IMX265 Progressive Scan CMOS Sensor [11]

Parameter	Value
Pixels (H × V)	2048 × 1544
Pixel size (H × V)	3.45 × 3.45 μm
Sensing area (H × V)	7.1 × 5.3 mm
Pixel depth	8/12 bit
Shutter type	global
Resolution	3.20 MegaPixels
Max frame rate	37.50 fps

An image of the sourcepoint is formed on a Mako G-319B camera, which uses a Complementary Metal-Oxide-Semiconductor (CMOS) sensor, the properties of which are given in Table 2. Using a CMOS sensor allows the pixels imaging the beam core to saturate without blooming effects ruining the image [9]. The visible SR is a direct representation of the distribution of the electrons at the sourcepoint.

The monitor was built and tested in the lab. A system of mirrors was set up to replicate the 7.37 m optical path from the sourcepoint to the lens, and images taken of a 1951 USAF target were used to characterise the system. Using QuickMTF software [12], the modulation transfer function (MTF) of the system was measured. The properties of the stage 1 beam halo monitor are shown in Table 3.

The monitor was installed in the storage ring, next to the visible light extraction line. Reference images of the

* Emily.Howling.2017@live.rhul.ac.uk

EMITTANCE MEASUREMENT ALGORITHM AND APPLICATION TO HIMM CYCLOTRON*

Yong Chun Feng^{†,1}, Rui Shi Mao¹, Xiao Juan Wei

Institute of Modern Physics, Chinese Academy of Sciences, 730000 Lanzhou, China

¹also at Lanzhou Kejintaiji Corporation, LTD, 730000 Lanzhou, China

Abstract

HIMM, a Heavy Ion Medical Machine, developed by Institute of Modern Physics, has been in operation since April 2020. The beam emittance of the cyclotron exit is measured with the most often used techniques, i.e. slit-grid, Q-scan and 3-grid at a dedicated beam line which is not the actual HIMM optical line. The high speed data acquisition architecture is based on FPGA, and motion control system is constructed based on the NI module.

The data post processing and emittance calculation is based on Python code with self-developed algorithm, including Levenberg–Marquardt optimization algorithm, thick lens model, dispersion effect correction, error bar fit, mismatch check, image denoise and “Zero-thresholding” calculation. The algorithm description and simulation are discussed in detail. The application of the algorithm to HIMM cyclotron is presented in this paper as well.

INTRODUCTION

The heavy ion medical machine (HIMM) is developed by the Institute of Modern Physics (IMP), which consists of two electron cyclotron resonance (ECR) ion sources, a cyclotron, a synchrotron ring and five nozzles [1]. The synchrotron has a compact structure with a circumference of 56.2 m. The layout of the HIMM complex is shown in Fig. 1. Up to now, the slow-extraction efficiency of HIMM has reached nearly 90% for all energies from 120 to 400 MeV/u. The spill duty factor has exceeded 90% at a sample rate of 10 kHz with the feedback-based slow-extraction technique applied [2, 3].

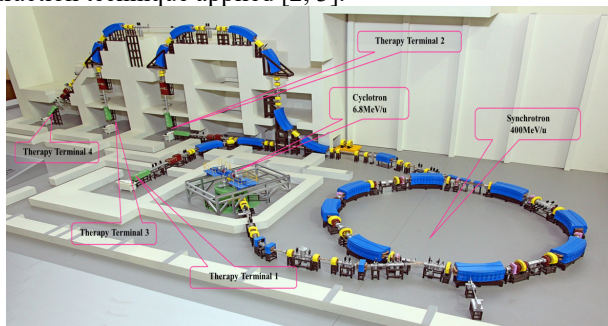


Figure 1: Layout of the HIMM complex.

Cyclotron, as the injector, plays a critical role in HIMM complex, which delivers the high quality beam to the ring through the MEBT (median energy beam transport line). The emittance and TWISS parameters measurement at the

exit of the cyclotron are essential. Before integrating the cyclotron into HIMM, a dedicated beam line is constructed temporarily at the laboratory, and the measurement of emittance is performed along it.

The emittance and TWISS parameters at the exit of the cyclotron are measured using three most commonly used methods, slit-grid [4-6], Q-scan [7-9] and 3-grid [8-10]. A cross-check is of capability to validate this measurement.

In this paper, optimization algorithm for Q-scan and 3-grid is introduced, in which dispersion correction and thick lens model fit are of the most importance in improving the reconstruction accuracy of the emittance. In addition, slit-grid algorithm, especially denoising in reconstructing the beam phase space is interpreted also. Both the optimization algorithm and denoising process can result in a positive improvement for emittance calculation from the view point of simulation and analytic derivation. Finally, the measurement results of the cyclotron are presented.

ALGORITHM DESCRIPTION AND SIMULATION

Optimization Algorithm for Q-scan and 3-grid

In the approximation of linear, beam transport along a lattice can be expressed in the form of matrix, which indicate how the transfer elements impose a function to the beam. From the view of matrix point, a transfer matrix can be formulated as

$$M = \begin{pmatrix} a & b \\ c & d \end{pmatrix} \quad (1)$$

without the loss of generality. The matrix must be symplectic, which is a remarkable property of a Hamiltonian system. After the implementation of the matrix, the squared distribution in the real space at the exit of the lattice element can be written as

$$\Sigma_{11}^f = a^2 \langle x_\beta^2 \rangle + D^2 \langle \delta^2 \rangle + 2ab \langle x_\beta x'_\beta \rangle + DD' \langle \delta^2 \rangle + b^2 \langle x_\beta'^2 \rangle + D'^2 \langle \delta^2 \rangle \quad (2)$$

, with the dispersion considered and chromaticity ignored. For a typical configuration of focus lens followed by a drift, the a and b can be expressed as

$$\begin{aligned} a(k) &= \cos\sqrt{k}l - \sqrt{k}L\sin\sqrt{k}l \\ b(k) &= \frac{1}{\sqrt{k}}\sin\sqrt{k}l + L\cos\sqrt{k}l \end{aligned} \quad (3)$$

with L the drift length, $k = B'/B\rho$, $B'l = C_1 + C_2l$, C_1 and C_2 for calibrated coefficient of magnet. For Q-scan scheme, the desired values, i.e., $\langle x_\beta^2 \rangle$, $\langle x_\beta x'_\beta \rangle$, $\langle x_\beta'^2 \rangle$, can be

* Work supported by NSFC (Nos.12105336), NSFC (Nos. 11775281), NSFC (Nos. 11905271) and the Natural Science Foundation of Gansu Province (No. 20JR10RA115)

† fengyongchun@impcas.ac.cn

DEVELOPMENT OF A PEPPER POT EMITTANCE MEASUREMENT DEVICE FOR THE HIT-LEBT

R. Cee*, C. Dorn¹, E. Feldmeier, T. Haberer, A. Peters, J. Schreiner, T. Winkelmann,
Heidelberg Ion Beam Therapy Centre, Heidelberg, Germany

¹also at GSI Helmholtzzentrum für Schwerionenforschung GmbH, Darmstadt, Germany

Abstract

The Heidelberg Ion Beam Therapy Centre (HIT) is a synchrotron based medical accelerator facility for the treatment of cancer patients with ions. Since the first treatment in November 2009 about 7000 patients have been irradiated with protons or carbon ions and, since July 2021, also with helium ions. In 2010 HIT started the operation of a test bench with a setup comparable to the LEBT at the accelerator. Since 2013 the test bench serves as a common low energy beamline of Siemens Healthcare and HIT with components from both partners. In parallel to ion source and RFQ research and development we have experimented with our proprietary pepper pot device. We plan to install the final version of the pepper pot into the LEBT section and use the measured beam distributions for the design of a new RFQ. With the recent redesign of the mask-target assembly we have increased the active area of the device and generated a possibility for an accurate pixel calibration by a specialised calibration mask. Our tool PePE (Pepper Pot Emittance Evaluation) offers different approaches for the reconstruction of the 4D emittance parameters from the raw image. The evaluation process was validated by a pepper pot image generated from a simulated beam with known properties.

INTRODUCTION

For reliable beam dynamics simulation and accelerator design the knowledge of the phase space occupied by the beam is of major importance. The pepper pot device is particularly suitable for characterizing the output beam of the ion source. Its vital component is the mask, a metal sheet with a regular grid of holes, reminding of the lid of a pepper pot thus giving the instrument its name. When inserted into the beam the mask cuts out a set of beamlets which are made, after a drift, visible on a scintillating screen. A digital camera records the light spots in a raw image which has to be processed with respect to the location and intensity of the beamlets. The beamlets have to be related to the holes giving not only the position but also the angle coordinate, the latter from the small difference between the beamlet position on the screen and the hole position on the mask. The hole spacing has to be chosen *small* enough to fulfil the demands on spatial resolution but *big* enough to avoid overlapping of the beamlets, leading to unfeasible images.

The resolution will in most cases be lower compared to e.g. a slit-grid-assembly but the major benefits of the pepper

pot are the fast data acquisition (single shot) and the 4D information including not only the real space (x - y) and the pure phase spaces (x - x' and y - y') but also the momentum space (x' - y') and the mixed phase spaces (x - y' and y - x').

TEST BENCH

The HIT test bench has its origin in 2010 when it was set up as a test facility for the third ion source branch for our low energy beam transport system (LEBT) [1]. After installation of the source and most of the beam line components into the productive accelerator, we continued to operate the test bench with alternating components. The exploratory focus is now on ion source optimisation, emittance measurement and RFQ characterisation.

The HIT test bench in its current state represents a LEBT with a subsequent RFQ accelerator (see Fig. 1). The ECR ion source for the production of $^{12}\text{C}^{4+}$, H_3^+ and $^4\text{He}^{2+}$ ions is directly coupled to a spectrometer dipole and followed by a dual stroke round aperture ($\varnothing 10$ mm, $\varnothing 20$ mm or out) for charge separation. The beam line behind the dipole comprises a triplet, a chopper for pulsed beam operation and a solenoid for the final matching of the beam into the RFQ. For beam alignment three steerer pairs are installed. The beam line is well equipped with beam diagnostic devices such as Faraday cups, beam transformers and profile grids. The pepper pot emittance meter with a mask, a quartz target, a mirror and a camera is located in a diagnostics chamber between chopper and solenoid. The diagnostic line downstream the RFQ contains three capacitive phase probes for time-of-flight resp. energy measurements.

The last subject of investigation has been the pepper pot device, which was, in its original form, developed in 2010 [2]. After having collected a number of measurement data for all available ions, we could draw our conclusions of how to improve the device. A couple of optimisations, described in the following section, have already been put into effect and measurements are in progress.

PEPPER POT HARDWARE

The pepper pot equipment is attached to two distinct actuators both mounted to the same diagnostics chamber: one holding the mask and the screen, the other one the mirror directing the light through a glass window to the camera installed on the flange. The distance between mask and screen is adjustable, realised by a fixed screen and a displaceable mask. The most important properties of mask and screen are summarised in Table 1.

* rainer.cee@med.uni-heidelberg.de

BEAM PROFILE MONITOR DESIGN FOR A MULTIPURPOSE BEAM DIAGNOSTICS SYSTEM

A. R. Najafiyani[†], F. Abbasi, Shahid Beheshti University, Tehran, Iran
Sh. Sanaye Hajari, F. Ghasemi, Physics and Accelerator Research School,
Nuclear Science and Technology Research Institute (NSTRI), Tehran, Iran

Abstract

Beam diagnostic tools are the key component of any accelerator. They provide the way to measure beam parameters in order to monitor the accelerator performance. The beam profile is a bridge to other beam parameters such as transverse position, size, divergence and emittance. Depending on the characteristics of the beam, there are different tools and methods for beam profile monitoring. A suitable diagnostic tool for measuring the beam profile with high resolution is scintillator view screens which are the oldest and most precise tools. This paper presents the beam profile monitor design for a multipurpose beam diagnostic system. This system is aimed to measure the beam profile, transverse parameter, momentum spectrum and current. The concerning issues in the beam profile monitor design such as image resolution, radiation damage and scintillator temperature distribution have been discussed.

INTRODUCTION

Diagnostic instruments are a set of equipment used to measure the various parameters of the particle beam in accelerators. A suitable diagnostic tool for high-resolution profile monitoring are scintillation screens that utilize the mechanism of the scintillation phenomenon. In this method, according to Fig. 1, the scintillation light is recorded by an optical system and processed in order to extract the beam parameters. We designed a scintillation screen monitor using YAG for a multipurpose beam diagnostics system that will be able to measure proton beams up to 200 keV energy and electron beams up to 10 MeV.

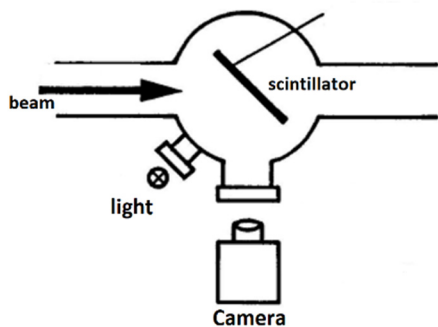


Figure 1: Layout of beam profile diagnostic system.

In this paper, the concerning issues in the beam profile monitor design such as image resolution, radiation damage, temperature distribution and charge accumulation on the scintillator have been discussed. Specially, using the

Geant4 Monte Carlo code, we have estimated the resolution of the scintillator view screen and the temperature distribution of the scintillator is simulated using Comsol software and its effect on measured beam profile has been addressed.

PROFILE MONITORING DESIGN

The design procedure includes, scintillator material selection, handling the thermal and charge accumulation issues and estimation and improvement of the measurement resolution.

Selection of Scintillation Material

For the scintillation material high light yield, resistance to radiation damage, vacuum compatibility, linear response and lower temperature sensitivity is demanded, YAG:Ce is a trade-off choice since it presents good scintillation yield and radiation damage resistance and low temperature dependence as discussed below [1].

Radiation Damage

Cavity and atomic displacement are the main types of radiation damage in scintillation crystals [2]. These lattice damage alters the energy of the crystal bond. As a result, optical parameters such as the yield and frequency of scintillation output light change [3]. Radiation damage is directly related to LET (the amount of energy that an ionizing particle transfers to the material per unit distance) of incident radiation, and the LET of each beam is directly related to its mass and charge and inversely related to its energy [4]. Therefore, the damage of the electron beams is generally small compared to the ion beams due to their mass.

[†]alireza.najafiyani2@gmail.com

COMMISSIONING OF THE SEM-GRID MONITORS FOR ELENA

M. McLean*, J. Cenede, G. Tranquille, CERN, Geneva, Switzerland
M. Hori, Max-Planck-Institut für Quantenoptik, Garching, Germany

Abstract

The Extra Low ENergy Antiproton ring (ELENA) is a compact ring for the further deceleration and cooling of the 5.3 MeV antiprotons delivered by the CERN Antiproton Decelerator. It decelerates antiprotons to a minimum energy of 100 keV, creating special challenges for the beam instrumentation. These challenges have been addressed by an extremely sensitive SEM-Grid (Secondary Emission Monitor) monitor which is also compatible with the Ultra High Vacuum (UHV) requirements of ELENA. Since November 2019, ELENA's H^- ion source has been used to test the SEM-Grid monitors and, since July 2020, the monitors have been used to commission the ELENA transfer lines. In this paper, a summary of the features of the SEM-Grid will be given together with an overview of its commissioning activities. An ingenious technique for testing the integrity of the grid wires which are not directly accessible will also be described.

INTRODUCTION

ELENA [1, 2] is a small synchrotron of 30.4 m circumference constructed recently at CERN and sketched in Fig. 1. The purpose of the machine is to decelerate antiprotons coming from the Antiproton Decelerator (AD) [3] at 5.3 MeV beam energy down to 100 keV. Multiple branching electrostatic transfer lines lead to the experimental zones. All the transfer lines are equipped with multiple SEM-Grid Profile Monitors to enable accurate and automated steering of the beam.

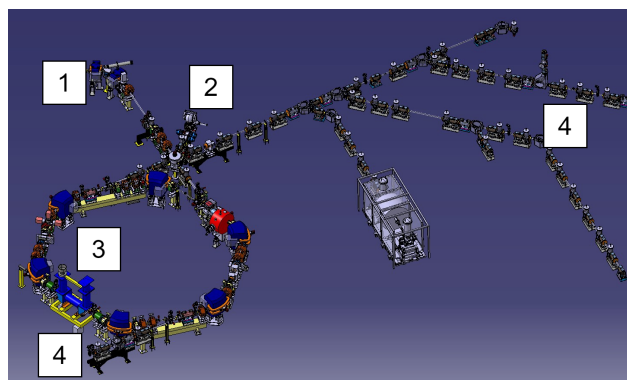


Figure 1: ELENA ring and transfer lines.
1 - Injection from AD
2 - H^- source
3 - ELENA ring with electron cooler
4 - Transfer lines

* mark.mclean@cern.ch

These monitors and electronics were initially developed by the ASACUSA collaboration based on an earlier design [4] used in the radiofrequency quadrupole decelerator facility, and then productionised, assembled, installed, and commissioned by CERN. Numerous issues were resolved during this process. The monitors were installed to observe protons, antiprotons and H^- ions at 100 keV to 5.3 MeV.

MONITOR OVERVIEW AND COMMISSIONING

Each monitor is composed of five stacked grids; one sensor grid for each plane (horizontal and vertical), sandwiched between three anode grids to attract any liberated electrons. The sense grids use 47 wires of $\text{Ø}20\ \mu\text{m}$, while the anode grids use 43 wires of $\text{Ø}12\ \mu\text{m}$. The sense wires are bigger to optimise the charge collection, while the anode wires are a compromise between mechanical strength and beam attenuation. The sense wires are on a $500\ \mu\text{m}$ pitch in the central region and 3 mm pitch at the sides, they are at ground potential. The anode wires are on a 1.5 mm pitch under a bias voltage of 60 V. When a particle hits one of the sensor grid wires, a few electrons are liberated and attracted to the anode wires. A charge then flows into the sensor wire to replace the lost electrons, and this charge is measured. Each monitor absorbs about 10% of the beam, therefore it is mounted on a pneumatic in-out mechanism so it can be removed from the beam path when not required. Figure 2 shows the different components of the SEM-Grid monitor.

A total 43 SEM-Grid Monitors are planned to be installed in the ELENA transfer lines. The installation has been progressing since early 2020, as the transfer lines were completed and as the parts to assemble the monitors became available.

Mechanics

The grids are supported by a guided bellows and connected to the electronics by two 50-way vacuum feedthroughs. All the in-vacuum parts of the monitor were designed to be compliant to stringent vacuum requirements regarding the materials used, the surface treatment and cleanliness, this is especially relevant to the detector grid which utilises a ceramic PCB. The guide rods have a vacuum compatible treatment of molybdenum disulfide (MoS_2) to avoid sticking.

Installation The monitor is assembled in a clean environment and placed in a spare tank to protect the grid during transport. The vertical position of the grid is measured in a metrology laboratory, and any offset is then corrected by a custom spacer. The monitor is then installed in a bake-out

4D BEAM TOMOGRAPHY AT THE UCLA PEGASUS LABORATORY

V. Guo*, P. Denham, P. Musumeci, A. Ody, and Y. Park,
 UCLA Department of Physics and Astronomy, Los Angeles, CA, USA

Abstract

We present an algorithm to tomographically reconstruct the 4D phase space of a beam distribution of a high brightness electron beam, based on the use of two fluorescent screens separated by a beamline containing a quadrupole triplet which can be used to impart arbitrary rotations to the beam phase space. The reconstruction method is based on generating a macroparticle distribution which matches the initial profile and then it is iteratively updated using the beam projections on the second screen until convergence is achieved. This process is repeated for many quadrupole current settings. The algorithm is benchmarked against GPT simulations, and then implemented at the UCLA Pegasus beamline to measure the phase space distribution for an upcoming high speed electron microscope experiment.

INTRODUCTION

In high brightness electron accelerators, the beam dynamics and transport is strongly influenced by the space charge fields associated with the details of the electronic distribution and its evolution along the beamline, which depends on each particle position and velocity [1]. In linear beam dynamics, it is sufficient to monitor the second order moments of the distribution which has a constant shape along the beamline, but as soon as non-linear forces (either external or internal) are applied, the distribution will evolve and change along the beamline. Having an accurate representation of the beam transverse phase space is then critical to predict and then optimize the beam behavior in many setups. For example in single-shot time-resolved electron microscopy, it has been pointed out that different electronic distribution can originate different space-charge induced aberrations and greatly affect the spatial resolution of the instrument [2].

While it is of great interest to know the shape of the transverse phase space distribution function, the experimental measurement of this quantity poses some challenges as beam profile monitors only record the spatial beam distribution (i.e. the projection of the 4D phase space volume onto the x - y plane) while the angular or transverse velocity distribution is harder to access.

Tomography is a well developed imaging technique that uses a set of projections to reconstruct a distribution in a space with higher dimensions. Typically, tomography is used to reconstruct the shape of an object in 3D from a complete set of 2D projections along different angles as for example in CAT scans. Applied to beam physics, tomography can be used to reconstruct the 4D phase space distribution from an appropriately chosen set 2D transverse beam profile (projections) [3–6].

* vgw618@g.ucla.edu

In this paper, we present the development of such a technique at the UCLA Pegasus Laboratory [7, 8] where fluorescent screens are used to record the spatial projections of a high brightness beams before and after a set of three quadrupoles with adjustable currents to change the rotation angles of the transverse phase space and enable a tomographic reconstruction. Importantly, the transformation of the phase space in these measurements does not provide projections for the entire range of rotation angles due to the limitation in the quadrupole currents or placement of the beamline components. Therefore, while usual tomography reconstructs the source volume from complete set of projections over the entire range of possible angles [9, 10], the algorithm for beam phase space reconstruction should be tolerant of this incomplete set of projections. We present here the MATLAB algorithm we used in the reconstruction which is based on sampling the 4D beam transverse phase space with a macroparticle distribution. The algorithm is shown to work well both on simulation and experimental data and is eventually expected to be used in a feedback loop to optimize the photocathode illumination to generate ideally shaped 4D transverse phase space distributions to improve spatial resolution in single shot time-resolved electron microscopy.

DATA COLLECTION

In order to perform a tomographic reconstruction, sufficient access to different rotation angles is needed. While the technique can be generalized and applied to other beamlines, in the following we focus on the setup currently installed at the UCLA Pegasus laboratory shown in Fig. 1. The measurement takes place in the area highlighted by the red square. The initial spatial distribution is recorded on screen 4 and the various projections are obtained changing the currents in the green quadrupoles with the beam profile recorded on the final YAG screen.

The current settings for the quadrupoles are chosen in order to maximize the range of angles the phase space rotates before hitting the final screen.

In order to do this, we write the beam transport matrix as a function of current settings on each of the quadrupole (I_1, I_2, I_3) using a smooth approximation for the quadrupole field gradient profile $G(z)$ along the axis:

$$G(I, z) = \frac{CI}{2} \left[\tanh \left(\frac{b}{2} \left(\frac{L}{2} - z \right) \right) + \tanh \left(\frac{b}{2} \left(\frac{L}{2} + z \right) \right) \right]$$

where L is the effective length of the quadrupole, b is the steepness parameter of the edges, and the nominal magnetic field gradient CI is simply proportional to the current setting of the quadrupole. For the quadrupoles used in the experiment $L = 0.078$ m, $b = 135$ m⁻¹ and $C = 0.45$ Tm⁻¹A⁻¹.

THE FIRST BEAM EXPERIMENT RESULT OF THE PROTOTYPE OF WIRE SCANNER FOR SHINE *

F. Z. Chen[†], B. Gao, J. Chen, Y.B. Leng

Shanghai Advanced Research Institute, Chinese Academy of Sciences, Shanghai, China

J. Wan, Shanghai Institute of Applied Physics, Chinese Academy of Sciences, Shanghai, China

Abstract

As a kind of quasi-non-destructive beam size monitoring, SHINE will employ dozens of wire scanners. The preliminary study is confronted with motion control difficulty. To reduce the ultrahigh coordinate about wire movement with beam loss data acquisition, a new method has been proposed in the SXFEL test platform. The strategy is utilizing the beam jitter, which is of the same magnitude with the beam size. Combine with the jitter of the beam position, we move tungsten wires in a few of different position to realize the measurement. This paper will present our experiment design as well as a furthermore plans about the prototyping design.

INTRODUCTION

As a quasi-non-destructive beam size and emittance measurement system, wire scanner is widely used in linear accelerators worldwide [1]. As a classic beam size measurement system, the measurement principle of wire scanner is very simple. It is assumed that the downstream secondary product flow is proportional to the intensity of the electron beam passing through the tungsten wire [2]. The secondary products mainly include high-energy electrons, gamma rays and secondary currents generated on tungsten wires. Therefore, the signal detected by the downstream photomultiplier is positive correlation with the beam intensity, and the size of the beam can be measured by accurately measuring the distance of the tungsten wire movement. In addition to the application of the wire scanner for accurate beam size measurement, one or several sets of such detectors can also be used to complete offline or online beam emittance measurement and energy dispersion measurement.

In this article, we discuss the hardware and software structure of the SHINE wire scanner prototype and the first beam experiment results.

IDEA

The initial setting is to use wire scanner to scan the beam transversal section at a uniform speed [3]. Take advantage of the high repetition frequency of the SHINE, the position of the wire and the beam interaction can be obtained. Combining the beam loss data, we can calculate the beam size using Gaussian fit.

Since the SHINE is still under construction, our wire scanner prototype is installed in the SXFEL facility for testing at present. It is differ from the hard X-ray free electron laser

facility with high repetition frequency(up to 1MHz), the current repetition frequency of the SXFEL facility just 2 Hz. Under the circumstances, the fast scan method requires high precision for the timing system, also the movement speed requirement for linear motor uniform scanning is too low. After the first preliminary experiment, we acquired that the beam size of the SXFEL is in the magnitude of several hundred microns, and the jitter of the beam position is about the same order of magnitude. This will introduce a noticeable uncertainty of measurement using the fast scan mode. However, it provides a new idea for the SXFEL experiment adopt a static testing method. We can make use of the beam jitter, acquire a step-by-step scanning method in the SXFEL wire scanner prototype principal verification stage.

The basic idea is fixing the position of the wire target, changing the original wire scanning motion mode of the wire sweeping the beam to the beam sweeping wire. We can get the beam loss signal and beam position signal in different beam positions due to beam jitter. The step-by-step static testing is using the CBPM to acquire the accuracy position(position resolution up to 200nm). The data acquisition system using external clock and external trigger come from electronic chamber, which can guarantee the synchronization of the beam loss and the impact point.

SYSTEM SETUP

The wire scanner system is comprised of the mechanical execution structure and the beam loss detector in the tunnel, the upper computer and the data acquisition board outside the tunnel. Figure 1 is the installation photo in the tunnel. From nearest to farthest, CBPM is upstream the mechanical execution structure, the beam loss detector is installed downstream parallel to the vacuum pipe.

After the tensile test of 10 μm tungsten wire and 20 μm tungsten wire, we chose 20 μm tungsten wire as the test wire for the first version of the prototype. The tungsten wire is mounted on the customized fork connected to the linear motor, it was distributed in three directions testing the beam size in the horizontal direction, the vertical direction and the oblique 45 degrees(see Fig. 2).

We use the linear motor of LinMot to drive the wire target. The main motion modes of the motor are as follows:

- Step by step test: In this mode, the scanner will move to the user defined position for several test, after that, it will move to another position. The sample interval is defined by the beam jitter.

* Work supported by National Nature Science Foundation of China(No.11375255)

[†] chenfz@sari.ac.cn

FAST MEASUREMENTS OF THE ELECTRON BEAM TRANSVERSE SIZE AND POSITION ON SOLEIL STORAGE RING

M. Labat*, A. Bence, N. Hubert, D. Pédeau, Synchrotron SOLEIL, Gif-sur-Yvette, France
 M. M. Patil, M. Caselle, A. Ebersoldt, E. Bründermann,
 Karlsruhe Institute of Technology, Karlsruhe, Germany

Abstract

On SOLEIL storage ring, three beamlines are dedicated to electron beam diagnostics: two in the X-ray range and one in the visible range. The visible range beamline uses the synchrotron radiation which is emitted in one of the ring dipoles and further extracted by a slotted mirror operated in surf-mode (surfing on the upper part of the synchrotron layer). The radiation in the visible range is then transported towards a diagnostic hutch in the experimental hall, allowing electron beam imaging at the source point onto a standard CCD camera. In the perspective of prototyping works for the eventually forthcoming upgrade of SOLEIL, and for the on-going commissioning of a new Multipole Injection Kicker (MIK), we recently installed in this hutch two new branches ended by two new cameras (a KALYPSO system and a standard CMOS camera). We report in this paper the first results obtained on those branches.

INTRODUCTION

SOLEIL storage ring presently delivers synchrotron radiation to 29 beamlines. The stability of the delivered photon beams, a main figure of merit for users, relies on an accurate monitoring of the electron beam orbit and electron beam size / emittance at users source points. The electron beam size / emittance is measured independently by two pinhole camera (PHC) systems, located at two different places of the ring. One of the PHC measurement is used in a feedback loop to maintain the vertical emittance within +/-5 %. However, with typical exposure times of 50–100 ms, those systems cannot follow fast beam dynamics features at the turn-by-turn scale for instance.

The installation of a new injection magnet and the perspective of an upgrade for SOLEIL recently revealed the need for an additional beam size diagnostic with a faster response.

We therefore decided to upgrade our visible range MRSV (*Moniteur de Rayonnement Synchrotron Visible*) beamline with two new branches. This work presents the preliminary results obtained on those branches.

EXPERIMENTAL SETUP

The experimental layout of the MRSV beamline is presented in Fig. 1. The synchrotron radiation of one of the ring dipoles (ANS-C01) is extracted using a slotted mirror operated in *surf-insertion* mode: the mirror is surfing on top of the synchrotron radiation layer to catch visible range

photons. Because of heat load issues, we can't operate the mirror in *slot-insertion* mode, i.e. centered on the beam axis with synchrotron radiation X-rays going through the slot, at high current. The synchrotron radiation is then transported via a set of mirrors down to a hutch in the experimental hall. On the beam path inside the tunnel are successively placed: a motorized slit to define the horizontal collection angle θ_x of the beamline and a spherical lens for refocussing. At the arrival on the optical bench in the hutch, the synchrotron radiation is splitted into several branches.

Initially, three branches were implemented (see pink boxes in Fig. 1): one with a fast diode for filling pattern measurement, one with a Streak Camera for bunch length measurement and one with a standard ethernet camera for a coarse imaging of the beam at the source point. We added two new branches to test higher resolution / higher speed imaging systems for beam size retrieval.

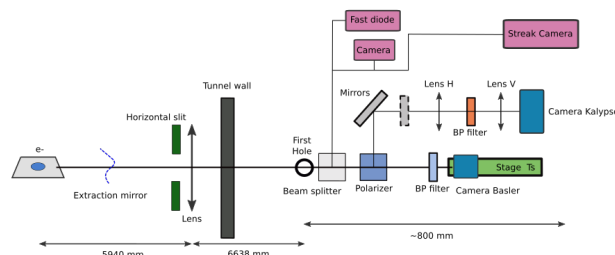


Figure 1: Layout of the MRSV beamline with its three initial branches in pink, and its two new branches.

BEAMLINE MODELING

To achieve an accurate imaging, an accurate modeling of the beamline is mandatory. We used for that the SRW (*Synchrotron Radiation Workshop*) code [1]. In Fig. 2 is first presented the simulated effect of using the extraction mirror in *surf* rather than in *full* (or *slot*) –insertion mode. Because of the dissymmetry of the extraction, there is nearly no more difference between the polarization components of the radiation.

After a first attempt of comparison between measured and simulated intensity distributions in the image plane of the MRSV beamline, we realized that the beamline was suffering from strong stigmatism: the image plane in y was few tens of centimeters downstream the image plane in x . Because the focussing lens in the tunnel is spherical, we immediately suspected the extraction mirror to introduce this stigmatism. To verify this interpretation, we simulated the effect of a

* marie.labat@synchrotron-soleil.fr

COMMISSIONING OF THE LHC INJECTORS BWS UPGRADE

J. Emery*, W. Andreatza, D. Belohrad, S. Di Carlo, J.C. Esteban Felipe, A. Goldblatt, D. Gudkov, A. Guerrero, S. Jackson, G.O. Lacarrere, M. Martin Nieto, A.T. Rinaldi, F. Roncarolo, C. Schillinger, R. Veness,
European Organization for Nuclear Research (CERN), Geneva, Switzerland

Abstract

A novel generation of fast Beam Wire Scanners (BWS), developed in the framework of the LHC Injectors Upgrade (LIU), has been recently deployed in the 3 LHC injector synchrotrons, accelerating protons from 160 MeV to 450 GeV, during the 2019-2020 LHC long shutdown. The monitors feature high precision motor controllers, high resolution wire position monitoring and wide dynamic range secondary particles detectors. This contribution will document the commissioning of the 17 new systems during the accelerator complex restart in 2021, which is an exciting and challenging phase in the life cycle of an instrument. A summary of the so far achieved levels of reliability, reproducibility, detectors/DAQ bandwidth, and overall accuracy, will be used to revisit the options for further improving the systems' performance in the future.

INTRODUCTION

The LHC Injectors Upgrade (LIU) Beam Wire Scanner (BWS) achieves high performances and reliability with completely new engineering concepts. After more than a decade of research and development within the instrumentation group at CERN [1–5], seventeen systems have been installed in the injectors complex during the second LHC long shutdown (LS2). The commissioning has been following the restart of the injectors in 2021, starting with the Proton Synchrotron Booster (PSB) with eight systems, Proton Synchrotron (PS) with five and Super Proton Synchrotron (SPS) with four. This paper, after introducing the new system features, will focus on the various commissioning stages that allowed to hand over the systems to the various accelerators operation crews.

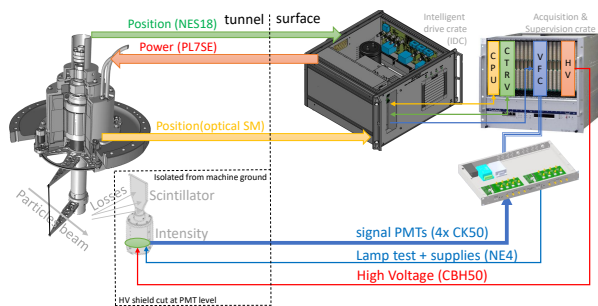


Figure 1: LIU BWS with its electronics at the surface (right) while mechanics and detectors are on the beam line (left).

* jonathan.emery@cern.ch

INSTRUMENT DESCRIPTION

A wire-scanner monitor is based on a very thin carbon wire made crossing the particle beam at high velocity [6]. This interaction produces a shower of secondary particles, which correlated to the wire position, allows reconstructing the transverse beam profile.

The new BWS features key innovations, with the kinematic unit having moving parts only in vacuum, using magnetic and optical means to transfer power and signaling from and to the air side. The position of the shaft is measured by a solid rotor resolver for trajectory control [7] and by a high accuracy optical encoder, developed in-house, to precisely infer the fork and wire position during a scan [8]. The encoder is based on the analysis of a laser beam focused on and then reflected by reflective and anti-reflective tracks engraved on the optical disc mounted on the shaft. Due to the high acceleration felt by the carbon wire the calibration of this system is essential to compensate for uncertainties of the wire trajectory for predefined speeds [9]. The secondary particle shower detection uses one scintillator coupled to four detectors equipped with different neutral density filters to cover the large dynamic range of beam energies and intensities across the LHC injectors [10]. The output signals are digitised simultaneously at high speed and processed to provide profile measurements for each particle bunch.

Figure 1 shows the instrument architecture. The kinematic unit and particle detectors (left side) are located in the accelerator tunnel. The stand-alone control unit and the VME acquisition system (right side) are in the surface service area. The communication from tunnel to surface is done with cables and optical fibers, with lengths above 150 m in some cases.

Hardware Test Procedures

Emphasis was made on the system testability when designing the LIU wire-scanner. Multiple procedures were implemented to quickly validate the systems after installation and any time a diagnosis is required.

The Open Loop Test (OLT) verifies the cabling, electronics and sub parts of the kinematic unit. The three phases motor is powered without current and position feedback, i.e. in open loop, similar to stepper motors. The scanner moves forward and backward by 3.14 rad in steps and an example of the measured motor currents (blue, green, orange) and shaft angle (red) is shown in Fig. 2. The levels are compared to references to detect any non-conformity. With this procedure, the system hardware commissioning can be carried out from the surface without the need of tunnel access to

PROPOSED RESEARCH WITH MICROBUNCHED BEAMS AT LEA*

A. H. Lumpkin†, Argonne Associate, Argonne National Laboratory, Lemont, IL 60439 USA

W. J. Berg, J. Dooling, Y. Sun, K.P. Wootton, Argonne National Laboratory, Lemont, IL 60439 USA

D. W. Rule, Silver Spring, MD, 20904 USA

A. Murokh, RadiaBeam Technologies LLC, Santa Monica, CA 90404 USA

P. Musumeci, UCLA, Los Angeles, CA 90095 USA

Abstract

Significant microbunching of an electron beam at 266 nm is projected with the co-propagation of electrons at 375 MeV and a UV laser pulse through a 3.2-cm period prebuncher undulator. Such microbunched beams will generate coherent optical transition radiation at a metal screen surface boundary or coherent optical diffraction radiation from a nearby metal surface (new model presented). With a 10% microbunching fraction, coherent enhancements of more than 7 million are modelled for a 300-pC charge. Diagnostic plans are described for beam size, divergence, electron microbunching fraction, spectrum, and bunch length on a single shot at the Argonne National Laboratory Linac Extension Area (LEA).

INTRODUCTION

One of the advantages of relativistic electron beams with microbunching at UV to visible wavelengths is the potential to generate coherent optical transition radiation (COTR) at a metal foil for diagnostics purposes. A significant microbunching fraction of at least 10% is expected for the case of a seed laser at 266 nm copropagating with a 375-MeV electron beam through a modulator undulator (3.2 cm period) at the Linac Extension Area (LEA) at Argonne National Laboratory [1,2]. Diagnostic plans have been made for the COTR-based characterization of the microbunched beam size (~100 microns), divergence (sub-mrad), microbunching fraction, spectrum, and bunch length (sub-ps), as well as coalignment of the laser pulse and electron beam as previously described [3]. For that case, COTR enhancements over OTR of more than seven million were calculated, and we expect a similar enhancement of coherent optical diffraction radiation (CODR). Thus, we propose the modification of the microbunching diagnostics station to support initial CODR experiments with beam transit through an aperture in a metal screen or near a metal edge at the second screen position of the interferometer. We would explore whether the coherence function for CODR provides a complementary beam size monitor.

EXPERIMENTAL ASPECTS

The Advanced Photon Source (APS) linac includes options for injection of beam from either a thermionic cathode (TC) rf gun or a photocathode (PC) rf gun into an S-

band linac with final beam energies of up to 500 MeV. The schematic of the facility is given in Fig. 1. For operations providing beam to the APS storage ring, beam from one of the two thermionic guns is used. For these proposed experiments, single micropulses from the PC rf gun with Cu cathode irradiated by a quadrupled Nd glass laser at 2 or 6 Hz would be used with electron beam parameters given in Table 1. The chicane is used for bunch compression from 2 ps down to $\sigma_t \sim 0.5$ ps.

At the end of the linac there is an option to transport beam with a bypass of the Particle Accumulator Ring (PAR) to the LEA building where the experiments can be performed. A schematic of the experimental geometry is shown in Fig. 2. After the modulator and dispersive section, there would be the diagnostics chamber which is repurposed from a previous FEL experiment [4]. This chamber has stepper actuators at two locations in z separated by 6.3 cm. The first is a normal imaging station with positions for a YAG:Ce screen plus 45-degree mirror or a metal foil at 45 degrees. When this latter 10- μ m thick Al foil is selected, it blocks the seed laser, and it also generates forward COTR as the beam exits from the back surface in the direction of the second mirror at 45 degrees which is 6.3 cm downstream. COTR is also generated at the front surface of this metal mirror. The combination of sources provides the COTR interferometry. By using near field (NF) focusing the microbunched beam size at the first screen can be measured, and by using far-field (FF) focusing the angular distribution pattern of the COTR interferences can be seen and divergences assessed. The expected COTR patterns have been previously reported [3,5], and an example is provided in the next section.

The YAG:Ce emissions are near 550 nm so a standard digital CMOS camera would be used for initial beam size imaging. The COTR and CODR would be narrowband at the wavelength of the UV seed laser so a UV sensitive imager is needed with a digital capability preferred. Multiple cameras would be used with beam splitters to provide NF, FF, polarized imaging, and spectra on a single shot for

Table 1: Linac Parameters for PC Gun Beam Used in the Proposed Tests

Parameter	Units	Value
Energy	MeV	375
Charge	pC	100-300
Emittance	mm mrad	2-4
Bunch length	ps	0.5-2.0

* Work supported in part by UChicago Argonne, LLC under Contract No. DE-AC02-07CH11357 with the U.S. Department of Energy, Office of Science, Office of Basic Energy Sciences.

† lumpkin@anl.gov

THE HL-LHC BEAM GAS VERTEX MONITOR - PERFORMANCE AND DESIGN OPTIMISATION USING SIMULATIONS

B. Kolbinger*, H. Guerin¹, O. R. Jones, T. Lefevre, J. W. Storey,
A. Salzburger, R. Veness, C. Zamantzas, CERN, Geneva, Switzerland
S. M. Gibson, R. Kieffer, Royal Holloway, University of London, Surrey, UK
¹also at Royal Holloway, University of London, Surrey, UK

Abstract

The Beam Gas Vertex (BGV) instrument is a novel non-invasive beam profile monitor and part of the High Luminosity Upgrade of the Large Hadron Collider (LHC) at CERN. Its aim is to continuously measure emittance and transverse beam profile throughout the whole LHC cycle, which is currently not possible using a single device. The BGV consists of a gas target and a forward tracking detector to reconstruct tracks and vertices resulting from beam-gas interactions. The beam profile is inferred from the spatial distribution of the vertices, making it essential to achieve a very good vertex resolution. Extensive simulation studies are being performed to provide a basis for the design of the future BGV. The goal of the study is to ascertain the requirements for the tracking detector and the gas target within the boundary conditions provided by the feasibility of integrating them into the LHC. This contribution will focus on the simulations of the forward tracking detector. Based on cutting-edge track and vertex reconstruction methods, key parameter scans and their influence on the vertex resolution will be discussed.

INTRODUCTION

Understanding the evolution of beam profile and size throughout the whole accelerator cycle of the LHC is of great importance for the optimisation of emittance, and hence luminosity. The BGV device is foreseen to provide an independent, continuous, non-invasive, and bunch intensity independent measurement of the beam profile throughout the accelerator cycle. Beam-gas collision products stemming from LHC protons, interacting inelastically with the BGV's gas target installed in the path of each circulating beam, are measured via tracking detectors (Fig. 1 A). The beam profile is determined from the spatial distribution of the reconstructed vertices of the collisions.

A BGV demonstrator device has been successfully installed, commissioned and operated during LHC Run 2 [1]. A vacuum pressure bump of 10^{-7} mbar extending over ≈ 2 m was provided by a gas injection system and acted as the target. The forward tracking detector was composed of several planes of scintillating fibres based on the LHCb SciFi detector modules [2]. It successfully demonstrated the feasibility to use inelastic beam gas interactions for beam monitoring. However, due to poor track quality and limited vertexing capabilities, the demonstrator failed to reconstruct the beam profile. A new design is currently under development based

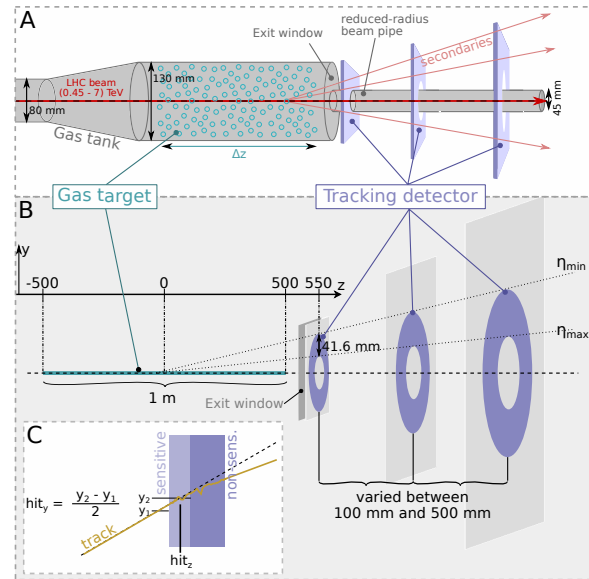


Figure 1: A: Sketch of the BGV. B: Generic simulation setup. The interaction region is shown in turquoise. The detector layers are shown in light grey, their active area in purple. The exit window (dark grey) is placed at $z = 545$ mm. C: Z-y cross-section of a detector layer.

on what has been learned from the BGV demonstrator and the results of detailed and complete simulations.

The true beam profile is extracted from the spatial distribution of reconstructed vertices via deconvolution of the vertex response of the BGV system, making the latter the most important figure of merit for the device's performance. However, a precise knowledge of the vertex response is difficult to achieve. It is therefore desirable to keep its width, i.e. the vertex resolution σ_v , low relative to the true beam width σ_b . At the foreseen location of the BGV, the smallest expected beam size will be $\sigma \approx 200 \mu\text{m}$ at 7 TeV. Assuming bunches with Gaussian transverse distributions with standard deviations of σ_b and a Gaussian vertex response with a width of σ_v , the following relation arises via deconvolution, error propagation and assuming negligible measurement uncertainty [3]: $\frac{\delta\sigma_b}{\sigma_b} = \frac{\sigma_v^2}{\sigma_b^2} \frac{\delta\sigma_v}{\sigma_v}$, where $\delta\sigma_b$ and $\delta\sigma_v$ denote the absolute beam size and vertex resolution uncertainties. This relation highlights the importance of a small σ_v relative to the beam size and precisely knowing the vertex resolution. Assuming a relative beam size error of ≤ 0.05 (see design specifications listed in Ref. [4]) and $\frac{\delta\sigma_v}{\sigma_v} \leq 0.1$, we arrive at an upper limit for the vertex resolution of $\sigma_v \leq 140 \mu\text{m}$.

* bernadette.kolbinger@cern.ch, corresponding author

NEW CERN SPS BEAM DUMP IMAGING SYSTEM

S. Burger*, E. Bravin, A. Churchman, F. Roncarolo, A. Topaloudis, F. Velotti, E. Veyrunes,
 CERN, Geneva, Switzerland

Abstract

As part of the LHC injector Upgrade (LIU), the CERN SPS is now equipped with a new Beam Dumping System (SBDS) designed to cope with the high power beams foreseen for the High Luminosity LHC (HL-LHC) era [1, 2]. Before reaching the dump, the proton beam (from 14 to 450 GeV) is vertically kicked and then diluted passing through a series of horizontal and vertical bumps. This prevents the dump damage, by reducing the power density per surface unit. The quality of each dump event must be verified, for which all SBDS parameters are logged and analysed in the so-called Post-Mortem dataset. An essential part of the verification is performed by a beam imaging system based on a Chromox screen imaged on a digital camera. The desired availability level (100%, to protect the dump) and the harsh radiation environment made the design extremely challenging. For example, it implied the need for a 17m long optical line made of high-quality optical elements, a special camera shielding (to minimise single event upsets) and a generally careful design accounting for maintenance aspects, mainly related to expected high activation levels. After giving an overview of the whole imaging system design with details on the chosen layout and hardware, this paper will discuss the DAQ and SW architecture, including the automatic, on-line, image selection for validating every dump event. This will be complemented with experimental results demonstrating the performance and reliability achieved so far.

THE NEW SPS INTERNAL DUMP

The new SPS beam dump is composed of a 5 m long absorber made of several blocks of graphite, Titanium Zirconium Molybdenum (TZM) and pure Tungsten material. It is covered by a 3 layer concrete, cast-iron and concrete/marble shielding. The weight of this assembly is 2 t for the absorber that is impacted by the beam and about 674 t for the shielding. It is located in sector 5 of the SPS machine.

To protect the block against high power density beams, the extracted protons are diluted in order to reach a non-destructive power density. The principle of the beam dumping is sketched in Fig. 1 with a simulated example of a Fixed Target type beam dump dilution shape, as expected at the front plate of the dump.

Instrumentation Specifications

The instrumentation, fundamental to the beam dump quality checks has been requested to fulfill the following main specifications:

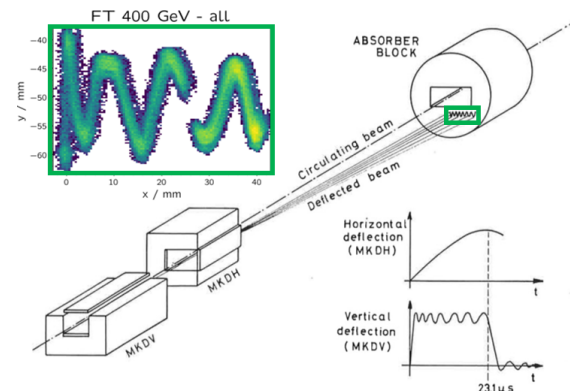


Figure 1: Principle of beam dumping and simulated example of a Fixed Target type beam dump dilution shape.

- All SPS beam dump events must be recorded. This means between $5 \cdot 10^9$ and $8 \cdot 10^{13}$ protons per event, with energy from 14 to 450 GeV.
- The imaging horizontal and vertical spatial resolution must be better than $200 \mu\text{m}$.
- The imaging system maintenance must be optimized to cope with high radiation levels.

The design of the new SBDS monitor is based on the so-called Beam TV (BTV) system, exploited in different versions and hundreds of units, throughout the whole CERN facility. A BTV system is based on the use of a screen interacting with the beam and generating photons (i.e. different processes depending on protons energy and screen materials) that are imaged on a camera system, thus providing the proton beam footprint. In the SBDS case, the image acquisition is synchronized with the beam extraction event. After calibration, the digitized images provide an accurate beam position and size to monitor quantitatively the dilution of the beam on the dump surface. As already mentioned above, the high radiation environment has heavily affected the new BTV system design choices, from the layout (i.e. need of a

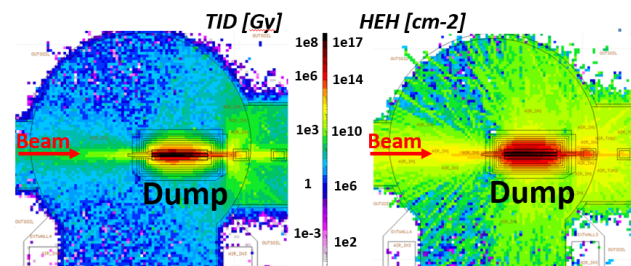


Figure 2: Fluka radiation simulations of the SBDS area showing the top view at the beam level.

* stephane.burger@cern.ch

A BEAM DIAGNOSTICS SYSTEM OF ELECTRON BEAM MELTING FOR ADDITIVE MANUFACTURING*

R. Kavak[†], E. Durna, M. G. Sanal, M. M. Sezer, ASELSAN A.S., Ankara, Turkey

Abstract

Electron beam melting has been used recently in additive manufacturing by various researchers. In those electron beam melting applications, the electron energy can be 60 to 100 keV, the beam current can be around 10 mA to 100 mA, and the beam spot size can be as small as 200 μm according to electron energy and beam current. Those parameters can result in very high beam power densities. The diagnostics of this powerful beam can be quite a problematic issue. As the electron beam current required for the application is quite similar to DC current, fast undestructive current measurement techniques for current beam profile and beam position are very limited in performance. Therefore, some destructive techniques to measure current and other beam properties are essential. As part of the beam diagnostics for electron beam melting application for additive manufacturing, the authors proposed a complete beam diagnostics system to measure the electron gun's capabilities and associate electromagnetic lens systems. The following properties have been diagnosed as part of this research work: i) Beam Current, ii) Beam Spot size for enlarged and focused beams, iii) Scanning velocity of the deflected beam, iv) Profile of the beam. The authors proposed methods to measure focused beam spot size and deflected beam scanning velocity using Secondary Emission Grid Sensors. Moreover, the authors proposed a new technique to measure beam profile using consecutively placed several copper plates with beam guiding holes of various diameters. The proposed beam profile measurement method effectively determines the useful beam radius for metal powder melting properties specifically to additive manufacturing applications.

INTRODUCTION

Recent advancements in engineering and material science require complex manufacturing processes [1]. For this reason, Additive Manufacturing (AM) challenges the traditional manufacturing methods in many cases [2]. According to the Additive Manufacturing Trend Report 2021 from HUBS, the global AM market grew 21 percent year-on-year to \$12.6 bn in 2020. They also predicted that the AM market will be more than doubled, reaching \$37.2 bn in 2026 [3]. The efficient usage of limited resources and the ability to produce complex shapes put AM forward when compared to traditional manufacturing [2, 4].

* Work supported by the Scientific and Technological Research Council of Turkey (TUBITAK) under grant number 3170014.

[†] rafetkavak@protonmail.com

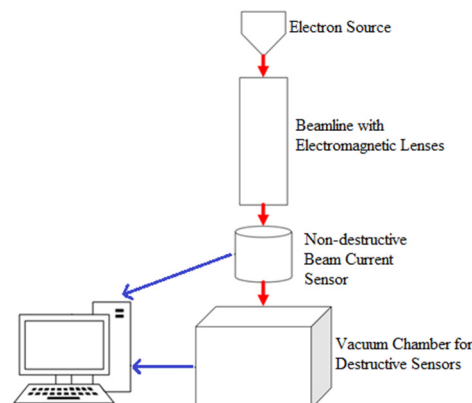


Figure 1: Overview of the EBM test setup and the proposed beam diagnostics system.

As the attention on AM has been dramatically increased among the researchers in the field, Electron Beam Melting (EBM) technique is getting used in the manufacturing process. EBM technique has been preferred to Selective Laser Melting (SLM) because of its advantages. One advantage is on that EBM provides higher beam power and beam scan velocity [5]. Another one is that EBM process occurs under a vacuum, but the SLM process works in an inert atmosphere. Therefore, oxidation of the parts is prevented in most cases for EBM [6].

An EBM system requires controlling several beam parameters in order to ensure the precision during manufacturing process. Some of them are beam power, beam spot size, beam scanning and jumping velocity [6]. The requirements of the EBM system are determined according to desired operating modes, and associated measurement mechanisms should be integrated to the calibration and test processes. Common EBM diagnostics methods are investigated in [7, 8].

In this paper, a beam diagnostics system is proposed for EBM process which diagnoses beam current, beam spot size for enlarged and focused beams, scanning velocity of the deflected beam, and profile of the beam. While proposed system makes use of SEM grid sensors to measure beam spot size and deflected beam scanning velocity, a novel method is put forward to measure the profile of the electron beam. Details of the EBM test system, and the proposed beam diagnostics system is described in the following sections.

SYSTEM DESCRIPTION

The EBM test system under investigation in this paper consists of three main parts, namely electron source, electromagnetic lenses, and test chamber. The source is where the electron beam is generated by Lanthanum Hexaboride (LaB_6) cathode at 60-100 kV. To manipulate the beam, sev-

DEVELOPMENT OF A PROFILE MONITOR USING OTR AND FLUORESCENCE FOR INJECTED BEAMS IN J-PARC MAIN RING*

Y. Hashimoto[†], Y. Sato, T. Toyama, T. Mitsuhashi, T. Nakamura, M. Tejima, M. Uota,
J-PARC Center, Tokai, Japan

also at Accelerator Laboratory, KEK, Tsukuba, Japan

H. Sakai¹, ¹Mitsubishi Electric System & Service Co., Ltd., Tsukuba, Japan

Abstract

A two-dimensional beam profile monitor having a high dynamic range approximately six digits of magnitude by using of Optical Transition Radiation (OTR) and fluorescence screens, Unit-1, has been operated in the injection-beam transport (3-50BT) line of the J-PARC main ring (MR) [1, 2]. This device contributes to the diagnosis of beam core and halo of intense proton beams before injection to MR, particularly measurement of beam cut effects by beam collimators located in upstream of the device is useful for beam shaping. We have been developing the second device, Unit-2, to be installed into MR for diagnosing on injected beams. By using the both of first and second devices, beam core and halo can be diagnosed in different phases. Property tests of the second device have been conducted at a test bench. But its longitudinal coupling impedance of several ohms (by Z/n value) is an issue. Then we have been studying the absorption of the rf power of the resonances up to about 1 GHz using SiC. In this paper, we discuss the characteristics of the developing device, and simulation results of reducing the coupling impedance.

INTRODUCTION

The key to increase beam intensity is how to reduce the beam loss, then the diagnosis of the beam halo with device of Unit-1 in operation has been an advantage. Following the Unit-1, it was planned to put a Unit-2 in MR [3, 4]. At the Unit-2, it will be able to diagnose a halo with a beam core and orbits of about 10 to 20 turns after the injection. Those two-dimensional information on the halo formation at the beginning of the circulation enables us to operate high-intensity beam with reflecting the correlation in the X-Y directions. In addition, by performing measurements synchronized with the Unit-1, it is possible to adjust the collimator balance between 3-50BT and MR, and to diagnose the transverse phase-space distribution of the injection beam including the two-dimensional XY coupling component. Furthermore, by only using the beam halo part of Unit-2 for the measurement of the circulating beam, the beam loss due to the time evolution of the two-dimensional distribution. It is also expected to diagnose resonance condition with such a temporal halo information.

Development as a basic monitor device has been completed, and basic measurements have been made on a test bench. The challenge for the current study is how to reduce the coupling impedance with MR circulating beams. At the

beginning of development, the impedance (Z/n) was set to almost zero in the frequency range up to 100 MHz. This reason was the MR's basic acceleration frequency of 1.67-1.71 MHz (corresponding to 3-30 GeV) was observed with high-frequency components up to about 100 MHz in the actual beam. However, recently, microwave instabilities have occurred in the region of several hundred MHz at the time of rf de-bunch in a slow extraction. For this reason, a requirement was imposed to reduce the impedance in the region up to around 1 GHz to zero as much as possible.

DEVICE CONFIGURATION

The concept of a high dynamic-range profile monitor is to increase the dynamic range of detection by using two types of screens. The beam core (about 2 digits) is detected by OTR from the titanium screen, and the beam halo (about 4 digits) is detected by the fluorescence from the alumina screen on the outer part [1, 2] (Fig. 1).

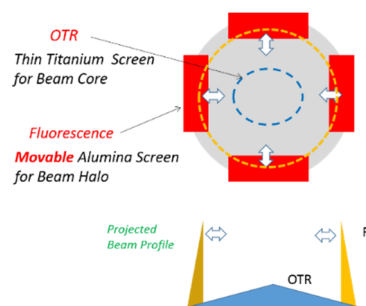


Figure 1: Conceptual screen layout.

In the Unit-2, the following five points were changed from the Unit-1 of 3-50 BT in order to install it in MR.

1. The diameter of the beam hole at the upper concave mirror was increased from 120 mm to 160.
2. Then the diameter of the concave mirror was increased from 300 mm to 350 mm to compensate for the light loss due to the large beam hole as above.
3. The vacuum chambers for the mirror and the target were separated.
4. The imaging point was positioned in the atmosphere to increase the yield of light with close optics.
5. Though conventional mirrors were made by depositing pure aluminium on the entire surface of polished Pyrex glass, considering radiation damage, in Unit-2 pure aluminium (A1050) was used as the base material and machined.

* Work supported by Grant-in-Aid for Scientific Research JP16H06288.

[†] email address: yoshinori.hashimoto@kek.jp

BEAM PROFILE MEASUREMENTS UTILIZING AN AMPLITUDE MODULATED PULSED FIBER LASER AT PIP2IT

V. Scarpine, R. Campos, N. Eddy, B. Fellenz, T. Hamerla, J. Ruan, R. Thurman-Keup,
 Fermi National Accelerator Laboratory, Batavia, IL USA
 M. El Baz, Université Paris Saclay, Orsay, France

Abstract

Fermilab is undertaking the development of a new 800 MeV superconducting RF linac to replace its present normal conducting 400 MeV linac. The PIP-II linac consists of a warm front-end generating 2 mA of 2.1 MeV H⁻ followed immediately by a series of superconducting RF cryomodules to 800 MeV. To limit the potential damage to the superconducting RF cavities, PIP-II will utilize laser-based monitors to obtain beam profiles via photoionization. This paper will present the results of transverse and longitudinal beam profile measurements using a prototype profile monitor that was tested with 2.1 MeV H⁻ beam at the PIP-II Injector Test (PIP2IT) accelerator. This prototype profile monitor utilizes a high repetition rate fiber laser and fiber optic transport into the PIP2IT enclosure. In addition, results will be shown of narrow-band electron detection from amplitude modulated laser pulses

THE PIP-II SUPERCONDUCTING LINAC

The PIP-II project at Fermilab is building a superconducting (SC) Linac to fuel the next generation of intensity frontier experiments [1]. Capitalizing on advances in superconducting radiofrequency (SRF) technology, five families of superconducting cavities will accelerate H⁻ ions to 800 MeV for injection into the Booster. Table 1 shows the main SC Linac beam parameters.

Table 1. PIP-II Linac Beam Parameters

Delivered Beam Energy (kinetic)	800 MeV
Particles per Pulse	6.7×10^{12}
Average Beam Current in the Pulse	2 mA
Pulse Length	550 μ s
Pulse Repetition Rate	20 Hz
Bunch Pattern	Programmable

Figure 1 shows the layout of the SC Linac. The β values represent the optimal betas where the corresponding cavity delivers the maximum accelerating voltage. A room temperature (RT) section accelerates the beam to 2.1 MeV and creates the desired bunch structure for injection into the SC Linac. In the SC section of the linac, strict particle-free and high-vacuum requirement place limitation on the design and type of beam instrumentation that can be used [2]. To meet these strict particle-free conditions, invasive beam instrumentation profiling devices, such as wire scanners, are forbidden. Non-invasive laser-based profile monitors will be developed as PIP-II SC Linac beam profiling instruments. Since the PIP-II linac accelerates H⁻ ions, laser induced photoionization ($H^- + \gamma \rightarrow H^0 + e^-$) will be used to

measurement beam profiles [3] in the region of PIP-II SC linac.

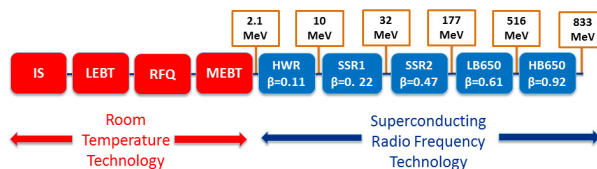


Figure 1: The PIP-II SC Linac technology map.

THE PIP-II INJECTOR TEST FACILITY

As part of the PIP-II R&D strategy, the project has developed and operated the PIP-II Injector Test (PIP2IT) facility. The PIP2IT accelerator covers the first 20 MeV of the PIP-II design [4]. The PIP2IT program performed an integrated system test of the room temperature warm front end (WFE), consisting of the ion source, LEBT, RFQ and MEBT [5], and the first two superconducting cryomodules. Figure 2 shows the layout of the PIP2IT accelerator.

The MEBT operates with 2.1 MeV H⁻ beam up to 5 mA which includes a bunch-by-bunch chopper allowing for any arbitrary beam pattern [6]. For PIP-II beam operations, the MEBT chopper will reduce the beam current from 5 mA to 2 mA before injection into the SC linac.

To test possible laser-based profiling techniques for PIP-II, a prototype laser profile monitor was installed in the PIP2IT MEBT.

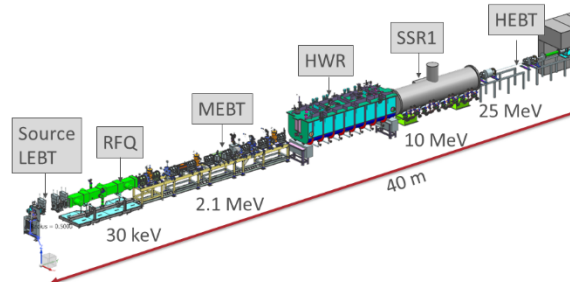


Figure 2: The beamline layout of the PIP-II Injector Test.

PROTOTYPE LASER-BASED BEAM PROFILER FOR PIP2IT

We have developed a prototype laser-based beam profiler to develop techniques that may be used at PIP-II. The prototype profile monitor is based on a low-power fiber laser with all-fiber optical transport through the linac [7]. The fiber laser is an Ytterbium seed laser with amplifier

REAL-TIME BEAM DETECTION AND TRACKING FROM PINHOLE IMAGING SYSTEM BASED ON MACHINE LEARNING

A. A. Nosych, U. Iriso, ALBA Synchrotron, Barcelona, Spain

Abstract

At ALBA Synchrotron each of the two in-air pinhole imaging systems is able to see several beam spots at once due to specific pinhole grid with 3x3 holes placed in the path of the X-ray fan. Each beam image has its own properties, such as source pinhole aperture size, its Point Spread Function (PSF) and copper filter thickness, all of which impact the electron beam size calculation. Until now, these parameters were applied manually to the pinhole device servers for numerical image analysis, so this semi-manual beam size calculator is subject to frequent adjustments and human monitoring.

This study looks at feasibility of training and pointing an Artificial Neural Network (ANN) at image stream coming from pinhole cameras in real time, track all detected beam spots and analyze them, with the end goal to automate the whole pinhole beam image processing.

INTRODUCTION

The ALBA Synchrotron is a 3 GeV third-gen light source located in Cerdanyola del Vallès (Barcelona, Spain). Currently it has 10 operational beamlines, comprising soft and hard X-rays that perform research in fields like material science, condensed matter, nanotechnology, biology and others. The facility provides more than 6000 hours of beam time per year and is available for the academic and the industrial sector, serving several thousand researchers every year.

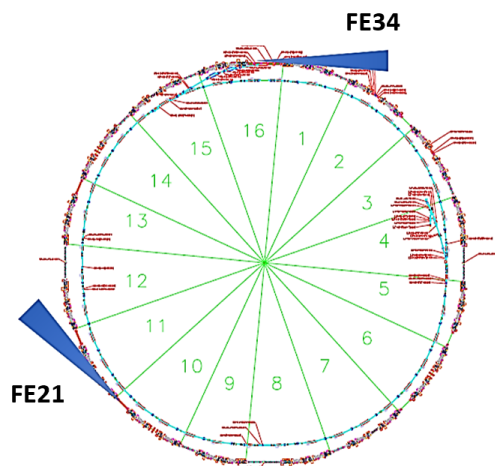


Figure 1: ALBA storage ring layout, and location of both in-air X-ray pinholes in sectors 1 and 11.

Measuring transverse size and emittance [1] of the electron beam at any moment of time is essential to control the machine performance. This measurement is carried out by two in-air X-ray pinhole cameras [2], whose location is shown in Fig. 1 and components laid out in Fig. 2.

Apart from emittance and beam size, the pinholes inevitably monitor beam position and stability. As the simple optics principle of a pinhole, it takes the synchrotron radiation coming from a bending magnet to obtain a magnified transverse image of an electron beam, which is analysed to infer the horizontal and vertical (H and V) electron beam size. Any movement of beam orbit will immediately be seen in the pinholes, and any problematic beam will be observed as blurred, out of shape, or different in size than usual.

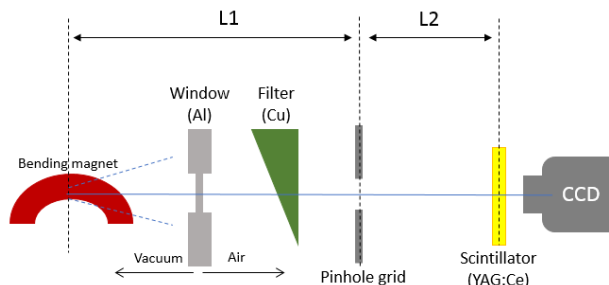


Figure 2: Component schematics of ALBA pinhole system (not to scale).

Since its commissioning in 2011 the storage ring has been operating with only one pinhole located at front-end 34 (FE34) [3], but in 2020 a second pinhole at front-end 21 (FE21) was installed for redundancy. It brings a few improvements with respect to FE34, the main of which is higher magnification. See Table 1 for a list of other differences.

Table 1: ALBA's Pinholes Compared

	FE21	FE34
L1	4.111 m	5.936 m
L2	15.357 m	13.828 m
Magnification	3.76	2.31
Visible beam spots	2	6
Al window thickness	1.5 mm	1 mm
Beam size at source	56, 26 μm	53, 23 μm

Both ALBA's X-ray pinhole lines are similar and consist of a chain of elements shown in Fig. 2. This type of pinhole system has previously been described in greater detail [2–4], so we will not focus on its functionality here. The elements important for this work are the copper wedge filter (an X-ray attenuator) and the pinhole grid itself.

The pinhole grid is motorized and has 4 degrees of freedom (lateral, vertical, rotational and pitch). It consists of apertures made by horizontal and vertical tungsten bars (Fig. 3): in total there are 9 rectangular holes of different size, with 3 squared. FE21 and FE34 share the 50x50 and 10x10 μm

FAST SCANNING DIAMOND DETECTOR FOR ELECTRON BEAM PROFILE MONITORING*

V. V. Konovalov[†], Applied Diamond, Inc., Wilmington, DE, USA
T. Miller, S. Bellavia, C. Brutus, P. Thieberger, and R. Michnoff,
Brookhaven National Laboratory, Upton, NY, USA

Abstract

The first prototype of a fast scanning diamond beam profile detector (DBPD) suitable for invasive high power CW electron beam core profile measurements in transmittance mode was developed. It consists of a multi-strip solid state diamond detector to scan with high speed (up to 1 m/s) and precision (about 5 μm) through the core of an electron beam. The diamond sensor was made from a thin polycrystalline diamond (PCD) plate with highly B-doped diamond conductive strips both grown by CVD. Transient currents from the multi-strip detector were measured with fast digitizing electrometers. Successful operation of the DBPD was demonstrated for pulsed (5 Hz) and CW (78 kHz) CeC beams, including the detector's ability to withstand a 20 sec insertion into the CW CeC beam core. The X-Y beam spatial profile was measured in one scan. Thermal modelling demonstrated a manageable thermal impact even from a relatively long insertion of the diamond sensor into the CW CeC core and very short (0.2 s) insertion into the CW LEReC beam core. Electrical impedance modelling of the detector and vacuum chamber assembly demonstrated minimal impact on beam line impedance with diamond sensor insertion.

INTRODUCTION

Recently, novel electron cooling systems for ion beams are being developed at Brookhaven National Laboratory, such as the Low Energy electron Cooling (LEReC) system, the first electron cooler without any magnetization, designed to maximize collision rates at the lowest energies available at the Relativistic Ion Collider (RHIC) [1], and the ongoing Coherent electron Cooling (CeC) Proof of Principle (CeC PoP) experiment, currently installed in the RHIC tunnel [2]. LEReC system produces 704 MHz electron bunches, modulated at 9 MHz to overlap Au-ion bunches, with 1.6 - 2.6 MeV electron energies and the beam power ranging from 10 to 140 kW. In the CeC experiment, the electron beam is produced by an electron gun followed by superconducting cavity and a 704 MHz superconducting LINAC producing a 15 MeV electron beam at up to 78 kHz repetition rate.

Efficient electron cooling requires a high quality, high power electron beam with tight parameters (energy and space trajectory). In order to achieve and maintain the required parameters and stability of the electron beam, its parameters have to be continuously monitored and feedback

control has to be developed [3]. Interference of beam diagnostic instrumentation with the beam may lead to degradation of beam parameters therefore, invasive and non-interceptive methods of monitoring are preferred. Invasive beam monitoring can be achieved by using highly transparent detectors made from low-Z materials absorbing $< 1\%$ of beam energy. However, existing detectors, e.g. wire scanners, are not suitable for invasive profile measurements of powerful continuous wave (CW) electron beams. As a result, the beam profile of these beams is currently monitored in low repetition pulsed mode and assumed to remain the same in CW mode. Common wire scanners have a rather short life-time even when used for pulsed beam monitoring. Their very thin wires are easily overheated and burned, thus contaminating the beam pipe with debris.

Diamond's unique combination of material properties: low energy absorption, tremendous radiation tolerance, ability to dissipate significant heat load, and stability of electronic properties over a wide temperature range, makes it an ideal material for high energy applications. Diamond radiation detectors (DRD) have been used for detection of many types of radiation demonstrating fast time response, high radiation stability, and ability to operate at high temperatures without cooling. DRDs have much longer lifetimes compared to radiation detectors made from other materials like silicon or plastic. Also the signals from gas-filled ion chambers and silicon detectors saturate under high-flux conditions. DRDs are an established technology as beam condition monitors in the highest radiation areas of all Large Hadron Collider experiments [4]. DRDs are used as X-ray beam position monitors for multiple synchrotron radiation and free electron laser sources, including NSLS-II at BNL [5], SOLEIL [6], and CEA at Saclay [7]. DRD was been used with a powerful 90 W/mm² white X-ray beam and demonstrated 11 orders of magnitude flux linearity and stable response over an 18 month time period [8]. DRD for electron beam profile and halo monitoring was developed and successfully tested for the XFEL/SPring-8 as a part of a system to protect undulator permanent magnets from radiation damage [9].

The first prototype of a fast scanning diamond beam profile detector (DBPD) suitable for invasive high power CW electron beam core profile measurements in transmittance mode has been developed and fabricated. Its research and development in significant degree was focused on future installation into the high power CeC and LEReC beam-lines at BNL and the detector design was tailored to the corresponding BNL requirements. Numerical modeling demonstrated that the DBPD prototype is suitable for direct

* Work supported by DOE SBIR under grant No. DE-SC0020498 (AD) and by BSA under DOE contract DE-AC02-98CH10886 (BNL).

[†] Email address: val@ddk.com.

DESIGN AND NUMERICAL INVESTIGATIONS OF SCINTILLATION BEAM LOSS MONITOR FOR PoIFEL*

R. Kwiatkowski[†], M. Krakowiak, S. Mianowski, R. Nietubyc, J. Szewinski
National Centre for Nuclear Research, Otwock, Poland

A. Wawrzyniak, National Synchrotron Radiation Centre SOLARIS, Krakow, Poland

Abstract

The Beam Loss Monitor (BLM) system is used mainly for machine protection and is particularly important in the case of high energy density of accelerated beam, when such a beam could lead to serious damages in the case of uncontrolled loss. Operational parameters of PoIFEL linear accelerator induced needs to install and operate the BLM system. The BLM concept for PoIFEL is based on several scintillation probes placed along the linear accelerator. The paper reports on numerical investigation of electron and X-ray radiation induced during fast electron losses. We also present design of BLM detectors and results of first tests of a prototype on the linear electron accelerator at Solaris research centre.

INTRODUCTION

The main purpose of Beam Loss Monitoring (BLM) system is to detect events of charged particle escaping from its designated path (beam pipe). Such a system, while not being coupled directly with the particle beam, is important from the point of view of machine protection. While above feature is crucial for facilities with high beam current and energy density, ability to detect interaction of particles with accelerator components, could also be used to indirect control of beam position and alignment and fine-tuning these parameters, also for low-power devices.

THE PoIFEL PROJECT

The Polish Free Electron Laser, PoIFEL, is planned to be operational in the 2024. It is a superconducting FEL, based on the TESLA SRF technology, which could operate in continuous wave (cw) and long pulse (lp) mode. Electron beam, generated in all-superconducting gun will be accelerated by four cavities and then delivered to either THz-undulator, or further accelerated and delivered to VUV-undulator. After passing through undulators, the electron will be used for other experiments (e.g. Inverse Compton Scattering). The maximum electron energies for the beamlines, a THz/IR line and VUV line, are equal to 79 and 154 MeV, respectively. The most important parameters of PoIFEL electron accelerator are listed in Table 1 [1, 2].

*The construction of PoIFEL received funding from the European Regional Development Fund in the framework of the Smart Growth Operational Programme and Regional Operational Programme for Mazowieckie Voivodeship.

[†]email: Roch.Kwiatkowski@ncbj.gov.pl

Table 1: The Parameters of Polfel Electron Beam (Maximal Values, Continues Wave Mode)

	Gun	VUV line	THZ line
Bunch charge [pC]	250	100	250
Repetition rate [kHz]	50	50	50
Bunch length [ps]	10	0.4	10
Beam energy [MeV]	4	154	79
Beam current [μ A]	12.5	5	12.5
Beam power [W]	-	770	940

BEAM LOSS AND MACHINE PROTECTION

Beam losses, i.e. deviation of beams from designed path, could be divided into two main classes: regular losses and irregular ones.

Regular Losses

Regular beam loss occurs as a part of normal accelerator operation and are generally unavoidable. However, they are typically localized on the collimator or aperture limits. Such losses could be used for machine diagnostics, e.g. injection studies, tail measurements or lifetime limitations. For further details, see e.g. [3, 4].

Irregular Losses

Irregular or uncontrolled (fast) losses, could happen as a result of misaligned beam, leaks in vacuum system, or other failure of accelerator components. The beam hitting accelerator walls could lead to, e.g.: vacuum lost (in case of melting the vacuum vessel wall), radiation damage of sensitive components (electronics), quench in superconducting circuits (in case of excessive heat deposition by colliding beam). Monitoring of fast losses could also be used to diagnose problems around the machine, like vacuum leaks, obstacles or microparticles in the line.

BEAM LOSS MONITOR TYPES

The Beam Loss Monitor, which in principle is a detector of ionizing radiation, could be built of a different sensor types. The selection of appropriate system is based on several factors, amongst which we can distinguish:

- intrinsic sensitivity
- ease of calibration
- radiation hardness
- reliability, robustness
- dynamic range
- temporal resolution
- shielding properties

THE BEAM LOSS MONITORING SYSTEM AFTER LHC INJECTORS UPGRADE AT CERN

M. Saccani*, E. Calvo, W. Viganò, C. Zamantzas, CERN, Geneva, Switzerland

Abstract

The LHC Injector Upgrade (LIU) project aims to increase the available brightness of the beams and improve the efficiency of the whole accelerator chain. The Beam Loss Monitoring (BLM) system is a key element of CERN's accelerator instrumentation for beam optimisation and machine protection by producing continuous and reliable beam loss measurements while ensuring safe operation. The new BLM system for the LHC injectors aimed to provide faster measurements with a higher dynamic range, to install more detectors along the beamlines, and to give the operator more flexible use. A review will be given on the versatility provided by the system to cover requirements from various accelerators and their transfer lines, focusing on the measurements and the operational scenarios.

INTRODUCTION

CERN Accelerator Complex

The High-Luminosity LHC (HL-LHC) upgrade requires the injector chain to produce beams with higher brightness. The LHC Injector Upgrade (LIU) project aims to meet the beam performance in terms of reproducibility, availability, and efficiency [1]. This project consisted of building a new H- linac (i.e. Linac4) and renovating the accelerator chain: The Proton Synchrotron Booster (PSB), the Proton Synchrotron (PS), and the Super Proton Synchrotron (SPS), with all their transfer lines.

The upgrade of the Beam Loss Monitoring (BLM) system in the injectors (i.e. BLMINJ) is an integral part of the LIU program and serves two main purposes: first, to automatically protect the accelerator equipment from damage if it

detects excessive losses, and second, to allow operators to observe in real-time losses and adjust machine parameters accordingly. The system development and installation took six years in total and included 322 detectors integrated along the beamlines between the Linac4 source and the SPS injection. This paper first describes the new BLMINJ system recently deployed, before focusing on the commissioning phase and the performance achieved.

BLMINJ SYSTEM ARCHITECTURE

In 2012, an architecture that met the BLMINJ specifications has been proposed [2]. The technical choices resulted in a generic, configurable and high-performance system, in addition to the reliability and availability expectations. The following sections describe the final design, the specification evolution, and the deployment solutions.

The BLMINJ system consists of detectors placed in strategic locations at the tunnel installation and Beam Loss Electronics (BLE) for acquisition & processing located on the surface buildings in a single rack per location, as shown in Fig. 1.

Detectors and Cabling

The BLM detectors are mounted outside the vacuum chamber and measure the secondary shower caused by stray particles interacting with the vacuum chamber walls or magnets. Sensitivity and detection efficiency depend on the size, technology, and positioning of the detector. The BLMINJ system accepts various types of loss monitors as input, all of which were characterised in detail in 2018 [3].

* mathieu.saccani@cern.ch

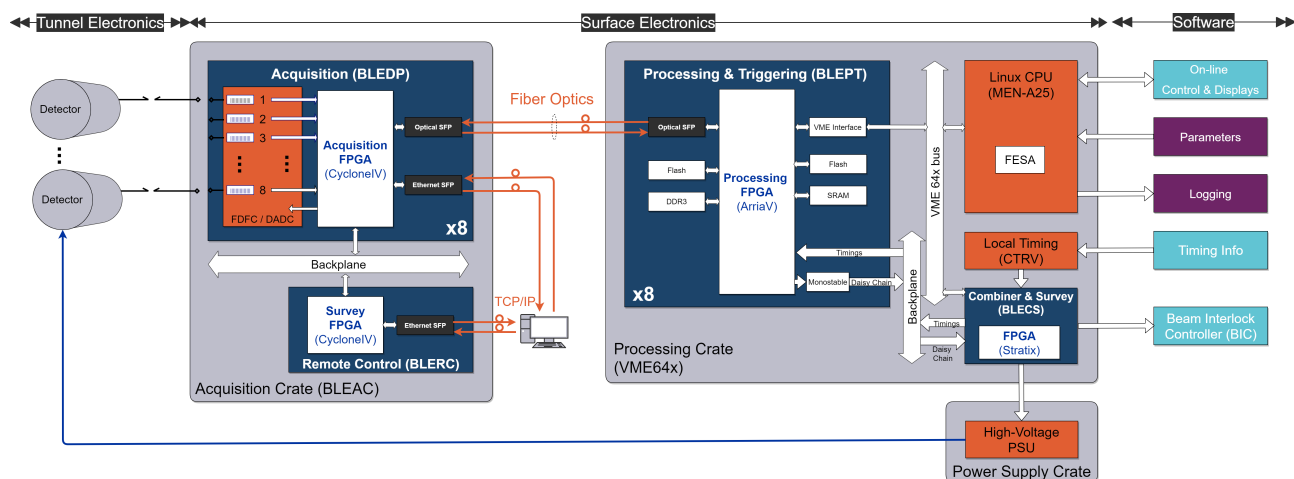


Figure 1: Schematic overview of the BLMINJ system architecture.

BEAM LOSS SIGNAL CALIBRATION FOR THE LHC DIAMOND DETECTORS DURING RUN 2

S. Morales^{*1}, B. Salvachua, E. Calvo, E. Effinger, C. Zamantzas, CERN, Geneva, Switzerland
C.P. Welsch, J. Wolfenden, University of Liverpool, Liverpool, United Kingdom
¹ also at University of Liverpool, Liverpool, United Kingdom

Abstract

Chemical Vapour Deposition (CVD) diamond detectors can be used as fast beam loss monitors in particle accelerators. In the Large Hadron Collider (LHC) at CERN, they are installed in the betatron collimation region, a high-radiation environment. In addition to their high-radiation tolerance, their main advantage is a time resolution of 1 ns which makes possible not only turn-by-turn, but also bunch-by-bunch loss measurements. An analysis of the LHC diamond beam loss monitor signals recorded during the last months of Run 2 (September 2018-November 2018) is presented with the aim of obtaining a signal-to-beam-loss calibration.

INTRODUCTION

The Large Hadron Collider (LHC) at CERN is the largest and most powerful accelerator ever built. It has a 27-kilometre long circumference and it is located 100 m underground. The LHC accelerates protons and ions up to a design energy of 7 TeV, with up to 2 556 particle bunches per beam and, on average, 1.15×10^{11} particles per bunch, achieved during Run 2 (2015-2018) [1].

Dipole electromagnets create a field of up to 8.33 T that is used to bend the trajectory of the beam particles along the accelerator. In order to reach and maintain the current of around 11 850 A required to produce this magnetic field, superconducting coils are employed in the LHC magnets [2]. Under these conditions, losses on the level of 30 mJ/cm^3 induced by a local transient beam loss of 4×10^7 protons could provoke a transition from superconducting to normal conducting state (quench) in the magnets and generate an accelerator downtime in the order of hours or even months [3]. Additionally, beam losses could damage the accelerator or detector equipment.

Driven by these concerns, a Beam Loss Monitoring (BLM) system is installed in the LHC. The system includes around 4 000 beam loss detectors placed all around the accelerator ring downstream the most probable loss locations. They measure continuously the beam losses and trigger a beam dump signal when the losses reach certain predetermined thresholds [4]. Even though it is seen mainly as a machine protection system, the signals from the beam loss detectors can also be used to provide a precise number of the lost beam particles and to identify the different loss mechanisms, making it a powerful diagnostics tool to improve the performance of the accelerator. This type of analysis has already been carried out in the past, but only considering

the signals from the Ionization Chamber (IC) BLM detectors [5–7]. This work aims at reproducing the same results using the signals from the Diamond BLM (dBLM) detectors that were under test in certain locations in the LHC during Run 2, which offer a bunch-by-bunch loss signal resolution and therefore could provide a more detailed information about the LHC beam loss patterns.

LHC BLM SYSTEM DETECTORS

The LHC BLM system includes four different types of beam loss detectors. The most relevant ones for this analysis are the IC BLMs and the dBLMs.

Ionization Chambers

The IC is the most common beam loss detector type in the LHC BLM system, with around 3 600 installed downstream the most probable loss locations. The IC is made of a stainless steel cylindrical tube which is 50 cm long, with a diameter of 9 cm and filled with nitrogen gas. It contains aluminium plates that are alternatively used as high voltage and signal electrodes. A voltage of 1.5 kV is applied between the electrodes, which generates an electric field of 3 kV/cm inside the chamber. The internal part of an IC BLM detector is shown in Fig. 1. The analog beam loss signal is induced when the lost beam particles or their products traverse the chamber and ionize the gas inside [8]. The signal is then continuously integrated and digitized in the front-end analog electronics using a Current-to-Frequency-Converter card that provides measurements every $40 \mu\text{s}$ [9]. The read-out electronics then converts the signal bits to Gy/s and keeps a history of the values by producing longer integration windows.



Figure 1: Internal part of an IC BLM detector showing the electrodes. The cables to the read-out electronics are located on the right side.

Diamond Detectors

The dBLM consists of a squared pCVD diamond detector which is 10 mm long and 0.5 mm thick. It offers a time resolution in the order of the ns which allows to record turn-by-turn and bunch-by-bunch beam loss measurements, as the nominal LHC bunches are separated by 25 ns [10]. These

* sara.morales.vigo@cern.ch

METHODOLOGY, CHARACTERISATION AND RESULTS FROM THE PROTOTYPE BEAM LOSS MONITORING ASIC AT CERN

F. Martina^{1,2,*}, C. Zamantzas, L. Giangrande, J. Kaplon, P. V. Leitao, CERN, Geneva, Switzerland
J. W. Bradley¹, C. P. Welsch¹, University of Liverpool, Liverpool, UK

¹also at Cockcroft Institute, Warrington, UK

²also at University of Liverpool, Liverpool, UK

Abstract

The characterisation of novel beam loss monitoring front-end converters, based on radiation-hardened application-specific integrated circuits (ASIC), is undergoing at CERN. An effective performance analysis of the newly developed ASICs plays a key role in their candidacy for the future installation in the HL-LHC complex. This work introduces the latest test-bed architecture, used to characterise such a device, together with the variety of audits involved. Special focus is given on the verification methodology of data acquisition and measurements, in order to allow a detailed study of the conversion capabilities, the evaluation of the device resolution and the linearity response. Finally, the first results of post-irradiation measurements are also reported.

INTRODUCTION

The Beam Loss Monitoring (BLM)[1, 2] is an essential protection system of particle accelerators, since a variety of phenomena cause beam particles to escape from the desired trajectory. These produce secondary particle showers, which lead to unwanted energy deposition in the various machine elements. Thus, the BLM system is mandatory to prevent equipment activation, damage and, like in the case of the LHC, the quench of its superconductive magnets [3–6].

In view of the HL-LHC upgrade [7], a major renovation of the BLM electronics is on-going covering parts both within the accelerator tunnel and in the surface buildings. To cope with the new specifications, the BLM system will be required amongst others to enhance its radiation tolerance to reach 100 MRad of TID (was 50 kRad), and to provide a faster acquisition period of 10 μs in comparison to the currently installed system (was 40 μs) [8–11].

The high radiation tolerance requirements cannot be achieved using only commercial components, and a custom radiation hardened Application Specific Integrated Circuit (ASIC) was necessary to be designed.

The device is able to convert the analogue currents produced by the ionisation chamber detectors [12, 13] into digital data streams. These are serialised [14] and transmitted via optical fibres to the back-ends [15], where the data is further processed to obtain the beam loss measurements.

The measurements are compared in real-time with pre-defined thresholds [16, 17], unique by location, to decide whether the beam is permitted to circulate or its extraction must be triggered. Since the front-end conversion capabil-

ities relies on the ASIC component, strict validation and performance characterisation on test-beds is required. Later, the post commissioning supervision will be carried on in conformity with the currently installed system [18–20].

In this report we will focus on the second version of the device, the BLMASIC, which implements similar concepts of current-to-frequency converter (CFC) as the currently operational system and an early prototype, studied in [21–24]. The validation has been performed using test-beds specifically designed to qualify the ASIC. In a previous paper [25], we presented a first version of the setup, which has since been significantly improved.

A brief description of the BLMASIC architecture and the methodology for the device validation are described in the following sections. Then, the test-bed assembly architecture, the batch data analysis software, as well as the first post-irradiation results are reported.

CONVERSION ARCHITECTURE

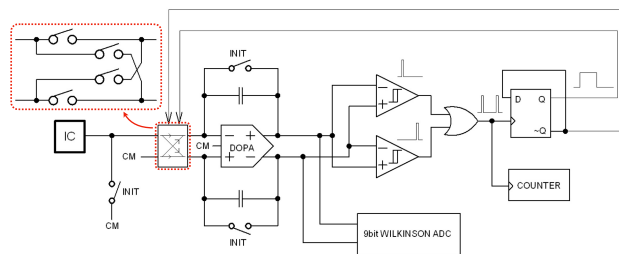


Figure 1: BLMASIC Conversion Architecture. "IC" represents the ionisation chamber detector (ideally modelled as an independent current source). "DOPA" is the input fully-differential amplifier configured as a current integrator. Quantisers and the toggling flip-flop are shown on the right.

The schematic architecture of the BLMASIC is shown in Fig. 1. The differential design of the circuit allows to double the internal signal swing and helps to improve the overall linearity response. Because of the configuration symmetry, it is possible to study its behaviour by splitting the complementary signal paths in two equivalent single-ended networks. Finally, the input current to measure is single-ended and the amplifier complementary input is connected to the circuit common-mode node, here considered as a neutral.

After the initialisation of the circuit, i.e. close the "INIT" switch, any charge injected by the ionisation chamber (IC) will be accumulated in the capacitors, producing a voltage

* francesco.martina@cern.ch, f.martina@ieee.org

NEW APPLICATIONS AND STUDIES WITH THE ESRF BEAM LOSS MONITORING AT INJECTION

E. Buratin*, N. Benoist, N. Carmignani, F. Ewald, J.-L. Pons, K. Scheidt
European Synchrotron Radiation Facility, Grenoble, France

Abstract

More than one year after the commissioning of the ESRF's new Extremely Brilliant Source (EBS), the Beam Loss Detectors (BLDs) are continuing to be used for extensive applications and studies, notably at injection. A total of 144 BLDs and 36 associated Libera Beam Loss Monitors (BLMs) are distributed in the EBS ring and the Booster. These BLDs allow to measure slow losses during user-mode operation and fast losses at injection, with a sub-orbit-turn time resolution. In this paper these fast beam loss dynamics are presented at injection for different lattice parameters, collimator-settings and beam conditions. We will also show the excellent correlation with results obtained from the injection efficiency diagnostic and the bunch length acquired with the Streak Camera.

INTRODUCTION

The new Extreme Brilliant Source (EBS) ring at the European Synchrotron Radiation Facility (ESRF) has been installed, commissioned and it is now operational since mid-2020. The 6-GeV and 200-mA electron beam has typically horizontal and vertical emittances of 120-pm and 10-pm, respectively, with a typical beam lifetime of above 20 hours. This allows to generate a coherent and bright x-ray beam for the scientific users [1].

One of the useful accelerator diagnostics present in EBS are the Beam Loss Detectors (BLDs), to measure the distribution of the lost electrons around the accelerator [2]. Since the EBS commissioning phase, 128 BLDs have been installed, calibrated, exploited for Machine Dedicated Time (MDTs) studies and USM-mode operation. Additional 8 BLDs have been installed in the Booster, 4 in the injection zone and 4 in the extraction area. And in the Transfer Line from Booster to the EBS ring another 4 extra BLDs had been installed. In March 2021 and for a couple of months other 4 BLDs have been positioned near the Radio Frequency (RF) cavities of cell 25 to study critical events and dynamics. The total of 144 units of BLDs are controlled by 36 Beam Loss Monitors (BLMs) [3, 4].

The BLDs can be used to measure slow losses during operation and fast losses at injection. In User-mode there are about $5 \cdot 10^7$ lost electrons per second around the EBS ring, while at each injection it is about $2 \cdot 10^9$ lost electrons in less than 3 ms. In this paper we concentrate mainly on the injection mode to understand the BLDs fast functionality, behaviour and performance, in order to improve and to optimize the EBS complex, and to correlate and to verify the BLDs signals with other diagnostics.

BLDS AT INJECTION MODE

The measurement of fast losses can be extremely useful to describe the beam dynamics and the quality of the injection process. At injection, the BLDs termination switches automatically to 50Ω , which is needed for the required time-resolution, thereby allowing these fast loss measurements.

For a standard 200-mA beam and a uniform filling pattern, the typical distribution of the injection losses is displayed on Fig. 1. In y-axis the BLD position is displayed, considering the standard 128 BLDs installed from cell 1 to cell 32. In x-axis the time is plotted up to 2800 μ s, equivalent to 1000 turns. The losses are differently distributed depending on BLD position, aperture limitations, machine and beam parameters. An interesting feature visible in Fig. 1 is a periodic recurrence, measured by some of the most critical BLDs, such as:

- BLD n.61, after the Insertion Device (ID) of cell 16, that is often one of the smallest gaps,
- BLD n.96, after the collimator of cell 24.

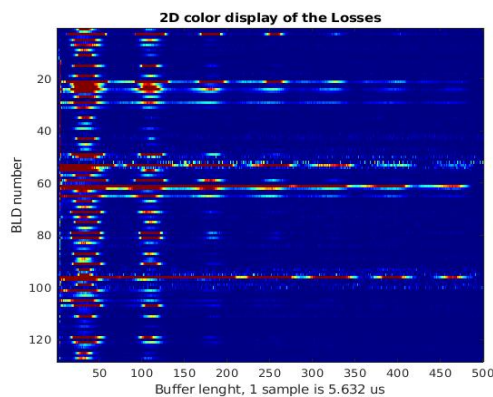


Figure 1: 2D color display of the Losses around EBS, for a 200 mA uniform-filling pattern beam.

The evolution of a single BLD can be analysed to identify the above-mentioned periodicity. In Fig. 2 the so-called Time-Resolved Beam Losses are displayed for the BLD n.96, installed in the middle of the fourth dipole after the collimator of cell 24. A big loss peak is present on the first turns, followed by damped oscillations with a 0.4 ms periodicity. These periodic losses are linked to bunch length oscillations occurring at injection, and presented below.

The evolution in time can also be summed-up so to generate a single value per BLD, the so-called Integrated Injection Losses. The distribution of these losses is reported in Fig. 3. The highest losses are registered on BLDs n.61 and n.96. At each injection, the Integrated

* elena.buratin@esrf.fr

APPLICATION OF THE CORIS360 GAMMA RAY IMAGER AT A LIGHT SOURCE

Y. E. Tan *, ANSTO, Clayton, Australia

D. Boardman, L. Chartier, M. Guenette, J. Ilter, G. Watt, ANSTO, Menai, Australia

Abstract

The CORIS360[®] is a gamma-ray imager developed at Australian Nuclear Science and Technology (ANSTO) for identifying and localising sources of radiation typically from gamma emitting radionuclides. The low EMI and low noise power supply features of the imaging technology have enabled it to have a low energy detection threshold and to detect photons as low as 20 keV. This report shall present the initial measurements performed at the Australian Synchrotron, in the storage ring and beamlines, where the imager is able to detect radiation from all sources of synchrotron radiation (dipole, wiggler and undulator). The radiation imaging results from the injection system and scrapers (to dump the stored beam) will be discussed. Future developments for imaging in pulsed radiation environments and time varying environments will also be discussed.

INTRODUCTION

Synchrotron light sources are a source of radiation with photon energies ranging from milli-eV up to 200 keV. Knowledge of the sources and distribution of ionising radiation is needed to ensure the safety of the people at the facility and also in the protection of equipment susceptible to damage. Simulation of the synchrotron radiation source and its distribution is straight forward however the result of secondary scatter in a complex environment is harder to predict. Therefore we have employed a gamma ray imager to evaluate its effectiveness in diagnosing sources of scattered radiation in the storage ring to detect potential problems and also inform if additional local shielding is required. In this report we present some of the strengths and weaknesses of the CORIS360[®] gamma ray imager [1] that has been used in this evaluation. In particular the imager is very sensitive and is able to detect sources of hard xray sources from dipole, wiggler and undulator sources. A current drawback of the system is that it requires a constant radiation source intensity. Therefore, the imager will not be suitable for situations with variable source intensities (scraping, transient beam loss) and pulsed sources (injector). The report will conclude with some of the future developments the team at ANSTO are pursuing to address some of these drawbacks.

CORIS360 GAMMA RAY IMAGER

CORIS360[®] is a novel gamma ray imager developed by ANSTO. Equipped with a 360° × 90° gamma and optical field-of-view (FOV), it can quickly identify and localise gamma-ray and X-ray sources of radiation with energies

between 40 keV and >3 MeV. The technology is designed around the theory of compressed sensing and employs two nested cylindrical tungsten masks that independently rotate around a single non-position sensitive detector, which enables a series of quasi-random (incoherent) linear projections of the scene plane to be measured. A compressed sensing approach to gamma-ray imaging had previously been presented in Ref. [2]. The cylindrical mask design provides the 360° × 90° FOV and the compressed sensing approach can localise gamma or X-ray sources of radiation with an order of magnitude fewer samples when compared to traditional imaging techniques, delivering fast results. A modular detector approach means different detectors can ‘plug & play’ into the system. CORIS360[®] currently uses two different geometry CLLBC detectors that have an energy resolution of ~4 % at 662 keV. A ~44 cm³ CLLBC detector is used for low to medium dose rate environments and ~ 2 cm³ detector is used for higher dose rate environments. The CLLBC detector is a dual gamma/neutron scintillator, and for neutron interactions the crystal produces an equivalent gamma energy of 3.1 MeV. During a single image acquisition, these spectroscopic detectors enable any part of the 40 keV to >3 MeV energy range to be imaged over the full system FOV. For this work, the low EMI and low noise power supply features of the imaging technology have enabled the low energy detection threshold to be reduced to 20 keV. A simple to use graphical user interface (GUI) provides the end user with an optical panorama with an overlay of the radiation location, which makes it easy to visualise where the source of radiation is. The GUI also provides the measured spectrum, radionuclide identification and indicates when neutrons have been detected.

MEASUREMENTS

Beamlines

The imager was first used at the beamlines to determine if it were sensitive enough to detect synchrotron radiation from a 1.3 T dipole, 1.9 T wiggler and 22 mm period undulator. In all three cases the imager was placed in the first optical enclosure, where the white beam slits and first optical mirrors were located and was able to detect scattered synchrotron radiation (secondaries that penetrate the vacuum chamber or shielding). Using the observation of the scattered radiation it is possible to identify issues along the optics as was observed on the MX2 beamline. Figure 1 shows how a defunct photon beam position monitor (BPM) appears to still be in the path of the beam. Or it can be used to inform the choice of local shielding that can be used to minimise scattered radiation and improve reliability and longevity of

* eugene.tan@ansto.gov.au

MACHINE-LEARNING BASED TEMPERATURE PREDICTION FOR BEAM-INTERCEPTIVE DEVICES IN THE ESS LINAC

E. M. Donegani*, European Spallation Source ERIC, Lund, Sweden

Abstract

“Where there is great power [density], there is great responsibility”¹. The concept holds true especially for beam-intercepting devices for the ESS linac commissioning. In particular, beam-intercepting devices will be subject to challenging beam power densities, stemming from proton energies up to 2 GeV, beam current up to 62.5 mA, pulses up to few milliseconds long, and repetition rates up to 14 Hz. Dedicated Monte Carlo simulations and thermo-mechanical calculations are necessarily part of the design workflow, but they are too time-consuming when in need of rapid estimates of temperature trends. In this contribution, the usefulness of a Recurrent Neural Network (RNN) was explored in order to forecast (in few minutes) the bulk temperature of beam-interceptive devices. The RNN was trained with the already existing database of MCNPX/ANSYS results from design studies. The feasibility of the method will be exemplified in the case of the Insertable Beam Stop within the Spoke section of the ESS linac.

INTRODUCTION

The European Spallation Source (ESS) in Lund (Sweden) is currently one of the largest science and technology infrastructure projects being built today. The facility will rely on the most powerful linear proton accelerator ever built, a rotating spallation target, 22 state-of-the-art neutron instruments, a suite of laboratories, and a supercomputing data management and software development centre [1].

The ESS accelerator high-level requirements are to provide a 2.86 ms long proton pulse at 2 GeV, with a repetition rate of 14 Hz. This corresponds to 5 MW of average beam power, with a 4% duty cycle on the spallation target [2].

A comprehensive suite of beam instrumentation and diagnostics [3] has started to support the commissioning and operation of the normal-conducting linac (NCL) section of the ESS linac. Additional devices and enabling systems are going to be deployed in the superconducting linac (SCL) section, as well as in the transport line to the tuning dump and to the spallation target.

In particular, the Beam Diagnostics Section is responsible for the design, procurement, test and operation of all the bulkiest beam-interceptive devices in both the NCL and SCL linac sections (see the list in Table 1). The beam instrumentation plays the most important role in the machine protection system by monitoring the beam parameters and stopping the beam operation before damages may occur.

Unfortunately, there is no straightforward expression for anticipating the energy deposition of a beam with high power

density within accelerator elements, because the deposited energy depends on many beam properties as well as on the material properties of the beam-interceptive device and the capabilities of its cooling system.

Dedicated Monte Carlo simulations and thermo-mechanical calculations in MCNPX [4] and ANSYS [5], respectively, are part of the standard detector design workflow at ESS. However, many relevant beam- and material-related parameters have to be taken into account for the timing consuming simulations and validation. For instance, on a standard laptop it takes several hours to compute the temperature as a function of the time as shown in Fig. 1, when simulating just 14 proton pulses onto the SPK IBS [6].

Table 1: List of the Bulkiest Beam-interceptive Devices in the ESS Proton Linac. (FC = Faraday cup, IBS = Insertable Beam Stop)

Device	Mean power	Peak Power
LEBT FC	0.005 W	0.0002 MW
MEBT FC	16 W	0.23 MW
DTL2 FC	170 W	2.43 MW
DTL4 FC	323 W	4.63 MW
SPK IBS	411 W	5.88 MW
MBL IBS	1575 W	22.5 MW

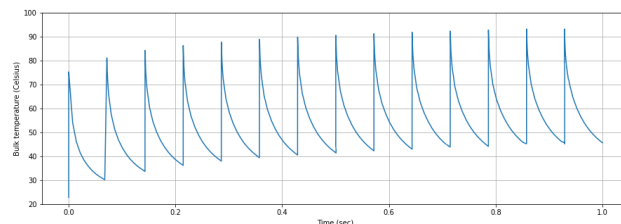


Figure 1: Temperature as a function of the time, calculated in ANSYS for the graphite bulk of the SPK IBS, after 73 MeV protons and 50 μ s long pulses, at 6 mA and 14 Hz.

Similarly, dedicated experiments and controlled damage tests are usually expensive and not always an option when the impact(s) of many parameters have to be studied. Therefore, in this contribution a Machine-Learning (ML) based method for the prediction of temperature trends within beam-interceptive devices was developed, not for detector design purposes, but for fast time-series forecasting. In the future, the method described in the next section can be expanded either for standard machine protection purposes or virtual diagnostics.

* Corresponding author: elena.donegani@ess.eu

¹ cit. Winston Churchill, 1906

BEAM EXTINCTION MEASUREMENT AT THE PIP-II INJECTOR TEST FACILITY*

Mathias El Baz[†], Université Paris Saclay, Orsay, France

Brian Fellenz, Vic Scarpine, Alexander Shemyakin, Randy Thurman-Keup, Fermilab, Batavia, USA

Abstract

The PIP-II particle accelerator is a new upgrade to the Fermilab accelerator complex, featuring an 800-MeV H^- superconducting linear accelerator that will inject the beam into the present Fermilab Booster. A test accelerator known as PIP-II Injector Test (PIP2IT) has been built to validate the concept of the front-end of such a machine. One of the paramount challenges of PIP2IT was to validate the bunch by bunch chopping system in the Medium Energy Beam Transport (MEBT). For PIP-II beam operations, the chopper will implement an aperiodic “Booster Injection pattern” that will roughly select two-fifth of the bunches, decreasing the beam current from 5 mA to 2 mA before injection into the cryomodules. Beam measurements have been taken by two Resistive Wall Current Monitors (RWCM) and recorded by a high bandwidth oscilloscope in order to validate the complete suppression of the chopped beam. This paper aims to present the beam extinction measurements at PIP2IT and their limitations.

INTRODUCTION

The PIP-II Injector Test facility, also called PIP2IT (see Fig. 1), is a model of what will be the Front End of PIP-II which will accelerate the H^- ion beam up to 25 MeV. The Front End is often divided into three sections: the Low Energy Beam Transport (LEBT), the Medium Energy Beam Transport (MEBT), and the High Energy Beam Transport (HEBT) which contains the superconducting RF Half-Wave Resonator and Single-Spoke Resonator cavities [1].

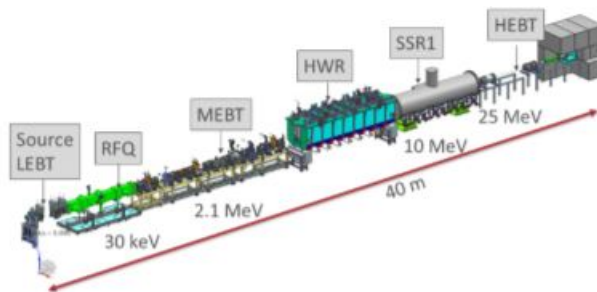


Figure 1: Sketch of PIP2IT.

At the exit of the RFQ, the beam is made of macro-pulses (typically 550 μ s), each of them made of short bunches at the frequency of 162.5 MHz.

The bunch-by-bunch chopping system is the heart of the MEBT and one of the most innovative parts of the PIP-II

* This work was supported by the U.S. Department of Energy under contract No. DE-AC02-07CH11359

[†] mathias.el-baz@universite-paris-saclay.fr

project. The chopper is made of two electric deflectors, called kickers, that kick a pre-programmable set of bunches onto an absorber downstream. The chopper is extremely demanding from a technical perspective, as the kickers voltage reaches 500 V while having the capability to turn on or off in a few nanoseconds [2].

MEASUREMENT SCHEME

Resistive Wall Current Monitor and Cabling

The beam is chopped in the MEBT but the extinction can be measured at any location after the absorber. The data were taken with two identical Resistive Wall Current Monitors (RWCM), one at the end of the MEBT and the other one after the SRF cavities in the HEBT.

A RWCM consists of a resistive gap along a conducting pipe. Charged particles traveling in the vacuum produce a Gaussian shape image current on the surface that has equal magnitude but opposite sign. When this image current passes through the resistive gap, a voltage signal is produced. A ferrite core forces the signal to go through the resistive ring gap made of ceramic rather than allowing it to flow through other conducting paths. The impedance of the ceramic gap is 2.36 Ω (Fig. 2) [3].

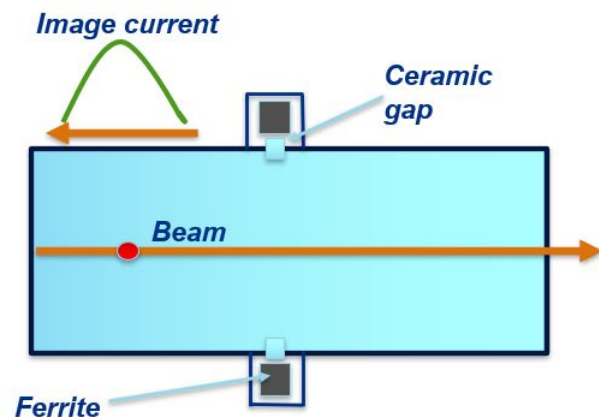


Figure 2: Schematic of the transverse slice of the RWCM.

The RWCM signals are recorded with a Rhode and Schwartz oscilloscope which has an 8 GHz bandwidth.

The same type of cables has been used for the 2 RWCM (but with different cable lengths!), with 4 different cables (including a long Helix cable) and 5 connectors. The Helix cable between the MEBT RWCM and the oscilloscope is 30 meters long and is 45 meters long between the HEBT RWCM and the oscilloscope.

MACHINE LEARNING METHODS FOR SINGLE SHOT RF TUNING

J. S. Lundquist*, S. Werin, Lund University, Lund, Sweden
 N. Milas, ESS, Lund, Sweden

Abstract

The European Spallation Source, currently under construction in Lund, Sweden, will be the world's most powerful neutron source. It is driven by a proton linac with a current of 62.5 mA, 2.86 ms long pulses at 14 Hz. The final section of its normal-conducting front-end consists of a 39 m long drift tube linac (DTL) divided into five tanks, designed to accelerate the proton beam from 3.6 MeV to 90 MeV. The high beam current and power impose challenges to the design and tuning of the machine and the RF amplitude and phase have to be set within 1% and 1° of the design values. The usual method used to define the RF set-point is signature matching, which can be a challenging process, and new techniques to meet the growing complexity of accelerator facilities are highly desirable. In this paper we study the use of ML to determine the RF optimum amplitude and phase, using a single pass of the beam through the ESS DTL1 tank. This novel method is compared with the more established methods using scans over RF phase, providing similar results in terms of accuracy for simulated data with errors. We also discuss the results and future extension of the method to the whole ESS DTL.

INTRODUCTION

The European Spallation Source (ESS) is a state of the art neutron science facility under construction in Lund, Sweden [1]. The basic process used by the facility is spallation, wherein one impinges a high neutron material, in this case Tungsten, with high energy protons, causing the target to shed excess neutrons. The high energy protons are provided by the ESS linear accelerator (linac), a 600 m long accelerator consisting of many different sections utilizing varied accelerator technologies in order to raise the proton energy from the 75 keV source output to the final 2.0 GeV arriving on the target. A crucial part of this machine is the 39 m long drift tube linac (DTL) divided into five tanks, designed to accelerate the proton beam from 3.6 MeV to 90 MeV. As the machine is expected to deliver beam of high current and power, a primary concern is to avoid slow beam losses, as these lead to radiation activation of surrounding equipment. In order to avoid such losses, proper and careful tuning of the RF fields is crucial. As a result the requirement for accuracy of the RF set point is to be within 1% in RF amplitude and 1° in phase [1]. In order to achieve this type of accuracy, much work has been performed in the last decades to develop new techniques to meet the growing scale and complexity of facilities [2–4]. Within this paper we will investigate how Machine Learning (ML) may serve this purpose. This paper presents our current strides in the development of a tuning

technique using ML, with simulated data used in such a way that a single pass through the untuned cavity could be sufficient for setting it up.

RF TUNING

RF Phase Scan

In order to be able to quantify how the beam responds to changes to the RF set-point, a diagnostic sensitive to the beam time of flight through the cavity must be used. For those cases a Beam Position Monitor (BPM) can be used. As the beam passes a BPM both the amplitude and phase of the fields excited on the BPM sensor by the passing beam are recorded. Although this phase alone doesn't hold much usable information for cavity tuning, by comparing two BPM phases we can get a fast measurement which is proportional to the time-of-flight, or looking with respect to acceleration in a RF cavity, the energy gain between the two devices. It is important to stress that this measurement is relative and that extracting the absolute values of the energy is not an easy task. For this technique, using only the relative phase changes has proven to be enough [2–4].

The BPMs are used to measure the energy gain (or time-of-flight) as a function of the set points in the accelerating cavity. As the BPM's measured phase is closely dependent on the energy of the beam, scanning RF amplitude and phase in a cavity and plotting out the resulting phase differences will give rise to different curves depending on the proximity to the ideal set point for the cavity. A few of these signature curves can be seen in Fig. 1, where the ideal set point can be found from the signature for the ideal amplitude $A_0 = 6.89$ kV, the ideal input beam energy $E_0 = 3.62$ MeV and the -35° phase set point.

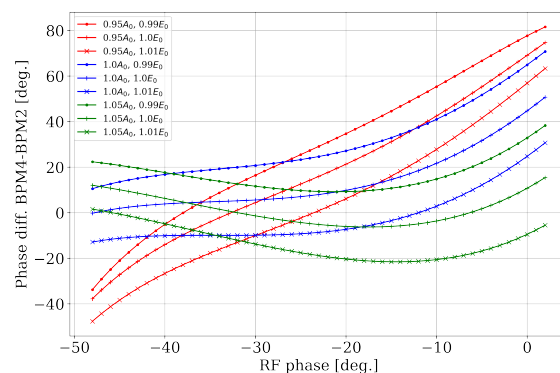


Figure 1: The phase curves for different RF amplitude and input energy set points. BPM phases simulated as comparison between two BPMs in the first DTL tank in the ESS linac.

* johan.lundquist@ess.eu

GOUBAU-LINE SET UP FOR BENCH TESTING IMPEDANCE OF IVUE32 COMPONENTS

Paul Volz*, A. Meseck, M. Huck, S. Grimmer
Helmholtz-Zentrum Berlin für Materialien und Energie (HZB), Berlin, Germany

Abstract

IVUE32 is the world first elliptical in-vacuum undulator, being developed at HZB. With a period length of 32 mm and a minimum gap of 7 mm, the 2.5 m long insertion device (ID) will be installed in the BESSY II storage ring, delivering soft X-rays to several beam lines. In-vacuum undulators put complex structures in close proximity of the particle beam which makes them susceptible to wake field effects. These effects can cause beam instabilities and unwanted heating of undulator components, possibly damaging them. Therefore understanding the impedance characteristics of the device prior to installation is paramount. Numerical studies, e.g. CST simulations of such complex structures become very resource intensive for high frequencies, making the ability to bench test such a device invaluable. A Goubau line is a single wire transmission line for high frequency surface waves that can mimic the transverse electric field of a charged particle beam out to a certain distance, allowing for impedance measurements of IDs outside of the working accelerator. The status of a Goubau-line set up, optimized for measuring IVUE32-components, will be presented.

INTRODUCTION

BESSY II is a third generation synchrotron light source with an electron beam energy of 1.7 GeV. There are 32 dipole magnets and 13 undulators supplying 48 beam lines with radiation ranging from infrared to soft X-ray. In September of 2018 the first in-vacuum undulator (IVU) CPMU17 [1] was installed in BESSY II to provide hard X-rays for the Energy Materials In-Situ Laboratory (EMIL) [2]. As previously described in [3] IVUs require shielding foils between their magnets and the accelerator beam. The second IVU for BESSY II, IVUE32 [4], is currently under development. The APPLE II configuration poses even greater design challenges than the planar CPMU17. IVUE32 features four individually movable magnet rows which requires a longitudinal slit in the shielding foils. The split shielding foils further complicate the design of the transition taper between the beam pipe and the undulator magnets.

Motivation

Without a vacuum chamber wall between the beam and the undulator magnets, both CPMU17 and IVUE32 change their geometry from a collimator to a cavity over the entire gap range. This has an impact on wakefield characteristics and beam dynamics. The impact on beam stability is difficult to simulate. Beam based impedance measurements using orbit bump and tune shift methods have been done for

the already installed CPMU17 with different gap settings [5]. Grow-damp and drive-damp methods have been utilized as well by M. Huck *et al.* [6]. The novel design of IVUE32 brings even more challenges as the shielding foil is split in the middle longitudinally to accommodate the different polarization settings. Therefore the impact on beam stability and accelerator operation are difficult to simulate and predict. Being able to measure impedance outside of the running accelerator is desirable to avoid complicated down time. As introduced in [3] a Goubau-line test stand is a possible way to measure impedance of insertion devices. Designed by Georg Goubau in 1950 [7] based on the work of Sommerfeld from 1899 [8], a Goubau-line is a transmission line that uses a single wire to transmit surface waves. Its transverse electric field can be used to mimic that of a charged particle beam. Goubau-line set ups have been successfully used to measure the impedance of accelerator components, for example at Argonne APS [9] or at Bergoz Instrumentation [10]. Studies of CPMU17s impedance suggest that the fill pattern at BESSY II induces effects up to a frequency of 20 GHz which is significantly higher than the aforementioned test stand examples.

The following sections will discuss the design parameters of a Goubau-line test stand, capable of measuring up to frequencies of 20 GHz.

THEORETICAL CONSIDERATIONS

The main parts making up a Goubau-line are a transmitter, a receiver and a dielectrically coated wire. Horn antennas are usually used as transmitter and receiver shown in Fig. 1. The



Figure 1: Schematic of a Goubau-line consisting of two conical horn antennas and a dielectrically coated wire similar to the design at Argonne APS [9].

transmitted waves are guided as transverse magnetic modes the coated wire. Figure 2 shows the orientation of electric and magnetic fields along the coated wire. The electric and magnetic fields are described by cylinder functions. These formulas are derived in Goubau's original paper [7] and in a revision considering modern computational advances by B. Vaughn *et al.* [11]. Three distinct regions can be considered: inside of the conductor, inside of the dielectric coating, and outside of the wire. The continuity of the fields across the interfaces of these regions can be used to numerically calculate the guided wave propagation constant [11] and

* paul.volz@helmholtz-berlin.de

DESIGN OF A MULTI-LAYER FARADAY CUP FOR CARBON THERAPY BEAM MONITORING*

K. Tang[†], R. S. Mao, Z. G. Xu, T. C. Zhao, Z. L. Zhao, K. Zhou

Institute of Modern Physics, Chinese Academy of Sciences (IMP/CAS), Lanzhou, China

Abstract

Because of determining the depth of Bragg Peak, range and energy of carbon beam are very important parameters in therapy. In order to measure those parameters rapidly, we design a multi-layer Faraday cup (MLFC). Simulation of proton beam and carbon beam are given in this paper. A prototype has 128 channels have been developed. Each consists of a 40 μm copper foil and 600 μm FR4 plate. A 128 channels electronics was used to measurement the deposited ions in each copper foil.

INTRODUCTION

China's first Heavy Ion Medical Machine (HIMM) developed by the Institute of Modern Physics (IMP) was approved to be registered at January 10, 2020. The main parameters at treatment place are listed in Table 1.

Table 1: Main Beam Parameters of HIMM

Parameters	Value
Ion	¹² C ⁶⁺
Beam energy	80~430 MeV/u
Intensity at treatment room	(2 pA ~ 0.4 nA)
Extraction time	2 s
Extraction cycle	8 s

It is very crucial that the difference between the radiation field achieved by patient and given by prescription is as small as possible. Two of most importance beam parameters which decide the radiation field are beam energy and beam energy distribution. Therefore, these parameters should be checked or calibrated before treating.

Overview of range verification of proton and light-ion beams have been given by W. T. Chu [1]. It involves ex vivo or off-line measurement method [2] and in vivo or on-line measurement method. MLFC (Multi Layer Faraday Cup) was proposed for testing Monte Carlo models [3]. And then it was first applied to verify proton range by Bernard Gottschalk at NPTC [4]. Now it has become a conventional tool and has been used in numerous proton therapy research center [5-13]. However, MLFC can only used for proton beam so far. Because, in proton therapy most of the primary particles will stop near Bragg Peak with no secondary fragments creation. But for carbon particles, there will be several charged secondary fragments such as H, He, Li, Be and B created. Those charged particles will be collected by charge meter as well as primary carbon particles.

After carefully analyzing the affection by secondary fragments and with Fluka simulation, the author find that the peak of beam charge collection curve was near Bragg Peak. So, we propose that use MLFC to measure carbon beam range and energy. In this paper, the measurement theory will be described firstly. And then, Fluka simulation result will be given. Finally, a prototype of MLFC are also given.

EXPERIMENT METHODS

Measurement Theory

The theory of MLFC is well-documented. A MLFC is a stack of metal collecting plates which separated from each other by thin insulating plates. MLFC is connected to a multi channel charge meter so that each active sheet of the MLFC is connected to one channel. Take proton beam for example, if a proton beam (for a therapy beam, beam energy are usually from 70 MeV to 250 MeV) inject into a MLFC, most proton particles will pass through several metal plates and insulating plate and stop near Bragg peak position in the last. When particles stop, each layer plate can collect the deposited charge. In other words, the MLFC can measure beam differential fluence as a function of depth [4].

As a result of statistical fluctuations, the effect of range straggling give a charge distribution. For a therapy proton beam, range straggling can be modelled by a Gaussian distribution [14-16]. Because proton is the lightest ion so no nuclear fragments created. Therefore, no extra charged particles or charged fragments affect the charge collection. So, we can use MLFC to measure the proton range and energy.

But for carbon beam, the situation is different. High energy charged fragment occur along the beam penetration path in materials. These charged fragments include H, He, Li, Be and B. Those fragments will continue move forward and will also be collected by charge meter as well as primary carbon particle. Its will have an affection on charge collection. Fortunately, the peak of these charged fragments are near the Bragg peak.

Differential Fluence v. Depth of Proton Beam

For proton therapy beam, the range distribution can be described by Gaussian function [14-16]

$$R_0(x) = I_0 \exp\left(-\frac{(x-R_0)^2}{2\sigma_0^2}\right) \quad (1)$$

Where I_0 is beam total charge, R_0 is beam range and σ_0 is the sigma of the Gaussian range straggling. The differential charge distribution as a function of depth in copper of a 70 MeV proton beam is simulated by Fluka (Fig. 1). The

* Work supported by the Young scientists Fund Grant NO.11905075

[†] email address: tangkai@impcas.ac.cn

DESIGN OF HYDROSTATIC LEVEL SYSTEM FOR THE APS-U STORAGE RING*

W. Cheng[#], D. Karas, G. Wang
Argonne National Laboratory, Lemont, IL, USA

Abstract

A Hydrostatic Leveling System (HLS) has been designed for the Advanced Photon Source Upgrade (APS-U) storage ring (SR) to characterize the relative floor motion along each Insertion Device Front End (IDFE) and the global floor motion of the SR tunnel. 3 HLS sensors will be installed alongside each IDFE. Two sensors will be mounted near the ID Beam Position Monitors (BPMs), which are located at either end of the ID. The 3rd HLS sensor will be mounted near the Grazing-Incidence Insertion Device X-Ray BPM (GRID xBPM), about 20 meters away from the source point. In addition, there will be 1 sensor installed in each of the 5 sectors in Zone-F where there are no ID beamlines. The HLS water network along each of the 35 IDFEs and 5 sectors in Zone-F are connected via valves to form a global network around the 1.1 km SR tunnel. The HLS will measure the vertical floor displacement at a total of 110 locations. Combined with the highly stable BPM/xBPM stands, the HLS can better characterize the electron and photon beam long-term stability. The HLS design is based on a two-pipe system for easy installation in tight spaces. In this paper, we present the design of the HLS system and preliminary performance of the first article units.

INTRODUCTION

Modern light sources have tight requirements of the beam stability. For example, the Advanced Photon Source Upgrade (APS-U) machine asks for an orbit stability [1] of 0.4 μm for short term (0.01 Hz – 1 kHz) and 1 μm for long-term (7 days). With careful design of the magnets, the supporting structure, Beam Position Monitor (BPM) electronics and the orbit feedback system, the short-term orbit stability can normally be achieved. However, the long-term stability is not obviously achievable even with the best modern electronics and feedback algorithms. The situation is even more complicated by comparing the stability of electron beam and photon beam. Long-term stability is affected by many factors including the mechanical/thermal stability of BPM/xBPM stands, BPM electronics long-term stability, utility system stability, ground motion, etc.

To achieve the long-term beam stability goals, all sources of mechanical motion of critical in-tunnel beam position monitoring devices must be carefully evaluated and appropriately addressed. This includes the effects of water and air temperature, as well as earth tides and diffusive ground motion. A Hydrostatic Leveling System

(HLS) is designed to quantify this floor motion.

The fundamental principle of the HLS is that any fluid seeks its own level. Given two reservoirs set at the same height and connected by a pipe or tube, the fluid level in each reservoir will be at the same absolute elevation. This is determined by the balance between gravity and air pressure. For small systems, the absolute elevation can be relative to some reference such as mean sea level. For larger systems, the curvature of the earth and other gravitational effects need to be considered. Given a reference point, the relative level of the fluid will vary as the sensor is moved up or down with respect to all the other sensors. While any fluid can be used, water has the advantages of a low viscosity (allowing for relatively rapid movement between reservoirs), it is non-toxic, is easily obtained, and if treated with sufficient care there will be no growth of biota in the reservoirs or tubing [2]. Specifically, the HLS requires that the system use demineralized water treated with fungicide.

3 HLS sensors per Insertion Device Front End (IDFE) will provide the necessary ground motion measurement. There will be a total of 105 HLS sensors to cover the 35 IDFEs. An additional sensor will be installed in each sector in Zone-F where there are no ID beamlines. This allows a global HLS network to be formed with a total of 110 sensors around the Storage Ring (SR).

Figure 1 illustrates the current HLS design for a generic sector in the APS-U SR. The B:P0 and A:P0 BPMs are mounted on invar stands on either side of the ID. The Grazing-Incidence Insertion Device (GRID) X-Ray BPM [3] in the IDFE is mounted on a granite table. 3 HLS sensors are mounted on the floor near the B:P0, A:P0 and GRID X-ray BPM stands. Water and air pipes will connect the sensors at each location. The invar stands and granite table will exhibit very good thermal stability given the tunnel ambient temperature will be stabilized within 0.1° C. Thus, we can assume that any ground motion measured by the HLS will be directly related to the change in position of the BPM sensors and any relative height differences between the BPMs can be characterized.

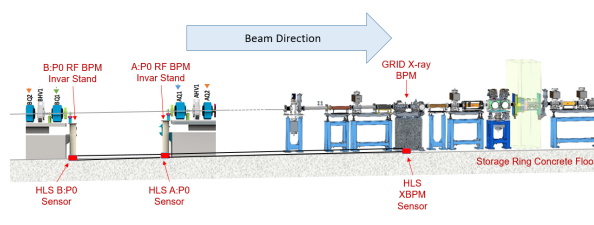


Figure 1: Hydrostatic Leveling System (HLS) for one of the APS-U IDFEs.

*Work supported by DOE contract No: DE-AC02-06CH11357

[#]wcheng@anl.gov

REAL-TIME LONGITUDINAL PROFILE MEASUREMENT OF OPERATIONAL H⁻ BEAM AT THE SNS LINAC USING LASER COMB*

Y. Liu[†], C. Long, and A. Aleksandrov

Spallation Neutron Source, Oak Ridge National Laboratory, Oak Ridge, TN 37831, USA

Abstract

We demonstrate a novel technique to measure the longitudinal profile of an operational hydrogen ion (H⁻) beam in a nonintrusive, real-time fashion. The measurement is based on the photoionization of the ion beam with a phase modulated laser comb – pico-second laser pulses with controllable temporal structure. The measurement technique has been applied to a 1-GeV, 1.4-MW H⁻ beam at the Spallation Neutron Source (SNS) high energy beam transport (HEBT). A stroboscopic photograph of the H⁻ beam micro bunch can be obtained by using a phase modulated laser comb. The entire measurement takes only 700 μs.

INTRODUCTION

Short-pulsed laser beam has been proposed to measure the longitudinal H⁻ beam profiles in the particle accelerators [1, 2]. The measurement is based on the photo neutralization of the ion beam where the electrons are detached from the ions by a focused laser beam, often named as laser wire, and the number or density of the detached electrons leads to the determination of the original ion density. The measurement is generally nonintrusive and can be conducted on operational particle beams. So far, laser wire based longitudinal profile measurements have been conducted on relatively low energy beams. One reason is that for the short-pulsed, high repetition rate lasers, the available peak power is in the range of 1-10 kW, which produces photodetachment yield below 10⁻⁴. Detection of such weak signals requires high sensitivity detectors such as photo-multiplier tube (PMT) and suffers from the large background noise in the low/medium-energy beam line.

In this paper, we describe the longitudinal profile measurement of 1-GeV H⁻ beam using a customized light source, referred to as a laser comb, which has multi-layer pulse structure with a peak power of more than 100 MW. The laser pulses can be phase modulated so that each comb tooth has a different phase delay with respect to the ion beam micro-bunches. When a phase modulated laser comb is applied to the ion beam, the photo-detached electrons are detected with a Faraday cup (FC). A stroboscopic photograph of the H⁻ beam micro-bunch can be obtained from the FC output with the measurement time of only 700 μs. This real-time measurement causes negligible beam loss

* This manuscript has been authored by UT-Battelle, LLC, under contract DE-AC05-00OR22725 with the US Department of Energy (DOE). The US government retains and the publisher, by accepting the article for publication, acknowledges that the US government retains a nonexclusive, paid-up, irrevocable, worldwide license to publish or reproduce the published form of this manuscript, or allow others to do so, for US government purposes. DOE will provide public access to these results of federally sponsored research in accordance with the DOE Public Access Plan (<http://energy.gov/downloads/doe-public-access-plan>).

[†] liuy2@ornl.gov

and therefore was conducted at different locations of the 1.4-MW neutron production H⁻ beam line.

LIGHT SOURCE DEVELOPMENT

Estimation of Laser Power Requirement

Photo neutralization is a non-resonant process with a very small cross section (~3×10⁻¹⁷ cm²). In laser-based H⁻ beam diagnostics, the photo-detached electrons are directly proportional to the product between photon and ion beam densities as expressed by

$$n_{det} = c\sigma n_b n_l \quad (1)$$

where c is the light speed, σ the photon-ion interaction cross-section, and n_b and n_l represent density functions of ion and photon beams, respectively.

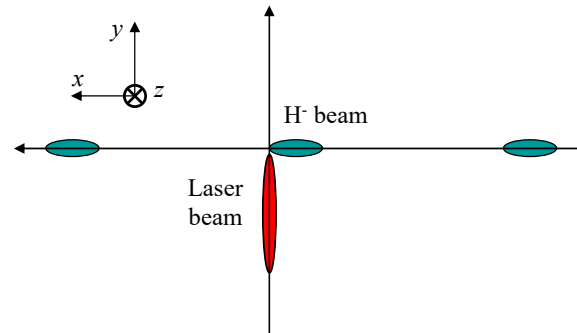


Figure 1: Schematic of laser-H⁻ beam interaction.

A typical laser-ion interaction scheme is shown in Fig. 1. Both n_b and n_l are assumed to have a Gaussian function distribution as

$$n_b = \frac{N_b}{(2\pi)^{3/2} \sigma_{bx} \sigma_{by} \sigma_{bz}} \exp \left[-\frac{(x-\beta ct)^2}{2\sigma_{bx}^2} - \frac{y^2}{2\sigma_{by}^2} - \frac{z^2}{2\sigma_{bz}^2} \right], \quad (2)$$

$$n_l = \frac{N_l}{(2\pi)^{3/2} \sigma_{lx} \sigma_{ly} \sigma_{lz}} \exp \left[-\frac{x^2}{2\sigma_{lx}^2} - \frac{(y-c(t-s))^2}{2\sigma_{ly}^2} - \frac{z^2}{2\sigma_{lz}^2} \right]. \quad (3)$$

Here N_b and N_l are ion and photon numbers, respectively, $\sigma_{bx,y,z}$ ($\sigma_{lx,y,z}$) represents the RMS size of the ion (photon) beam along the ion beam propagation, photon beam propagation, and vertical direction, respectively, and s denotes the phase delay in longitudinal profile scan. For pulsed beam with low duty factor, the overall photodetachment yield over one micro bunch of the ion beam can be calculated by integrating n_{det} over an entire space and time as

$$\eta = \frac{c\sigma}{N_b} \iiint_{-\infty}^{+\infty} n_b n_l dx dy dz dt$$

BUNCH-RESOLVED 2D DIAGNOSTICS – STREAKING COMBINED WITH INTERFEROMETRY*

M. Koopmans^{†1}, J.-G. Hwang, A. Jankowiak¹, M. Ries, G. Schiwietz

Helmholtz-Zentrum Berlin für Materialien und Energie GmbH (HZB), Berlin, Germany

¹also at Humboldt-Universität zu Berlin, Berlin, Germany

Abstract

Due to the complexity of the fill pattern in the BESSY II electron-storage ring, bunch-resolved diagnostics are required for machine commissioning and to ensure the long-term quality and stability of operation. In addition, low- α operation and a possible VSR upgrade demand bunch-length measurements with picosecond resolution. Therefore, a dedicated beamline equipped with a fast streak camera was set up and successfully commissioned. Couplings between time- and space-coordinates also call for bunch-selective and correlated multi-parameter detection methods. Thus, the beamline and the streak camera have been made capable of direct beam-profile imaging and interferometry of the vertical beam size using the X-ray blocking baffle method. The horizontal or vertical dimension can additionally be imaged with the streak camera and bunch-resolved 2D measurements are possible. Imaging the vertical direction, the characteristic dip in the center of the interference pattern from the π -polarized synchrotron radiation can be observed and is used to extract bunch resolved information about the vertical beam size. The streak camera measurements are validated with direct imaging measurements with a regular CCD camera at the beamline and compared to model calculations. The results are converted into absolute values by a calibration with the BESSY II pinhole monitors.

INTRODUCTION

The BESSY II electron storage ring provides synchrotron radiation (SR) to a very diverse user community. In standard user operation a complex fill pattern features multiple bunch types for dedicated applications. Special operation modes like single bunch or low- α operation for short pulses are offered for few weeks a year [1, 2]. In addition, a new operation with a second orbit is tested and developed [3] and a possible upgrade to a variable pulse length storage ring (VSR) is envisioned [1].

Non-invasive bunch resolved diagnostics are needed for maintaining and improving of existing as well as for commissioning and development of new operation modes. For this purpose dedicated diagnostic beamlines have been installed. A new beamline dedicated for bunch resolved longitudinal diagnostics equipped with a fast streak camera has been commissioned and is in full operation since mid 2020 [4]. Although this beamline is optimized for maximum photon flux, it has extremely good transverse imaging capabilities.

* Work supported by the German Bundesministerium für Bildung und Forschung, Land Berlin and grants of the Helmholtz Association
[†] marten.koopmans@helmholtz-berlin.de

Furthermore, the streak camera features an entrance aperture with a horizontal slit. Depending on the beamline settings, it is possible to image either a slice corresponding to the horizontal or the vertical direction of the initial electron beam in the horizontal direction of the streak camera. In combination with the streak camera an RMS resolution down to 120 μm was reached for direct imaging in the transverse direction. It was also shown that bunch position fluctuations below 10 μm (RMS) can be measured applying a statistical analysis method to single shot streak camera images [5].

To overcome the resolution limit of direct imaging, a combination of interferometry with the streak camera is investigated to become sensitive to bunch sizes below 120 μm [6]. For this goal the interference in the vertical direction originating from the X-ray blocking baffle using π -polarized SR turned out to be very promising. This method is similar to the obstacle diffractometer method introduced in Ref. [7, 8].

VERTICAL BEAMLINE IMAGING

A simplified schematic of the longitudinal diagnostics beamline at BESSY II, which contains the components relevant for the vertical imaging, is shown in Fig. 1. The SR beam first passes the X-ray blocking baffle and is then collimated through an intermediate focus with the M1 ellipsoid and the M2 toroid mirrors, which are replaced by lenses in the schematic. Then a polarisation filter, followed by a 90° rotation of the SR beam with a periscope (not shown in Fig. 1) and a 700 nm bandpass filter (10 nm FWHM bandwidth) are used to obtain a clear interference pattern, which is finally detected with a regular CCD or the streak camera. Additionally, a slit with an opening aperture of 2 mm is used to cut out approximately an eighth of the collimated beam for improved coherence due to the varying quality along the beam profile. The region with a minimal wavefront error was chosen by adjusting the slit position to optimize the

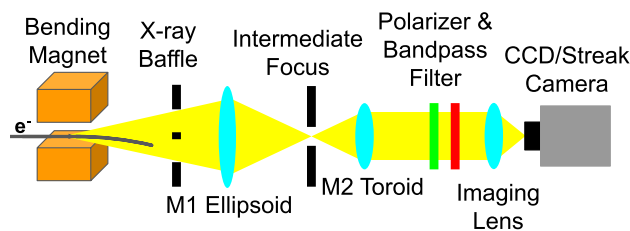


Figure 1: Schematic of the relevant objects for vertical imaging at the longitudinal diagnostics beamline at BESSY II. The two mirrors are replaced by lenses in this linearized drawing by keeping the main optical properties (M1 for point-to-point focussing and M2 for collimation).

ABSOLUTE BUNCH LENGTH MEASUREMENTS OF LOW ENERGY BEAMS USING ACCELERATING RF CAVITY

Ji-Gwang Hwang*, Helmholtz-Zentrum Berlin, Berlin, Germany
Tsukasa Miyajima, Yosuke Honda,

High Energy Accelerator Research Organization (KEK), Ibaraki, Japan
Eun-San Kim, Korea University Sejong Campus, Sejong, Republic of Korea

Abstract

The experimental technique has been proposed and demonstrated by authors for measuring the temporal distribution and absolute bunch length of picosecond-level low-energy electron bunch generated by an electron gun using radial electric and azimuthal magnetic fields of an accelerating (TM₀₁ mode) radio frequency cavity. In this scheme, an accelerating RF cavity provides a phase-dependent transverse kick to the electrons, resulting in the linear coupling of the trajectory angle with the longitudinal position inside the bunch like a transverse deflecting cavity. In this paper, we show a detailed estimation of various aspects of the temporal resolution of this method with feasible parameters and deconvolution of the Gaussian distribution for accurate reconstruction of the temporal distribution.

INTRODUCTION

Energy Recovery Linac (ERL) demonstrators [1–3] are established to demonstrate physical challenges and key technologies of the generation, acceleration, transport, and energy recovery of high brilliance and high average current beams in superconducting cavities. The beam quality assurance in those high-brightness and high-current injectors is crucial. Therefore, a diagnostics beamline is mostly installed at the end of the injector to gauge beam quality in six-dimensional phase spaces [4, 5]. A transverse deflecting cavity that has a dipole mode to imprint the temporal information into transverse momentum is widely adopted [6–8] to measure a temporal distribution as well as absolute bunch length. This is a space-charge-free method but it has a technical difficulty to transport low-energy beams without the deterioration of beam qualities to the cavity where is typically located far downstream of the injector due to the limited space in low-energy injectors. As a complementary way to measure longitudinal beam properties near the electron gun, the zero-phase method [9] is also used. This method yields a linear RF chirp in the longitudinal phase space by using an accelerating cavity with a zero-crossing phase and transforms the longitudinal phase-space distribution to the transverse direction by dispersion function originated by a dipole magnet. However, it is not suitable for high current beams because the longitudinal phase space is strongly distorted at higher bunch charge by longitudinal space charge forces [10] while the beam is transported to the dipole magnet located far downstream of the gun. We have been proposed and demon-

strated [11, 12] a new method that uses radial EM fields of an accelerating cavity to measure the temporal distribution and absolute bunch length using existing instruments in the beamline such as a corrector magnet and a screen monitor.

RESOLUTION OF THE METHOD

To utilize the method, it demands a corrector magnet for adjusting the initial beam offset and angle, an accelerating cavity (TM₀₁ mode), and a screen monitor located downstream of the cavity. The schematic layout is shown in Fig. 1.

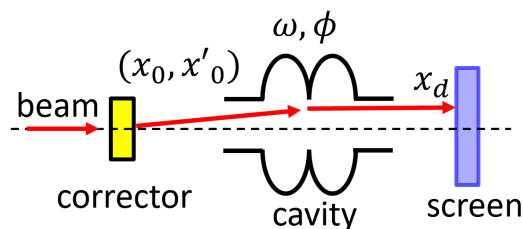


Figure 1: Schematic layout for the proposed method.

The initial beam offset x_0 and angle x'_0 are defined at the position of the corrector magnet. The beam passes the center of the cavity when the offset is vanished at the corrector position, i.e. $x_0 = 0$. With an on-axis beam, the temporal resolution R_t of the method is given by [12]

$$R_t = \frac{\sqrt{\sigma_c^2 + 2\sigma_{x0}\sigma_c}}{|d_{12}x'_0|\omega}, \quad (1)$$

where σ_c is the spatial resolution of the screen monitor, σ_{x0} is the initial beam size at the screen monitor without the offset and angle, d_{12} is the deflection coefficient associated with an initial angle, and $\omega = 360 \text{ deg} \times f$, where f is the frequency of the cavity. With a state-of-the-art technique for the screen monitor [13] that has been proven measurements of a beam size of 1.44 μm using a 200 μm thick LYSO:Ce scintillator, the temporal resolution of our method can be improved enormously. Assuming that the initial beam angle is 16 mrad which is equivalent to 1/3 of the cavity radius for a 1.3 GHz superconducting cavity and d_{12} of -0.0324 mm/deg/mrad measured at a beam energy of 390 keV, the temporal resolution is calculated as a function of the spatial resolution of the screen monitor at various initial beam sizes.

As shown in Fig. 2, the method with a spatial resolution of the screen monitor of 1.44 μm yields temporal resolutions of 32 fs, 50 fs, and 70 fs for initial beam sizes of 20 μm , 50 μm ,

* ji-gwang.hwang@helmholtz-berlin.de

CHARGE MEASUREMENTS IN SwissFEL AND RESULTS OF AN ABSOLUTE CHARGE MEASUREMENT METHOD

G. L. Orlandi*, P. Craievich, M. M. Dehler, R. Ischebeck, F. Marcellini, D. Stäger
Paul Scherrer Institut, 5232 Villigen PSI, Switzerland

Abstract

A comparative measurement campaign of the beam charge was carried out at SwissFEL using the following instruments: Faraday-Cup (FC), Wall-Current-Monitor (WCM), Integrating-Current-Transformer (Bergoz Turbo-ICT-2) and the reference cavity of the Beam-Position-Monitor (BPM). The goal of the measurement campaign was to determine an absolute charge measurement method for a general purpose of instrument calibration and machine routine operation. Results of the absolute charge calibration method proposed for SwissFEL will be presented.

INTRODUCTION

In the electron linac driven SwissFEL – the X-ray laser facility of Paul Scherrer Institut (PSI, www.psi.ch) – two undulator lines can be simultaneously supplied at a maximum repetition rate of 100 Hz by electron bunches with a charge in the range 10-200 pC and energy of 6.2 GeV and 3.3 GeV, respectively. A 2-bunch train of charge is emitted by a photocathode with a time duration of a few ps for the single bunch and a time macro-structure of 28 ns, accelerated by a 3 GHz RF booster and 6 GHz RF linac and compressed up to a few fs by two magnetic chicanes. The two bunches are split apart by a RF kicker into a magnetic switchyard to be finally injected into the ARAMIS and ATHOS undulator lines [1, 2], respectively.

The measurement of the bunch charge at the different acceleration stages of a linac driven Free-Electron-Laser (FEL) is relevant for characterizing the beam features such as the transverse emittance and peak current, for monitoring the correct transport of the beam through all the acceleration and compression stages, for protecting the machine from possible accidental beam losses and for a legal certification of the charge-per-hour accelerated by the machine.

In SwissFEL, the charge of each single bunch of the 28 ns long macro-structure can be measured at different position of the machine. Just downstream of the gun, a standard Bergoz ICT and a Bergoz Turbo-ICT-2 [3] can measure the integrated charge of the bunch train and the charge of the single bunch, respectively. At the gun, a Faraday-Cup (FC) and a Wall-Current-Monitor (WCM) are also available. The FC was initially installed just downstream of the SwissFEL gun to measure the dark current. The WCM is used in SwissFEL to measure the electron bunch charge and mainly to synchronize the photocathode laser and the radio frequency of the RF gun. In addition to the Turbo-ICT in the gun, three more Turbo-ICTs are available along the ARAMIS electron beam line as well as two Turbo-ICTs can provide

the charge readout at the beginning and at the end of the ATHOS electron beam line. A further monitor of the beam charge is represented by the cavity-BPM. The charge dependent signal of the monopole RF cavity of the BPM is used to normalize the dipole signal of the adjacent RF cavity which instead depends on the product of the charge and position of the bunch. The normalized dipole signal is hence processed to determine the bunch position in the horizontal and vertical directions. In SwissFEL, about two hundred cavity-BPMs are distributed all along the machine. The monopole RF signal of the cavity-BPMs has been so far calibrated against the charge readout of a reference Turbo-ICT-2 in order to provide an additional and a quite densely localized charge readout of the single bunch at 100 Hz.

The absolute calibration of the charge monitor is a crucial and sensitive issue in all the particle accelerators and, in that sense, SwissFEL does not makes an exception. The determination of an absolute method of charge calibration is even more stringent and necessary in linac facility where different charge monitors designed, realized and calibrated by distinct manufactures – quite often by a third party – are all together integrated in the machine as in the SwissFEL.

At the beginning of the SwissFEL project an agreement was signed between PSI and Bergoz for the realization of a fast Integrating-Current-Transformer (ICT) able to discriminate the 28 ns macro-structure of the SwissFEL beam in the charge range 10-200 pC. The company provided PSI with Turbo-ICT-2 sensors equipped with a factory calibration certification and a native front-end readout electronics. In order to perform a correct integration of the Turbo-ICT with the most general machine environment of the signal control and timing system of SwissFEL, the Turbo-ICT native electronics was interfaced with the standard back-end readout electronics in use at PSI.

Manufacturer company and PSI share a distinct role and action domain in the ICT set-up and operation. The company is responsible for the sensor calibration and front-end readout electronics while PSI is responsible for the back-end readout electronics and operations. Consequently, a clear recognition of the actions for bug-fixing and system improvements as well as every possible intervention of recalibration of a Turbo-ICT or correction of a charge readout discrepancy between different ICTs requires a complex formal procedure with possible local breaks of the machine operations as well as a large investment of beam time and manpower resources.

In order to ensure to PSI an absolute calibration procedure to be applied to all the charge monitors in operation at SwissFEL, the decision to develop in-house an independent charge measurement and calibration method was taken and realized as in the following described.

* gianluca.orlandi@psi.ch

COMMISSIONING OF THE CRYOGENIC CURRENT COMPARATOR (CCC) AT CRYRING*

D. M. Haider[†], A. Reiter, M. Schwickert, T. Sieber, F. Ucar,
GSI Helmholtz Centre for Heavy Ion Research, Darmstadt, Germany
H. De Gersem, N. Marsic, W. F. O. Mueller, TU Darmstadt, Darmstadt, Germany
M. Schmelz, R. Stolz, V. Zakosarenko³, Leibniz IPHT, Jena, Germany
M. Stapelfeld, Friedrich-Schiller-University Jena, Jena, Germany
T. Stoehlker^{1,2}, V. Tympel, Helmholtz Institute Jena, Jena, Germany
¹also at GSI Helmholtz Centre for Heavy Ion Research, Darmstadt, Germany
²also at Institute for Optics and Quantum Electronics, Jena, Germany
³also at Supracon AG, Jena, Germany

Abstract

Accurate non-destructive measurement of the absolute intensity of weak ion beams ($< 1 \mu\text{A}$) in storage rings is often restricted to special beam conditions and, even then, is associated with large uncertainties and tedious calibration procedures. However, experiments with rare ions in particular depend on excellent current resolution. In order to make these beams accessible, the Cryogenic Current Comparator (CCC) monitors deviations of the DC beam current on a scale of nA and compares the signal to a calibrated reference current. At the heavy-ion storage ring CRYRING at GSI a CCC prototype for FAIR was installed and first results of the commissioning are reported here. Preceding the operation with beam, a careful design of the beamline helium cryostat was required to provide the stable cryogenic environment needed for CCC operation. Mechanical and electro-magnetic perturbations that interfere with measurement of the beam's faint magnetic field are suppressed by the internal structure of the system and a superconducting magnetic shield, while the remaining interference can be filtered with adequate signal processing. In this way, a current resolution in the nA range was demonstrated.

INTRODUCTION

In the second half of 2020, a Cryogenic Current Comparator (CCC) was installed at the heavy-ion storage ring CRYRING at GSI to serve as the prototype for a total of up to five CCC installations at FAIR. A CCC monitor consists of a cryogenic system supporting the stable operation of the sensing unit and a CCC detector as developed within the CCC collaboration at the FSU Jena [1] and the Leibniz IPHT [2]. The FAIR prototype consists of a newly manufactured beamline cryostat that has been developed with ILK Dresden[§] at GSI specifically for the needs at FAIR [3]. The particular CCC detector (FAIR-Nb-CCC-XD [1]) that is installed is part of the same design family (CCC-XD) as

*Work supported by AVA – Accelerators Validating Antimatter the EU H2020 Marie-Curie Action No. 721559 and by the BMBF under contract No. 5P18SJR1.

[†]d.haider@gsi.de

[§]ILK Dresden gGmbH, Dresden, Germany

[¶]Model PT415 from Cryomech Inc, Syracuse, NY, USA

[‡]Datasheet, Sylomer SR28, Getzner Spring Solutions GmbH, Germany

the one developed for the use at the Antiproton Decelerator at CERN [4] with extended dimensions to accommodate the FAIR beamlines with a diameter of 150 mm. Both, the cryostat and the CCC detector, were tested separately in a laboratory environment.

Herein, we will introduce the first results of the commissioning of the assembled setup in an accelerator setting. In the following, the configuration of the detector setup at the CRYRING is presented and the effect of the environment on the performance of the CCC is discussed.

BEAMLINE SETUP

The CCC beamline setup (see Fig. 1) is based on a helium bath cryostat with a volume of 80 l, a gas-cooled heat shield with a nominal throughput of 15 l/day and a local cryocooler-based liquefier from Cryomech[¶] with a performance of up to 19.4 l/day. At the moment, the cold operating time is limited to 7 days due to an excessive heat load and an oscillating gas flow to the liquefier. The additional heat input that leads to an increased evaporation rate of 22 l/day is most likely due to the installation of heating foils for the bake-out of the UHV beamline which is surrounded by the cryostat (c.f. Fig. 2). In this area, the cryogenic CCC detector and the heat shield is placed as close to the beamline as possible and the additional material from

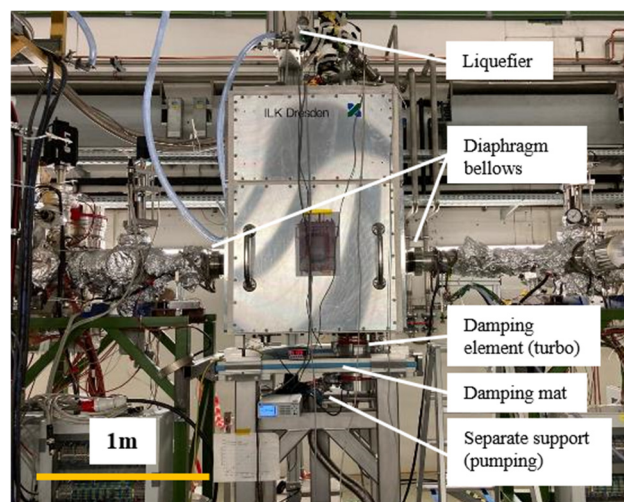


Figure 1: CCC beamline setup at the CRYRING.

LONGITUDINAL IMPEDANCE MEASUREMENTS WITH STREAK CAMERA AT BEPC II ELECTRON STORAGE RING*

D. C. Zhu[†], W. Zhang, Y. F. Sui, J. H. Yue, J. S. Cao, J. Q. Wang
Institute of High Energy Physics, Chinese Academy of Sciences, Beijing, China

Abstract

We measure the bunch length at BEPC II electron storage ring using a dual sweep streak camera at visible light diagnostic beamline. The impedances estimated by a series $R+L$ impedance model. Resistive impedance of $R=446\pm 21 \Omega$ is obtained by measuring loss factor from measured synchronous phase advancing with streak camera. An inductance impedance of $L=23.3\pm 1.8$ nH has been estimated by measuring single bunch lengthening with beam current. Both loss factor and inductance are close to the impedance budget. Besides, the streak camera is also used to measure synchronous phase at low current as RF voltage changing from 0.85 MV to 1.65 MV.

INTRODUCTION

BEPC II is a double-ring e^+e^- collider that operates in the τ and charm region. The energy reached to 2.474 GeV, the highest collision energy by far in Feb. 2021. Beam-based experiments are made to determine the longitudinal impedance. Some parameters are shown in Table 1.

Table 1: Main Parameters of BEPCII

Parameters	Value	unit
Energy	2.474	GeV
Revolution frequency	1.2421	MHz
RF frequency	499.8	MHz
RF voltage	1.65	MV
Momentum compaction factor	0.0189	--
Synchrotron tune	0.02767	--
Energy spread	6.9×10^{-4}	--

LONGITUDINAL IMPEDANCE

The longitudinal broadband coupling impedance of the storage ring can be divided into real and imaginary parts. The real part is a resistance, can be characterized by the loss factor as an energy loss of the bunch. The imaginary part does not cause energy loss, but it leads to energy transfer inside the bunch, and results in bunch lengthening and energy spread growth. We measure the impedance with streak camera, the real part resistance from synchronous phase shift measurement, and the imaginary part from bunch lengthening measurement.

Synchronous Phase Shift

The parasitic energy loss induced by real part resistance is dependent on charge in the bunch as $\Delta E = -k_l q^2$. In

terms of voltage it becomes $\Delta V = -k_l q$ or $\Delta V = -k_l \frac{I_b}{f_0}$, where I_b is the bunch current and f_0 is the revolution frequency. For the reason of energy balance of the bunch, the current-dependence synchronous phase shift $\Delta\varphi_s$ can be derived from the equation as follows:

$$V_0 \cos(\varphi_s) \Delta\varphi_s = k_l \frac{I_b}{f_0} \quad (1)$$

where V_0 is the RF voltage, φ_s is the synchronous phase at zero current. The time shift is:

$$\Delta\tau = \frac{k_l I_b}{\omega_{RF} V_0 \cos(\varphi_s) f_0} \quad (2)$$

Streak camera at BEPC II is OptoScope SC-10 from Optronis. For synchronous phase shift measurement, it works at synchroscan sweep mode with the frequency of 249.9 MHz (1/2 RF frequency). Ten reference bunches are injected in adjacent even buckets with 0.1 mA per bunch and a total current of 1mA. The reference bunches have fixed low intensity so that have long beam lifetime. The main bunch is injected in an odd bucket, its current changes from 0.5 mA to 10 mA with a step of 0.5 mA. Since just synchroscan sweep plate is applied, the image has two profiles in the central part, the left profile is main bunch while the right profile is reference bunch, as in Fig. 1.

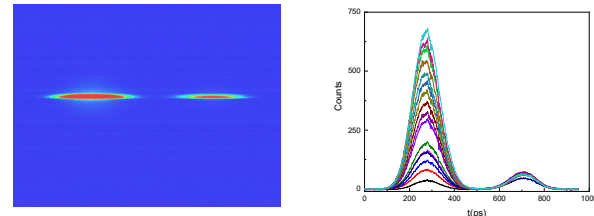


Figure 1. Left: Bunch image captured by streak camera. Right: Bunch profile with main bunch current from 0.5 mA to 10 mA.

The profile data are fitted with asymmetric Gaussian distribution [1, 2]:

$$I(z) = I_0 + I_1 \exp \left\{ -\frac{1}{2} \left(\frac{(z-\bar{z})}{[1+\text{sgn}(z-\bar{z})A]\sigma_z} \right)^2 \right\} \quad (3)$$

I_0 is the initial pedestal, I_1 is the maximum value of the distribution, σ_z the longitudinal rms size, \bar{z} the center of the distribution, and A the asymmetric coefficient.

Time jitter of main bunch profile can be reduced by subtracting the reference bunch profile's center time. By linear fitting the corrected profile center time data with current, the time shift $\Delta\tau = 0.32 \pm 0.02$ ps/mA is obtained, as in Fig. 2. The loss factor is calculated with Eq. (2) as $k_l =$

* email address : zhude@ihep.ac.cn

TIME DOMAIN PHOTON DIAGNOSTICS FOR THE ADVANCED PHOTON SOURCE UPGRADE*

K. P. Wootton[†], W. Cheng, G. Decker, S.-H. Lee, N. S. Sereno, B. X. Yang
Argonne National Laboratory, Lemont, IL 60439, USA

Abstract

With swap-out injection and a third-harmonic bunch lengthening cavity, time domain diagnostics will be beneficial tools for optimisation of the Advanced Photon Source Upgrade electron storage ring. In the present work, we present plans for time-domain X-ray and visible photon diagnostics for the Advanced Photon Source Upgrade. Particular emphasis is given to implementation of visible light streak cameras and X-ray bunch purity monitors as time domain photon diagnostics.

INTRODUCTION

The Advanced Photon Source (APS) storage ring presently provides beams to user X-ray beamlines. The Advanced Photon Source Upgrade (APS-U) project is currently underway to increase the brilliance of photon beams to user beamlines [1–3]. Several user programs take advantage of the pulsed time-of-arrival of X-rays corresponding to the storage ring fill pattern. As these user programs are anticipated to continue during Advanced Photon Source Upgrade (APS-U) operations, we plan to provide temporal photon beam diagnostics for the optimisation and diagnostics of accelerator operations.

In the present work, we motivate time-domain photon diagnostics for the APS-U storage ring. We outline the time distribution of photons for beamlines at APS-U. Proposed techniques for time-domain photon diagnostics are summarised. Finally, we describe the proposed changes to the existing beamline configuration to employ these diagnostics.

FILL PATTERN AND BUNCH PROFILE

Fill patterns of the APS are controlled by the radiofrequency (rf) of the main rf cavities (352 MHz), and the storage ring circumference (1104 m). This accommodates 1296 buckets.

At present, the APS operates three fill patterns for routine user operations. Essentially, these are either bunches equally-spaced, or a camshaft fill ('hybrid mode', $1 + 8 \times 7$), with 1 bunch, and 8 trains of 7 bunches spaced at 2.84 ns [4]. For APS-U operations, a 48-bunch mode and 324-bunch mode are foreseen, with 324 bunches operating in bunch trains with ion-clearing gaps and guard bunches [5]. A camshaft fill pattern is not envisaged for future APS-U operations. These fill patterns and bunch lengths are summarised in Table 1 below.

* Work supported by the U.S. Department of Energy, Office of Science, Office of Basic Energy Sciences, under Contract No. DE-AC02-06CH11357.

[†] kwootton@anl.gov

Table 1: Temporal Structure Corresponding to Fill Patterns of APS and APS-U Storage Rings

Description	Bunch Spacing (ns)	Bunch Length (ps)	Ref.
APS Fill Patterns:			
324 bunches	11.4	25	[6]
24 bunches	153	40	[6]
Hybrid (1, 8×7)	2.84	50, 32	[4]
APS-U Fill Patterns:			
324 bunches	11.4	88	[2]
48 bunches	77	104	[2]

So for APS-U, the proposed bunch lengths to be measured are of the order ~ 100 ps, with a minimum bunch spacing of 11.4 ns. We propose to use bunch length measurements sensitive on the picosecond time scale [7].

TIME DOMAIN PHOTON DIAGNOSTICS

At present, the APS operates temporal diagnostics at the 35-BM bending magnet diagnostic beamline [8–11]. Specifically, this includes bunch length measurement and bunch purity monitoring. These two temporal diagnostics are outlined below.

Bunch Length Measurement

For the existing APS, the bunch lengths can be reasonably approximated as Gaussian in profile. However, for bunches in the future APS-U storage ring, the operation of the higher harmonic cavity to lengthen the bunch results in a bunch distribution that potentially departs significantly from a Gaussian approximation [12]. This motivates experimental techniques to measure the bunch temporal profile without assumption about the bunch shape.

For APS-U, bunch length measurements will be performed using a visible light streak camera [13]. Visible light streak cameras have been employed as a bunch length diagnostic at APS since its commissioning [14–18]. Synchronising the vertical (fast) sweep with the storage ring rf ('synchroscan') has been usefully employed in studies of longitudinal dynamics in the storage ring [19–23]. The streak camera can be synchronised with the third subharmonic of the storage ring main rf frequency (117 MHz), derived from the APS-U timing and synchronisation system [24].

Bunch Purity Monitor

Ensuring bunch purity in the fill pattern is essential to the operation of some user X-ray experiments at APS. At the

TERAHERTZ DIAGNOSTIC FOR THE ADVANCED PHOTON SOURCE PARTICLE ACCUMULATOR RING*

K. P. Wootton[†], W. J. Berg, S.-H. Lee, N. S. Sereno, J. L. Steinmann¹

Argonne National Laboratory, Lemont, IL 60439, USA

¹also at Karlsruhe Institute of Technology, Karlsruhe, Germany

Abstract

Electron beam microbunching instabilities can present operational limits on the practical operation of storage ring accelerators. In the present work, we outline components of a synchrotron radiation diagnostic beamline for the Advanced Photon Source Particle Accumulator Ring operating at frequencies up to approximately 1 THz.

INTRODUCTION

The Particle Accumulator Ring (PAR) is an electron storage ring at the Advanced Photon Source (APS). The principal function of the ring is an accumulator ring, damping multiple (<30) injections from the linac into a single bunch [1]. For the Advanced Photon Source Upgrade (APS-U), we require accumulation of charge in a single bunch up to 20 nC [2]. At such high charges, measurement and control of electron beam instabilities may be important [3].

The intensity of coherent synchrotron radiation (CSR) is dependent on the longitudinal bunch profile. Observation of CSR can provide a sensitive diagnostic tool to detect instabilities. We propose an extension of the optical synchrotron radiation diagnostics port to support the detection of long wavelengths of incoherent synchrotron radiation (ISR) and CSR in the terahertz range, without installing a new beam port and without disturbing existing optical synchrotron radiation diagnostics.

In the present work, we outline the design of the PAR terahertz diagnostic beamline. Performance requirements of the beamline are outlined. The operating principles of the proposed instruments are summarised. Implementation of the beamline subsystems is outlined.

THEORY

We have chosen a spatial separation of the terahertz and optical frequencies because of the different opening angles of synchrotron radiation. For bending magnet radiation, an approximation to the vertical opening angle Θ_{vert} is [4]:

$$\Theta_{\text{vert}} = 1.66188 \times \left(\frac{c}{fR} \right)^{(1/3)} \text{ [rad]}, \quad (1)$$

where c is the speed of light in vacuum, f is the frequency of synchrotron radiation (much less than the frequency corre-

sponding to the critical photon energy), and R is the bending radius.

The waveguide cutoff frequency of a rectangular chamber describes the frequency limit for waves that can propagate in the beam pipe: whether or not they are directly emitted by the bunch. The low-frequency cutoff is limited by the cutoff frequency of the synchrotron light monitor port acting as a waveguide. For a waveguide with rectangular profile, the cutoff frequency f_c is defined as:

$$f_c = \frac{c}{2a}, \quad (2)$$

where a is the larger dimension of the waveguide. The bending magnet vacuum chamber defines the input aperture to the beamline, and is rectangular in profile. For a waveguide of dimension 100×40 mm [5], the low-frequency cutoff frequency is 3 GHz.

Rather than synchrotron radiation, waves propagating at frequencies above cutoff could be wakefields from the beam pipe, cavities, or other components. This can distort the measurement at lower frequencies. Hence, we must also consider the formation length of the (bending magnet) synchrotron radiation which is at significantly higher frequency. A cutoff frequency f_{cutoff} incorporating the formation length of synchrotron radiation is given by [6–9]:

$$f_{\text{cutoff}} = \sqrt{\frac{\pi}{6}} c \sqrt{\frac{R}{h_c^3}}, \quad (3)$$

where h_c is the chamber gap height. For a bending radius of $R = 1$ m, and chamber gap height of $h_c = 0.04$ m, $f_{\text{cutoff}} = 27$ GHz. The detector should therefore be sensitive at frequency ranges higher than 27 GHz. The high frequency limit is bound by the length scale of longitudinal bunch substructure that may produce CSR (extending up to a few hundred GHz).

The longitudinal impedance due to synchrotron radiation for the PAR at an electron beam energy of 470 MeV is illustrated in Fig. 1 [5]. Additionally, the minimum focus point size is reduced at higher frequencies. A good compromise seems to be 100 GHz to approximately centre on this frequency range, and where the focus point size matches the detector acceptance.

A problem is that the timescale of electron bunch instability substructures in the PAR is undetermined. Simulations have been performed of the longitudinal impedance due to the PAR vacuum components [10], and there are also measurements of the loss factor [11]. We suspect that the bunch may be far above the microbunching instability threshold, with potentially <10 ps substructures.

* Work supported by the U.S. Department of Energy, Office of Science, Office of Basic Energy Sciences, under Contract No. DE-AC02-06CH11357. Partial support of J.L.S. by “Matter and Technologies” of Helmholtz Association.

[†] kwootton@anl.gov

SCHOTTKY SIGNAL FROM DISTRIBUTED ORBIT PICK-UPS

O. Marquversen[†], Steen Jensen, CERN-SY-BI, Geneve, Switzerland

Abstract

In the CERN Extra Low ENergy Anti-proton (ELENA) ring, intended for the deceleration of antiprotons, the longitudinal Schottky signal is obtained by summing the multiple electrostatic pick-up (PU) signals that are also used to measure the closed orbit. The signals from the individual PUs are phase-compensated to a single, common longitudinal location in the machine and added in the time domain. In this contribution, the related theoretical phase compensation is calculated and compared to measurements. We show how the cross correlation between the Schottky noise from the individual PUs can be used to find the correct phase-compensation for an optimal signal-to-noise ratio (SNR). This improvement in terms of SNR is, as expected, proportional to the square root of the number of PUs. The capability of the system to measure both, the bunched and the un-bunched low intensity ($\sim 3 \cdot 10^7$ H⁻ @ 100 keV / 144 kHz) beams is confirmed by the experimental results presented. Furthermore, the inter-bunch phase correlation is briefly addressed and, for the case of bunched beams, the Schottky signal levels once down converted to different harmonics of the revolution frequency (f_{rev}) are presented. In applications where the coherent beam signal dominates the spectrum and limits the dynamic range of the signal processing system, a down-conversion to a non-integer multiple of the RF harmonic is proposed as a way to reduce the coherent signal level.

THE MEASUREMENT SYSTEM

The digital part of the CERN ELENA orbit measurement system is implemented on in-house designed VME Bus Switched Serial - Digital Signal Processor – Field Programmable Gate Array Mezzanine Card (VXS-DSP-FMC) carrier boards, carrying FPGAs, FMCs and DSPs with the possibility to transmit data between them via the VXS bus [1]. The key features of the VXS-DSP-FMC carrier, used in this extension of the ELENA orbit system [2], is the possibility to synchronize local oscillators across cards for all down-converters and pass real-time data between DSPs.

The orbit system already uses the sum and the delta signals from all PUs, as these analog signals are connected to inputs of the ADCs. To extract the longitudinal Schottky signal only the sum signals are used. Each PU sum signal is individually down-converted by a configurable harmonic of the revolution frequency. In ELENA, the Schottky system functionality is typically used for un-bunched beam, whereas the orbit system functionality is used for bunched beam. Using the same down-mixers, the two functions can operate on different harmonics while sharing the same hardware in a time-multiplexed fashion or operate simultaneously if using the same harmonic. The

relative phase difference between the individual local oscillators (LOs) used in the down-converters must be kept minimal for a successful phase compensation, otherwise it would introduce an unwanted phase shift between the various down-converted signals. The zero phase between LOs is obtained by a simultaneous reset of the phase accumulators in the Direct Digital Synthesis (DDS) used as local oscillators.

The expected bandwidth of the longitudinal Schottky signal in ELENA depends on the beam energy and the cooling status and is 50 Hz – 200 Hz times the chosen Schottky harmonic. The sampling time, and hereby the bin width of the resulting Fast Fourier Transformation (FFT), can be chosen from 20 ms to 650 ms per spectrum, resulting in a bin width range of 48 Hz to 1.5 Hz. Up to a total of 128 spectra can be sampled on one or two energy levels during the ELENA cycle where beam cooling is performed.

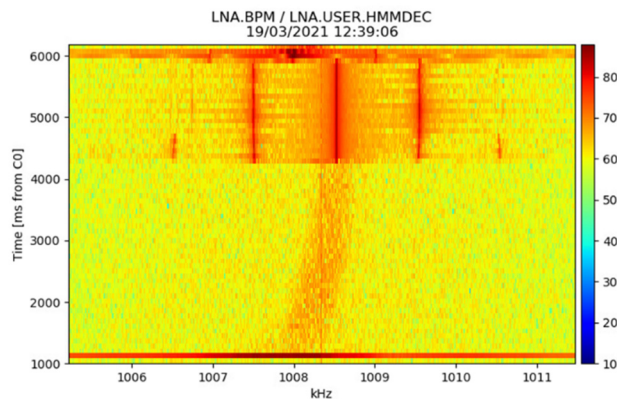


Figure 1: The measurement shows longitudinal Schottky in ELENA [3] as a function of time i.e. for both un-bunched and bunched beam.

The measurement shown in Fig. 1 is performed, on a flat 100 keV energy level in the ELENA deceleration cycle, using the phase compensating technique i.e. phase-compensating and adding 16 PUs down-converted from the 7th harmonic of the revolution frequency, with $f_{RF} = 4 f_{rev}$ in the bunched part. The beam is injected at approximately 1080 ms relative to machine cycle start (C0), it is then debunched, slightly changed in energy using the electron cooler and re-bunched at approx. 4250 ms.

LONGITUDINAL SCHOTTKY SIGNALS

A single particle circulating in an accelerator will, on a sum PU, generate a series of Dirac pulses spaced in time by the revolution time τ_{rev} , i.e. a Dirac comb. The Fourier series of this signal is given by:

$$s(t) = \frac{1}{\tau_{rev}} \sum_{n=-\infty}^{\infty} e^{j \cdot n 2\pi \frac{t}{\tau_{rev}}} \quad (1)$$

For beam diagnostics purposes typically, a particular harmonic is selected for the Schottky signal observation. The

[†] Ole.Marquversen@cern.ch.

TWO COLOR BALANCED OPTICAL CROSS CORRELATOR TO SYNCHRONIZE DISTRIBUTED LASERS FOR SHINE PROJECT*

Chunlei Li, Lie Feng, Jinguo Wang, Wenyan Zhang, Xingtao Wang, Bo Liu†
 Shanghai Advanced Research Institute, Chinese Academy of Science, Shanghai, China

Abstract

The planned Shanghai high repetition rate XFEL and extreme light facility (SHINE) generate X-ray light pulses in femtosecond range. For photoinjector drive laser, seed laser, and time resolved pump-probe experiments it is crucial to synchronize various slave laser oscillator to the master reference laser with a long term stability of better than 10 fs. For this purpose two color balanced optical cross correlator for locking slave laser to master laser is under developing.

In this paper, we report on the progress of the development of a background free two color balanced cross correlator (TCBOC) to synchronize 800 nm slave laser to 1550 nm master laser. The synchronization system is being tested by linking a commercial Ti:sapphire oscillator to a locally installed timing reference source.

INTRODUCTION

At present, FELs are the only facilities that can generate bright, coherent hard X-ray pulse with temporal durations below 100 fs and up to 10^{13} photon per pulse [1]. High precision timing synchronization systems are critical for FELs because X-ray temporal duration is highly sensitive to the overall synchronization between the injector laser, the Linacs, and the bunch compressors. Moreover, for the seeded FELs, timing jitter between the seed laser and the electron bunch must be minimized. Finally, the relative timing jitter between the FEL output and the pump laser must be controlled with a precision better than the FEL pulse duration for pump probe experiments aiming high temporal resolution [2].

The optical synchronization system for SXFEL and under consideration for the SHINE is based on an ultra-stable mode locked master laser locked to a low noise RF oscillator generating hundreds of fs light pulse of 1550 nm. The master laser is phase locked to the low noise RF master oscillator of the accelerator to ensure stable operation and small jitter. The timing information is contained in the precise repetition frequency of 238 MHz of the pulse train and distributed via actively length stabilized fiber links to remote locations.

Recently, one scheme has been demonstrated that pulsed-optical timing stability distribution system using polarization maintaining fibers can deliver sub femtosecond timing stability over kilometer-scale distances [2]. One of the key components of the synchronization system is the two color balanced cross correlator (TCBOC) which provides a method to lock slave laser systems to the timing reference with less than 10 fs accuracy [3]. This balanced

optical cross correlation scheme was firstly suggested by Franz X. Kärtner group to perform pure timing measurements in the optical domain [4], and have been developed to achieve sub femtosecond precision [5-7].

PRINCIPLE OF TWO COLOR BALANCED CROSS CORRELATOR

FH: Fundamental harmonics of input pulses; DM: Dichroic mirror; HM: high reflective mirror; GVD: Silica slab for group velocity delay. V1 and V2: output voltage from photodetector.

The principle of two color balanced cross correlator is shown in Fig. 1. Two optical pulses with different central wavelength are input to a BBO crystal in a forward pass and reverse pass configuration, where one pulse is from the master laser and the other pulse is from slave laser. A third light pulse of their sum frequency will be created when they overlap spatially and temporally. As they propagate through the BBO crystal, they walk through each other due to different group velocity. Therefore, different amount of sum frequency light is generated depending on their temporal overlap in the forward and reverse pass. The generated sum frequency pulses are separated from input pulses by dichroic mirror and measured by two identical channels of a balanced photodetector. Therefore, the difference of the sum frequency pulse cancels the intensity fluctuations of input pulses, and the generated voltage signal is only proportional to the time separation of input pulses. Base on this principle, one can detect timing fluctuations significantly smaller than the pulse duration itself. Another advantage it that this method is immune to temperature variations due to the timing detection is performed directly in the optical domain.

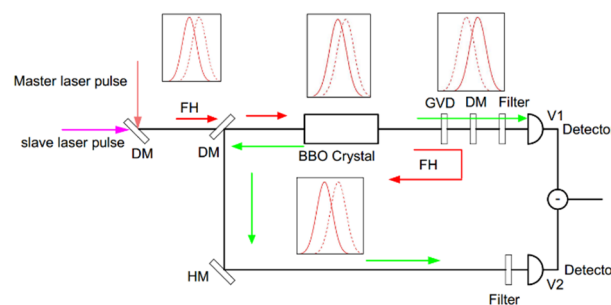


Figure 1: Principle of timing detection using TCBOC.

Supposing two Gaussian-shaped input pulses with their intensities $I_1(t)$ and $I_2(t)$, the intensity of generated sum frequency light is expressed by the convolution of the two input pulses:

$$I_{sum}(t) \propto \int_{-\infty}^{\infty} I_1(\tau) I_2(t - \tau) d\tau \quad (1)$$

* Work supported by Shanghai Municipal Science and Technology Major Project (Grant No. 2017SHZDZX02)

† email address liubo@zjlab.org.cn

OBSERVATION AND ANALYSIS OF ISLAND PHENOMENON IN THE STORAGE RING LIGHT SOURCE*

Yunkun Zhao, Sanshuang Jin, Jigang Wang[†], Baogen Sun[‡], Fangfang Wu, Tianyu Zhou, Ping Lu, Leilei Tang,
National Synchrotron Radiation Laboratory (NSRL),
University of Science and Technology of China (USTC), Hefei, China

Abstract

In the previous experimental investigations and measurements using the radio-frequency (RF) phase modulation method to study the longitudinal beam characteristics of the Hefei Light Source-II (HLS-II), we found that the longitudinal bunch distributions under different modulation frequencies and amplitudes have great difference. In order to further explore island phenomenon and better understand beam motion associated with external RF phase modulation, the streak camera is exploited to effectively observe the longitudinal bunch profile and distribution in single-bunch filling mode. In addition, the dependence between island size, bunch dilution effect and modulation frequency are also discussed in detail. This is meaningful for researching the impact of RF noise on longitudinal beam dynamics, beam manipulation, and machine maintenance and debugging.

INTRODUCTION

In accelerators, the investigation of the nonlinear longitudinal beam dynamics [1, 2] is of great physical significance and engineering value. This is particularly important for studying and exploring the mechanism of beam instability, analysis of beam evolution, observation of longitudinal bunch characteristics, and beam manipulation. In the actual operation of accelerators and synchrotron radiation light sources, particle motion is generally disturbed by RF noise, wakefields, power supply ripple, vibration, etc. There is no doubt that these disturbances will cause changes in beam motion and machine performance due to RF phase and voltage modulations. A part of the theoretical analysis and experimental measurements have been demonstrated that this RF modulation has significant advantages as that of suppressing the coupled bunch instability, improving the beam lifetime, and performing beam manipulation in phase space. Therefore, the RF phase modulation (RFPM) technique was preferred introduced into the HLS-II storage ring to deeply research longitudinal beam characteristics and effectively improve beam lifetime in recent research work [3, 4]. However, it is a pity that the exploration of the nonlinear longitudinal beam dynamics is not comprehensive and ambiguous in the presence of the RFPM error noise. Moreover, some clerical

errors need to be corrected in reference [3]. As a consequence, the motivation of this article is to further investigate the nonlinear beam dynamics in HLS-II based on the RFPM approach. The main research contents include the observation of resonance island phenomenon, characterization of island size, and study of transient beam response.

THEORETICAL MODELLING AND ANALYSIS

In the synchrotron radiation light sources, when charged particles are suffered from RFPM, the effective parametric resonance Hamiltonian equation can be expressed as [1, 2]

$$H(\delta, \phi) = \frac{\omega_s \delta^2}{2} + \omega_s \tan \phi_{s0} [\sin \phi \cos (a_m \sin \omega_m t) + \cos \phi \sin (a_m \sin \omega_m t)] - \omega_s \cos \phi \cos (a_m \sin \omega_m t) + \omega_s \sin \phi \sin (a_m \sin \omega_m t) - \omega_s \sin \phi \tan \phi_{s0} \quad (1)$$

In Eq. (1), ω_s denotes the synchronous oscillation angular frequency with $\omega_s = 2\pi f_s$, in which f_s denotes the synchrotron oscillation frequency. It is noted that ϕ_{s0} is determined by the synchrotron phase ϕ_s , namely equivalent to $\phi_{s0} = \pi - \phi_s$. a_m indicates the modulation amplitude, and ω_m indicates the angular frequency of RFPM that is satisfied with $\omega_m = 2\pi f_m$ where f_m is the modulation frequency. δ and ϕ are the energy deviation and the phase, respectively.

In the case that the RFPM frequency is close to the synchrotron frequency, for which the violent first-order parametric resonance can be produced at this time. After through coordinate transformation (J, ψ) and a series of simplifications and ignoring non-parametric resonance terms, the time-averaged Hamiltonian can be described by [5]

$$\langle H \rangle_t = (\omega_s - \omega_m) J - \frac{\omega_s J^2}{16} - \frac{\omega_s a_m}{2} (2J)^{\frac{1}{2}} \cos \psi \quad (2)$$

By introducing the feature function g , the solution of the above Eq. (2) can be written as

$$\begin{cases} g_1(x) = -\frac{8}{\sqrt{3}} \sqrt{x} \cos \frac{\pi x}{3}, & (\text{SFP}, \psi = \pi) \\ g_2(x) = \frac{8}{\sqrt{3}} \sqrt{x} \cos \left(\frac{\pi}{3} + \frac{\pi x}{3} \right), & (\text{SFP}, \psi = 0) \\ g_3(x) = \frac{8}{\sqrt{3}} \sqrt{x} \cos \left(\frac{\pi}{3} - \frac{\pi x}{3} \right), & (\text{UFP}, \psi = 0) \end{cases} \quad (3)$$

* Work supported by the National Natural Science Foundation of China under Grant 12075236, Grant 12005223, Grant 51627901, and Grant 11705203, the Anhui Provincial Natural Science Foundation under Grant 1808085QA24, and the Fundamental Research Funds for the Central Universities under Grant WK2310000080.

[†] wangjg@ustc.edu.cn

[‡] bgsun@ustc.edu.cn

DESIGN AND SIMULATION OF THE COUPLING STRUCTURE FOR SINGLE RESONANT CAVITY BUNCH LENGTH MONITOR*

Huanxiang Tuo, Qing Luo, Fangfang Wu, Tianyu Zhou, Ping Lu, Baogen Sun[†]
National Synchrotron Radiation Laboratory (NSRL),
University of Science and Technology of China (USTC), Hefei, China

Abstract

The measurement of the bunch length can better realize the monitoring of the beam, because the bunch length is one of the important longitudinal parameters of the beam. In this paper, a new single-cavity bunch length monitor is proposed, whose coupling structures consist of two kinds of filters. One is a low pass filter, the other is a band pass filter. The coaxial low-pass filter is used to couple out low-frequency signals, and the band-pass filter is used to couple higher-frequency signals. According to the beam characteristics of the National Synchrotron Radiation Laboratory (NSRL) based on the tunable infrared laser energy chemistry research large-scale experimental device (FELiChEM), we perform simulation in CST. The simulation results show that the monitor can measure the bunch length of the FELiChEM device very well, and the simulation measurement error is less than 2%.

INTRODUCTION

FELiChEM is a large-scale experimental device built by the National Synchrotron Radiation Laboratory of the University of Science and Technology of China. The device has high pulse intensity, continuously adjustable wavelength, and the bunch length is on the order of ps [1]. The bunch length monitor based on the resonant cavity is a non-intercepting measurement and has little effect on beam. Therefore, this measurement method is suitable for measuring the bunch length of FELiChEM. When the beam moves from the beam tube through the resonant cavity, several characteristic modes will be excited in the cavity [2–4]. We extract the desired electromagnetic field, and then process it electronically to get the bunch length information. Compared to conventional double-cavity bunch length monitor, the single-cavity bunch length monitor more compact [5]. In this paper, we designed a single-cavity beam bunch length monitor and its coupling structure based on the beam current parameters of FELiChEM.

THEORETICAL ANALYSIS

In the resonant cavity, for the Gaussian distributed beam, the Fourier expansion is performed, and the n -th harmonic amplitude is obtained [6] as shown in Eq. (1).

* Work supported by the National Key Research and Development Program-X-ray free electron laser principle and key technology research Grant 2016YFA0401900, and Grant 2016YFA0401903, the Natural Science Foundation Grant 12075236.

[†] bgsun@ustc.edu.cn

$$I_n = 2I_0 \exp\left(-\frac{n^2\omega_0^2\sigma_\tau^2}{2}\right) \quad (1)$$

In Eq. (1), I_0 denotes the beam fundamental wave amplitude. ω_0 represents the fundamental angular frequency. n denotes the harmonic order and σ_τ is the bunch length.

According to Eq. (1), we can get Eq. (2).

$$V_n = I_n \times Z_n = 2I_0 \exp\left(-\frac{n^2\omega_0^2\sigma_\tau^2}{2}\right) \times Z_n \quad (2)$$

Where V_n represents the voltage value obtained by harmonic detection, and Z_n is the shunt impedance of the cavity that can be obtained through actual measurement.

Let $\omega_1 = n_1\omega_0$, $\omega_2 = n_2\omega_0$, then

$$\begin{cases} V_1 = I_1 \times Z_1 = 2I_0 \exp\left(-\frac{\omega_1^2\sigma_\tau^2}{2}\right) \times Z_1 \\ V_2 = I_2 \times Z_2 = 2I_0 \exp\left(-\frac{\omega_2^2\sigma_\tau^2}{2}\right) \times Z_2 \end{cases} \quad (3)$$

where ω_1 and ω_2 are the angular frequencies of multiple harmonics, and V_1 and V_2 are the corresponding measured harmonic voltage values respectively.

The above term in Eq. (3) is divided by the following term to get Eq. (4).

$$\frac{V_1}{V_2} = \frac{Z_1}{Z_2} \exp\left[\frac{(\omega_2^2 - \omega_1^2)\sigma_\tau^2}{2}\right] \quad (4)$$

Let $K = \frac{Z_2}{Z_1}$, which can be obtained by actual measurement, then

$$\exp\left[\frac{(\omega_2^2 - \omega_1^2)\sigma_\tau^2}{2}\right] = K \frac{V_1}{V_2} \quad (5)$$

$$\sigma_\tau = \sqrt{\frac{2}{(\omega_2^2 - \omega_1^2)} \ln\left(K \frac{V_1}{V_2}\right)} \quad (6)$$

It can be seen from Eq. (6) that is necessary to measure the harmonic voltage values of two different frequency modes to obtain the bunch length.

The beam current parameters of FELiChEM are shown in Table 1. According to Table 1, the designed single-cylindrical resonant cavity needs to resonantly output an electromagnetic field with a multiple frequency mode of 0.476 GHz. Equation (7) represents the resonant frequency formulas of cylindrical resonators [7].

$$\begin{cases} f = \frac{c}{2} \sqrt{\left(\frac{p}{l}\right)^2 + \left(\frac{v_{nm}}{\pi r}\right)^2}, & (TM) \\ f = \frac{c}{2} \sqrt{\left(\frac{p}{l}\right)^2 + \left(\frac{\mu_{mn}}{\pi r}\right)^2}, & (TE) \end{cases} \quad (7)$$

FEMTOSECOND FIBER LINK STABILIZATION TO TIMING SYNCHRONIZATION SYSTEM FOR SHINE PROJECT*

Lie Feng, Jinguo Wang, Chunlei Li, Wenyan Zhang, Xingtao Wang, Bo Liu†
Shanghai Advanced Research Institute, Chinese Academy of Science, Shanghai, China

Abstract

The under-construction Shanghai high repetition rate XFEL and Extreme light facility (SHINE) project has a high precision requirement for the timing synchronization system on femtosecond timescale over more than 3-km long optical fiber links, therefore, an ultra-low noise reference signals from the optical master oscillator (OMO) transmission is play an important role. For this purpose, a fiber link stabilization units based on balanced optical cross-correlators to stable the long-distance fiber link is under developing.

In this paper, the latest progress of the fiber link stabilization experiment and measured results for the performance will be reported.

INTRODUCTION

FELs facilities can generate bright, coherent X-ray pulses with temporal duration below 100 fs and up to 10^{13} photon per pulse [1]. Such high brightness and ultra-short pulses light source facilities put forward higher requirements for the accuracy of timing synchronization system. The traditional RF method cannot meet the XFEL's femtosecond precision synchronization requirements on femtosecond timescale. According to the timing synchronization schemes of several major FELs facilities under operation all over the world, such as FLASH, the European XFEL, and FERMI FEL [2-5], we have conducted research on femtosecond synchronization system as is shown in Fig. 1. For such a timing system, it is essential to stabilize the long-distance fiber link to provide the drift and jitter-free reference pulsed optical signals to multiple terminals, including photo-injector laser, seed laser, RF system, user experiment stations, bunch arrival time monitors and so on.

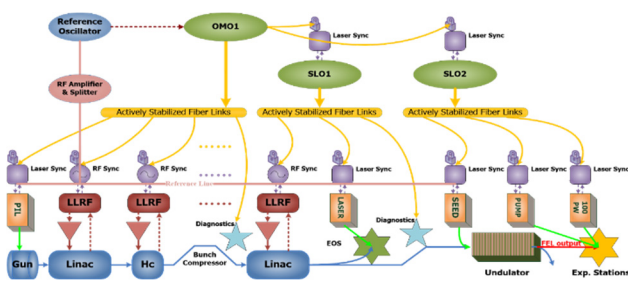


Figure 1: Schematic of typical femtosecond synchronization system.

* Work supported by Shanghai Municipal Science and Technology Major Project (Grant No. 2017SHZDZX02)

† Email address liubo@zjlab.org.cn

Fiber link stabilization system based on a mode-locked fiber laser (OMO), which locked on a RF master oscillator (RMO), using the a phase detector called balanced optical cross-correlators (BOC) due to its attosecond timing resolution, long-term stability, amplitude invariance and robustness against environmental fluctuations.

PRINCIPLE OF FIBER LINK STABILAZAION

BOCs is a highly sensitive method to measure timing fluctuations between optical pulses and it can be also employed to detect time of flight fluctuations of pulses circulating in a fiber link [5]. Figure 2 shows the timing detection principle of BOC, the relative timing of both input optical pulse is to be measured by the double-pass configuration. BOC is based on the second-harmonic generation (SHG) between two orthogonal polarizations pulses in a non-linear crystal PPKTP [6, 7]. The forward two pulses with a time delay Δt transmitted through the dichroic mirror (DBS1), overlap in the crystal and generate the SH1. The residue fundamental pulse is reflected by the DBS2, and backward into the crystal second time, generate another second harmonic signal SH2. A balanced photodetector receives the both SHG signals separately, and the output indicates the time delay of both input pulses.

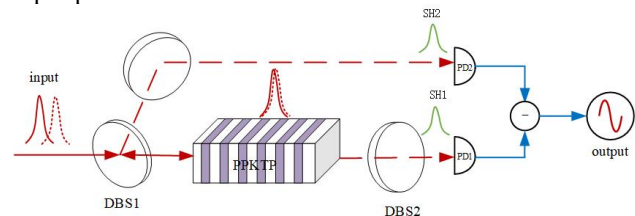


Figure 2: Principle of BOC.

Figure 3 illustrates the operation principle of fiber link stabilization using a BOC. Since the mode-locked laser can provide ultra-low noise optical and microwave signals in the form of optical pulse trains, it has great advantage as the optical master oscillator (OMO) for the high precision timing synchronization system.

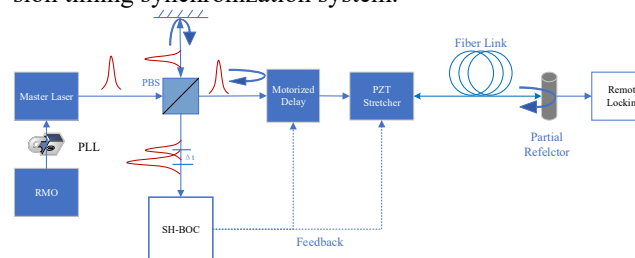


Figure 3: Operation principle of fiber link stabilization.

DEVELOPMENT OF AN ON-LINE BUNCH LENGTH MONITORING SYSTEM AT PLS-II USING AN ULTRAFAST PHOTODIODE

W. Song, Pohang University of Science and Technology, Pohang, Korea

G. Hahn[†], D. Kim, Y. Joo, Y. Lee and T. Ha, Pohang Accelerator Laboratory, Pohang, Korea

J. Hwang, Helmholtz-Zentrum Berlin, Berlin, Germany

Abstract

Users of time-resolving experiments at 3rd generation synchrotron light sources deem online bunch length and filling pattern monitoring as an important real-time diagnostic. We developed an on-line monitoring system that can measure bunch lengths and filling pattern using a photodiode, a wideband pre-amplifier, and a sampling digitizer. Two different methods were evaluated to reconstruct the bunch lengths: Gaussian deconvolution method as an approximation scheme and Fourier analysis as a method to restore the original signal by using the power transmission characteristics of the electronic devices in the system, including a bias-tee, a wide band amplifier and cables, as well as the photodiode. A bunch lengthening experiment has been conducted to compare and verify the results of those two methods of the photodiode and the result of the streak camera images by changing the overall gap voltage of the superconducting RF cavities. In this paper, we elaborate upon the said photodiode-based measurement techniques, and present the experimental results.

INTRODUCTION

Pohang Light Source (PLS-II) is a 3rd generation light source and is designed to form a bunch train with 470 RF buckets placed 2 ns apart in a synchrotron of 281.82 m (accelerated RF frequency of 500 MHz, harmonic number of 470). Since 2019, to support time-resolving experiments, PLS-II has applied filling-pattern profiling to operation by selectively injecting electron beams into each bucket to control the amount of charge for each bunch. The 1B diagnostic beamline uses a streak camera to observe longitudinal properties of the beam, such as electron beam filling pattern and bunch length. The streak camera has a high temporal resolution and sensitivity, and so is appropriate for fine longitudinal beam measurements; however, it can only manually monitor specific events due to its incapability of making continuous measurements.

Filling pattern measurement mainly uses a beam position monitor (BPM). However, BPM has low resolution, and the signal sum value from 4 pickups makes signal analysis difficult. To solve this problem, at the 2008 Australian Synchrotron, D. J. Peake measured the filling pattern using a photodiode [1]. During normal operation (250~400 mA) of the PLS-II storage ring, the average RMS bunch length is about 19~21 ps. A high-speed readout system is required to measure the single bunch length. Therefore, we built and tested a diagnostic device that continuously measures bunch length and filling pattern information using an ultrafast MSM (Metal-Silicon-Metal) photodiode.

[†] garam@postech.ac.kr

EXPERIMENTAL SETUP

The simple schematic diagram in Fig.1 (a) presents the filling pattern and bunch length monitoring system with the photodiode. An MSM photodiode (Hamamatsu G4176-03) with a rise time of 30 ps always observes the radiation produced by the bunch train. The optical signal is converted to an electric signal by the photodiode and passes through the Picosecond 5541A 26 GHz bandwidth bias tee and a wide bandwidth amplifier (Mini-Circuits ZX60-14012L) to amplify the low photocurrent. A Pico Technology Picoscope 9404-16, a sampling digitizer, was used as the readout device. Picoscope 9404-16 has a maximum 2.5 TS/s random sampling and 500 MS/s real-time sampling, and 16 GHz analog input bandwidth is suitable for filling pattern and bunch length measurement.

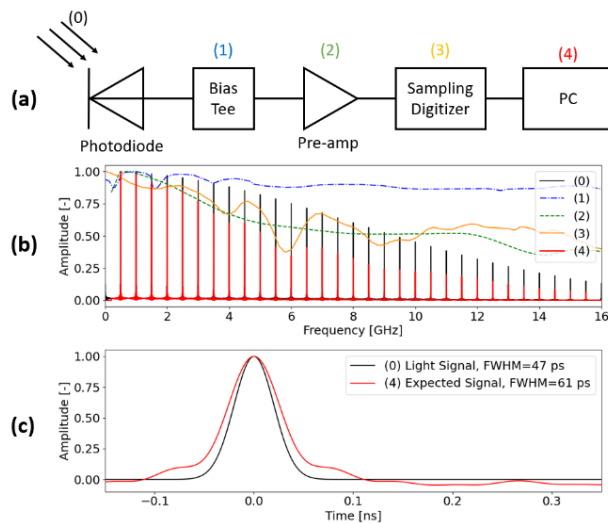


Figure 1: Experimental configuration and signal flow. Synchrotron radiation(0) is incident on the photodiode. The signal passed through the bias tee(1) and amplifier(2) is sampled by the sampling digitizer(3) then, the signal measured by the PC(4) is read. (b) When a Gaussian signal (0) with a standard deviation of 20 ps is input, the spectrum of the signal in (0), (4) and the gain of (1), (2), (3) electronics. (c) The original signal is distorted as it passes through the electronics.

ANALYSIS METHOD

Single bunch length is about 20 ps, and when converted to a frequency band, the bandwidth (-3 dB) is about 10 GHz. The high frequency broadband signal is difficult to accurately measure bunch length because the bandwidth and time constant of electronics are distorting the original

BROADBAND CHARACTERIZATION OF A COMPACT ZERO-BIAS SCHOTTKY DIODE DETECTOR WITH A CONTINUOUS WAVE THz SYSTEM*

R. Yadav^{†,1}, S. Preu, Terahertz Devices and Systems, TU Darmstadt, Darmstadt, Germany
A. Penirschke, High Frequency Tech., Mittelhessen Univ. of Applied Sciences, Friedberg, Germany
¹also at High Frequency Tech., Mittelhessen Univ. of Applied Sciences, Friedberg, Germany

Abstract

Over the last few decades several types of Terahertz (THz) detectors have been developed to maturity, paving the way for various potential applications such as diagnostics of THz generation at particle accelerators. An important class are zero-biased Schottky diode THz detectors that are frequently applied at accelerator facilities for operation at room temperature. Zero-biased Schottky diode THz detectors are having lower noise compared to biased ones due to the absence of shot noise. Here we demonstrate the sensitivity of Schottky detectors using a commercial continuous wave photomixing THz system as source. Both, a commercially available as well as a research-grade compact quasi-optical detector with improved video bandwidth are compared from 0.05 to 1.2 THz in terms of sensitivity. At 1 THz, the research grade quasi optical detector shows 7 dB higher dynamic range than the commercial one.

INTRODUCTION

Terahertz (THz) radiation generated either from Free Electron Lasers (FELs) or by Coherent Synchrotron Radiation (CSR) sources with high brilliance and power open doors for research and applications (low and high power) in THz domain [1]. Ultra-short pulses with picosecond length are available at several FELs have higher power compared to other table top THz sources and provide the opportunity for characterizing targets at atomic scale and beyond [2, 3]. Optical pump-probe THz (or vice versa) experiments are frequently applied to study matter and materials. These experiments are affected from time jitter as there is no natural phase locking, so that electro-optical sampling is not optimized to use in such cases. This means direct detectors have to be used. For studying the transient behavior, however, the detectors have to be sufficiently fast, with a time constant of the order of a few ps at least. Bolometers and hot-electron detectors [4] are not suitable for such studies. Also, Bolometers need to operate at cryogenic conditions which make the whole setup big, bulky and expensive. Schottky diode- [5, 6] and Field Effect Transistors (FETs)-based [2, 3] are handy, easy to use, plug-play and less expensive operating costs compared to their cryogenic counterparts with reported time constants in the range of 6-20 ps [3, 5].

* We are grateful to the Hesse ministry of science and culture (HMWK) for funding the position of Mr. Rahul Yadav. Thankful to ACST GmbH for providing the Schottky diode and commercial detector.

[†] yadav@imp.tu-darmstadt.de

Continuous wave (CW) sources are such as FEL, photomixers and p-i-n diode can be used as THz sources [7] for various experiments such as spectroscopy, medical imaging, communication etc. The available Schottky diodes and FETs THz detectors can be used for these applications. Schottky diodes can rectified the signal upto the cut-off frequencies, while FETs can be used far beyond their cut-off frequencies in higher THz domain. Both are faster and sensitive compared to other counterparts available to the date. In this work, we characterize the zero-bias Schottky diode detectors: Both commercial available and modified research graded [5, 8]. The dynamic range of both are detectors is compared. This is part of the ongoing work for optimizing the Schottky diode and FETs THz detectors for applications at Particle accelerators and in future in other domains too.

THEORY

The Schottky barrier diode consists of metal-semiconductor junction. Quasi-vertical schottky barrier diodes [9] developed by ACST GmbH has been used in both, the commercial and the research grade THz detectors. The cross section is shown in Fig. 1.

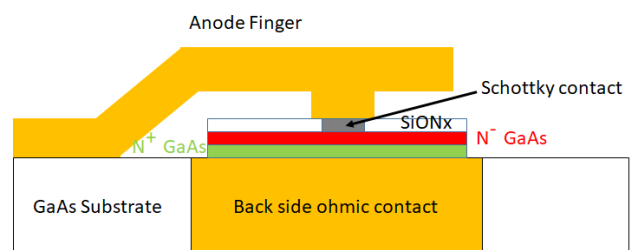


Figure 1: Cross section schematic of a quasi-vertical Schottky diode [9].

The diode is fabricated on a Gallium Arsenide (GaAs) substrate. The Anode and cathode are vertically fabricated, in contrast to the traditional horizontal contacting. This reduces the parasitic capacitance and series resistance. The quasi-vertical structure helps to keep the field distribution uniform across the anode finger and prevents current overloading when the ohmic contact is small, opposite to what there in case of Whisker-contacted Schottky diodes. Also, quasi-vertical structures help to keep the noise level low compared to Whisker-contacted as the anode and ohmic contact are not located on the same plane, reducing the cross link of the fields. The modified Schottky diode reduces

MODAL ANALYSIS OF ELECTROMAGNETIC COUPLING BETWEEN SMA-FEEDTHROUGH ELECTRODE AND BEAM FOR WIDEBAND BEAM MONITOR

T. Suwada*, High Energy Accelerator Research Organization (KEK),
also at SOKENDAI (The Graduate University for Advanced Studies), Tsukuba, Japan

Abstract

The direct simultaneous detection of electron (e^-) and positron (e^+) bunch signals was successfully performed for the first time by a wideband beam monitor at the e^+ capture section of the SuperKEKB factory. This monitor can measure a time interval between the e^- and e^+ bunches, their bunch lengths, bunch intensities, and transverse beam positions, depending on the phase of accelerating structures. For this purpose, a new beam monitor with wideband pickups simply using SMA feedthroughs and a wideband detection system based on a real-time oscilloscope was developed to investigate their capture process at the capture section and to maximally optimize the e^+ intensity. The required specification for the new monitor is to simultaneously detect the e^+ and e^- bunches generated in the capture section within the resolution of pico-second level with a sufficient dynamic range in the time-interval and bunch-length measurements. In this report, the basic design and numerical results based on a modal analysis of electromagnetic couplings between SMA-feedthrough and beam are in detail given.

INTRODUCTION

The SuperKEKB B-factory [1] (SKEKB) is a next-generation B-factory that is currently in operation at KEK, after the KEK B-factory [2] (KEKB) was discontinued in 2010. The SKEKB is a e^+e^- collider with asymmetric energies; it comprises 4 GeV e^+ (LER) and 7 GeV e^- (HER) rings. The target luminosity ($8 \times 10^{35} \text{ cm}^{-2}\text{s}^{-1}$) of the SKEKB, that is, the rate of e^- and e^+ collisions, is 40 times the peak luminosity of the KEKB. To improve the collision rate, the development of a powerful and stable e^+ source is one of the key elements in this experiment. The SKEKB injector linac [3] is an e^-/e^+ linear accelerator for the SKEKB; the KEKB injector linac [4] was upgraded for the abovementioned purpose. The requirements for the injector linac are full energy injection into the SKEKB rings with the e^- and e^+ bunch charges of 5 and 4 nC, respectively. The injector linac should deliver high-current e^+ beams to the SKEKB. The e^+ production and capture section are described in detail elsewhere [3].

Since both the electrons and positrons with approximately equivalent amounts of bunch charges are generated at the target, not only the positrons but also the electrons are simultaneously captured and accelerated (or decelerated) in the capture section with a certain time interval that is dependent on the operational condition of the capture section. The time

interval between the e^- and e^+ bunches is very short with a time range from 135 to 265 ps.

The time interval between the e^- and e^+ bunches, their bunch lengths and intensities for each e^- and e^+ bunch are very important parameters that can be fundamentally investigated on the basis of detailed beam dynamics at the capture section. However, they have never been measured because the time interval is too short to detect them independently, while they are generally simulated on the basis of beam dynamics in multidimensional transverse and longitudinal phase spaces. Thus, it is a challenging to experimentally verify and elucidate complicated beam dynamics for both positrons and electrons in the capture section in order to fully understand them and to maximize the e^+ intensity under an optimized operation condition.

For this purpose, new beam monitors with not only wideband pickups but also a wideband detection system were installed at the capture section to simultaneously detect e^- and e^+ signals during the summer shutdown of 2019. They are essential diagnostic instruments to fully investigate the e^- and e^+ capture process and to maximally optimize the e^+ intensity. Both the electrons and positrons generated at the target are formed into their steady bunched beams through their phase slip process in accelerating structures of the capture section. Thus, the experimental tests were successfully carried out at the e^+ capture section of the injector linac [5].

In this report a very wideband beam monitor with SMA-feedthroughs has been designed, and the modal analysis of electromagnetic coupling between SMA-feedthrough and beam is described on the basis of analytical methods with electromagnetic couplings between two coaxial structures.

WIDEBAND BEAM MONITOR SYSTEM

Mechanical Structure

A photo picture of the wideband beam monitor is shown in Fig. 1.

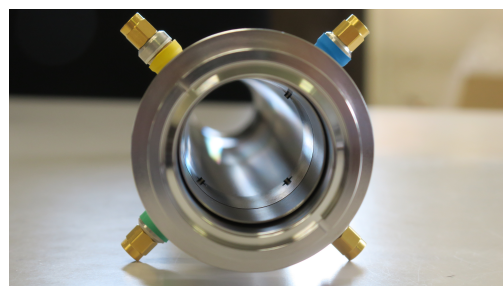


Figure 1: Photograph of the new beam monitor.

* tsuyoshi.suwada@kek.jp

BUNCH ARRIVAL TIME MEASUREMENT SYSTEM TEST FOR SHINE*

Y. M. Zhou[†], S. S. Cao, J. Chen, Y. B. Leng[#]
 Shanghai Advanced Research Institute, CAS, Shanghai, China

Abstract

To achieve high-precision synchronization between electron bunches and seeded lasers, a femtosecond resolution bunch arrival time measurement system (BAM) is required at SHINE (Shanghai High repetition rate XFEL aNd Extreme light facility). The bunch signal from a GHz-bandwidth cavity monitor is mixed with a reference signal from the device synchronization clock in the RF front-end. Then, the generated IF signal is collected by the digital acquisition system. In the pre-research stage, four sets of cavity monitors with different frequencies and load quality factors and three sets of analog front-ends with different schemes were performed, but now only one monitor with the attenuation time constant of 200 ns was installed for beam experiment testing. The system can measure the bunch charge, bunch arrival time, and bunch flight time. The first results will be presented in this paper.

INTRODUCTION

Shanghai High repetition rate XFEL aNd Extreme light facility (SHINE) is the first hard X-ray FEL facility in China, which started construction in April 2018 [1]. It will be used to generate brilliant X-rays between 0.4 and 25 keV at pulse repetition rates of up to 1MHz. Some important parameters are shown in Table 1.

Table 1: Main Parameters of the SHINE

Parameter	Value
Beam energy/ GeV	8.0
Bunch charge/ pC	100
Max repetition rate/ MHz	1
Pulse length/ fs	20-50
Photon energy/ keV	0.4-25
Total facility length/ km	3.1

The high-precision synchronization between the electron beam and the seed laser is of great significance to the debugging and operation of the accelerator. The SHINE project has very high requirements for the bunch arrival time measurement. The cavity probe has the characteristics of high resolution and high sensitivity. Therefore, the bunch arrival time monitor (BAM) system based on the radio frequency (RF) resonant cavity method can be used as an auxiliary measurement tool for the beam distribution area and the FEL section. It is hoped to accurately measure each bunch with a resolution better than 25 fs @100 pC.

*Work supported by Ten Thousand Talent Program and Chinese Academy of Sciences Key Technology Talent Program

[†]zhouyimei@zjlab.org.cn

[#]lengyongbin@sinap.ac.cn

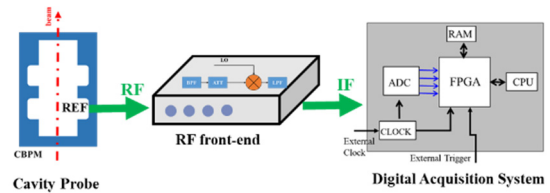


Figure 1: System block diagram.



Figure 2: Photos of CBPM 200.

SYSTEM STRUCTURE

The BAM system is mainly composed of three modules, as shown in Fig 1. The cavity probe is used to couple beam electromagnetic fields, including beam charge, beam arrival time, and position information. The function of the RF front-end is to filter, amplify, and down-convert the high-frequency signal into an intermediate frequency (IF) signal. A real-time online digital IQ demodulation algorithm is implemented in FPGA to extract beam position and phase information. All signal processing will be completed in the tunnel.

Cavity Probe

In general, the design of the reference cavity is relatively simple compared to the position cavity. Therefore, the two will be designed jointly, but the reference cavity is mainly used for bunch arrival time measurement. We have designed four sets of cavity probes with different frequencies and load quality factors. The detailed design parameters and test results can be found in Ref [2]. So far, the manufacturing and laboratory testing of three CBPM200 probes have been completed, as shown in Fig.2. The cold tests with a network analyzer have been performed, the results are presented in Table 2. The S-parameter spectrum of the reference cavity is relatively close to the simulation result. The frequency of the three sets of cavities is within ± 6 MHz of the design value, and the bandwidth is within ± 0.2 MHz of the design value, which meets the design requirements. The three CBPM200 probes have been installed on the beam test platform of the SHINE. The experimental beam mainly comes from the Shanghai soft X-ray FEL (SXFEL) facility.

BUNCH COMPRESSION MONITOR BASED ON COHERENT DIFFRACTION RADIATION AT EUROPEAN XFEL AND FLASH

Ch. Gerth* and N. M. Lockmann
 Deutsches Elektronen-Synchrotron, Hamburg, Germany, EU

Abstract

Bunch compression monitors (BCMs) based on the detection of coherent diffraction radiation have been installed at the European XFEL for a beam-based stabilisation of the accelerating phases as well as monitoring of bunch lengths. The monitor systems comprise zero-bias Schottky and pyro-electric detectors in combination with low and high pass filters. The detector responses and filters are matched to the spectral ranges of the coherent part of the emitted diffraction radiation which is given by the particular beam energy and bunch lengths after each bunch compression stage. In this paper, we describe in detail the experimental setup of the BCMs. The last BCM has been calibrated with the help of a transverse deflecting structure to establish a (rms) bunch length monitor in the range of a few tens of femtoseconds, and results from compression scans are presented. To enable operation at megahertz repetition rates of the superconducting accelerator, a correction method for the signal pileup of the pyro-electric detectors has been applied. Installation of the same BCMs is foreseen at FLASH within the FLASH2020+ upgrade project.

EUROPEAN XFEL

High-gain, single-pass free-electron lasers (FELs) require high-brightness electron bunches with kiloampere peak currents, which are longitudinally compressed in several stages by off-crest acceleration in combination with magnetic dipole chicanes. Figure 1 depicts schematically an overview of the European XFEL accelerator [1] with three radio-frequency (RF) accelerating sections (L_1, L_2, L_3) followed by bunch compression chicanes (BC_1, BC_2, BC_3). The settings of the compression stages were optimised for various bunch charges [2] as the electron bunches can be affected by collective, non-linear effects at these high peak currents. To establish the correct compression settings and ensure stable, long-term FEL operation, monitoring of the bunch compression is mandatory.

Bunch compression monitors (BCM) based on the detection of coherent diffraction radiation (CDR) have been installed after each of the three BC chicanes as is indicated in Fig. 1. CDR is generated by an electron bunch passing through an aperture in a screen and, therefore, is non-invasive to the electron beam. BCM1 has been installed after L_2 at higher beam energies, as this leads to a smaller emittance and, therewith, beam size and reduces the risk of beam losses at the aperture.

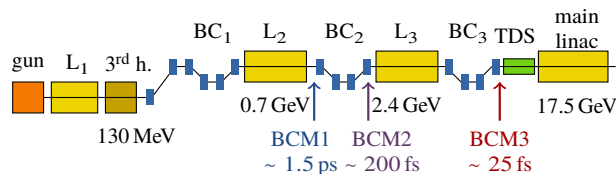


Figure 1: Schematic overview of the European XFEL accelerator. The positions of the BCMs and nominal rms bunch lengths for a bunch charge of 250 pC are indicated.

BCM SETUP

A BCM consists of a screen station mounted in the electron beamline for the generation of CDR as well as an optics and detector unit for transport and detection of the CDR.

Screen Station

Figure 2 shows a CAD image of the screen station and CDR screen which is mounted on a remotely-controllable vacuum feed-through (screen mover). The screen consists of solid aluminum, and the screen normal has an angle of 45° with respect to the electron beam axis. The radiator area at the bottom ($32 \text{ mm} \times 80 \text{ mm}$, 1 mm-thick) is depicted enlarged in the right part of Fig. 2 and comprises two apertures with effective diameters of 5 mm and 7 mm in the projection of the electron beam axis. The surface of the CDR screen has been machined with a diamond milling cutter and has a roughness $< 1 \mu\text{m}$. Backward CDR is emitted perpendicular to the electron beam axis and enters the optics and detector unit through a fused silica vacuum window at BCM1 and BCM2 and a diamond vacuum window at BCM3.

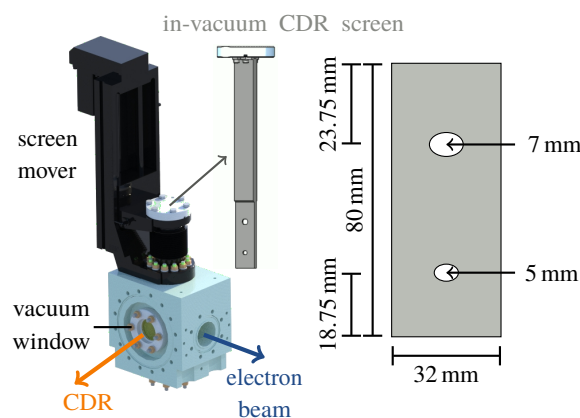


Figure 2: (Left) CAD model of the screen station and CDR screen. (Right) The radiator area enlarged with dimension.

* christopher.gerth@desy.de

PROPOSED LONGITUDINAL PROFILE DIAGNOSTICS FOR OPTICAL STOCHASTIC COOLING OF STORED ELECTRONS IN THE IOTA RING*

A. H. Lumpkin†, Fermi National Accelerator Laboratory, Batavia, IL 60510 USA

Abstract

The Fermilab Integrable Optics Test Accelerator (IOTA) ring optical stochastic cooling (OSC) experiment is designed for a low nominal beam current (~0.1 microAmps of 100-MeV electrons) to reduce intrabeam scattering (IBS), and during cooling, OSC is expected to reduce the bunch length from ~200 ps to ~130 ps. These equilibrium bunch lengths can be measured using a streak camera and the optical synchrotron radiation (OSR) generated in a ring dipole by the circulating beam as demonstrated on a small ring elsewhere recently. The same model streak camera has been installed on IOTA, and one expects the integrated system will have sufficient sensitivity and resolution for measuring the evolution and equilibrium values of the bunch length during OSC experiments.

INTRODUCTION

Optical stochastic cooling (OSC) experiments [1] are an extension to optical frequencies of stochastic cooling experiments for particle beams performed previously in the microwave regime [2]. They are motivated by an increase in the cooling bandwidth by up to 3 orders of magnitude in principle. Complementary experiments on OSC for electrons are being implemented at 1 GeV at the Cornell Electron Storage Ring (CESR) in an arc bypass [3] and at 100 MeV at the Fermilab Integrable Optics Test Accelerator (IOTA) ring [4]. This latter experiment will use two undulators (with resonant wavelength of 0.95 μm) in a straight section of the ring for the “pickup undulator” (PU) and the “kicker undulator” (KU). An optical delay path is used to match the transit time of the photon emitted in the PU with the same electron that emitted it (after the transit of a magnetic chicane) in the KU. Small longitudinal kicks to the electrons can result in a cooling effect on the momentum offset with appropriate delay tuning.

One of the predicted signatures of successful optical stochastic cooling in the Fermilab IOTA ring is reduction of the bunch length. The IOTA OSC experiment is designed for a low nominal beam current (~0.1 microAmps of 100-MeV electrons) to reduce intrabeam scattering (IBS), and during cooling, OSC is expected to reduce the bunch length from ~200 ps to ~130 ps [4]. These equilibrium bunch lengths can be measured using a streak camera and the optical synchrotron radiation (OSR) generated in a ring dipole by the circulating beam. A similar measurement was previously performed at the Advanced Photon Source with a Hamamatsu C5680 synchroscan streak camera operating at 117.3 MHz [5]. In this case, synchronous summing of

OSR resulted in a bunch length measurement of 354 ± 12 ps using only 389 electrons circulating at 425 MeV. At IOTA, an existing streak camera has been modified to operate at the 11th harmonic of the ring’s revolution frequency of 7.50 MHz and has been installed on an OSR port in support of the OSC experiments. The integrated system will have sufficient sensitivity and resolution for measuring the evolution and equilibrium values of the bunch length during OSC.

EXPERIMENTAL ASPECTS

A brief description of the FAST/IOTA facility is given in this section plus that of the streak camera system being implemented to support OSC experiments.

The FAST Electron Injector Linac

The Integrable Optics Test Accelerator (IOTA) electron injector at the FAST facility (Fig. 1) begins with an L-band rf photoinjector gun built around a Cs₂Te photocathode (PC [6]). When the UV component of the drive laser, described elsewhere [7] is incident on the PC, the resulting electron bunch train with a 3-MHz micropulse repetition rate exits the gun at <5 MeV. Following a short transport section with a pair of trim dipole magnet sets, the beam passes through two superconducting rf (SCRf) capture cavities denoted CC1 and CC2, and then a transport section to the low-energy electron spectrometer. In this case this dipole is off so 25-MeV beam is transported to and through the cryomodule (CM2) with an exit energy of 100 MeV. Generally, a single bunch of ~100 pC is transported to the IOTA ring for injection into it.

The IOTA Ring

The IOTA ring is a multipurpose research accelerator which normally circulates electrons injected from the linac at 100 or 150 MeV and with a 7.50-MHz revolution frequency. Currents have been stored from a few mA to a single electron. The target area for the OSC experiments is 83,000 e⁻, or 0.1 μA and lower. There are 8 dipoles in the ring lattice as shown in Fig. 2, and the streak camera was installed on the M3R OSR port. Signal is shared with one of the standard FLIR CMOS digital cameras used for e-beam transverse size measurements via OSR.

Streak Camera

A C5680 Hamamatsu streak camera with an S20 PC operating with the M5675 synchroscan vertical deflection unit will be phase locked to 82.50 MHz as shown in Fig. 3. The synchroscan unit was selected over the slow sweep unit plugin with a trigger rate of 500 kHz at 2-ns sweep and

* Work supported by Fermi Research Alliance, LLC under Contract No. DE-AC02-07CH11359 with the U.S. Department of Energy, Office of Science, Office of High Energy Physics.

† Lumpkin@fnal.gov

COMPARISON OF FESCHENKO BSM AND FAST FARADAY CUP WITH LOW ENERGY ION BEAMS

R. Singh^{*1}, S. Lauber^{1,2,3}, W. Barth^{1,2,3}, P. Forck¹, M. Miski-Oglu^{1,2}, T. Reichert¹, V. Scarpine⁴,
T. Sieber¹, D. Sun⁴

¹GSI Helmholtz Center for Heavy Ion Research, Darmstadt, Germany

²Helmholtz Institute Mainz, Mainz, Germany

³Johannes Gutenberg-University, Mainz, Germany

⁴Fermilab, Batavia, IL, USA

Abstract

A comparison between Fast Faraday Cup and Feschenko longitudinal bunch shape detectors was recently performed at HELIAC Advanced Demonstrator beamline at GSI. Feschenko bunch shape monitor (BSM) uses the time to space conversion by means of secondary electrons emitted from a wire correlated to a rf deflector [1], while the fast Faraday cup (FFC) measures the deposited charge in a cup geometry matched to $50\ \Omega$. The FFC design aims to minimize the bunch shape dilution due to field polarization and secondary electrons produced on irradiation [2]. An He^{1+} with $100\ \mu\text{A}$ average current and $1.4\ \text{MeV/u}$ kinetic energy is utilized for this comparison. A buncher upstream of the detectors was operated to focus the beam longitudinally. The results are discussed in this contribution.

INTRODUCTION

Longitudinal charge distribution measurements are essential for the commissioning and optimization of linear accelerators. The emergence of new nonlinear beam dynamics concepts employing a variation of particle synchronous phases different from the traditional $-30\ \text{deg}$ resonance acceleration pattern, e.g. KONUS [3], EQUUS [4] has called for better understanding of longitudinal phase space and relevant instrumentation. Charge distribution measurements of non relativistic heavy ions beams are not feasible with electromagnetic-field sensing devices like capacitive pickups because the field distribution is elongated in comparison to charge distribution. A commonly used instrument for longitudinal beam profile measurements is the Feschenko bunch shape monitor (BSM), which relies on the time-to-space conversion of electrons emitted when the beam interacts with a wire [5]. Alternatively, there has been several designs for a Fast Faraday Cup (FFC), which intend to avoid the induction of image charges on the cup before the charges are deposited on the cup while maintaining a $50\ \Omega$ geometry [6–8]. Recently, longitudinal charge distribution measurement using coherent transition radiation in GHz regime has been investigated [9]. Although BSMs and FFCs are widely used, no benchmarking of these devices among each other is known to us. In this contribution, we compare both of these monitors under similar beam and machine conditions and the experimental results are discussed.

* r.singh@gsi.de

The tests were performed at the Helmholtz Linear Accelerator (HELIAC) *Advanced Demonstrator* beam line at GSI [10]. The HELIAC components marked in grey were not installed. Various charge states and ion species were delivered to the test setup by the GSI High Charge State (HLI) injector with an kinetic beam energy of $1.4\ \text{MeV/u}$ and a duty cycle of up to 25% in the regime of some $30\text{--}100\ \mu\text{A}$ average current. The beam line is equipped with phase probe sensors, a slit-grid emittance measurement device, beam position monitors, beam profile grids as well as Feschenko BSMs. Recently a test Fast Faraday Cup was made available on loan from Fermilab for comparison with Feschenko BSMs, which was installed to the preliminary line setup with a beam pipe substituting the cavities. The test beamline (with the cavities to be installed) is shown in Fig. 1.

BUNCH SHAPE MONITOR

The bunch shape monitor of Feschenko type provides for precise measurements of heavy ion beams with an accuracy of up to $\pm 0.5\ \text{deg}$ at an rf frequency of $108\ \text{MHz}$ [5]. It consists of three main parts: a thin filament in the beam line, an optical system and an electron multiplier. The thin filament is irradiated by the heavy ion beam, and thus emits secondary electrons in all directions. The optical system, which is entered by the secondary electrons through a pinhole at the border of the beam pipe, provides for the suppression of noise and translates the time dependent electron current $I(t)$ to a spatially resolved signal $I(z)$, primarily with use of an deflecting electric field. A narrow part of the spatial signal is steered to enter the secondary electron multiplier, where it is measured. Thus, $I(z)$ is scanned successively by steering and subsequently available for readout. The installed version of the Feschenko BSMs optical system features additional bending magnets for further noise reduction [1].

A measurement series with the Feschenko-BSMs has been successfully used to calculate the longitudinal phase portrait of the bunch with use of an advanced tomographic reconstruction technique at the HELIAC *Advanced Demonstrator* beam line [11]. Although a useful device, there are couple of shortcomings of the BSM, first of which is the averaged nature of the measurement, i.e. measurement at each phase is a different macropulse which does not allow resolving the bunch length variations between consecutive macropulses.

Content from this work may be used under the terms of the CC BY 3.0 licence (© 2021). Any distribution of this work must maintain attribution to the author(s), title of the work, publisher, and DOI

NEW X-BAND RF DEFLECTOR FOR FEMTOSECOND DIAGNOSTICS OF LCLS-II BEAMS*

V. A. Dolgashev[†], H. Bassan, S. Condamoor, A. Haase, P. Krejcik, T. Maxwell, J. Wang,
SLAC National Accelerator Laboratory, Menlo Park, CA, USA

Abstract

An X-band Transverse deflector CAVity (XTCAV) has been successfully developed for femtosecond electron and X-ray pulse temporal diagnostic at the Linear Coherent Light Source (LCLS). The working frequency for the deflector is 11.424 GHz. New free electron laser LCLS-II has two undulator beamlines, one Soft-X-Ray (SXR) and another Hard-X-Ray (HXR). The HXR line deflector is made of two one-meter long XTCAVs. We have designed, built, installed and commissioned another, 1.5 meter long X-band deflector in the Soft-X-Ray beam line. Both HXR and SXR deflectors share one klystron. RF power is transmitted from a 50 MW klystron to a tunnel in an overmoded circular waveguide and then directed to either of the deflectors using a remotely controlled variable RF power splitter. The power split ratio can be changed arbitrarily, and both deflectors can work simultaneously. The system is successfully commissioned and operational. In this article, we provide details on the development and commissioning of the new deflector.

INTRODUCTION

LCLS is the world's first hard X-ray free electron laser. It allows for X-ray snapshots of atoms and molecules at work, providing atomic resolution detail on ultrafast timescales to reveal fundamental processes in materials, technology and living things [1]. One of the most important tools for electron beam diagnostics in LCLS is X-band transverse deflecting structures [2, 3]. XTCAVs are used in the LCLS accelerator for bunch length and beam longitudinal phase space measurements. The high frequency time variation of the deflecting fields streaks the electron bunch while the resulting transverse beam shape measured on a profile monitor represents the absolute bunch length [2, 3]. The LCLS-II is an evolution of the original LCLS with a much higher pulse repetition rate, it is also will benefit from the diagnostic capabilities of the XTCAVs. In LCLS-II there are two X-ray beam lines: HXR line and SXR line. To achieve femtosecond resolution, the XTCAVs are driven by a SLAC 50 MW XL-4 klystron. The klystron and its high voltage modulator are the most expensive components of the system. Rather than purchase a second XL-4 klystron and modulator we chose to use one klystron with a power splitter [4]. This paper will provide details of upgrading the original HXR system with its original two-cavity-deflector, and the addition of a new, simultaneously operated single-cavity deflector on the SXR beamline. The new layout is shown in Fig. 1.

* Work supported by the U.S. Department of Energy Contract No. DE-AC02-76SF00515.

[†] dolgash@slac.stanford.edu

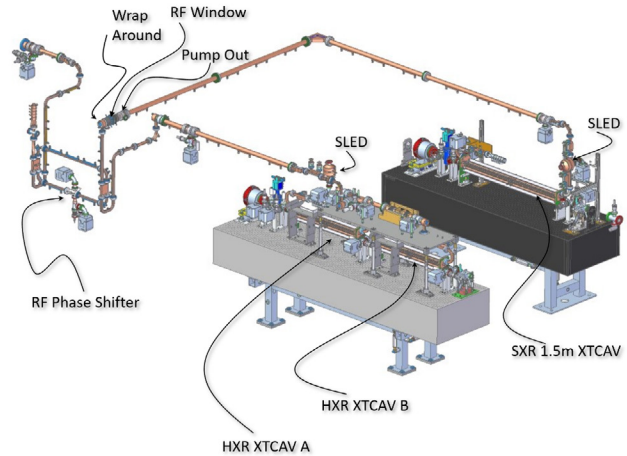


Figure 1: System layout showing the rf deflectors (XTCAVs) of HXR and SXR beam lines. RF power from klystron is coming from the left. LCLS electron beam direction is from the left to right.

Upgrade Goals and Approach

The aim of the modernization was to create a system for measuring the longitudinal phase space of electron beams with a femtosecond resolution, which allows reconstructing the temporal structure of an X-ray pulse in an FEL for alternating operation in two X-ray beams. The goal of the upgrade was to build a system for measuring the longitudinal phase space of electron beams with a femtosecond resolution, which allows reconstructing the temporal structure of FEL X-ray pulse for interleaved operation in two X-ray beamlines, HXR and SXR, at LCLS repetition rate of 120 Hz. To achieve this, we proposed following:

- Build, tune and install a new, longer RF deflector in the Soft X-Ray beamline.
- Build, tune, install a new SLED rf-pulse compressor for operation with new 1.5 m deflector.
- Build, and install a multi-megawatt RF variable power splitter based on a remotely controlled phase shifter.
- Move HXR SLED closer to HXR deflector, install both HXR and SXR SLEDs downstream after the rf power splitter.
- Upgrade the control system for operation with the copper linac, then upgrade it for superconducting linac of LCLS-II.

BUNCH ARRIVAL-TIME MEASUREMENT WITH ROD-SHAPED PICKUPS ON A PRINTED CIRCUIT BOARD FOR X-RAY FREE-ELECTRON LASERS*

B. E. J. Scheible[†], S. Mattiello, A. Penirschke, TH Mittelhessen, Friedberg, Germany
M. K. Czwalinna, H. Schlarb, Deutsches Elektronen-Synchrotron, Hamburg, Germany
W. Ackermann, H. De Gersem, TU Darmstadt, Darmstadt, Germany

Abstract

The all-optical synchronization system implemented in the European X-ray free-electron laser (EuXFEL) is to receive an upgrade. The modifications are intended to allow operation with consistently high accuracy in a 1 pC mode, which is required for various user experiments. The lower charges, e.g. a factor of 20, lead to a reduced signal strength at the pickups and thus to a decreased resolution. A significant potential for improvement has been identified in a modified pickup structure and transmission network, which provide the transient voltage signal to subsequent parts of the synchronization system. One solution for a broadband pickup structure with short signal paths, large active surfaces and minimum aperture diameter could be achieved by connecting rod-shaped pickups to a combination network on a printed circuit board, which will be mounted in the beamline. In this contribution the proposed design is introduced and analyzed by electromagnetic field simulations.

INTRODUCTION

A stable high-resolution synchronization system is indispensable in fourth generation light sources, specifically linac-based free-electron lasers (FELs). To exploit their potential, it is necessary to synchronize various subsystems, distributed in the km-long facilities, with fs precision [1, 2].

There are two commonly used approaches for synchronization systems in FELs. The first is based on resonant cavities synchronized to the low-level rf, for example implemented at the LCLS [3]. In contrast the second uses a train of laser pulses, synchronized to the main rf clock, as an optical reference, which is correlated to the transient signal induced by the coasting bunch [4]. Though the additional installation of an optical distribution as well as a laser oscillator with sufficient rate, timing stability and short pulse duration is costly, these systems have advantages for high resolution synchronization in large facilities [2, 4]. The European X-ray free-electron laser (EuXFEL) [5], FERMI@Elettra [6] and the SwissFEL [7] are some of the notable examples, where the optical scheme is in operation. Furthermore, such a synchronization system will be used for SHINE [8].

One substantial criterion for the classification of light-sources is the pulse duration [9]. For many experiments it is favorable to have short pulses in atomic time scales, which

can be achieved when the bunch charges are reduced [10]. Yet the non-invasive electro-optical arrival-time measurement, a key challenge in synchronization, depends on transient fields of the electron beam [1, 4] and thus is a limiting factor for a reliable low charge operation of current FELs.

To extend the EuXFEL parameter range towards low charges, the bunch arrival-time monitors (BAMs) need to be improved. Following a former design upgrade, the EuXFEL's operating synchronization system is capable to operate with 20 pC bunches and with resolution well below 6 fs r.m.s. for higher charges [11, 12]. After the successful completion of the ongoing design update, the BAM is planned to achieve a consistently high accuracy with 1 pC bunches.

In this paper a possible design and intermediate stages are presented after a brief introduction to the current BAMs.

ELECTRO-OPTICAL BAM

The arrival time of a single bunch is measured relative to an optical reference in the BAM, which is one end-station of the all-optical synchronization system. As a reference, 1 ps short laser pulses [13] are emitted from an optical laser oscillator synchronized to the master rf oscillator [2]. The laser pulse distribution system is actively stabilized by piezo fibre stretchers and free-space delay stations [2, 5].

The operation principle of electro-optical BAM, introduced in [4], can be divided into the rf part and the electro-optical correlation to the reference laser pulse.

In the rf part, the transient electric fields of coasting bunches couple with button-type pickups and induce a bipolar voltage signal [4]. State-of-the-art BAMs are equipped with four cone-shaped pickups [14] evenly distributed around the beam pipe. The signals are transmitted via coaxial cables [14] while each pair of opposite pickups is combined to compensate for the beam position [13].

Afterwards, the voltage signal is applied to a Mach-Zehnder-type electro-optical modulator (EOM), where the signal is probed by the optical reference [4]. By another free-space delay station the working point is set exactly to the voltage signal's zero crossing (ZC) for a perfectly timed bunch [4, 13]. Any temporal deviation causes a modulation voltage that effects the amplitude of the probing reference pulse [4]. In the operating range the amplitude difference is proportional to the arrival time [5] and therefore the relative timing can be determined by comparing the modulated pulse to unaltered reference pulses [4]. The information is retrieved and digitized in the data acquisition and the results are used to stabilize the operation by a feedback-loop [4, 5, 13].

* This work is supported by the German Federal Ministry of Education and Research (BMBF) under contract no. 05K19RO1

[†] bernhard.scheible@iem.thm.de

Content from this work may be used under the terms of the CC BY 3.0 licence (© 2021). Any distribution of this work must maintain attribution to the author(s), title of the work, publisher, and DOI

DESIGN OF THE BUNCH-LENGTH MONITORS FOR THE NEW SUPERCONDUCTING LCLS LINAC

E. Aneke[†], T. Maxwell, A. Fisher, L. Sapozhnikov, B. Jacobson
SLAC National Accelerator Laboratory, Menlo Park, CA 94025, USA

Abstract

The LCLS x-ray free-electron laser at SLAC uses the third km of the original 3-km copper linac. We are now installing LCLS-II, a superconducting linac that replaces the first km. Two undulators, for hard and soft x rays, will be driven by bunches from either linac. One of the solutions developed at SLAC involves a pyroelectric detector, which converts the infrared emitted by the electron bunch into voltage by measuring fast changes in the temperature of the detecting crystal. Not only are the pyrodetectors used at SLAC but also a method with gap diodes. The radial electric field produced by the bunches leaks through a ceramic gap in the beampipe and is collected by a horn antenna and conveyed through a one millimeter waveguide. The waveguides act as a filter, only passing shorter wavelengths and a zero-bias Schottky diode measures the power. In both methods, a portion of the spectral energy emitted by the bunch is intercepted. After normalizing to differentiate between bunches of the same length with different charge, the detected signal is sensitive to only changes in bunch length. This poster discusses the mechanics and optics behind the LCLS-II bunch length monitors' operations and plans for collaboration.

BACKGROUND

This paper describes the physics requirements and implications for instrumenting the single-shot relative bunch length monitors (BLM) based on coherent edge radiation (CER) at the end of the LCLS-II bunch compressor chicane. It also describes the physics requirements and implications for instrumenting single-shot, diode-based relative bunch-length monitors (BLEN) based on radiation picked up from a ceramic break in the vacuum pipe and coupled to a GHz detection diode [1, 2].

PYROELECTRIC DETECTOR

The superconducting linac will have two stages of bunch length compression with off-crest RF phasing to energy-chirp the bunch. Afterwards, compression is then achieved in 4-dipole bunch compressor chicane named: BC1 and BC2. The critical final peak current of 1 kA is generated after these stages, with a nominal 100 pC charge per bunch. The final peak current, which is directly related to the final bunch length, must be stable to < 10% rms from pulse to pulse. The goal is to also have the peak current stable over much longer time periods (e.g., one week), until manual intervention is eventually required [1].

The compression system, and in turn, the final peak current, will be very sensitive to time-dependent variations in things such as: RF phasing, accelerator gradient, bunch charge, and laser timing from the gun. Maintaining the

peak current over longer time scales will require a longitudinal feedback system based on continual single-shot electron beam measurements. Such a system has already been described for the LCLS and requires at least one single-shot relative bunch length monitor located immediately after each chicane. A measurement of the absolute bunch length is not necessary for feedback purposes. It is sufficient to produce a relative signal which is approximately proportional (inversely proportional) to the peak current (electron bunch length) over a reasonable dynamic range [1].

Bunch length monitors in the injector and immediately prior to the undulators will also be of great importance, but are not necessary of the critical longitudinal feedback system. The pyroelectric detector diagnostic method as a BLM is the only the single-shot monitors needed for the critical longitudinal feedback system integrated in the BC chicanes. This is crucial to the integrity of LCLS-II operations [1].

A mirror with a long, vertical slot for the electron beam will be insertable into the beamline to reflect the upstream CER from the fourth bend magnet (B4) out of the vacuum chamber. The CER will then be sent up into the optics box containing the diagnostic. See Fig. 1 [3].

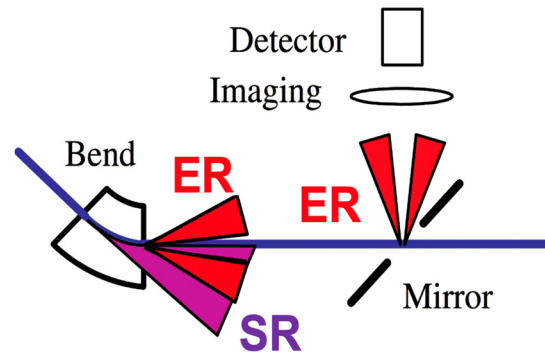


Figure 1: Diagram of the capture of edge radiation.

Once in the optics box, the CER will be guided by a couple of off-axis parabolic mirrors. Then it will pass 4 insertable filters followed by a beam splitter. It is meant to image the CER onto two identical pyroelectric detector elements. There are two pyroelectric detectors for redundancy in the event of a single element failure. Detectors will include preamplifiers with remotely selectable gain [1]. See Figs. 2 and 3.

DESIGN OF WALL CURRENT MONITOR IN BRING AT HIAF

Peilin He[†], Yongliang Yang, Xincan Kang, Xiaotao Liu, Zhiguo Xu, Ruishi Mao
Institute of Modern Physics, Chinese Academy of Sciences, Lanzhou, China

Abstract

The Wall Current Monitor (WCM) can monitor the longitudinal beam shape, beam stability, beam longitudinal emittance and intensity, which has been applied widely in the laboratories of high-current proton accelerators. Many accelerators such as CERN-PS, CERN-CLIC, J-PARC and CSNS-RCS have designed different WCMs according to their respective accelerator beam parameters. In order to provide the high-intensity heavy-ion accelerator facility (HIAF)-BRing high-frequency system of with the intensity of each harmonic beam to compensate for wake field; and to observe the changes of the bundle length during the injection, acceleration, and extraction of the bundle, it is planned to place a WCM in HIAF-BRring. According to physical requirements, the lower limit of the WCM working bandwidth is expected to reach 10 kHz, and the upper limit can reach 100 MHz. According to this bandwidth requirement, a WCM structure is designed, and its theoretical bandwidth is 2 kHz~400 MHz, which fully meets the demand. This article gives a detailed and comprehensive introduction to the overall design of this WCM, the selection of various components, design calculations and related simulation calculations. At present, the WCM has completed the procurement and processing of various components, while offline and online testing has not been carried out owing to time constraints. It is expected to be installed on the Heavy Ion Research Facility in Lanzhou-Cooling Storage Ring (HIRFL-CSR) for online testing in August.

PRINCIPLE OF WCM

When the beam passes through the vacuum pipe, its AC component will produce a constant-amplitude and inverse-phase mirror current on the wall of the vacuum pipe. The WCM uses this principle to measure the longitudinal information of the beam. Its schematic diagram and the corresponding equivalent circuit are shown in Fig. 1.

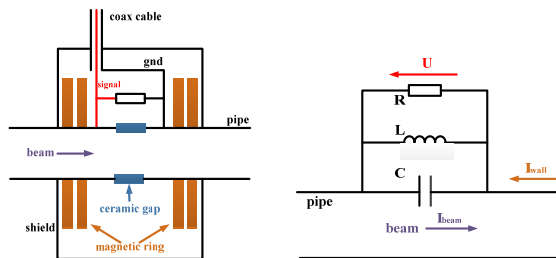


Figure 1: the schematic diagram and the corresponding equivalent circuit of WCM.

Cut the vacuum pipe and install a section of ceramic ring, connecting a resistor across the two ends of the ceramic ring, the induced wall current(mirror current) will

produce a voltage which is proportional to the beam current on this resistor. By directly measuring the voltage signal, the intensity signal of the beam pulse can be measured [1].

Ceramic Gap

The main purpose of adding a ceramic ring is to isolate the vacuum pipe, making the induced wall current flow to the resistance. In addition, after welding with the vacuum pipe, it can also make the magnetic ring, shield and other parts outside the vacuum, which makes it easy to control the vacuum performance index of the whole device.

Its equivalent capacitance value is:

$$C_{gap} = (\epsilon_0 \epsilon_r S) / t \quad (1)$$

The characteristic impedance of the ceramic ring is:

$$Z = 377 \frac{t}{2\pi r_0} \frac{1}{\sqrt{\epsilon_r}} \quad (2)$$

Where ϵ_0 is the vacuum dielectric constant, ϵ_r is the relative dielectric constant, S and t are the side area and thickness of the ceramic ring. $r_0 = (r_{in} + r_{out}) / 2$, r_{in} and r_{out} are the inner and outer radius of the ceramic ring.

Magnetic Ring

The magnetic ring is filled outside the vacuum pipe and inside the shielding shell, acting as a role to increase the inductance. Its equivalent inductance value is:

$$L = \frac{\mu_0 \mu_r}{2\pi} h \ln\left(\frac{b}{a}\right) \quad (3)$$

Where μ_0 is the vacuum permeability, μ_r is the relative permeability, h is the thickness of the magnetic ring, a and b are the inner and outer diameter of the magnetic ring.

Signal Pick-up Resistance

Because resistors have certain inductance and capacitance characteristics under high frequency, the signal pickup resistor of WCM uses multiple non-inductive resistors connected across the ceramic gap in parallel, and in order to achieve matching, the equivalent resistance value R must be equal to the characteristic impedance Z of the ceramic ring.

Working Bandwidth

Upper cutoff frequency:

$$f_H = \frac{1}{2\pi RC_{gap}} = \frac{r_0}{377S\epsilon_0\sqrt{\epsilon_r}} \quad (4)$$

Lower cutoff frequency:

[†] hpl@impcas.ac.cn

PSB H^0 - H^- MONITOR CALIBRATION AND COMMISSIONING

A. Navarro*, S. Bart, D. Belohrad, C. Bracco, E. Renner, F. Roncarolo, J. Tassan-Viol,
 CERN, Geneva, Switzerland

Abstract

During the LHC Long Shutdown 2 (LS2), the H^- LINAC4 replaced the proton LINAC2 as Proton Synchrotron Booster (PSB) injector. In each of the four PSB rings, the injection region was upgraded to accommodate the necessary elements for a proper H^- charge exchange injection system. Four beam dumps (one per ring), installed downstream the stripping foil, prevent the unstripped H^- particles from being injected in the ring. The H^0 H^- monitors, consist of four titanium plates placed a few centimetres upstream of the dump, intercept partially stripped H^0 or not stripped H^- ions and allow a continuous monitoring of the stripping efficiency, providing an interlock signal to block the injection process in the case of severe degradation or breakage of the foil, which would heavily damage the dumps.

This contribution focuses on the commissioning and operation of these new systems. It describes the results from the calibration campaigns, performed by comparison to beam current transformer measurements during special periods with low intensity beams and no stripping foil, and during normal operation, when it was already possible to monitor stripping inefficiencies below 1% and compare different beams and stripping foil types.

INTRODUCTION

The LHC high luminosity programme (HL-LHC) [1] calls for the production and acceleration of brighter beams from the injectors [2]. During the Long Shutdown 2 (LS2) at CERN, the new LINAC4 accelerator [3] was connected to the Proton Synchrotron Booster (PSB). It provides a 160 MeV H^- particle beam. With respect to the LINAC2, the increase of injection energy from 50 to 160 MeV doubles the relativistic factor $\beta\gamma^2$ at PSB injection allowing the beam brightness to be doubled. The beam from LINAC4 consists of four individual pulses, separated by a 1 μ s particle-free gap and a pulse length that depends on the number of turns injected per ring. The pulses are then distributed to the corresponding booster rings for injection.

To inject the H^- beam in the PSB, a new charge exchange injection system [4] was installed in each ring. This new system reduces injection losses which were unavoidable in the previously used multi-turn injection. Figure 1 shows a schematic representation of the new injection system which comprises a stripping foil, a set of four pulsed dipole magnets (BSW) [5] and four horizontal kickers (KSW) [6] (Not indicated in the picture).

The first magnet (BSW1) acts as a septum generating a high-field region for the circulating beam and a field-free region for the injected H^- beam. It is followed by 3 bumper

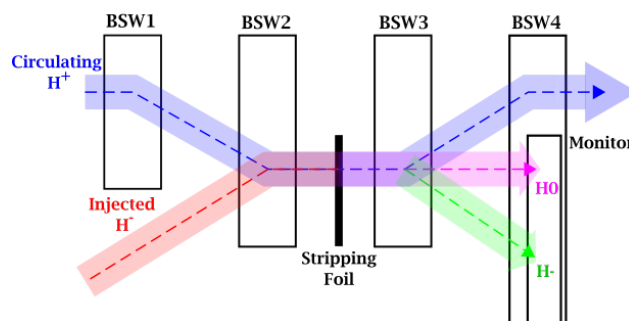


Figure 1: Schematic representation of PSB H^- Charge injection system.

magnets (BSW2-4) that help merging the injected beam with the circulating beam. The stripping foil (about 20 mm wide and 20 mm high) is made of carbon with a density around $200 \mu\text{gcm}^{-2}$. It strips electrons from the incident H^- particles. The characteristics of the used stripping foil have been optimized to provide sufficient stripping efficiency ($> 99\%$) while minimizing emittance blow-up. After the stripping foil, fully-stripped protons are injected into the circulating beam while the partially-stripped and unstripped ions are collected by a dedicated dump.

PSB H^0 - H^- BEAM CURRENT MONITOR

The injection region geometry and the very limited space available preclude extraction of the unstripped or partially stripped ions. For that reason, four internal Ti_6Al_4V dumps, one per ring, were installed downstream of the stripping foil, within the vacuum chamber of the chicane magnet BSW4, as shown in Figs. 2 and 3. The geometry of the dump provides an unobstructed passage for the circulating beam during injection as well as for the injected proton beam, whilst providing optimal protection of the downstream elements by absorbing a few percent of the unstripped beam during regular operation, and also by absorbing the full beam in the event of a foil failure. In Figs. 2 and 3 the dump is represented in black.

The H^0 H^- monitors (represented in red in Figs. 2 and 3) are installed 4 cm upstream from the face of the dump. The dump is far enough from the detectors to prevent secondary electrons coming from the dump affecting the signal of the monitors. The H^0 H^- monitors consist of four titanium plates: two 22 mm wide central plates and two 18 mm wide external plates with around 1 mm separation between the plates which allows to supplement the intensity measurements with some beam positioning information. The two outer plates are expected to measure H^- particles while

* araceli.navarro.fernandez@cern.ch

HIGH SPEED PARALLEL DIGITAL SIGNAL PROCESSING STRUCTURE IN BUNCH-BY-BUNCH POSITION MEASUREMENT BASED ON FPGA*

Ruizhe Wu, Leilei Tang[†], Ping Lu, Bao-gen Sun, National Synchrotron Radiation Lab. (NSRL), University of Science and Technology of China (USTC), Hefei, Anhui, China

Abstract

In storage ring, the measurement of bunch-by-bunch positions can help to obtain abundant beam dynamics characteristic information, diagnose the instability of beam motion and provide a basis for the suppression of instability. However, the measurement of bunch-by-bunch requires one analog-to-digital converter (ADC) with high sampling rate and one processor with fast digital signal processing (DSP) ability. With the development of electronics, high sampling rate ADCs are no longer a problem. Therefore, high-speed DSP has become the key. In this paper, a parallel digital signal processing architecture based on polyphase decomposition is proposed. This architecture realizes the GHz DSP speed on the programmable gate array (FPGA), which can be used as the infrastructure of high-speed DSP in the bunch-by-bunch position measurement system.

INTRODUCTION

Beam diagnostics is an indispensable part of synchrotron light source to ensure its stability in operation. In beam diagnostics, the beam position monitor (BPM) used to monitor electron beam can obtain the position and current intensity information of the beam, then shows the running state of the synchrotron light source. In recent years, with the improvements of digital devices in terms of working frequency, DSP is of interest in the field of BPM.

With different DSP dealing rates, different types of beam information can be obtained by BPM:

- Closed Orbit: Sample at 10Hz for high precision position measurement. The average value of multi turn beam position in the storage ring can be obtained.
- Fast Orbit: Sample at 10kHz for fast orbit feedback. The average value of multi turn beam position in the storage ring can be obtained.
- Turn-By-Turn: Sample at the time for the bunch to move one turn in the storage ring. The average position data of all bunches in the storage ring can be obtained.
- Bunch-By-Bunch: Sample at the time interval between adjacent bunches. The position of each bunch in the storage ring can be obtained.

At present, BPM can obtain the beam information from closed orbit to turn-by-turn through the development of digital devices [1]. However, the obtain of bunch-by-bunch beam information usually imposes higher requirements on DSP dealing capacity. Hence the BPM of bunch-by-bunch, limited by the DSP part, is still in its initial stage.

The DSP part of BPM is usually implemented with FPGA. By coding, digital logic can be mapped to FPGA, so as to achieve various digital logic functions. This great programming flexibility of FPGA is provided by its internal interconnect bus architecture, but this architecture also limits its processing speed to about 500 MHz. Therefore, the DSP speed of BPM is basically at 500 MHz, and then it is difficult to realize the DSP work of bunch-by-bunch.

In FPGA, static timing analysis technology [2] can verify the correctness of digital circuit timing and predict the working frequency of digital system implemented by FPGA.

$$F_{max} \leq \frac{1}{T_{co} + T_{logic} + T_{routing} + T_{su} - T_{skew}} \quad (1)$$

As shown in the Eq. (1), the highest DSP speed F_{max} depends on T_{co} , T_{logic} , $T_{routing}$, T_{su} and T_{skew} parameters. Among them, T_{co} and T_{su} are intrinsic parameters of FPGA that cannot be changed. $T_{routing}$ and T_{skew} are dynamic parameters in FPGA implementation process optimized by Tcl timing constraints, but its change is quite limited. Therefore, only the code logic T_{logic} can be modified to achieve the high speed DSP structure meeting the requirements of bunch-by-bunch.

The high speed parallel DSP structure proposed in this paper will be described in five parts: selection of DSP form, analysis of DSP structure, implementation of DSP structure, data parallelization and performance of parallelization implementation.

SELECTION OF DSP FORM

Generally, in DSP digital filters has two forms, finite impulse response FIR and infinite impulse response IIR.

FIR is a stable all zero structure with linear response characteristics. While IIR, a structure with both poles and zeros, has no linear phase response. If IIR needs to realize linear phase response, it needs to use all-pass filter for correction, which consumes additional digital logic resources. Moreover, due to the nonlinear influence caused by the quantization effect in hardware implementation, the poles of IIR will change and even become unstable [3].

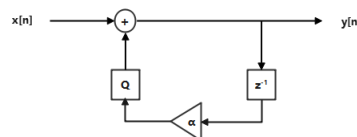


Figure 1: IIR transfer function.

As shown in Fig. 1, the IIR transfer function $\frac{1}{1-\alpha z^{-1}}$ has been transformed into the block design form of state-space

* National Synchrotron Radiation Laboratory

[†] tanglei@ustc.edu.cn

SUB-ns SINGLE-PARTICLE SPILL CHARACTERIZATION FOR SLOW EXTRACTION

T. Milosic*, R. Singh, P. Forck
 GSI Helmholtz Centre for Heavy Ion Research, Darmstadt, Germany

Abstract

With the recent developments on improving spill quality at GSI/FAIR, appropriate measurement devices have come into focus again. In contrast to commonly used scaler-based approaches where events at a certain sample frequency are counted, we present a measurement concept resolving single-event detector timestamps in the sub-ns regime leveraging a well-established off-the-shelf TDC VMEbus module. This allows for high-resolution time structure information with respect to the ring RF as well as evaluation of inter-particle separation distributions. This yields insightful information for specific experiments at GSI whose efficiencies are heavily limited by pile-ups and detector dead times. We will present the concept of the measurement setup and exemplary data taken in recent campaigns in context of spill microstructure improvements for slow extraction.

INTRODUCTION

Recent experiments measuring and optimizing slow-extraction spills at GSI/FAIR led to promising results [1]. The focus on spill quality introduced the demand to complement traditional counter-based approaches with single-particle detection at higher time resolution. Ideally, this would allow to resolve bunches and directly access the particle-interval information. Both is not possible with scalars even at high latching rates.

This goal can be achieved by fast time-to-digital converters (TDCs). They turn logic input signals, such as discriminated detector signals, into precise timestamps. Figure 1 schematically depicts timing events derived from two input signals and recorded by a TDC. Time-structure information

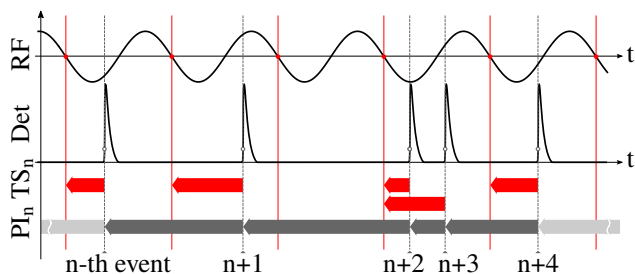


Figure 1: Single-particle events used to characterize spills.

is extracted from the detector event by correlating it with the SIS18 cavity RF or, alternatively, with a custom clock. The red arrows TS_n mark the difference between a detector event and the preceding slope-sensitive zero-crossing of the RF reference. This data is histogrammed at a user-definable bin

size and time slice, providing a reconstruction of the time structure confined to the RF period range.

Similarly, the particle-interval (also *separation*) information PI_n is retrieved as the difference between consecutive detector timestamps as represented by gray arrows. Event data grouped in time slices is histogrammed with user-definable bin sizes and total range. The particle-interval distribution is useful to evaluate and optimize reduced efficiencies as a consequence of dead times of specific experiments.

Two application targets are considered. An online tool allows to assess spill characterization for operating and experiments. Furthermore, offline analysis preserving full information of the raw data is available. The TDC module comes with some limitations for which, in particular high-performance, online analysis is a challenge. However, the setup presented is capable to make use of the TDC ASICs performance to its fullest even in online mode.

HARDWARE SETUP

A system leveraging a high-precision TDC already existed as part of the ABLAX suite [2]. It is based on a RIO3 VMEbus controller, a CAEN V1290N TDC module and a custom software stack on top of LynxOS. Being limited to a net detection rate of $\ll 100$ kEvents/s and the increasing challenge to maintain the environment this gave rise to a new development from scratch but using the same TDC module.

Constrained to the VMEbus, the new system uses a x86-64 MEN A25 controller [3] paired with a PMC White Rabbit FAIR timing receiver node (FTRN) [4] (Fig. 2). The con-



Figure 2: VMEbus mainframe configuration.

troller is based on the Intel(R) Pentium(R) CPU D1519 with 4 cores supporting 2 threads per core through hyper-threading at 1.50 to 2.10 GHz and 8 GiB of RAM. It has been equipped with a 1 TB mSATA SSD to store data locally.

Time-to-Digital Converter

The V1290N TDC VMEbus module is build around CERN's HPTDC ASIC [5] and is still available from CAEN.

* t.milosic@gsi.de

TESTS OF DIGITAL BPM SIGNAL PROCESSORS FOR SHINE*

L.W. Lai[†], Y.B. Leng, Y.M. Zhou, W.M. Zhou, X. Yang, J. Wan, H.S. Wang,
SSRF, Shanghai Advanced Research Institute, Chinese Academy of Sciences, Shanghai, China

Abstract

Digital signal processors that can handle 1 MHz bunch rate BPM signal processing is under development for SHINE. At the same time, two general purpose processor prototypes for all BPM signal sampling and processing have been developed. One uses 14bits ADC, the other uses 16bits ADC. Both processors have been completed. This paper will introduce the tests of the processors and the related performance evaluations.

INTRODUCTION

Shanghai High repetition rate XFEL and Extreme light facility (SHINE) is a 3 km long hard X-ray FEL facility built underground in Shanghai. The designed beam repetition rate is 1 MHz. The project was initiated at the end of 2018. Now the research of key technologies has entered the final stage. There will be three types of BPMs located in different parts of the machine, including stripline BPM, cold button BPMs, and cavity BPM. The required BPM system resolution is 10 μm , 50 μm and 200 nm at 100 pC respectively.

BPM electronics will use independent RF front-end modules and digital signal processors. Different RF front-end modules will be designed to meet the signal characteristics requirements of different BPM types. The design of the RF front-end modules will not be introduced here. All three types of BPM will use unified digital signal processor hardware. The processor will be used for signal processing of different BPMs through the development of corresponding FPGA firmware and software [1]. The processor mainly contains 4 channels ADCs for sampling, FPGA for signal processing and ARM for system control and communication. Considering the beam dynamic range and the required system performance, the relative resolution of the processor should be better than 0.1%.

The processor is designed as a 1U height standalone instrument. The processor consists of a FPGA carrier board and an ADC daughter board. The boards are connected through FMC connector. The sampled data from ADCs are transmitted to FPGA through the JESD204B protocol. Another FMC connector is reserved for a WRN timing board. Figure 1 is the structure of the processor. Other interfaces including a Ethernet port, serial port, JTAG, SD slot, et al. Table 1 lists the specification of the processor. Except for the generic BPM processor, another direct RF sampling processor for cavity BPM also has being developed, the

hardware is completed but firmware is still in progress, it will not be introduced here.

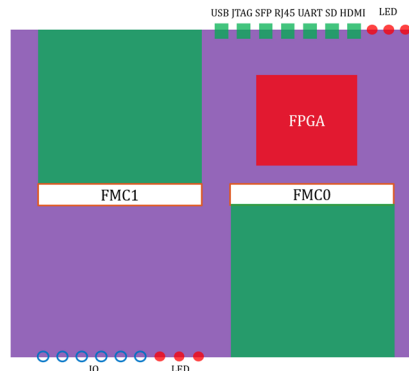


Figure 1: Processor structure.

Table 1: DBPM Specifications

Parameter	Value
Channels	4
Bandwidth	≥ 1 GHz
ADC bits	≥ 14
Max ADC rate	≥ 500 MSPS
FPGA	Xilinx Zynq Ultra+MPSoC
Clock	External
Trigger	Ext./Self/Period
SFP	≥ 2
Interlock	Lemo
DDR	≥ 512 MB
Software	Arm-Linux/EPICS
Relative resolution	$\leq 0.100\%$

In order to cultivate qualified vendors for SHINE, two processor prototypes were developed at the same time. One processor uses 14 bits ADCs, the other two uses 16 bits ADCs. The maximum sampling rate of all ADCs is 1 GSPS. The development of the processors has been introduced in previous conference paper [2]. Recently, all the two processor prototypes come to the final stage. The tests of the processors will be introduced here.

*Work supported by Youth Innovation Promotion Association, CAS (Grant No. 2019290); The National Key Research and Development Program of China (Grant No. 2016YFA0401903).

[†]Corresponding author: lailongwei@zjlab.org.cn

THE FACET-II DATA ACQUISITION SYSTEM*

S. J. Gessner†, SLAC National Accelerator Laboratory, Menlo Park, CA, USA

Abstract

The Data Acquisition System (DAQ) at FACET-II is designed to address the challenge of collecting synchronized, time-stamped data from a variety of diagnostics spread throughout the kilometer-long linac and experimental area. The EPICS control system is used to read out data from devices at FACET-II via Channel Access (CA) over the network. This poses a problem for collecting image data at the 30 Hz beam rate. With image sizes ranging from 0.3-10 Megapixels, the data rate from a single camera can be as high as 0.6 Gbps and there are nearly 100 cameras deployed at FACET-II. Simultaneous image acquisition from just a few of these cameras would overwhelm the network. The FACET-II DAQ solves this problem by coordinating the camera IOCs to write their image data to network-attached storage (NAS) and then validating time-stamps to confirm synchronization.

INTRODUCTION

FACET-II [1] at SLAC uses EPICS [2] to control and retrieve data from diagnostics and devices spread throughout the kilometer-long accelerator and experimental area. The principle diagnostics for experiments at FACET-II are digital cameras. FACET-II hosts nearly 100 digital cameras and more than half of them are dedicated to the experimental area. Communication with the cameras is handled by the Channel Access (CA) network protocol. CA is the appropriate tool for monitoring and managing devices, but data rates are limited by the network. This poses a challenge for data acquisition (DAQ) because we require simultaneous images from multiple cameras corresponding to a single shot. The beam rate at FACET is 30 Hz and the average image size is over 1 Megapixel, equal to 2 MB/frame. FACET users commonly request datasets utilizing ten or more cameras, which yields a data rate of ≈ 5 Gbps. This rate can easily overwhelm the network, which utilizes both 1 GbE and 10 GbE switches, and may disrupt accelerator applications.

The FACET-II DAQ avoids the problem of acquiring data over the network by coordinating camera Input-Output Controllers (IOC) to save their data to a Network Attached Storage (NAS) drive located on the same switch as the camera servers. With this approach, the camera data never leaves the switch and network traffic is maintained at an acceptable level.

HARDWARE, LAYOUT, AND TOPOLOGY

The majority of cameras at FACET are AVT Manta and Mako GigE-interface devices running on Advantech Sky 8201 servers. Each server can host up to 12 cameras. FACET

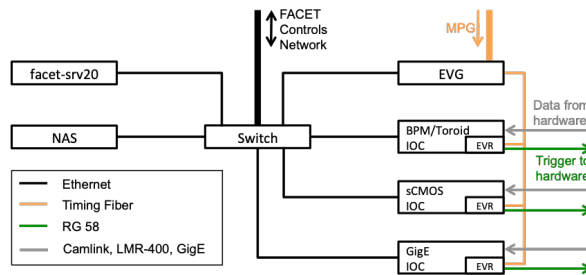


Figure 1: Network topology in FACET Sector 20. Note that the EVG has been relocated to the FACET injector in Sector 10.

also uses scientific-CMOS cameras in the experimental area. All servers run areaDetector [3] IOCs. There are 7 camera servers along the linac and 9 camera servers located in Sector 20 (S20), the experimental area. The camera servers in S20 collect the majority of the data requested by users via the DAQ. A control server called facet-srv20 and NAS drive are also located in S20 and connected to the same switch as the camera servers. The NAS uses bonded ports to maximize data rate onto the drive. The topology of the network in S20 is shown in Fig. 1. The layout of the machine is shown in Fig. 2 and the distribution of the cameras is shown in Table 1.

DATA SOURCES AND SYNCHRONIZATION

In addition to camera images, the FACET-II DAQ also collects data from a variety of sources. This includes devices that update at the beam rate, such as beam position monitors (BPM), toroids, and photo-multiplier tubes (PMT), as well as devices that update asynchronously, such as magnet currents, motor positions, and temperatures. The beam-synchronous devices produce scalar data and are included in SLAC's beam-synchronous acquisition (BSA) infrastructure [4]. BSA devices store data in a rolling buffer with 2800 events. The length of the buffer was chosen for compatibility with the legacy SLC Control Program (SCP) [5]. The buffer exists on the IOC hosting the device, and each IOC can support multiple buffers with unique event definitions. For example, if the nominal beam rate at FACET is 30 Hz, an event code (EC) may be used to specify a lower rate (e.g. 10 Hz) or a rate subject to conditions (e.g. beam destination). Events are timestamped and tagged with a pulse ID number. The pulse ID is a rolling value that updates at 360 Hz. The maximum pulse ID is 131040, which is also a legacy of the SCP. This implies that the pulse IDs are not unique, but a buffer of length 2800 will not contain duplicate pulse IDs. BSA buffers are centrally managed by the Event Generator

* This work performed under DOE Contract DE-AC02-76SF00515.

† sgress@slac.stanford.edu

Content from this work may be used under the terms of the CC BY 3.0 licence (© 2021). Any distribution of this work must maintain attribution to the author(s), title of the work, publisher, and DOI

STUDY OF SOLUTIONS FOR INTERFACING ILSF BEAM DIAGNOSTICS TOOLS TO CONTROL SYSTEM

P. Navidpour, F. A. Mehrabi, S. Mohammadi Alamouti

Iranian Light Source Facility, Institute for Research in Fundamental Sciences, Tehran, Iran

Abstract

There is an ongoing study at Iranian Light Source Facility (ILSF) aims to determine control solutions for a variety of diagnostics tools that will be placed at various locations around the facility. In this paper, an overview of the possible control solutions with a focus mostly on the low-level part of the control system is reported.

INTRUCTION

The ILSF synchrotron light source is under design and construction and now that the basic design phase of the diagnostics subsystems is finished, our job in the control and diagnostics group is to study and document the possible control solutions for each diagnostics tools. However, the study is still in progress and our choices are not finalized yet. The diagnostics tools we will discuss in this paper are Fluorescent Screen (FS) and Optical Transition Radiation (OTR) systems, Beam Loss Monitors (BLM), Fast Current Transformer (FCT), Integrating Current Transformer (ICT), Faraday Cup (FC), and Direct Current Transformer (DCCT). These tools are categorized into three sections and the control solution is discussed for each one.

CAMERA BASED DIAGNOSTICS TOOLS

Camera based diagnostics tools have applications in measuring the size and profile of the beam. There are several FS/OTR and SRM stations at various locations around the facility. Table 1 summarizes the location and controllable components for each of these tools.

Table 1: Camera Based Diagnostics Tools and their Controllable Components

Tool	Location	Qty	Controllable Component
FS/OTR	Linac Diagnostics line, LTB, Booster, BTS, Storage ring	20	Stepper Motors, CCD Cameras, Single-Board Computers
SRM	LTB, Booster, BTS, Storage ring, Diagnostics beamline	9	Streak Camera, CCD Cameras

The standard we choose to transfer the image data from the camera to the IOC depends on the required frame rate and the image quality. For a typical 2-4-megapixel camera that we will use in FS/OTR systems, we presume that the required speed demand will not exceed 1000 Mbps. This makes the GigE solution a good choice in terms of much longer cable it supports compared to the Firewire, and also, its simplicity and much lower cost compared to other non-Ethernet based standards.

For the Streak camera, with a high bandwidth demand of about 2 Gbps, we will use CoaXPress (CXP) interface to send data from the camera to a frame grabber that is installed on a PC workstation. In the future, depending on the community support and commercial availability of the required equipment, other network-based solutions like 10 GigE might be used as well. Table 2 gives a summary of camera based diagnostics tools control specification and its IOC platform.

Table 2: Control Requirements and IOC Platform for the Camera Systems

Camera	Interface	Data Rate	Frame Grabber	IOC
CCD Camera	GigE	320 Mbps	No	PC
Streak Camera	CXP	2000 Mbps	Yes	PC

All camera systems have PC-based IOCs. This PC runs the camera EPICS IOC, areaDetector modules [1], and applications such as ImageJ to calculate some parameters and visualize the image data.

A simplified layout of the control interface of the camera based diagnostics tools at ILSF is shown in Fig. 1. There will be one workstation PC in the instrumentation area that is used as the EPICS IOC for FS/OTR and SRM cameras. Another workstation PC that hosts the CXP frame grabber is used as the EPICS IOC of the streak camera and SRMs that are located in the diagnostics beamline. The latest one will be located somewhere near the beamline instrumentation area to ease the access of the engineers to it.

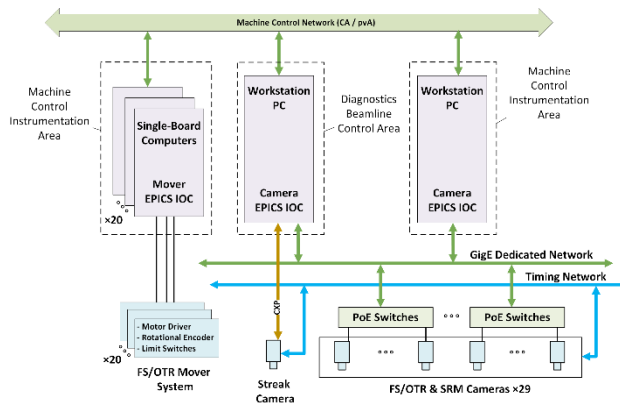


Figure 1: An example of the possible control solution for camera based diagnostics tools.

Each FS/OTR stations has a mover system that is controlled by a single-board computer (e.g. BeagleBone Black). The board runs soft IOCs to interface the mover

BUNCH-BY-BUNCH 3D MEASUREMENT SYSTEM IN HLS-II*

Ruizhe Wu, Leilei Tang, Bao-gen Sun, Fangfang Wu, Jiang Wang, Zeran Zhou, Ping Lu[†]
 National Synchrotron Radiation Laboratory (NSRL),
 University of Science and Technology of China (USTC), Hefei, Anhui, China

Abstract

In order to improve the performance of Hefei Light Source (HLS-II), it is necessary to study various problems of nonlinear beam dynamics in the storage ring, so as to optimize the beam filling mode and injection mode, and then improve the intensity and brightness of HLS-II. In beam dynamics, bunch-by-bunch can provide detailed information of beam bunches and help beam researchers to study the problems of beam bunches deeper. Therefore, HLS-II diagnostics group has developed an on-line bunch-by-bunch three-dimensional measurement system based on high bandwidth and high speed oscilloscope.

SYSTEM STRUCTURE AND FUNCTION OVERVIEW

The measurement system uses SDS6204 H12 Pro oscilloscope of Siglent company [1] as the front end of signal processing to collect bunch-by-bunch signal. The front-end oscilloscope uses the 0.1Hz trigger signal provided by HLS-II timing system. The signal processing back-end of the system is the win10 virtual machine created by Zstack IAAS platform [2]. In the back-end, all signal processing programs are written with LabVIEW. In these programs, calab writes the PV variable of EPICS into the IOC of CentOS system, and then displays the results of back-end signal processing through OPI, as Fig. 1.

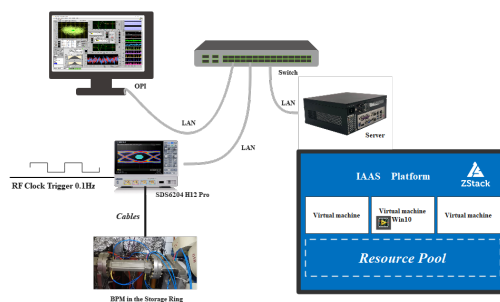


Figure 1: Overall structure of the system in HLS-II.

Driven by the 0.1 Hz trigger signal, the system updates every 10 seconds. Each time it is triggered, the back-end program will collect waveform data from four channels of BPM for 500 μ s. The waveform data records 2266 circles of bunch-by-bunch. Through these data, various information of bunch-by-bunch can be calculated, such as time, amplitude, intensity and transverse information. Moreover, the

system can obtain turn-by-turn information and the tune of each bunch through the waveform data.

OPI INTERFACE

Templates are provided for recommended software and authors are advised to use them. Please consult the individual conference help pages if questions arise.

After obtaining the three-dimensional information of bunch-by-bunch, the 3D position information of 2266 circles of bunch-by-bunch can be displayed through the three views function of OPI interface to clarify the distribution of the bunch-by-bunch centroid. As shown in Fig. 2, the OPI interface shows the bunch-by-bunch three-dimensional centroid distribution under the normal state, while in Fig. 3 it shows the bunch-by-bunch three-dimensional centroid distribution under the injection state. In the three views on the left are measured by stripline BPM and the three views on the right are measured by button BPM. And different colors in three views represent the average results of different numbers of bunch-by-bunch bunches.

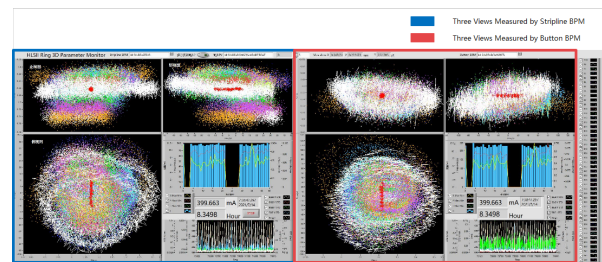


Figure 2: Three views under the normal state.

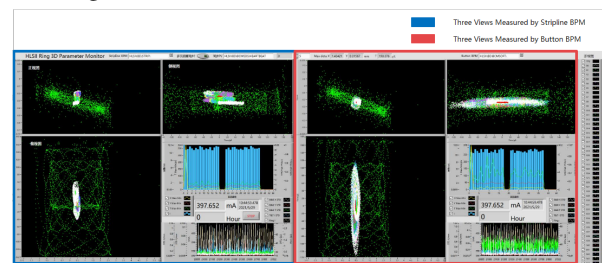


Figure 3: Three views under the injection state.

Moreover, the OPI interface also provides bunch-by-bunch tracking interfaces to track a specific bunch, as shown in Fig. 4. In Fig. 4(a), the upper left part is a two-dimensional diagram of the bunch-by-bunch current intensity. For this part, the abscissa is the number of 45 bunches in one circle, and the ordinate is the number of cycles of bunches running in the storage ring, while its colors indicate different current intensities. The lower left part shows the average current intensity of 2266 cycles for each bunch in

* National Synchrotron Radiation Laboratory
[†] lup@ustc.edu.cn

HIGH-RESOLUTION, LOW-LATENCY, BUNCH-BY-BUNCH FEEDBACK SYSTEMS FOR NANOBEAM PRODUCTION AND STABILISATION

P. N. Burrows, D. R. Bett, N. Blaskovic Kraljevic, T. Bromwich, G. B. Christian, C. Perry, R. Ramjiawan, John Adams Institute, Oxford, UK

Abstract

High-precision intra-bunch-train beam orbit feedback correction systems have been developed and tested in the ATF2 beamline of the Accelerator Test Facility at the High Energy Accelerator Research Organization in Japan. Two systems are presented: 1) The vertical position of the bunch measured at two stripline beam position monitors (BPMs) is used to calculate a pair of kicks which are applied to the next bunch using two upstream kickers, thereby correcting both the vertical position and trajectory angle. This system was optimised so as to stabilize the beam offset at the feedback BPMs to better than 350 nm, yielding a local trajectory angle correction to within 250 nrad. Measurements with a beam size monitor at the focal point (IP) demonstrate that reducing the trajectory jitter of the beam by a factor of 4 also reduces the observed wakefield-induced increase in the measured beam size as a function of beam charge by a factor of c. 1.6. 2) High-resolution cavity BPMs were used to provide local beam stabilization in the IP region. The BPMs were demonstrated to achieve an operational resolution of ~20 nm. With the application of single-BPM and two-BPM feedback, beam stabilization of below 50 nm and 41 nm respectively has been achieved with a closed-loop latency of 232 ns.

INTRODUCTION

A number of in-construction and proposed future particle accelerator designs feature trains of particle bunches with bunch-separation intervals in the ranges of nanoseconds to tens or hundreds of nanoseconds. For example, the International Linear Collider (ILC) design [1] calls for bunch trains comprising thousands of bunches separated in time by around 500 ns with a train repetition frequency of 5 Hz; the Compact Linear Collider (CLIC) design [2] specifies bunch trains comprising several hundred bunches separated in time by around 0.5 ns, with a train repetition frequency of 50 Hz. Free-electron lasers based on similar accelerating technologies as ILC and CLIC, such as the European XFEL [3], have respectively similar bunch-train time structures. Beam control at such facilities calls for beam position monitors (BPMs) that can resolve bunches on an intra-train (ideally bunch-by-bunch) timescale, with submicron position resolution in single-pass mode. The designs of such BPM and feedback systems are presented here.

STRIPLINE BPM SYSTEM AT ATF2

The system was developed by the Feedback on Nanosecond Timescales (FONT) group [4] and it was deployed, commissioned and tested at the Accelerator

Test Facility (ATF) [5] at KEK. The layout of the BPMs is shown in more detail in Fig. 1. The design goal for the FONT5 system is to stabilize the vertical beam position to the 1 μm level at the entrance to the final-focus system. This requires BPMs capable of resolving bunches separated in time by around 100 ns, and with a position resolution at the submicron level. For tests of the FONT system the ATF is operated in a mode whereby a train of two or three bunches is extracted from the damping ring and sent down the ATF2 beam line. The bunch separation is determined by the damping ring fill pattern and typically is chosen to be between 140 ns and either 154 ns (3-bunch mode) or 300 ns (2-bunch mode).

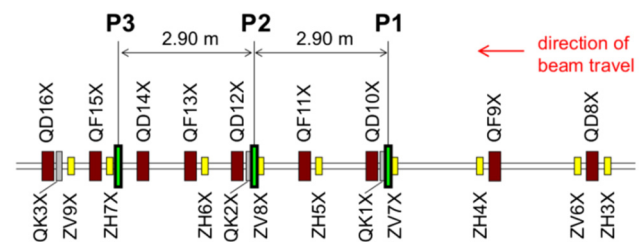


Figure 1: Layout of the FONT BPMs (P1, P2 and P3) in the ATF2 extraction line; quadrupole (“Q”) and dipole corrector (“Z”) magnets are indicated.

The FONT5 BPM system (Fig. 2) consists of three stripline BPMs (Fig. 3) each of which is instrumented with an analogue processor, and a custom multichannel digitizer. Stripline BPMs were used due to their inherently fast, broadband response and capability to resolve bunches with the required time resolution. In the FONT5 system, only the vertical plane of the BPMs is routinely instrumented.

The FONT5 analogue processors’ (Fig. 4) function [6] is to deliver the stripline pickoff-pair difference and sum signals in a form that can be easily recorded by the digitizer for calculation of the position-dependent, beam charge-independent ratio of the two. Ten processors were built and are used in beam operations at ATF2. A single BPM processor can be used to process the beam position data in either the horizontal or vertical plane; from here on only the vertical plane is considered. The BPM processor outputs are digitised by a custom digital feedback processor board (Fig. 5). The board has nine analogue signal input channels digitised using ADCs with a maximum conversion rate of 400 MS/s, and two analogue output channels formed using DACs, which can be clocked at up to 210 MHz. The digital signal processing is based on a Xilinx Virtex5 FPGA. The FPGA is clocked with a 357 MHz source derived from the ATF

ADAPTIVE CONTROL AND MACHINE LEARNING FOR PARTICLE ACCELERATOR BEAM CONTROL AND DIAGNOSTICS*

A. Scheinker[†], Los Alamos National Laboratory, Los Alamos, USA

Abstract

In this tutorial, we start by reviewing some topics in control theory, including adaptive and model-independent feedback control algorithms that are robust to uncertain and time-varying systems, and provide some examples of their application for particle accelerator beams at both hadron and electron machines. We then discuss recent developments in machine learning (ML) and show some examples of how ML methods are being developed for accelerator controls and diagnostics, such as online surrogate models that act as virtual observers of beam properties. Then we give an overview of adaptive machine learning (AML) in which adaptive model-independent methods are combined with ML-based methods so that they are robust for and applicable to time-varying systems. Finally, we present some recent applications of AML for accelerator controls and diagnostics. In particular we present recently developed adaptive latent space tuning methods and show how they can be used as virtual adaptive predictors of an accelerator beam's longitudinal phase space as well as all of the other 2D projections of a beam's 6D phase space. Throughout the tutorial we will present recent results of various algorithms which have been applied at the LANSCE ion accelerator, the EuXFEL and LCLS FELs, the FACET plasma wakefield accelerator facility, the NDCXII ion accelerator, and the HiRES compact UED.

INTRODUCTION

The control of charged particle beams in particle accelerator facilities is a very challenging task due to the time variation and complexity of the beams and of the machines. Accelerators are typically composed of hundreds-thousands of coupled components which include radio frequency (RF) resonant cavities used for acceleration as well as magnets for focusing of the beams. The performance of large RF systems is known to drift with time due to external disturbances such as vibrations in the case of superconducting cavities and temperature fluctuations for normal conducting cavities which perturb their resonant frequencies. On slower time scales environmental temperature changes result in slight variation of RF cables or analog RF components such as mixers or local oscillators which also introduces phase and amplitude shifts in the highly sensitive high frequency RF systems. The performance of magnets is also perturbed and uncertain due to issues such as power source ripple, hysteresis, and misalignments.

Charged particle beams themselves are also highly complex and time-varying objects which live in a 6 dimensional phase space (x, y, z, p_x, p_y, p_z) which is impossible to mea-

sure directly or quickly. While newer electron machines are able to measure 2D longitudinal phase space projections (z, E) hadron machines are many times limited to scalar beam position or current monitor-based measurements online. More detailed measurements are possible but typically rely on slow emittance scans or wire scanners, which cannot be performed online in real-time without disrupting operations. Furthermore, both hadron and electron machines suffer from time-varying initial phase space distributions at their sources and undergo complex collective effects such as space charge forces. In the case of highly relativistic intense electron beams collective effects such as coherent synchrotron radiation are also an issue.

Because of all of the complexities and uncertainties described above, advanced controls and diagnostics are of great importance in the accelerator community. Control theory methods, including adaptive and model-independent feedback control algorithms exist which are robust to uncertain and time-varying systems and we provide some examples of their application for particle accelerator beams at both hadron and electron machines. We also discuss recent developments in machine learning (ML) and show some examples of how ML methods are being developed for accelerator controls and diagnostics, such as online surrogate models that act as virtual observers of beam properties. Then we give an overview of adaptive machine learning (AML) in which adaptive model-independent methods are combined with ML-based methods which are used to train surrogate models directly from raw data.

ADAPTIVE CONTROL

Model-independent feedback methods have been developed by the control theory community with an emphasis of robustness to un-modeled disturbances and changes to system dynamics. One classic adaptive control result is given for a scalar linear system of the form

$$\dot{x}(t) = ax(t) + bu(t), \quad (1)$$

where the values of a and b are unknown. Such a system cannot be stabilized with simple proportional integral derivative (PID)-type feedback, but if the sign of b is known, for example if $b > 0$, a stable equilibrium of (1) can be established at $x = 0$ by the following nonlinear controller

$$u(t) = \theta(t)x(t), \quad \dot{\theta}(t) = -kx^2(t), \quad k > 0. \quad (2)$$

This approach does not depend on a detailed knowledge of system dynamics, but has major limitations which are: 1). The sign of the unknown term b must be known and cannot be time-varying. 2). The presence of an arbitrarily small

* Work supported by Los Alamos National Laboratory

[†] ascheink@lanl.gov

IDENTIFICATION OF THE INTER-BUNCH AND INTRA-BUNCH BEAM DYNAMICS BASED ON DYNAMIC MODAL DECOMPOSITION (DMD)*

C. Rivetta^{†1}, SLAC National Accelerator Laboratory, Menlo Park, USA

T. Mastoridis, Physics Dept. California Polytechnic State University, San Luis Obispo, CA, USA

J. Fox, Physics Dept. Stanford University, Palo Alto, USA

¹also at Nadeval LLC, Palo Alto, USA

Abstract

The beam dynamics in circular and linear particle accelerators have been studied defining physics-driven / model-driven models that have been used for operation of the machine, diagnostics and feedback system designs. In this paper, a data-driven technique is evaluated to characterize the inter-bunch / intra-bunch beam dynamics in particle accelerators. The dynamic modal decomposition (DMD) is an equation-free, data-driven method capable of providing an accurate decomposition of a complex system into spatiotemporal coherent structures that can be used for short-time future state prediction and control. It does not require knowledge of the underlying governing equations and only uses snapshots in time of observables from historical, experimental, or black-box simulations. The application of the DMD algorithm to particle accelerator cases is illustrated by examples of the collective longitudinal motion of the bunches in a circular storage ring and the transverse motion of a bunch circulating in an accelerator.

INTRODUCTION

The beam dynamics in circular and linear particle accelerators have been studied defining a framework for design and operation of machines as well as the background for future research in the topic [1]. Based on this framework, multiple studies were conducted in order to delineate models of the beam dynamics to create diagnostic tools and design feedback systems to stabilize the beam and improve the machine performance [2]. These physics-driven / model-driven models are commonly used during the operation of the machine and their parameters are obtained via measurements to provide both diagnostic tools to the control room operators and design tools to set the feedback systems.

There is another option to create models for dynamic systems that does not require the previous knowledge of the physical system. Data-driven modeling and control of complex systems is a field that is having a large impact in engineering and physical sciences. Those complex systems generally evolve on a low-dimensional attractor that can be characterized by spatiotemporal coherent structures. In this paper, we present the dynamic mode decomposition (DMD), and apply it to characterize the intra-bunch and inter-bunch beam dynamics. As example, the analysis of the coupled longitudinal beam dynamics of bunches in a

circular accelerator is presented. Results from simulation are compared with results using traditional methods based on model-driven analysis. The analysis of the transverse dynamic of a single bunch is used as an example to show the application of the DMD algorithm to characterize the intra-bunch motion.

DYNAMIC MODAL DECOMPOSITION

Generalities

The DMD method originated in the fluid dynamics community as a method to decompose complex flows into a simple representation based on spatiotemporal coherent structures [3]. The particular characteristic of DMD is that it is an equation-free, data-driven method capable of providing an accurate decomposition of a complex system into spatiotemporal coherent structures that can be used for short-time future state prediction and control. DMD has a number of uses, classified in three primary tasks:

- **Diagnostics.** In particular, the algorithm extracts key low-rank spatiotemporal features of many high-dimensional systems, allowing for physically interpretable results in terms of spatial structures and their associated temporal responses.
- **State estimation, future-state prediction, and system identification.** Another application of the DMD algorithm is associated with using the spatiotemporal structures that are dominant in the data to construct dynamical models of the underlying processes observed.
- **Control.** The ultimate goal of the algorithm is to define viable and robust control strategies directly from the data sampling or the models identified by the algorithm. This is the most challenging task due to the dynamics associated is nonlinear and the DMD creates a linear model based on the data taken.

Background

The main objective is to characterize the intra-bunch / inter-bunch dynamics of the beam based on measurements. The beam dynamics can be represented by a set of ordinary differential equations (ODE),

$$\frac{dx(t)}{dt} = f(x(t)) \quad \text{with } x \in R^{2n} \text{ or } x \in C^n$$

ODEs in general are used to describe the inter-bunch dynamics. Partial differential equation (PDE) are used to represent

* Work supported by the DOE contract #DE-AC02-76SF00515.

[†] chrivetta@nadeval.com